

**Some pages of this thesis may have been removed for copyright restrictions.**

If you have discovered material in Aston Research Explorer which is unlawful e.g. breaches copyright, (either yours or that of a third party) or any other law, including but not limited to those relating to patent, trademark, confidentiality, data protection, obscenity, defamation, libel, then please read our [Takedown policy](#) and contact the service immediately ([openaccess@aston.ac.uk](mailto:openaccess@aston.ac.uk))

"STRUCTURAL OPTIMIZATION"

BY

DAVID WILLIAM CHARLES ELLIOTT

A THESIS SUBMITTED FOR THE DEGREE OF

DOCTOR OF PHILOSOPHY

DEPARTMENT OF CIVIL ENGINEERING

UNIVERSITY OF ASTON IN BIRMINGHAM

SEPTEMBER 1971

*Thesis*  
*519.28*  
*ELL*

3 DEC 71 145272

"STRUCTURAL OPTIMIZATION"

BY

DAVID WILLIAM CHARLES ELLIOTT

A THESIS SUBMITTED FOR THE DEGREE OF

DOCTOR OF PHILOSOPHY

DEPARTMENT OF CIVIL ENGINEERING

UNIVERSITY OF ASTON IN BIRMINGHAM

SEPTEMBER 1971

*Thesis*  
*519.28*  
*ELL*

3 DEC 71 145272

#### THE AUTHOR

The author graduated from the Department of Civil Engineering, University of Aston in Birmingham, in 1967 having completed a four-year sandwich course. The following period until September 1971 was spent as a postgraduate student engaged in full time research in the above department. The work presented in this thesis has been carried out during this period.

No part of this work has been submitted in support of an application for another degree or qualification.



## SYNOPSIS

Two non-linear programming algorithms for the minimum weight of structural frames are presented in this thesis. The first, which is applied to rigidly jointed and pin jointed plane frames subject to deflection constraints, consists of a search in a feasible design space. Successive trial designs are developed so that the feasibility and the optimality designs are improved simultaneously. It is found that this method is restricted to the design of structures with few unknown variables.

The second non-linear programming algorithm is presented in a general form. This consists of two types of search, one improving feasibility and the other optimality. The method speeds up the 'feasible direction' approach by obtaining a constant weight direction vector that is influenced by dominating constraints. For pin jointed plane and space frames this method is used to obtain a 'minimum weight' design which satisfies restrictions on stresses and deflexions. The matrix force method enables the requirements to be expressed in a general form and the design problem is automatically formulated within the computer. Examples are given to explain the method and the design criteria are extended to include member buckling.

Fundamental theorems are proposed and proved to confirm that structures are inter-related. These theorems are applicable to linear elastic structures and facilitate the prediction of the behaviour of one structure from the results of analysing another, more general, or related structure. It becomes possible to evaluate the significance of each member in the behaviour of a structure and the problem of minimum weight design is extended to include shape. A method is proposed to design structures of optimum shape with stress and deflexion limitations. Finally a detailed investigation is carried out into the design of structures to study the factors that influence their shape.

## SYNOPSIS

Two non-linear programming algorithms for the minimum weight design of structural frames are presented in this thesis. The first, which is applied to rigidly jointed and pin jointed plane frames subject to deflexion constraints, consists of a search in a feasible design space. Successive trial designs are developed so that the feasibility and the optimality of designs are improved simultaneously. It is found that this method is restricted to the design of structures with few unknown variables.

The second non-linear programming algorithm is presented in a general form. This consists of two types of search, one improving feasibility and the other optimality. The method speeds up the 'feasible direction' approach by obtaining a constant weight direction vector that is influenced by dominating constraints. For pin jointed plane and space frames this method is used to obtain a 'minimum weight' design which satisfies restrictions on stresses and deflexions. The matrix force method enables the design requirements to be expressed in a general form and the design problem is automatically formulated within the computer. Examples are given to explain the method and the design criteria are extended to include member buckling.

Fundamental theorems are proposed and proved to confirm that structures are inter-related. These theorems are applicable to linear elastic structures and facilitate the prediction of the behaviour of one structure from the results of analysing another, more general, or related structure. It becomes possible to evaluate the significance of each member in the behaviour of a structure and the problem of minimum weight design is extended to include shape. A method is proposed to design structures of optimum shape with stress and deflexion limitations. Finally a detailed investigation is carried out into the design of structures to study the factors that influence their shape.

## SYNOPSIS

Two non-linear programming algorithms for the minimum weight design of structural frames are presented in this thesis. The first, which is applied to rigidly jointed and pin jointed plane frames subject to deflexion constraints, consists of a search in a feasible design space. Successive trial designs are developed so that the feasibility and the optimality of the designs are improved simultaneously. It is found that this method is restricted to the design of structures with few unknown variables.

The second non-linear programming algorithm is presented in a general form. This consists of two types of search, one improving feasibility and the other optimality. The method speeds up the 'feasible direction' approach by obtaining a constant weight direction vector that is influenced by dominating constraints. For pin jointed plane and space frames this method is used to obtain a 'minimum weight' design which satisfies restrictions on stresses and deflexions. The matrix force method enables the design requirements to be expressed in a general form and the design problem is automatically formulated within the computer. Examples are given to explain the method and the design criteria are extended to include member buckling.

Fundamental theorems are proposed and proved to confirm that structures are inter-related. These theorems are applicable to linear elastic structures and facilitate the prediction of the behaviour of one structure from the results of analysing another, more general, or related structure. It becomes possible to evaluate the significance of each member in the behaviour of a structure and the problem of minimum weight design is extended to include shape. A method is proposed to design structures of optimum shape with stress and deflexion limitations. Finally a detailed investigation is carried out into the design of structures to study the factors that influence their shape.

SYNOPSIS

Two non-linear programming algorithms for the minimum weight design of structural frames are presented in this thesis. The first, which is applied to rigidly jointed and pin jointed plane frames subject to deflexion constraints, consists of a search in a feasible design space. Successive trial designs are developed so that the feasibility and the optimality of the designs are improved simultaneously. It is found that this method is restricted to the design of structures with few unknown variables.

The second non-linear programming algorithm is presented in a general form. This consists of two types of search, one improving feasibility and the other optimality. The method speeds up the 'feasible direction' approach by obtaining a constant weight direction vector that is influenced by dominating constraints. For pin jointed plane and space frames this method is used to obtain a 'minimum weight' design which satisfies restrictions on stresses and deflexions. The matrix force method enables the design requirements to be expressed in a general form and the design problem is automatically formulated within the computer. Examples are given to explain the method and the design criteria are extended to include member buckling.

Fundamental theorems are proposed and proved to confirm that structures are inter-related. These theorems are applicable to linear elastic structures and facilitate the prediction of the behaviour of one structure from the results of analysing another, more general, or related structure. It becomes possible to evaluate the significance of each member in the behaviour of a structure and the problem of minimum weight design is extended to include shape. A method is proposed to design structures of optimum shape with stress and deflexion limitations. Finally a detailed investigation is carried out into the design of structures to study the factors that influence their shape.

### ACKNOWLEDGEMENTS

The author wishes to express his gratitude to Professor K. I. Majid, B.Sc., Ph.D., C.Eng., M.I.C.E., M.I.Struct.E., for his continued encouragement, advice and enthusiasm throughout the duration of this project.

In the preparation of this thesis the author would like to thank Miss Pat Sage for tracing the diagrams and his wife for her very efficient and patient typing of the script.

Finally, the author would like to thank the Atlas computer staff at Chilton for their prompt service and the Science Research Council for their financial support.



SYMBOLIZATION

$\underline{a}$	diagonal matrix of member areas.
$a$	cross-sectional area.
$a_1 \dots a_9$	equation coefficients (Chapter 2).
$\underline{b}$	benefit vector.
$b$	stiffness parameter.
$c_i$	objective function coefficient.
$c_1 \dots c_{10}$	equation coefficients (Chapter 2).
$c_{oi}$	effect of member removal defined by equation (6.49).
$d$	stiffness parameter (Chapter 2), constant.
$e$	stiffness parameter (Chapter 2), increment.
$\underline{f}$	member flexibility matrix (Chapter 3), matrix of member forces due to unit axial loads (Chapters 6, 7 and 8).
$f_{ij}$	force in member $i$ due to unit loads at the ends of member
$g_i(x)$	behaviour function.
$g_i(m_{i-1}, m_i)$	function representing cost of $i$ -th segment.
$g_{\min}$	minimum element of $\underline{G}$ .
$h_1$	length of columns.
$h_2$	vertical distance between apex and eaves.
$\underline{i}$	unit vector.
$i, j, k$	counters.
$k$	non-dimensional ratio $h_2/h_1$ (Chapter 2).
$\underline{k}, \underline{k}'$	vectors indicating position of variables between bounds (Chapter 4).
$k_i, k_i'$	elements of $\underline{k}$ and $\underline{k}'$ .
$\underline{l}$	vector of member lengths.
$l_i$	length of member $i$ .
$l_t, l_c$	length of tensile and compressive member (Chapter 1).
$l_p$	direction cosine.

$\underline{m}$	vector of redundant moments (Chapter 1).
$m_i$	$i$ -th moment.
$m_p$	direction cosine.
$\underline{n}$	vector of weighted redundant moments (Chapter 1).
$n$	counter.
$n_g$	number of groups.
$n_p$	direction cosine.
$p_i$	force acting in member $i$ .
$p_t, p_c$	tensile force and compressive force (Chapter 1).
$\underline{p}$	vector of member forces.
$p$	counter.
$p_{iq}$	force in member $q$ due to unit load at node $i$ .
$p_w$	pressure caused by wind velocity of $W$ m.p.h.
$p_{72}$	pressure caused by wind velocity of 72 m.p.h.
$q$	non-dimensional quantity $L/h_1$ (Chapter 2).
$r$	radius of gyration (Chapter 5), variation factor (Chapters 6, 7, 8).
$r$	variation factor.
$r^*$	force in redundant member (Chapter 6).
$s_{ij}$	element of slope matrix.
$s_{ij}^*$	element of modified slope matrix.
$t_1, t_2, t_3, t_4$	tolerances.
$u$	variable.
$u_{\text{new}}, u_{\text{old}}$	present and previous values of $u$ .
$u_f, u_n$	feasible and non-feasible values of $u$ .
$u_a, u_b$	value of $u$ at boundary points $a$ and $b$ .
$v_j$	slack variable (Chapter 1).
$v_i$	volume of feasible structure on removal of member $i$ (Chapter 7).
$v$	variable.

$\underline{m}$	vector of redundant moments (Chapter 1).
$m_i$	$i$ -th moment.
$m_P$	direction cosine.
$\underline{n}$	vector of weighted redundant moments (Chapter 1).
$n$	counter.
$n_g$	number of groups.
$n_P$	direction cosine.
$p_i$	force acting in member $i$ .
$p_t, p_c$	tensile force and compressive force (Chapter 1).
$\underline{p}$	vector of member forces.
$p$	counter.
$p_{iq}$	force in member $q$ due to unit load at node $i$ .
$p_w$	pressure caused by wind velocity of $W$ m.p.h.
$p_{72}$	pressure caused by wind velocity of 72 m.p.h.
$q$	non-dimensional quantity $L/h_1$ (Chapter 2).
$r$	radius of gyration (Chapter 5), variation factor (Chapters 6, 7, 8).
$r$	variation factor.
$r^*$	force in redundant member (Chapter 6).
$s_{ij}$	element of slope matrix.
$s_{ij}^*$	element of modified slope matrix.
$t_1, t_2, t_3, t_4$	tolerances.
$u$	variable.
$u_{\text{new}}, u_{\text{old}}$	present and previous values of $u$ .
$u_f, u_n$	feasible and non-feasible values of $u$ .
$u_a, u_b$	value of $u$ at boundary points $a$ and $b$ .
$v_j$	slack variable (Chapter 1).
$v_i$	volume of feasible structure on removal of member $i$ (Chapter 7).
$v$	variable.



$v_{\text{new}}, v_{\text{old}}$	present and previous values of $v$ .
$v_f, v_n$	feasible and non-feasible values of $v$ .
$v_a, v_b$	value of $v$ at boundary points $a$ and $b$ .
$w$	variable.
$w_h$	uniformly distributed load due to wind pressure.
$w_v$	uniformly distributed load due to vertical forces.
$w_{ij}$	weight per unit run of $i$ -th section possible for group $j$ .
$w_{aX}, w_{aY}, w_{aZ}$	components of $W_a$ .
$\underline{x}$	vector of variables.
$\underline{x}^q$	vector of variables at $q$ -th design point.
$\underline{x}_v$	$v$ -th solution vector.
$x_i$	$i$ -th variable (Chapter 4), deflexion at node $i$ (Chapters 6 and 8).
$x_i^o, x_i^u$	lower and upper bounds of $i$ -th variable.
$x_i^i$	new value of variable $x_i$ .
$x_{bi}, x_{bi}^i$	values of variable $x_i$ on boundary of feasible design space.
$x_i^*$	element of new deflexion vector.
$y$	non-dimensional quantity $x^*/x$ (Chapter 6, 7).
$y^*$	value of $y$ after member removal.
$y_i$	most recent non-feasible value of variable $x_i$ .
$y_j$	distance of extreme fibre from neutral axis of member $j$ .
$z, z(x)$	objective function.
$z^i$	previous value of objective function.
$z_o$	objective function of a reference design.
$A$	cross-sectional area.
$A_i^o, A_i^u$	lower and upper bounds of $i$ -th area group.
$A_{ij}$	$j$ -th section specified for area group $i$ .
$\underline{A}$	displacement transformation matrix.
$\underline{A}_b, \underline{A}_r$	submatrices of $\underline{A}$ .

$\underline{B}$	load transformation matrix.
$\underline{B}_b, \underline{B}_r$	submatrices of $\underline{B}$ .
$C$	constant (Chapter 1).
$C_T$	sum of objective function coefficients.
$\underline{C}$	unit load matrix.
$D$	material density (Chapters 1 and 2), distance moved (Chapter 4), constant (Chapters 6, 7, 8).
$E$	Young's modulus of elasticity.
$\underline{F}$	overall flexibility matrix.
$\underline{F}_{bb}, \underline{F}_{br}, \underline{F}_{rb},$ $\underline{F}_{rr}$	submatrices of $\underline{F}$
$\underline{G}$	vector of normalised constraints.
$G_j(x)$	constraint function.
$G_{Ni}(x)$	i-th normalised constraint.
$G_N^T, G_N^C$	tensile and compressive normalised constraints.
$H$	horizontal force.
$I$	second moment of area.
$\underline{I}$	unit matrix.
$I_{ij}$	element of unit matrix.
$\underline{K}$	overall stiffness matrix.
$\underline{K}^*$	new overall stiffness matrix.
$K, K'$	sum of elements $k_i$ and $k'_i$
$K_{ij}$	element of $K$
$K_{ij}^o, K_{ij}^u$	lower and upper bound values of $K_{ij}$
$\underline{L}$	load matrix.
$\underline{L}_b, \underline{L}_r$	submatrices of $\underline{L}$ corresponding to external loads and redundant forces.
$L_{ric}$	c-th redundant force when i-th load case acts.
$L_i$	total length of area group i.

$L$	span of portal frame (Chapter 2), frame dimension (Chapters 6 and 8).
$\underline{M}$	vector of moments.
$\underline{M}^o$	vector of basic statically determinate moments.
$M_{1ij}$	moment at 1st end of member $j$ when load case $i$ acts.
$M_h$	moment acting at eaves.
$M_p$	plastic moment.
$M_{p_g}$	fully plastic moment of group $g$ .
$M_{p_{ij}}$	fully plastic moment of $i$ -th section possible for group $j$ .
$M_V$	fixed end moment due to vertical force $V$ .
$M'_1 \dots M'_r$	linearly independent residual moments.
$\underline{N}$	vector of weighted moments.
$\underline{N}^o$	vector of weighted statically determinate moments.
$\underline{O}$	null matrix.
$P_{kq}$	force in member $q$ under load system $k$ .
$P, Q, R$	local member axes.
$R$	represents redundant forces (Chapter 1), non-dimensional quantity $S/h_1$ (Chapter 2).
$\underline{R}$	removal matrix.
$\underline{R}^*$	updated removal matrix.
$\underline{R}_j$	submatrix of $\underline{R}$ corresponding to the removal of member $j$ .
$R_1, R_2$	redundant forces.
$\underline{S}$	slope matrix.
$\underline{S}^*$	modified slope matrix.
$S$	length of rafters.
$\underline{T}$	vector of limiting values.
$T_j$	limiting value.
$V$	structural volume (Chapter 1), vertical force (Chapter 2).

$W$	weight of structure (Chapter 1), wind velocity (Chapter 2)
$W_a$	force acting at end of a member.
$W_v$	applied load at location $v$ (Chapter 1).
$\underline{X}$	joint displacement vector.
$\underline{X}^*$	new joint displacement vector.
$\underline{X}_b$	displacements corresponding to $\underline{L}_b$
$\underline{X}_r$	displacements corresponding to $\underline{L}_r$
$X, Y, Z$	overall reference axes.
$X_D$	deflexion at joint D.
$X_j$	$j$ -th behaviour variable (Chapter 1)
$X_j^o, X_j^u$	lower and upper bound values of $X_j$ .
$Y_C$	vertical deflexion at joint C.
$\underline{Z}$	vector of member displacements.
$Z_1, Z_2, Z_3$	objective function values.
$\underline{\alpha}$	vector necessary for formation of direction vector.
$\alpha_i$	element of $\underline{\alpha}$ (Chapter 4 and 5), proportional increase in area of member $i$ (Chapters 6, 7 and 8).
$\alpha$	proportional increase of member areas.
$\underline{\beta}$	vector necessary for formation of direction vector.
$\beta_i$	element of $\underline{\beta}$ .
$\beta_{ij}$	rotation in member $i$ for mechanism $j$ .
$\gamma$	order of $\underline{F}$ .
$\delta$	member extension (Chapter 3).
$\delta A, \delta a$	change in area.
$\delta_k$	Kronecker delta.
$\delta_{vj}$	distance $W_v$ moves for mechanism $j$ .
$\delta u, \delta v$	step length in variables $u$ and $v$ .
$\delta v_i$	change in volume due to removal of member $i$ .

$\underline{\delta x}$	direction vector.
$\underline{\delta x}^*$	possible direction vector.
$\delta x_i, \delta x_i^*$	elements of $\underline{\delta x}$ and $\underline{\delta x}^*$ .
$\delta x_{\min}^*, \delta x_{\max}^*$	minimum and maximum values of $\underline{\delta x}^*$ .
$\delta z_i$	change in objective function due to i-th variable.
$\varepsilon$	maximum permissible strain (Chapter 1), small incremental change.
$\varepsilon, \rho, \nu, \phi, \theta$	constants (Chapter 6).
$\eta$	number embodying strut imperfections.
$\theta_D$	rotation at joint D.
$\lambda$	step length.
$\lambda_j$	Lagrangian multiplier.
$\underline{\lambda}_j$	subvector of matrix $\underline{f}$ corresponding to unit loads at ends of member j.
$\lambda_p$	allowable load factor for collapse.
$\mu$	constant.
$\underline{\pi}$	vector of final member forces.
$\pi_i$	force in member i.
$\pi_{ij}$	force in member i while member j is changing.
$\sigma$	member stress.
$\sigma_e$	Euler critical stress.
$\sigma_t^*, \sigma_c^*$	allowable tensile and compressive stresses.
$\sigma_{m_{ij}}$	permissible stress in bending, member j, load case i.
$\phi$	angle of inclination.
$\chi$	matrix of displacements due to unit loads.
$\chi_{ij}$	displacement at node i due to unit loads at the ends of member j.
$\underline{\psi}$	vector of displacements after changing structure.

## CONTENTS

$\psi_{ij}$	displacement at node i due to alterations in member j.
$\psi_{Ej}$	displacement of node j due to external loading after removal of member i.
$\psi_{Dij}$	displacement at node j due to self load vector corresponding to member i after removal of member i.
$\underline{\Delta}$	vector of permissible displacements.
$\Delta_j$	allowable displacement at node j.
$\Delta_u, \Delta_v, \Delta_w$	Kronecker deltas.

1.1	Historical Context of Optimal Design Methods	1
1.1.1	Structural Optimization as a Linear Problem Using Linear Programming Algorithms	1
1.1.2	Structural Optimization Using Non-Linear Programming	15
1.1.3	Structural Configuration as a Design Variable	25
1.2	The Stages for the Design Work	31
CHAPTER 2	SYSTEM SEARCH	34
2.1	Introduction	34
2.2	The Discrete Constraints	34
2.3	Determination of the Optimum Design	35
2.4	Optimization by Non-Linear Programming	45
2.5	Design Charts for Truss and Beam Frames	54
2.6	Design Examples	59
2.7	Design of Six Jointed Frame	61
2.8	Non-Linear Objective Functions	63
2.9	Conclusions	65
CHAPTER 3	FORMULATION OF THE OPTIMUM DESIGN PROBLEM	68
3.1	The Finite Element Method	68
3.2	Automatic Construction of the Load Transformation Matrix	72

$\psi_{ij}$	displacement at node i due to alterations in member j.
$\psi_{Ej}$	displacement of node j due to external loading after removal of member i.
$\psi_{Dij}$	displacement at node j due to self load vector corresponding to member i after removal of member i.
$\underline{\Delta}$	vector of permissible displacements.
$\Delta_j$	allowable displacement at node j.
$\Delta_u, \Delta_v, \Delta_w$	Kronecker deltas.



CONTENTS

	Page
SYNOPSIS	i
ACKNOWLEDGEMENTS	ii
SYMBOLIZATION	iii
CONTENTS	xi
CHAPTER 1 INTRODUCTION	1
1.1 Historical Review of Optimum Design Methods	2
1.1.1 Structural Optimization as a Linear Problem using Linear Programming Algorithms	5
1.1.2 Structural Optimization using Non-Linear Programming	16
1.1.3 Structural Configuration as a Design Variable	28
1.2 The Scope for the Present Work	31
CHAPTER 2 DYNAMIC SEARCH	34
2.1 Introduction	34
2.2 The Deflexion Constraints	34
2.3 Determination of the Optimum Design	35
2.4 Optimization by Non-Linear Programming	46
2.5 Design Charts for Pitched Roof Frames	54
2.6 Design Examples	59
2.7 Design of Pin Jointed Frame	61
2.8 Non-Linear Objective Function	63
2.9 Conclusions	66
CHAPTER 3 FORMULATION OF THE OPTIMUM DESIGN PROBLEM	68
3.1 The Matrix Force Method	69
3.2 Automatic Construction of the Load Transformation Matrix	77



	Page
CHAPTER 4      SOLUTION OF THE DESIGN PROBLEM	79
4.1      Introduction	79
4.2      The Mathematical Problem	79
4.3      Normalisation of the Constraints	81
4.4      The Boundary Solution Vector	83
4.5      The Searching Procedure	85
4.6      The Constant Weight Direction Vector	90
4.7      The Determination of the Step Size	101
4.8      The Non-Linear Programming Algorithm	103
CHAPTER 5      DESIGN EXAMPLES	108
5.1      Hand Example	108
5.2      2-Dimensional Braced Truss	116
5.3      Schwedler Dome Design	118
5.4      Buckling of Members	118
5.5      Tower Design	122
5.6      Cantilever Designs	123
5.7      Conclusions	130
CHAPTER 6      THEOREMS OF STRUCTURAL VARIATIONS	132
6.1      Introduction	132
6.2      The Theorems of Structural Variations	135
6.2.1 Assumptions	135
6.2.2 The Unit Load Matrix	136
6.2.3 Analysis Under Unit Loads	139
6.2.4 Variation of Forces with Those of Member Areas	139
6.2.5 Variation of Deflexions with Proportional Changes in Areas	145
6.2.6 Variation of Deflexions with Individual Areas	147

	Page
6.3 Application to a Plane Frame	154
6.4 General Applications of the Theorems	157
6.5 Conclusions	158
CHAPTER 7 SHAPE AS A DESIGN PARAMETER	159
7.1 Introduction	159
7.2 Design for Optimum Shape	160
7.2.1 Assumptions	162
7.3 The Tactics of Geometrical Synthesis	163
7.3.1 Dominating Stress Constraints	163
7.3.2 Dominating Deflexion Constraints	167
7.3.3 The Preparation of the Benefit Vector	169
7.4 The Mathematical Programming	171
7.4.1 Determination of a Feasible Solution	173
7.5 The Design Procedure	178
CHAPTER 8 DESIGN STUDIES	181
8.1 Introduction	181
8.2 Hand Design	181
8.3 Design of Hanging Structures	185
8.4 Design of Trusses	190
8.5 Design Including Self Weight	193
8.6 Design of Cantilever Truss	196
8.7 Conclusions	199
CHAPTER 9 SUGGESTIONS FOR FURTHER WORK	200
REFERENCES	203
PUBLISHED WORK	206

CHAPTER 1INTRODUCTION

Maximum economy as a direct aim of structural design became a feasible proposition for research in the 1940s. This was brought about by the advent of better methods of analysis and the branch of mathematics called Operations Research together with the need, in the aerospace industry for minimum weight design methods. The digital computer, probably the most important single tool in optimum design, was also at this time becoming a commercial reality. The vast decrease in time required for calculations, that this augered, meant that the goal of designing real optimum structures was possible, if distant. It soon became obvious that many different optimizing techniques would be produced, some for general cases but most for specific problems, from which perhaps an optimum technique could be selected.

When embarking upon an optimum structural design, one of the first problems encountered is deciding upon a function which will evaluate the merit of any particular design. By far the most popular measure of merit has been the weight of the structural material involved as this seems to be reasonably straightforward. A more realistic function however would have to include factors accounting for construction and fabrication costs, savings intrinsic with standardisation and maintenance. The total merit of a structure even includes such seemingly unquantifiable items as functional value, aesthetic merit, scrap value, and it has been suggested that the expected cost of a failure, based on the probability of failure during the lifetime of the structure, be included.

There exists a range of methods of structural analysis which can be used to predict the behaviour of a particular design. The refinements of these methods have enabled the designer to have increasing confidence that successive analyses bear a reasonably close approximation to the actual behaviour of the structure. When this is the case a change in design based on a merit function judgement has a real meaning.

Having decided upon a suitable method of analysis, it became the object of the designer to place within the computer the production of trial designs, the merit evaluation of each, and, based upon these successive evaluations, the metamorphosis of the design from the input structure to the final optimum result without outside interference.

### 1.1 Historical Review of Optimum Design Methods

Optimality in the design of structures has attracted the attention of many research workers in recent years. However, one of the earliest mentions of weight in connection with structural frameworks was made by Maxwell (1) in 1869. Maxwell stated that for all frames, under a given system of applied forces, the member forces and lengths were related in the following relationship:

$$\sum_{i=1}^n p_i l_i = C \quad \dots 1.1$$

where  $p_i$  is the force acting in member  $i$  of length  $l_i$  in a pin jointed structure of  $n$  members. The constant term  $C$  was shown to be a function of the applied forces and the co-ordinates of their points of application.

Maxwell immediately realised the importance of this theorem to the engineer, arising from the fact that the strength of a member is, in general, proportional to its section. Following from this the strength

required of a member is proportional to the stress which it has to bear, so that its weight will be proportional to its stress multiplied by its length. Hence the sum of these products gives an estimate of the total quantity of material required by a framework to support the systems of external loads.

Maxwell pursued this no further and the fact lay dormant until 1904 when Michell (2) added that if  $\sigma_t^*$  and  $\sigma_c^*$  were the greatest tensile and compressive stresses allowable then the least volume  $V$  of material in a given frame consistent with safety could be obtained from

$$V = \sum l_t p_t / \sigma_t^* + \sum l_c p_c / \sigma_c^* \quad \dots 1.2$$

The first term in this expression refers to the tensile members of the framework and the second term to the compressive members. It is noticeable that this expression is merely the sum of the products of the lengths and sectional areas of the members. Manipulation of equations (1.1) and (1.2) revealed that in a statically determinate frame in which  $V$  was least, then

$$2 \sigma_t^* \sigma_c^* V + (\sigma_t^* - \sigma_c^*) C$$

was also least

$$\text{i.e.} \quad (\sigma_t^* - \sigma_c^*) \{ \sum l_t p_t + \sum l_c p_c \} \quad \text{was least}$$

$$\text{or} \quad \sum_{i=1}^n l_i |p_i| \quad \text{was least} \quad \dots 1.3$$

Michell then applied the principle of virtual work and stated that a frame attained the limit of economy of material possible in any framed structure under the same applied forces, if the space occupied by it could be subjected to an appropriate small deformation, such that the strains in all the bars of the frame were increased by equal fractions of their lengths,



not less than the fractional change of length of any element of the space. If the space subjected to the deformation extended to infinity in all directions, the volume of the frame was a minimum relative to all others, otherwise it was a minimum only relative to those within the same finite boundary. Planar frames were then produced using orthogonal curves, which were found to satisfy his stated requirements.

An example of a centrally loaded beam is given in Figure (1.1). A single force  $F$ , is applied at  $C$ , the middle point of the line  $AB$ , and is balanced by equal parallel forces at  $A$  and  $B$ . The minimum frame is composed of the two quadrantal bars  $DF$  and  $EG$ , having their common centre at  $C$ . Structural members also include all the radii of the quadrants, and their four tangents  $AD$ ,  $AE$ ,  $BF$ , and  $BG$ . The orthogonal system is indicated by the dotted lines and extends to infinity.

Michell showed that under each of the loading arrangements presented there was a unique geometry for the structure of absolute minimum weight. However, Michell's theory really gives an inverse design method in which a given orthogonal network provides an optimal design required by a specific loading condition. The method does not produce the net required by a specified loading system. Furthermore the theories are extremely limited in practical use, covering only pin-jointed statically determinate frameworks subject to a single load condition and stress criteria, with no side constraints on design variables. Deflexion criteria were not considered and it is difficult to include design considerations such as strut formulae and restriction on the number of bars or the effect of alternative loading cases.

The difficulties incumbent in overcoming these limitations were found to be insurmountable until better methods of analysis were available and as a result nothing was heard of maximum economy as a direct aim of structural design for many years.

### 1.1.1 Structural Optimization as a Linear Problem Using Linear Programming Algorithms

One of the earliest methods of analysis used to formulate the problem of optimum structural design was the rigid plastic theory. This was because of the ease to which it lends itself to formulate the equations of structural behaviour. Heyman (3, 4) tackled the problem by stating that the general state of a frame of "r" redundancies could be expressed as the sum of one arbitrary fixed equilibrium state and r linearly independent residual states. In this way, for stability, the bending moments at all cross-sections in the frame should satisfy

$$-M_p \leq M^* + c_1 M'_1 + c_2 M'_2 + \dots + c_r M'_r \leq M_p \quad \dots 1.4$$

where  $M_p$  is the relevant plastic moment,  $M^*$  is the basic equilibrium bending moment at the section,  $M'_1, \dots, M'_r$  are the linearly independent residual moments and  $c_1 \dots c_r$  are associated constants. Only concentrated loads were considered. As a result the bending moments throughout the frame varied linearly and the points of maximum bending moment coincided with the points of application of the loads. Inequalities of the type (1.4) were written for every critical section and the fully plastic moments solved using Dines' method to minimize the weight of the frame which Heyman assumed to be proportional to the product of member length and plastic moment value.

In a similar manner to Heyman, Foulkes (5, 6) assumed a continuous range of selection was available for the design parameters, which were again the member plastic moments, and that the weight of a section was linearly related to these design parameters. The merit function to be minimized was therefore once again given by

$$z = \sum_{i=1}^n l_i M_{p_i} \quad \dots 1.5$$

The constraints of the problem were formed using the virtual work equations associated with rigid-plastic mechanisms. The result was that for a design to be allowable then for every possible mechanism

$$\frac{\sum_i M_{p_i} \beta_{ij}}{\sum_v W_v \delta_{vj}} \geq \lambda_p \quad \dots 1.6$$

where  $M_{p_i}$  is the fully plastic moment of member  $i$ ,  $\beta_{ij}$  is the total rotation in that member for mechanism  $j$ ,  $W_v$  is an applied load at location  $v$ ,  $\delta_{vj}$  is the distance  $W_v$  moves through for mechanism  $j$  and  $\lambda_p$  is the allowable load factor for collapse.

This problem could be solved using linear programming techniques such as the simplex method, however, it was soon realised that in any but the simplest frames the construction of the constraints would become very lengthy due to the number of conceivable collapse mechanisms. Added to this problem would be the possibility that perhaps the critical mechanism had been overlooked which tended to undermine the confidence in any result obtained.

Livesly (7) also formulated the problem in a linear manner using the theory of plastic collapse and assumed that the structure was only acted upon by concentrated forces. In a given problem therefore, there was only a fixed set of points in the structure at which plastic hinges would occur. This was because the maximum bending moment in each member occurred either at an end or at a point where a load was applied. The set of points at which plastic hinges could occur was then subdivided into smaller groups, each group corresponding to points at which the member cross-sections were known to be equal due to practical considerations.



With a frame having  $r$  redundancies the equations of equilibrium were expressed as follows

$$\underline{M} = \underline{a}_i \underline{m}_i + \underline{M}^0 \quad \dots 1.7$$

A certain length of member was associated with each group and by multiplying equation (1.7) by this length a similar expression for the weighted moments was obtained to be

$$\underline{N} = \underline{A}_i \underline{m}_i + \underline{N}^0 \quad \dots 1.8$$

The matrices  $\underline{a}_i$  and  $\underline{A}_i$  depended only on the geometry of the frame, while the column vectors  $\underline{M}^0$  and  $\underline{N}^0$  depended also on the applied loading. The vector  $\underline{m}_i$  was the vector of redundant moments. The fully plastic moments selected for the members, capable of supporting the induced moments  $\underline{M}$ , were to satisfy the inequality

$$M_{p_g} \geq \max_j |M_j| \quad \dots 1.9$$

where  $M_{p_g}$  was the fully plastic moment of group  $g$  and the right hand side of the inequality represents the modulus value of the maximum moment occurring in group  $g$ . An inequality of this type was associated with each group. The lightest structure would thus be the one in which the above inequality (1.9) held in every case. The total weight of the structure was once again assumed to be given by equation (1.5) which may be re-written here in terms of the weighted moments as

$$z = \sum_g \left( \max_j |N_j| \right) \quad \dots 1.10$$

If a set of  $\underline{m}_i$  can be found which minimizes this function then the associated critical design which is given by equation (1.9) will be the least weight structure.

Using this method Livesley was able to produce a computer program to design frames, which supported loads entirely by the bending action of members, with a capacity of 32 moment points and 16 redundancies. It was suggested that, although only one load case could be considered without deflexion limitations, the method of solution was so rapid and automatic that it could supply a rough guide in the initial stages of design work.

Since the work of Michell it was concluded that the stresses in the members of a determinate truss must be at their limiting values for the weight of the structure to be a minimum. This concept of a fully stressed or a simultaneous failure mode design has been of prime importance and is valid for a large class of applications. However if extensions were to be added to the basic problem such as multiple loading conditions, side constraints on design variables and deflexion constraints, the fully stressed concept would lead to erroneous results. Kicher (8) examined the relationship between the minimum weight design and the simultaneous failure modes design using simple linear-elastic structural systems and a Lagrange multiplier technique for minimization. The structural constraints were generally of the type

$$G_j(x_i) \geq T_j \quad \dots 1.11$$

where  $G_j(x_i)$  was a function of the design variables defining a particular mode of behaviour which was restricted by the scalar quantity  $T_j$ . These constraints were transformed into equalities through the addition of slack variables  $v_j$  in the following manner

$$G_j(x_i) - T_j - v_j^2 = 0 \quad \dots 1.12$$

Using Lagrangian multipliers,  $\lambda_j$ , these equality constraints were then incorporated into a function, that was extremised in order to minimize the weight function  $z(x_i)$ , giving

$$F(x_i, \lambda_j, v_j) = z(x_i) - \sum \lambda_j [G_j(x_i) - T_j - v_j^2] \quad \dots 1.13$$

The values of the associated Lagrangian multipliers gave a method of determining which are the active constraints at the optimum result. This was because when  $\lambda_j \neq 0$ , the corresponding constraint became active.

Using this technique Kicher was often able to determine beforehand which constraints would control the minimum weight design. Together with other researchers Kicher came to the following conclusions concerning the nature of optimum structures:

- (1) The minimum weight designs of a large class of structural systems subject to a single load case are indeed fully stressed.
- (2) The minimum weight designs of statically determinate trusses, with stress limitations only, are governed by at least as many constraints as there are members. That is, the stress in each member must be at its bound in at least one load condition.
- (3) The minimum weight designs of structures that are subjected to a multiplicity of load conditions and are statically indeterminate or have buckling modes dependent on the load conditions will not, in general, be fully stressed.

The majority of early work carried out on optimum design for civil engineering structures made use of the rigid-plastic theory and as a result did not allow for any control over the deflexions of the minimum weight structure. The limitation of deflexion, however, is of prime importance in the design of many structures, particularly sway frames. Rubinstein and Karagozian (9) introduced facilities to control deflexions in the rigid-

plastic minimum weight design of tall frames by simply assuming, from experience, that 60% of the sway deflexion of frames was due to beam flexibility. The plastic moments of the beams were assumed to vary linearly throughout the storeys of the frame and mechanisms were formed only due to collapse in the beams. Virtual work equations for the various mechanisms were used to form the strength constraints. The deflexion constraints were then formulated in terms of the energy of the beams. The simplex method of linear programming was used to make the optimum selection of plastic moments for the beams and having located the appropriate collapse mechanism suitable sections were chosen for the columns.

This offered a rational preliminary design of multistorey framed structures. However there was no limitation on the amount of sway deflexion due to the column flexibility which could render deformations greater than desired. Furthermore, being based upon rigid plastic mechanisms, safety was not ensured for frames in which instability was significant.

A more rigorous method of including controls over the deflexions of frames during optimisation was developed by Majid and Anderson (10) using a technique of piece-wise linearisation mentioned by Hadley (11). The matrix force method of structural analysis was used to formulate the constraints as this would yield only as many deflexion equations as loading positions. The resulting non-linear constraints were found to contain terms of the type  $l/A$ ,  $l/I$ ,  $R/A$  and  $R/I$ , where  $A$  and  $I$  were respectively the area and second moment of area of the various member groups. The quantity  $R$  represents the redundant forces throughout the frame which were themselves unknown being dependent upon the sectional properties. The variables  $A$  and  $I$  were not independent and therefore one could be removed by expressing it in terms of the other. When designing pin-jointed frames,

however, the members were assumed to deform in an axial manner. In this way bending was ignored and the constraints only included terms of the type  $1/A$  and  $R/A$ . Similarly when considering the design of sway frames it was found convenient to neglect axial deformations compared with those due to bending and as a result the constraints only included functions with terms of the type  $1/I$  and  $R/I$ .

Before carrying out piece-wise linearisation it was necessary to make substitutions into the constraints in order to separate the variables. These substitutions necessitated the inclusion in the design problem of additional constraints adding to its complexity. Two different linearisation techniques were used, but in both methods the original non-linear function is split into  $p$  segments and replaced by a piece-wise linear function which coincided with the original function at  $(p + 1)$  positions.

The Minit method of linear programming developed from the simplex algorithm was originally used to solve the resulting approximated linear problem. This method, however, was unsuitable for non-convex problems as it resulted in cycling between non-feasible local optima. The problem was finally solved using the simplex method as the solutions obtained throughout this procedure are feasible. However, considerable computation was found necessary. Although a guarantee of a local optimum was available within certain limitations, the method employed included facilities to leave a local optimum and search for a better one. This minimum weight design method was found to be applicable only to small bare frames. The restriction of frame size was due to the technique of piece-wise linearization which required a considerable amount of computer time and storage to obtain a solution. The accuracy of the solution depended upon the number of segments into which the non-linear functions were divided for linearization. This had the drawback that the additional constraints introduced



into the problem required large computer storage facilities.

Several researchers have proposed using first order Taylor series approximations to the constraint functions in order to define a linear programming problem which, in the neighbourhood of the current best solution, would approximate to the non-linear problem. This forms the basis of the cutting plane method which was used by Moses (12) to optimize the design of linear elastic structures subject to separate loading cases with deflexion as well as stress limitations. At each design point, defined by the vector of variables  $\underline{x}^q$ , the structural optimisation was transferred from the non-linear form of the type:

$$\left. \begin{aligned} &\text{minimize } z(x_i) \\ &\text{subject to } G_j(x_i) \leq T_j \\ &\text{and } x_i^o \leq x_i \leq x_i^u \\ &i = 1, 2, \dots, n \quad j = 1, 2, \dots, m \end{aligned} \right\} \dots 1.14$$

to the linear form of the type

$$\left. \begin{aligned} &\text{minimize } z(x_i^q) + \sum_{i=1}^n \frac{\partial z(x_i^q)}{\partial x_i} (x_i - x_i^q) \\ &\text{subject to } \sum_{i=1}^n \frac{G_j(x_i^q)}{\partial x_i} (x_i - x_i^q) = 0 \\ &\text{and } x_i^o \leq x_i \leq x_i^u \\ &j = 1, 2, \dots, m \quad i = 1, 2, \dots, n \end{aligned} \right\} \dots 1.15$$

a first order Taylor series approximation. In these formulations the terms  $x_i^o$  and  $x_i^u$  were respectively the lower and upper bound values of the  $i$  th design variable, and the term  $x_i^q$  represented the  $i$  th variable at the  $q$  th design point. The total number of variables was  $n$  and the total number of constraints  $m$ .

A solution was found to the linearised problem of equations (1.15) using the simplex method. However, this did not necessarily satisfy the original non-linear constraints of equations (1.14) and thus might have necessitated an all round uniform increase of the design variables to render the solution acceptable. This entire procedure was then repeated at the current acceptable design point and the process continued until successive designs yielded the same value for the merit function.

The computational effort involved in procedures of this type was increased only modestly as the size of the structural design increased. This was provided that the additional constraints were linear or nearly so. The method, however, showed to be efficient with only a few non-linear constraints. This was due to the increasing likelihood of obtaining an unfeasible design from the linearised problem, which in turn necessitated an increase in the weight of the structure.

Toakley (13) introduced limitations on the deformed shape of a structure using both rigid plastic and elastic methods of analysis. By assuming an initial deformed shape an optimum rigid plastic design was obtained. This was then analysed using an elastic plastic analysis program developed by Jennings and Majid (14) to determine the actual deformations, and axial forces in the members. The constraints were then reformulated using the new deformed shape and a further rigid plastic optimum design was obtained.

This procedure continued until two successive designs were identical at which point discrete sections were selected for the members with plastic moments greater than those corresponding to the optimum design achieved. This however did not guarantee, in all cases, that the final design would not collapse due to instability before the required load factor was reached.

The problem of discrete section design as opposed to a design which assumes that a continuous spectrum of member sizes is available was also tackled by Toakley (15). It was stated that even though selection of the next largest available section might lead to a design satisfying the constraints it did not follow that it would be the optimum design when discrete sections were assumed.

In the case of statically determinate frameworks the problem was expressed using a dummy unit load method as

$$\begin{array}{l}
 \min z = \sum_i \sum_j L_i A_{ij} \delta_{ij} \\
 \text{where } \sum_j \delta_{ij} = 1 \\
 i = 1, 2, \dots, n \\
 \text{subject to the deflexion criteria} \\
 \frac{1}{E} \sum_q p_{iq} P_{kq} l_q \sum_j \sum_r \delta_{jr} / A_{jr} \leq T_i \\
 \text{and stress criteria} \\
 \sum_j A_{ij} \delta_{ij} \geq |P_{kq} / \sigma_{kq}|
 \end{array} \quad \left. \begin{array}{l} \\ \\ \\ \\ \\ \\ \end{array} \right\} \dots 1.16$$

where  $A_{ij}$  is the  $j$ th section specified for area group  $i$  and  $\delta_{ij}$  are 'zero-one variables' in that they may take values of only zero or one in the final solution. The total length of members to be made up from section  $i$  is  $L_i$  whereas the length of an individual member  $q$  is  $l_q$ . The force in member  $q$  under load system  $k$  is  $P_{kq}$  and the force in this same member due to a unit load at node  $i$  is  $p_{iq}$ . The quantity  $\sigma_{kq}$  is the allowable working stress in the member under load system  $k$ , while  $E$  and  $T_i$  are respectively Young's modulus for the material and the maximum value for the deflexion at node  $i$ .



When designing rigid jointed frames the problem was formulated in a manner very similar to Livesley using rigid plastic theory. If  $M_{p_{ij}}$  is the fully plastic moment of the  $i$  th section possible for group  $j$ ,  $w_{ij}$  is the weight per unit run of that section and there are  $v$  possible sections for group  $j$  then the following relationship expresses  $M_{p_j}$  the plastic moment of group  $j$  at any instant

$$M_{p_j} = \sum_{i=1}^v M_{p_{ij}} \delta_{ij} \quad \dots 1.17$$

where once again  $\sum_{i=1}^v \delta_{ij} = 1$

and the objective function becomes

$$\min z = \sum_i \sum_j L_j w_{ij} \delta_{ij} \quad \dots 1.18$$

To solve these mixed integer continuous variable programming problems Toakley devised a method which involved the use of Gomory's Algorithm (16).

A search method was also proposed based on the fact that there were a fixed number of different possible designs and that an upper and lower bound on the objective function could be obtained. Each design falling between these limits was analysed, and if feasible, gave a new upper bound solution. Repetition eventually led to an optimum design when all possible designs had been considered.

This method was satisfactory, for discrete variable minimum weight design, provided that there were few integer variables. Otherwise Gomory's algorithm had to be used to solve the problem. This algorithm, however, suffered from numerical drawbacks and convergence to the optimum was only certain in simple cases.

By using an elastic analysis program developed by Jennings and Majid (17) to evaluate the axial forces in a frame and the unit load method to determine joint displacements, Toakley (18) was able to produce a fully automatic procedure for the minimum weight design of statically determinate pin jointed space frames subject to deflexion controls. The deflexion constraints were linearised by a substitution of the type

$$x_i + 1/A_i^u = 1/A_i \quad \dots 1.19$$

where the unknown area sectional properties  $A_i$  are replaced by variables  $x_i$  in the programming problem.  $A_i^u$  is an upper value for the area of the  $i$ th area group. As a result of this the objective function became non-linear of the form

$$z = \sum_i L_i / (x_i + 1/A_i^u) \quad \dots 1.20$$

This function however was shown to be strictly convex and a global optimum was obtained using a non-linear programming technique such as piece-wise linearisation.

### 1.1.2 Structural Optimisation using Non-Linear Programming

In general all of the previously described methods approximate the basic non-linear problem of optimal structural design to a linear one that can be solved by means of a linear programming technique such as the simplex method. There are however algorithms which treat the various constraints in their basic non-linear form and as a result can provide greater generality and flexibility. Such methods come under the headings 'hill climbing techniques', 'gradient projection', 'methods of steepest descent' or 'methods of feasible directions'. These are sequential design

methods which generate a new trial design based on the results of an analysis of the previous trial design so as to minimize the objective function. They all have in common a basic equation which is repeatedly employed to generate the  $(q + 1)$ st design point from the  $q$ th design point

$$\underline{x}^{q+1} = \underline{x}^q - \lambda \underline{\delta x}^q \quad \dots 1.21$$

where  $\underline{x}^{q+1}$  and  $\underline{x}^q$  are vectors containing the values of the design variables at the  $(q + 1)$ st and  $q$ th design points respectively. The vector  $\underline{\delta x}^q$  defines the direction of travel within the design space and  $\lambda$  is the distance to be travelled in this direction in a single step.

The methods that are proposed for locating the optimum design differ only in the methods that are used to determine which way to go in the design space, that is when obtaining the direction vector  $\underline{\delta x}$ , and when deciding how far to move in this direction,  $\lambda$ . There are techniques which modify the design in a relatively undirected manner making little use of the properties of the current trial design apart from whether it is feasible or non-feasible. On the other hand there are highly directed algorithms hoping to reduce the number of iterations required for location of the optimum by making much use of the properties of the current trial design to give each re-design an optimum significance.

The methods of analysis which are employed for any particular design are only dependent upon the type of structure or the wishes of the designer. These may include items such as stress, deflexion and buckling under a multiplicity of loading cases.

Schmit and Kicher (19) used a steepest descent algorithm to compare the optimum designs of various configurations of a three bar truss subject to several load cases with limitations on member stress and truss

deformations. This method of search comprised two stages. In the first stage, applicable when the current trial design lay inside the design space, was a steepest descent mode of search which reduced the value of the objective function at the greatest possible rate. To achieve this the direction vector  $\underline{\delta x}$  of equation (1.21) was made up of elements  $\delta x_i$  such that

$$\delta x_i = \partial z / \partial x_i \quad \dots 1.22$$

where  $z$  was, once again, the function to be minimized and represented the weight of the structure. This direction was pursued until a trial design was obtained having at least a single behaviour property on the verge of violation. At this point the second stage of the process was initiated. Movement in this stage maintained the weight of the structure constant and attempted to improve the feasibility of the design. The problem under consideration was one of three variables and the constant weight direction vector was chosen from three predetermined possibilities made up from elements of the type

$$\delta x_{ij} = x_i - \frac{z I_{ij}}{\partial z / \partial x_i} \quad \dots 1.23$$

$$i = 1, 2, 3 \quad j = 1, 2, 3$$

where  $I_{ij}$  is the relevant element of a unit matrix. The element  $\delta x_{ij}$  represents the  $i$ th element of the  $j$ th possible constant weight direction vector. These three possible directions of travel were chosen arbitrarily and each one of them defined movement from the current boundary design point toward one of the three co-ordinate axes of the design space.

Each of these vectors was considered in turn to calculate a possible value of the step length  $\lambda$ . To do this a series of polynomials was formed which expressed the behaviour of the structure as a function of

the distance of travel . When solved individually the polynomials gave the distances of travel to the corresponding constraint hyper-surfaces. The first real root that resulted from the solution of these polynomials that satisfied all the constraints within a tolerance and yielded a significant change in the design variables was selected as  $\lambda$ . Should the first direction vector fail to yield such a value, the second was considered, and if after consideration of the third direction vector no  $\lambda$  was available the process was terminated.

In this investigation a linear elastic analysis technique was employed and it was found that a weight saving could be made if the correct selection of material and frame configuration was chosen. Also an entirely different optimum design could be chosen from the available individual optimums with a slight alteration of design specifications.

Schmit and Morrow (20) added to this basic problem buckling constraints and found that the optimum configuration of the members became more rigid and the member materials tended to be of lighter weight. The optimum solution however, was still obtained by comparison of several trial three bar frameworks and the design problem remained one of three variables.

The steepest descent mode of the search procedure remained the same as the previous investigation, however when in the constant weight mode of travel three additional predetermined direction vectors were added to the three previously employed. Each of these vectors indicated a direction, maintaining constant weight, parallel to a co-ordinate axis.

As before each possible direction vector was considered in turn until a feasible distance of travel  $\lambda$  was obtained. Solving all the roots of all the equations, formed to express the behaviour of the frame in terms of the step size, however was already found to be laborious. A more



efficient method using Sturms functions and the Newton-Raphson method was therefore developed to obtain only the two most probable roots in alternative directions of travel. This necessitated an initial approximation of the two roots as being the distances to the nearest lower bound and upper bound constraints. The constraint equations were then successively checked until one was found that would be violated by one of the current possible step lengths. This constraint was then solved by refining the approximation using Sturms functions and the Newton-Raphson method. The root achieved in this manner replaced that which was responsible for the violation and the process was continued until all the equations had been checked. Should both roots thus obtained have represented an insignificant change of the design variables the next constant weight direction vector was considered, and so on, until an acceptable root was obtained or, failing this, the process terminated.

In Multi-dimensional design spaces this method of step length determination soon becomes time consuming as the constraints are highly non-linear. As a result Schmit and Mallet (21) investigated an accelerated incrementation technique for step lengths without knowledge of actual boundary distances. A further new innovation entailed the introduction of a design parameter hierarchy. This made it possible for the decisions regarding configuration of a truss and the materials of its members to be made during the searching procedure in an automatic fashion. This additional facility increased the size of the three bar truss problem to one of nine variables. These were the material densities  $D$ , member areas  $A$ , and the angles of inclination of the bars  $\phi$ . The weight function to be minimized therefore became non-linear and of the form

$$z = \sum_{i=1}^3 d D_i A_i / \sin \phi_i \quad \dots 1.24$$

where  $d$  is a constant depending on the size of the frame.



Due to the fact that the formulation of the design problem included density as a variable it was necessary to obtain expressions for Young's modulus and the maximum allowable stresses in terms of this variable as both are dependent upon it. This was done by fitting a curve to the series of points obtained when plotting these properties against the density of a range of known materials. The process assumed that a continuous spectrum of materials was available and the expressions obtained were non-linear. Due to these substitutions the design problem yielded a set of highly non-linear constraints with a non-linear objective function.

Once again, to solve this problem successive trial designs were generated by a method of alternate steps. The direction of steepest descent employed was much the same as before but the alternate step of constant weight used a modified random direction. The formula of design generation as given by equation (1.21) was also modified. In the case of steepest descent this became:

$$\underline{x}^{q+1} = \underline{x}^q - 2^j \lambda \underline{\delta x}^q \quad \dots 1.25$$

$j$  being an integer, of zero initial value, which was incremented in value by one when the current trial design was feasible, and where  $\lambda$  was the smallest step length which yielded a significant change in the design variables.

When this particular mode of travel yielded an infeasible design the previous trial design was examined for its proximity to the constraints. In the case of an interior point of the design space a new steepest descent direction vector was obtained using the properties of the objective function at this point. The integer  $j$  was once again set to zero and the new direction pursued. This process was continued until a feasible set of parameter values was achieved representing a design lying near the boundary

of the acceptable design space. At this stage a sideways step was taken into this space before the steepest descent mode was once again employed. The sideways step was represented by the formula

$$\underline{x}^{q+1} = \underline{x}^q + \underline{\delta x}^q \quad \dots 1.26$$

The vector  $\underline{\delta x}$  represented distance and direction and was formed by modifying a set of generated random numbers to allow for near active design variable limits. The relative magnitudes of the various types of design variables, the length of the step size to be taken and the constant weight condition also affected this vector.

The use of this technique in association with the three bar truss required, on average, approximately 300 redesign attempts to reach a point after which successive redesigns were of the same weight. Once having located a boundary the search was found to essentially follow the boundary to the optimum point, a feature of the gradient projection method.

Brown and Ang (22) found that the gradient projection method of non-linear programming, developed by Rosen (23) for the solution of general mathematical models, could be adapted for the requirements of structural design optimisation. Rosen's method was applied to the problem of the least weight elastic design of rigid frames with a non-linear, non-dimensional objective function of the form

$$z = \frac{1}{z_0} \sum_i L_i w_i \quad \dots 1.27$$

where the weight per unit run  $w_i$  of the material used by group  $i$  was given by a non-linear function of the design parameters which were the moments of inertia of the various member groups. The quantity  $z_0$  represented the weight of a reference design.

Once again the formula that generated a design from a previous trial design is given by equation (1.21). From an initial feasible design the gradient of the objective function was followed until a boundary design was achieved. At this point the direction or gradient vector  $\underline{\delta x}$  was modified so as to move along the gradient of the design space boundary while further decreasing the weight of the structure. If the current boundary was concave, movement of this type resulted in an infeasible design. This was then modified to bring it back into the acceptable region. In the gradient projection method, as described by Rosen and Hadley, techniques were given to obtain an optimum step length to be taken in the current direction of travel. However, in Brown and Ang's investigation it was found more convenient to use a constant step length  $\lambda$  given by

$$\lambda = 0.01 \sqrt{\sum_i (x_i^u - x_i^o)^2} \quad \dots 1.28$$

where  $x_i^u$  and  $x_i^o$  are respectively the upper and lower bound values imposed on the  $i$  th design variable. The boundary points from which to project gradients were obtained by interpolation between current feasible and non-feasible designs.

This method provided a sound mathematical basis on which to develop a rational design method. However, the search procedure may, by following the boundary, be trapped into a local optimum by dominating local features of the design space. To overcome this inability to move into the feasible area it was necessary to commence a design at several initial design points and to compare the various solutions obtained.

Schmit and Fox (24) used a steepest descent type algorithm with an integrated analysis-synthesis concept. This method formulated the problem as an unconstrained minimization in a design space. Each point, as well as representing a set of values for the design variables, also

represented values for the behaviour variables such as stresses and deflexions. In the previous non-linear studies a proposed design was generated and this was followed by an analysis that gave the values of the behaviour variables. The integrated approach however sought an improved design and acceptable values of the behaviour variables simultaneously. The procedure was based on the fact that a set of simultaneous equations can be solved by finding the minimum of a function that is made up from the squares of the residuals of the algebraic system. Mathematically if the following algebraic system defines the analysis of a structure

$$\begin{bmatrix} L_1 \\ L_2 \end{bmatrix} = \begin{bmatrix} K_{11} & K_{12} \\ K_{21} & K_{22} \end{bmatrix} \begin{bmatrix} X_1 \\ X_2 \end{bmatrix} \quad \dots 1.29$$

then the unknown behaviour parameters  $X_1$  and  $X_2$  which satisfy these equations, the rest being known, may be found by minimizing the following function

$$z_1(X_1, X_2) = (K_{11}X_1 + K_{12}X_2 - L_1)^2 + (K_{21}X_1 + K_{22}X_2 - L_2)^2 \quad \dots 1.30$$

In the actual design problem  $L_1$  and  $L_2$  represented the loads applied to a structure and the  $K$  terms were elements of the overall stiffness matrix relating deflexions and applied loads. These latter terms were themselves functions of the design variables. Equation (1.30) was adapted so that the  $K$  terms are included as variables in the following manner

$$\begin{aligned} z_2(X, K) = z_1 + \sum_j \{ \{X_j^o - X_j\}^2 + \{X_j - X_j^u\}^2 \} \\ + \sum_i \{ \{K_{ij}^o - K_{ij}\}^2 + \{K_{ij} - K_{ij}^u\}^2 \} \end{aligned} \quad \dots 1.31$$

where  $X_j^o$  and  $X_j^u$  are respectively the lower and upper bounds of the  $j$  th behaviour variable and  $K_{ij}^o$  and  $K_{ij}^u$  are respectively the lower and upper bounds of the element  $K_{ij}$  in the stiffness matrix. The significance of

the curly brackets in this context was defined by

$$\{D\}^o = \begin{cases} 0 & \text{if } D \leq 0 \\ 1 & \text{if } D > 0 \end{cases} \quad \dots 1.32$$

and

$$\{D\}^n = D^n \{D\}^o \quad n > 0 \quad \dots 1.33$$

Before explaining the action of this further, it is convenient to state the final unconstrained minimization problem. Given the terms  $L_i$ ,  $X_j^o$ ,  $X_j^u$ ,  $K_{ij}^o$  and  $K_{ij}^u$  together with an initial structure of weight  $W_o$  the problem was that of finding the design variables  $x_i$  and behaviour variables  $x_j$  that minimized the following expression

$$z_3(x, X) = \{W - W_o\}^2 + z_2(X, K) \quad \dots 1.34$$

where  $W$  is a function expressing the weight of the structure in terms of the design variables. After each steepest descent step of the optimization algorithm,  $W_o$  was replaced by the current weight of the structure. Successive steepest descent steps were taken until a weight  $W$  was achieved for which it was impossible to minimize the function  $z_3$  further. Should any variable during the course of the optimization, whether a design or a behaviour variable, wish to exceed its allotted limits the action of the curly brackets in equation (1.31) would automatically penalise  $z_3$ . This also applied should an attempt be made inadvertently to increase the weight of the structure at any stage.

This method of search seemed to suggest that the integrated design approach could improve the efficiency of locating an optimum design. It had, however, the drawback, in common with many of the other methods



described, that it might only be applied to individual designs, and not in a general fashion. Even this was only possible after a considerable amount of tedious algebraic manipulation by the designer.

As an alternative to the foregoing iterative approaches, Palmer (25) utilized the method of dynamic programming, developed by Bellman (26), to optimize the design of structures to which the lower bound theorem of plastic theory applied. He developed a sequential design method based on the construction of statically admissible force fields. The structure to be designed was split into convenient segments and the cost of each segment was then expressed as a function of variables which defined the interaction between segments. The values of the moments at each end of the segments could be such variables. In this way the total cost of a structure divided into  $n$  segments became

$$z_n(m) = \sum_{i=1}^n \{g_i(m_{i-1}, m_i)\} \quad \dots 1.35$$

where  $g_i(m_{i-1}, m_i)$  was the function representing the cost of the  $i$ th segment expressed in terms of the moments  $m_{i-1}$  at its first end and  $m_i$  at its second end.

To evaluate the minimum of this function the following procedure was carried out. The end condition  $m_0$  of the structure as a whole was assumed to be known and the range of costs of the first segment for a finite range of end conditions  $m_1$  was obtained. That is, all possible values of  $g_1(m_0, m_1)$  were evaluated giving all possible costs of the first segment. Following this each value of  $m_1$  was taken in turn as a possible first end condition of the second segment. All the values of  $m_2$ , the second end condition, were then used to evaluate every possible value for  $g_2(m_1, m_2)$ . This resulted in  $s^2$  possible costs for the first two segments,



where  $s$  is the number of finite values into which each end condition was divided. The  $s$  combinations of  $m_1$  and  $m_2$  which yielded minimum cost for each  $m_1$  were represented by

$$z_2(m_2) = \min_{m_1} \{ g_2(m_1, m_2) + z_1(m_1) \} \quad \dots 1.36$$

where  $z_1(m_1) (= g_1(m_0, m_1))$  represented the costs of the first segment alone. Each of these  $s$  optional combinations of  $m_1$  and  $m_2$  was now taken in turn with all values of  $m_3$ . The  $s$  combinations of  $m_1$ ,  $m_2$  and  $m_3$  which yielded minimum cost for each  $m_2$  were represented by

$$z_3(m_3) = \min_{m_2} \{ g_3(m_2, m_3) + z_2(m_2) \} \quad \dots 1.37$$

giving all the optional costs of the first three segments.

This process was continued until all  $n$  segments had been considered. The  $s$  possible optimal structures, given by

$$z_n(m_n) = \min_{m_{n-1}} \{ g_n(m_{n-1}, m_n) + z_{n-1}(m_{n-1}) \} \quad \dots 1.38$$

were then obtained, from which the actual optimum cost could be chosen by comparison. The actual optimum policy, as regards end moments, was selected by tracing back through the successive stages the various values of the moments, and the associated optimal design then followed. Simple enumeration of all possible combinations of the end moments would have required  $s^n$  calculations of the cost of the complete structure, but using dynamic programming reduced this to  $s + (n-1)s^2$  calculations. This algorithm seemed to be ideally suited for a computer, depending on simple operations which are repeated many times. The method was only efficient however when the inter-action between different segments of the structure could be described

by a relatively small number of variables. This was due to the fact that a minimization process was carried out at each stage. Should too many variables be involved the computation time may become unacceptably long. This is due to the fact that each of the variables is divided into a finite range of possible values, and that every possible combination of variable values, at every stage, is evaluated for minimization purposes.

### 1.1.3 Structural Configuration as a Design Variable

In all of the previously cited investigations, except that of Michell, the structural design was given beforehand apart from the problem of sizing the already present members. The following studies are specifically concerned with the problem of design in a broader sense, where both the location as well as the sizes of the members are to be determined for an optimum design.

Pearson (27) developed a technique based on expressing the forces in all the members in terms of the unknown forces in a set of redundant members. This was followed by random variation of the design variables to determine the successive steps necessary to minimize the weight function. In this way it was found that the redundant members were absent from the optimal design when subject to a single set of loads. This result, in a limited sense, constituted a selection of members as well as sizes.

The approaches of Hemp (28) and Chan (29) were based on the Michell theory. The continuum of space, however, was replaced by a mesh of discrete points at which structural joints might occur. Structures were assembled by pin-ended members each connecting two of these nodes. The structure of minimum volume was considered to be that which maximized the virtual work of the external forces provided that at no point in the structure did strains exceed their maximum allowable value. This concept

was expressed in linear programming form as follows

$$\max z = \underline{L}' \underline{X} \quad \dots 1.39$$

$$\text{subject to} \quad \varepsilon \underline{1} \leq \underline{A} \underline{X} \leq \varepsilon \underline{1}$$

where  $\underline{L}$  was a column vector of the applied loads and  $\underline{X}$  was a column vector containing the vectorially equivalent nodal displacements. The matrix  $\underline{A}$  depended on the geometry of the frame and related the joint displacements with the member extensions. The limiting values of these extensions were obtained by premultiplying the vector of member lengths  $\underline{1}$  with a scalar equal to the maximum permissible strain  $\varepsilon$ .

Dorn, Gomory and Greenberg (30) also treated the topology of pin-jointed frames as a design variable. This was achieved by optimizing over a wide class of possible structures whose elements were all selected from a prescribed admissible set. The problem was once again formulated as a linear program and it was found by interpretation of the dual problem that minimizing the weight was equivalent to maximizing the work done by the external loads. The simplicity of the design problems that were attempted however contrasted with the size of the solution that was necessary.

Palmer and Sheppard (31) found dynamic programming a useful tool when optimizing the geometry of a pin-jointed cantilever truss, making it possible to include member inclination as a design variable without excessive calculation. This was due to the fact that the problem was expressed as a design sequence involving only a few variables at each stage. The statically determinate cantilever considered was subjected to a single point load only and divided into a series of links. The cost of each link was then expressed as a function of the forces acting on the link, as well as the co-ordinates of the points at which they acted. The topology of the

cantilever was fixed beforehand but the geometry was optimized by assuming a range of finite positions that each joint could assume. Only stress constraints were considered so that having obtained the final geometry the sectional properties necessary for the members were readily available. Although only one example was considered the results obtained from this investigation represented a considerable weight saving over conventional geometries. This was found to be the case when both a continuous range of sections, and a discrete set of sections was assumed available.

As described earlier Schmit and Mallet included structural geometry as a continuous variable by introducing the angles of inclination of the members of a truss into a design parameter hierarchy. Once again the topology was considered fixed beforehand but a steepest descent algorithm was used to obtain the optimum configuration which remained statically indeterminate throughout.

Dorn, Gomory and Greenberg obtained geometrical configurations for planar trusses subject to a single set of loads. Trusses optimized under these conditions, without deflexion limitations, were found to be statically determinate and therefore fully stressed. In general, however, trusses may be designed for multiple sets of loads and an optimal structure need be neither statically determinate or fully stressed.

When dealing with a more general case Dobbs and Felton (32) found it mathematically convenient to use non-linear programming. The nodal pattern concept was adopted to obtain an initial structural configuration as being that where each node was connected to every other node by a member. This made the initial structure highly redundant. The steepest descent algorithm was used to repeatedly readjust the member areas in an attempt to reduce the overall weight. During this process certain cross-sectional areas approached zero value. The corresponding members were removed from

the structure after each steepest descent mode of the algorithm never to re-enter the design. In this way the topology of the truss was reduced until an optimum was achieved.

From the series of trusses designed in this investigation it was found that, even under several loading conditions, the optimum structural configuration was statically determinate. In reality, however, it is clear that this is not the case when a non-optimal nodal pattern is chosen for the initial structure. The inclusion of deflexion constraints may also force the optimum structure to be statically indeterminate.

Most of the above workers did not specify whether a rigorous investigation had been carried out to prove that either, the designs obtained were global optima or, indeed, local optima. The majority neglected deflexion limitations entirely and many concentrated on statically determinate structures. Finally when designing for optimum structural shape, in every case, it is either the geometry or the topology of the frame that is varied, but never both.

## 1.2 The Scope for the Present Work

It has been demonstrated that the minimum weight design of frames by the simple plastic theory can be made into a linear programming problem by introducing a number of simplifying assumptions. However, if any other structural theory is used, or if stress and deflexion limitations are taken into consideration, the programming problem becomes non-linear.

A frame which satisfies strength requirements may be unsatisfactory due to the development of unacceptable deflexions at the working load level. When both stresses and deflexions are to be restricted in an elastic frame, non-linear programming techniques can be used to obtain a minimum weight



design. Previously developed methods have not resulted in an automatic optimum design procedure for general statically indeterminate structures.

When producing successive trial designs of a frame suitable estimates must be made of the required section properties, if the design time is not to be excessive. A 'Dynamic Search' method of non-linear programming is presented in Chapter 2 that improves the feasibility and the optimality of the design simultaneously. This method is used to design, for minimum weight, a family of fixed base pitched roof frames for which the elastic deflexions are restricted by B.S.449.

The method is used to produce design charts which are presented and can be used directly for design purposes. These can be used to select the optimum pitch of a frame and optimum sections for the members. A method is given to make use of the fact that a continuous set of sections is not available in the safe load tables. The effects of using a non-linear objective function are also investigated.

The problem of obtaining an optimum design for an elastic frame, subject to strength and deflexion requirements, is presented in a general form in Chapter 3. An algorithm to solve this problem is presented in Chapter 4. The design problem is automatically formulated and solved by means of a computer program. The program can be used to design both plane frames and space frames under several loading conditions. Several designs are presented in Chapter 5 where the design criteria are extended to include member buckling.

Structures are all analysed by use of the same fundamental basic principals. This immediately indicates that they must be closely related, each one being a part of a more general structure. Hitherto, the significance of this fact and its implications, has not been seriously considered and hardly utilised.



In Chapter 6 a number of fundamental theorems are proposed and proved, to confirm that structures are inter-related. These theorems facilitate the prediction of the behaviour of one structure from the results of analysing another, more general, or related structure. With these theorems the variations in member forces and joint deflexions of a structure are studied when one or more of its members are varied or removed. The use of these theorems in the analysis and design of structures is explained and illustrative examples are given to show their versatility.

The problem of minimum weight design is extended in Chapter 7 to include shape. The shape of a structure, both its topology and geometry, is of major significance. Its determination however is difficult, involving all the design requirements. Since the work of Michell there has been little theoretical investigation to establish the optimum shape of a structure.

In Chapter 7 the theorems of structural variations put forward in Chapter 6 are employed to prove that it is possible to evaluate the significance of each member in the behaviour of a structure. This makes it possible to calculate, in advance, the economy achieved by altering its topology. A theoretical method is proposed to design structures, for minimum volume, with stress as well as deflexion requirements and where the shape of the structure is a basic design variable.

The problem turns out to be a new type of non-linear programming whose constraints and objective function are themselves continuously changing. A method is given to extend the non-linear programming procedure of Chapter 4 to deal with this new situation.

In Chapter 8 a detailed investigation is carried out into the design of structures to study the factors that influence their shape.

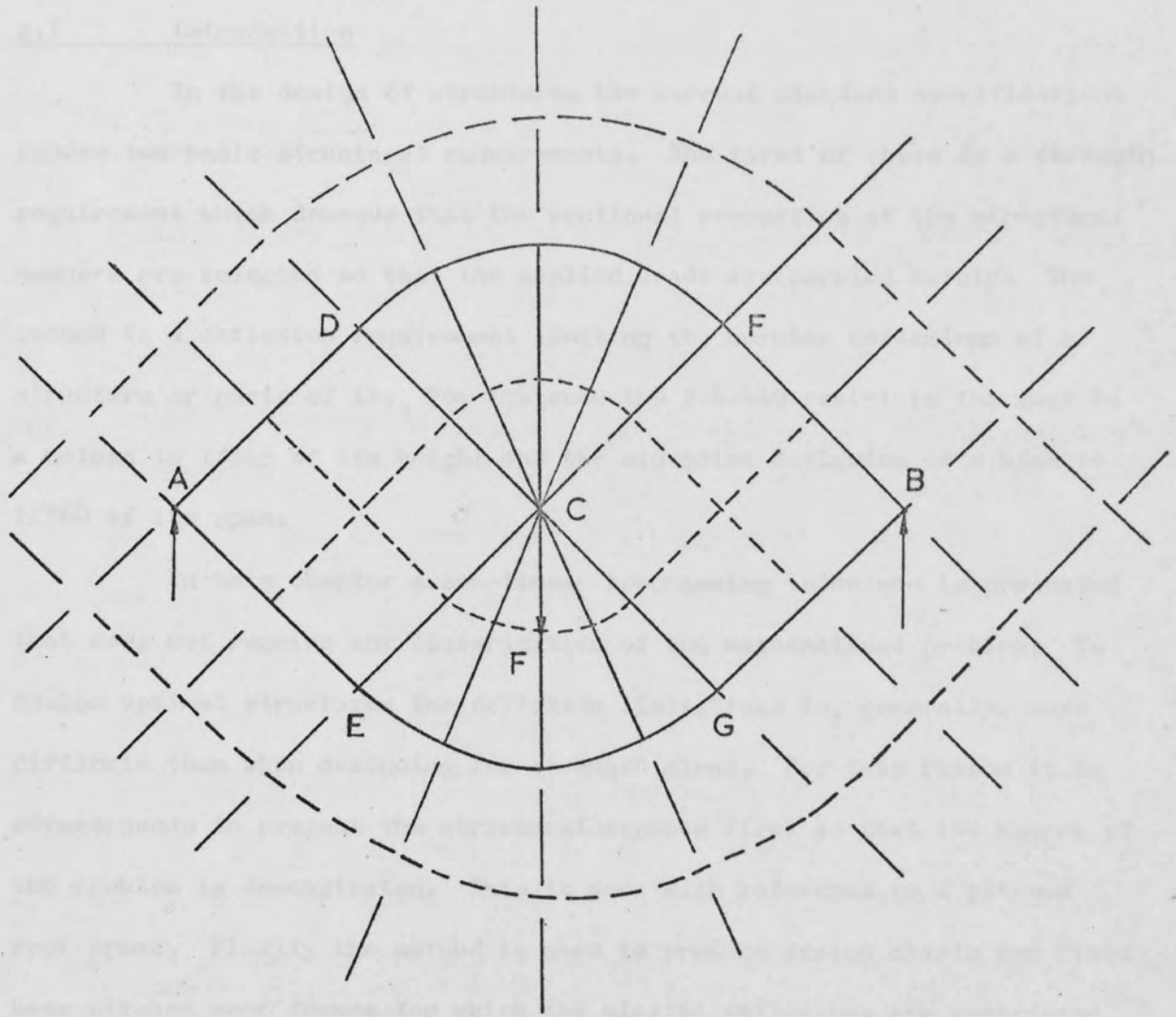


Figure 1.1. Michell structure.

## CHAPTER 2

### DYNAMIC SEARCH

#### 2.1 Introduction

In the design of structures the current standard specifications impose two basic structural requirements. The first of these is a strength requirement which demands that the sectional properties of the structural members are selected so that the applied loads are carried safely. The second is a deflexion requirement limiting the working deflexions of a structure or parts of it. For instance the B.S.449 restricts the sway in a column to  $1/325$  of its height and the mid-point deflexion of a beam to  $1/360$  of its span.

In this chapter a non-linear programming technique is presented that does not require any linearisation of the mathematical problem. To design optimal structures for deflexion limitations is, generally, more difficult than when designing for strength alone. For this reason it is advantageous to present the structural aspects first so that the nature of the problem is demonstrated. This is done with reference to a pitched roof frame. Finally the method is used to produce design charts for fixed base pitched roof frames for which the elastic deflexions are restricted by B.S.449.

#### 2.2 The Deflexion Constraints

The deflexion constraints are derived using the matrix displacement method of structural analysis. This method expresses the internal member forces in terms of the joint displacements and then proceeds to solve a set of joint equilibrium equations in order to determine the unknown displacements. This method is popular because it does not involve

the concept of redundancies and deals with statically determinate and indeterminate structures with equal efficiency. The vector of applied forces  $\underline{L}$  is related by the overall stiffness matrix  $\underline{K}$  of the structure to the resulting displacement vector  $\underline{X}$  in the following manner

$$\underline{L} = \underline{K} \underline{X} \quad \dots 2.1$$

A pitched roof frame is selected to derive the deflexion constraints. The forces acting on the frame are shown in figure (2.1). The deflexions caused by the combination of wind loading and vertical loading can be calculated by adding together those due to these loads when acting separately.

The amount of computation necessary is considerably reduced when advantage can be made of symmetrical or anti-symmetrical properties in the structure. In figure (2.2a) the horizontal wind load is replaced by equivalent horizontal loads  $H$ , and moments  $M_h$  acting at the eaves. This loading causes anti-symmetric deformation of the frame with the horizontal displacement and the rotation at each of the eaves being equal. In figure (2.2b) the vertical U.D. load is replaced by a set of equivalent point loads  $V$  and  $0.5V$  and fixed end moments  $M_v$ . This loading results in symmetrical deformation of the frame. It is simpler therefore to derive the deflexion constraints for each equivalent loading and then combine them for the general case.

For anti-symmetrical deformation, shown in figure (2.2a), the overall stiffness equations can be constructed in terms of the horizontal sway  $X_D$  and the eaves rotation  $\theta_D$  of joint D, thus

$$\begin{bmatrix} H \\ M_h \end{bmatrix} = \begin{bmatrix} 2b_1 & 2d_1 \\ 2d_1 & 2e_1 + 1.5e_2 \end{bmatrix} \begin{bmatrix} X_D \\ \theta_D \end{bmatrix} \quad \dots 2.2$$

in which

$$\left. \begin{aligned} b_1 &= 12 E I_1 / h_1^3 \\ d_1 &= -6 E I_1 / h_1^2 \\ e_1 &= 4 E I_1 / h_1 \\ e_2 &= 4 E I_2 / S \end{aligned} \right\} \dots 2.3$$

Here the suffixes 1 and 2 refer to the columns and the rafters respectively,  $E$  is the modulus of elasticity,  $S$  is the length  $BC$  of the rafters and  $I$  is the second moment of area of a member.

Solving equations (2.2) for the horizontal displacement  $X_D$  gives

$$X_D = [ (2Rh_1^3 H + 3Rh_1^2 M_h) I_1 + 1.5h_1^3 H I_2 ] / (7REI_1^2 + 36EI_1 I_2) \dots 2.4$$

where

$$\left. \begin{aligned} R &= S/h_1 = 0.5 \sqrt{(4k^2 + q^2)} \\ q &= L/h_1 \\ k &= h_2/h_1 \end{aligned} \right\} \dots 2.5$$

The span of the frame is  $L$  and  $h_2$  is the vertical distance between the apex and the eaves. The non-dimensional quantities  $R$ ,  $q$  and  $k$  define the geometry of the frame.

When considering the symmetrical deformation of the frame under the set of equivalent vertical loads the overall stiffness equations are obtained in terms of the vertical deflexion of the apex  $Y_c$  and the eaves rotation  $\theta_D$  as

$$\begin{bmatrix} V \\ M_v \end{bmatrix} = \begin{bmatrix} 2(b_1 \tan^2 \phi + b_2 \sec^2 \phi) & 2(d_1 \tan \phi - d_2 \sec \phi) \\ 2(d_1 \tan \phi - d_2 \sec \phi) & 2(e_1 + e_2) \end{bmatrix} \begin{bmatrix} Y_c \\ \theta_D \end{bmatrix} \dots 2.6$$

Where  $\phi$  is the angle of pitch of the rafters. Once again  $\theta_D$  is eliminated from these equations and the following expression for  $Y_c$  is obtained

$$Y_c = [V(cI_1 + dI_2) - M_v(aI_2 - bI_1)] / [(eI_1 + fI_2)(cI_1 + dI_2) - 2(aI_2 - bI_1)^2] \quad \dots 2.7$$

where

$$\left. \begin{aligned} a &= 6 E \sec \phi / R^2 h_1^2 \\ b &= 6 E \tan \phi / h_1^2 \\ c &= 4 E / h_1 \\ d &= c/R \\ e &= 24 E \tan^2 \phi / h_1^3 \\ \text{and } f &= 24 E \sec^2 \phi / R^3 h_1^3 \end{aligned} \right\} \quad \dots 2.8$$

Considering the idealised displacement diagram of Figure (2.2.c), if the joint B has moved a distance to position B' then joint C at the apex moves vertically to C' so as to maintain its position on the centre line of the frame. A vector diagram of displacements can be produced to show the relationship between these two displacements, this is given in Figure (2.2.d). From this diagram it is evident that

$$X_D = Y_c \tan \phi \quad \dots 2.9$$

It follows that the function defining vertical displacement, equation (2.7), defines the horizontal displacement at the eaves when multiplied by the tangent of the angle of pitch.  $X_D$  due to the vertical loading only is therefore given by

$$X_D = [V(cI_1 + dI_2) - M_v(aI_2 - bI_1)] \tan \phi / [(eI_1 + fI_2)(cI_1 + dI_2) - 2(aI_2 - bI_1)^2] \quad \dots 2.10$$



For the general case of Figure (2.1.c), when vertical and horizontal forces are acting simultaneously the vertical deflexion  $Y_c$  of the apex is given by equations (2.7), while the horizontal deflexion  $X_D$  is given by the sum of the right hand sides of equations (2.4) and (2.10).

Thus

$$X_D = \frac{I_1 [2Rh_1^3 H + 3Rh_1^2 M_h] + 1.5Hh_1^3 I_2}{7 REI_1^2 + 36EI_1 I_2} + \frac{[V(cI_1 + dI_2) - M_v(aI_2 - bI_1)] \tan \phi}{(eI_1 + fI_2)(cI_1 + dI_2) - 2(aI_2 - bI_1)^2} \quad \dots 2.11$$

It is noticed that, for the symmetrical and general case, there are two displacements which need to be constrained. These are the vertical displacement  $Y_c$  and the horizontal displacement at the eaves  $X_D$ . According to B.S.449,  $Y_c$  should not exceed  $L/360$  while  $X_D$  should not exceed  $h_1/325$ . To determine which of these deflexions dominate it is noticed that when considering the symmetrical case alone the vertical deflexion dominates the design if

$$L/360 < h_1 / 325 \tan \phi \quad \dots 2.12$$

This follows from equation (2.9) which states that the horizontal deflexion may be replaced by  $Y_c \tan \phi$  and therefore the restrictions imposed by B.S.449 become

$$Y_c < L/360 \quad \dots 2.13$$

and  $X_D = Y_c \tan \phi < h_1/325$

Equation (2.12) is obtained by eliminating  $Y_c$  from these equations.

Now  $L = qh_1$ , and  $\tan \phi$  is obtained from the geometry of the frame as follows

$$\tan \phi = h_2 / 0.5L \quad \dots 2.14$$

but  $k = h_2/h_1$  and  $q = L/h_1$  and therefore

$$\tan \phi = 2k/q \quad \dots 2.15$$

Substituting this into equation (2.12) it follows that the vertical deflexion dominates the design when

$$qh_1 / 360 < qh_1 / 650k \quad \dots 2.16$$

i.e. when  $k < 0.554$

Thus at a critical value of  $k = 0.554$  and of

$q = q' = 2 \times 0.554 / \tan \phi$  both deflexion constraints are effective. In figure (2.3) values of  $q'$ , the critical value of  $q$ , are plotted against  $\phi$  and for any frame of a given pitch and a given ratio  $q$  other than  $q'$ , the horizontal sway of the columns dominates the design when  $q > q'$ . On the other hand the vertical deflexion dominates the design when  $q < q'$ . For the general case, the dominant deflexion constraint is also dependent on the horizontal wind force as this exaggerates the sway of one column while reducing the sway of the other. As the two displacements are no longer directly related to each other by the geometry of the frame, the task of deciding which of these will dominate the final design becomes complicated. The manner in which this is decided upon is given later.

### 2.3 Determination of the Optimum Design

Before entering into the details of the optimization problem there are a number of assumptions that are made in conjunction with the minimum weight design of structures. First of all it should be pointed

out that it is not assumed that the lightest structure is always the cheapest. The lightest structure has, however, a good claim to be considered as the best possible design. The minimum weight design approach makes a number of assumptions. For instance despite the fact that there is only a finite number of member sections it is usually assumed that an infinite number of sections are available to choose from.

A second assumption is that there is a smooth curve relating the weight  $w$  per unit length of a member to some of its structural constants. In reality the weight of a member is linearly related to the cross-sectional area and an elastic minimum weight design correctly uses this for the design of pin-jointed structures. For rigidly jointed structures, as is the case here, the design variables are the second moments of area and an elastic minimum weight design must incorporate these into an objective function which indicates the weight of the structure.

Returning to the portal frame, the design problem is to select sections for the members of the frame so that the weight of the frame is minimum and the deflexion limitations imposed by B.S.449 are not violated. The total weight of the frame  $z$  is given by

$$z = D ( 2h_1 A_1 + 2SA_2 ) \quad \dots 2.17$$

where  $D$  is the density of the material while  $A_1$  and  $A_2$  are the cross-sectional areas of the columns and rafters respectively. The unknown cross-sectional properties appearing in the expressions for deflexions are the second moments of area  $I_1$  and  $I_2$  and it is these that must replace the cross sectional areas in the objective function.

At present it is reasonable to assume that the weight per unit length  $w$  and the second moment of area of a section are related in the

following manner

$$w = c I^d \quad \dots 2.18$$

where  $c$  and  $d$  are constants. This approach is similar to that adopted by Heyman (3, 4) for relating  $w$  to  $M_p$ . Equation (2.18) can be used to form the objective function by re-writing equation (2.17) as

$$z = 2h_1 c I_1^d + 2S c I_2^d \quad \dots 2.19$$

An objective function of this form is non-linear. In order to linearise this function it is necessary to replace equation (2.18) by a linear relationship such as

$$w = e + f I \quad \dots 2.20$$

where  $e$  and  $f$  are constants. The error involved in this linearisation process is very small. This is because in a region about the optimum design curve (2.19) is flat and approximates very closely to the linearised form, using equation (2.20). Equation (2.17) may now be re-written as

$$z = 2h_1 (e + f I_1) + 2S (e + f I_2) \quad \dots 2.21$$

which may be simplified to

$$z = D' + D'' (2h_1 I_1 + 2S I_2) \quad \dots 2.22$$

where  $D'$  and  $D''$  are constants. Since  $S = R h_1$ , the weight of the frame is minimized when  $z$  is

$$z = I_1 + R I_2 \quad \dots 2.23$$

is minimum. Equation (2.23) is thus used as the objective function for the portal frame optimization problem and can be rearranged to read

$$I_1 = -R I_2 + z \quad \dots 2.24$$

This is the equation of a straight line in  $I_1$  and  $I_2$  with a slope

$$dI_1 / dI_2 = -R.$$

The design which minimizes the objective function is the best of a set of feasible designs. The feasible design space can be defined by replacing  $Y_c$  in equation (2.7) with  $L/360$  and  $X_D$  in equation (2.11) with  $h_1/325$  and then converting these equations into inequalities. For the general case of horizontal and vertical loading acting together this results in two deflexion constraints. After re-arranging these are

- 1) The horizontal deflexion constraint  $G_1$  which is given by

$$G_1 = a_1 a_2 I_1^4 - (a_3 - a_2 a_4 I_2) I_1^3 - (a_5 I_2 - a_2 a_6 I_2^2) I_1^2 - (a_7 I_2^2 - a_2 a_8 I_2^3) I_1 - a_9 I_2^3 \geq 0 \quad \dots 2.25$$

and

- 2) The vertical deflexion constraint  $G_2$  given by

$$G_2 = c_1 c_2 I_1^2 - (c_3 - c_2 c_4 I_2) I_1 - c_5 I_2 + c_2 c_6 I_2^2 \geq 0 \quad \dots 2.26$$

where the terms  $a$  and  $c$  depend upon the geometry of the frame and the applied loading, and are defined to be:

$$c_1 = ec - 2b^2$$

$$c_2 = L/360$$

$$c_3 = cV + bM_v$$

$$c_4 = ed + cf + 4ab$$

$$c_5 = Vd - aM_v$$

$$c_6 = fd - 2a^2$$



$$c_7 = (2h_1 H + 3M_h) Rh_1^2$$

$$c_8 = 7RE$$

$$c_9 = 1.5Hh_1^3$$

$$c_{10} = 36E$$

$$a_1 = c_1 c_8$$

$$a_2 = h/325$$

$$a_3 = c_3 c_8 \tan \phi + c_1 c_7$$

$$a_4 = c_6 c_8 + c_4 c_{10}$$

$$a_5 = c_1 c_9 + c_4 c_7 + (c_3 c_{10} + c_8 c_5) \tan \phi$$

$$a_6 = c_1 c_{10} + c_4 c_8$$

$$a_7 = c_5 c_{10} \tan \phi + c_6 c_7 + c_4 c_9$$

$$a_8 = c_6 c_{10}$$

and  $a_9 = c_6 c_9$

The actual boundaries of the feasible space are obtained by using equalities in equations (2.25) and (2.26). Thus

$$\begin{aligned} & a_1 a_2 I_1^4 - (a_3 - a_2 a_4 I_2) I_1^3 - (a_5 I_2 - a_2 a_6 I_2^2) I_1^2 \\ & - (a_7 I_2^2 - a_2 a_8 I_2^3) I_1 - a_9 I_2^3 = 0 \end{aligned} \quad \dots 2.27$$

and

$$c_1 c_2 I_1^2 - (c_3 - c_2 c_4 I_2) I_1 - c_5 I_2 + c_2 c_6 I_2^2 = 0 \quad \dots 2.28$$

The value of the constraint  $G_1$  or  $G_2$  on the boundary of the feasible space, defined by equations (2.27) and (2.28), is zero respectively. When the values of both  $G_1$  and  $G_2$  are greater than zero the current design point

is in the interior of the feasible space.

The optimum design of a given portal frame is obtained when the objective function (2.23) touches one of the above boundary equations. Therefore the optimum condition is obtained by differentiating equations (2.27) and (2.28) as implicit functions and setting  $dI_1/dI_2$  in each case to the slope of the objective function which is  $-R$ . In this manner it is found that the horizontal deflexion constraint is active when the design variables  $I_1$  and  $I_2$  are such that

$$R = \frac{3a_9 I_2^2 - a_2 a_4 I_1^3 + (a_5 - 2a_2 a_6 I_2) I_1^2 + (2a_7 I_2 - 3a_2 a_8 I_2^2) I_1}{3(a_3 - a_2 a_4 I_2) I_1^2 - 4a_1 a_2 I_1^3 + 2(a_5 I_2 - a_2 a_6 I_2^2) I_1 + a_7 I_2^2 - a_2 a_8 I_2^3} \quad \dots 2.29$$

and that the vertical deflexion constraint is active when

$$R = (c_5 - c_2 c_4 I_1 - 2c_6 c_2 I_2) / (c_3 - 2c_1 c_2 I_1 - c_2 c_4 I_2) \quad \dots 2.30$$

In order to select the optimum set of sections, it is necessary to assume which of the constrained deflexions will be critical. Should the frame have a low  $q = L/h_1$  value and be subjected to high horizontal wind forces it is reasonable to assume that the horizontal sway criteria will dominate the design. In this case equations (2.27) and (2.29) are solved simultaneously for  $I_1$  and  $I_2$ . On the other hand if the frame has a low angle of pitch and low horizontal wind forces it is more probable that it will be the vertical deflexion governing the final design. In this case equations (2.28) and (2.30) are solved.

In situations where it is uncertain which of the constraints will dominate care must be taken that an optimum set of sections obtained by solving equations (2.27) and (2.29) do not violate the vertical deflexion

constraint (2.26). Conversely a solution obtained by solving equations (2.28) and (2.30) must not violate constraint (2.25). In this manner both deflexion constraints are satisfied.

The number of possible feasible solutions obtained by solving the various pairs of non-linear simultaneous equations is reduced by deriving  $d^2I_1/dI_2^2$  of the constraints and only selecting the set of sections that gives a positive second derivative for the dominating constraint. This ensures that the solution is a minimum.

In certain cases the procedure outlined above will not locate the optimum design. This is illustrated with the aid of figure (2.4) in which equations (2.27) and (2.28) are represented diagrammatically by curves (1) and (2) respectively. The feasible design space is shown shaded. Various objective functions, of constant  $z$ , are also shown as parallel straight lines. It is noticed that points such as A and B, where an objective function is tangential to one of the constraints, are not feasible. In this case the optimum design is given by point C where  $z_3$  intersects both curves,  $z_3$  being greater than both  $z_1$  and  $z_2$ . The optimum condition is thus obtained when the objective function passes through a node of the feasible design space.

It is convenient in connection with figure (2.4) to illustrate the use of an accurate objective function where in equation (2.17) the areas  $A_1$  and  $A_2$  of the columns and rafters are substituted by non-linear expressions in  $I_1$  and  $I_2$ . This would render the objective function  $z_3$  non-linear as shown by  $z_3$  in the figure. It is noticed that this function also touches the feasible space at point C, thus giving the same optimum design. This indicates that using a linearised objective function in I is reasonable in most cases and particularly when the objective function touches the feasible space at a node.

#### 2.4 Optimization by Non-Linear Programming

The 'dynamic search' procedure to be described here was developed to solve the portal frame design problem, but it can be extended to other problems, and is presented in a general form.

For an  $n$ -dimensional problem with variables  $u, v, w$ , etc., the proposed method keeps  $n-2$  variables constant while a search is carried out for an optimum solution in the plane of two variables. Once such an optimum solution is located in the  $u$ - $v$  plane, say, either  $u$  or  $v$  is kept constant and a new variable  $w$  is introduced into the search operation. For instance if  $u$  is to be kept constant the search will be carried out in the  $v$ - $w$  plane. In this manner all the  $n$  variables are repeatedly considered until a final optimum point is located. This procedure may be likened to a cutting plane method as the feasible design hyper-space is cut by planes which are orthogonal to all but two of the co-ordinate axes. The best solution is located in each plane and the next plane passes through this current best point thus ensuring continual improvement of the solution within the confines of the constraints.

In figure (2.5) a convex feasible design space is shown shaded. The boundary line JBDCTX is on a plane where all the variables except  $u$  and  $v$  are constant. Nodes such as J and T are formed when the individual constraints intersect on such a plane. All movement to the optimum design is carried out within the feasible region and therefore to initiate the search procedure an initial feasible solution is required. Such a solution is represented by point A in the figure. In normal structural problems this point may be arrived at by first setting all the variables at lower bound values and increasing them proportionally until a feasibility check shows that all the constraints are satisfied.

Point B is on the boundary of the feasible space where the value of the objective function, shown dashed, is less than that given by point A. For this reason point B is an improvement upon the initially selected feasible solution. As point A lies inside the feasible region point B may be obtained by moving from A in the direction of steepest descent. That is perpendicular to the lines of constant  $z$  so that this function decreases at the greatest rate possible. Any point such as B' gives a smaller value of the objective function but is unacceptable since it lies outside the feasible space.

Moving from point B a new improved solution such as that represented by point C is sought. It is noticed that movement along the line of constant objective function towards G improves the feasibility of the design by moving away from the boundary of the design space. On the other hand movement towards point F along the tangent to the boundary at B improves the optimality by reducing the objective function. This latter direction of travel however is at the expense of feasibility. For the actual direction of travel, a line BC is selected intermediate to BG and BF intersecting the feasible boundary line at C. Line BC is chosen so that its slope  $\partial u / \partial v$  is the average of the slopes of the objective function  $-R$  and the violated constraint  $(\partial u / \partial v)_c$  at point B, i.e.

$$(\partial u / \partial v)_{BC} = 0.5 [(\partial u / \partial v)_c - R] \quad \dots 2.31$$

where suffix BC refers to line BC and suffix c refers to the violated constraint. It is noticed that travel in the direction BC improves the optimality of the solution while the search is being continued within the feasible space. Further improved solutions can be obtained until a point such as D is reached where the value of the objective function in this particular plane of search is minimum.



The movement from one feasible point to another, such as from B to C, is carried out by taking a series of step lengths, such as that from B to H. The new values  $u_{\text{new}}$  and  $v_{\text{new}}$  of the variables are calculated from

$$u_{\text{new}} = u_{\text{old}} + \delta v \left( \partial u / \partial v \right)_{BC} \quad \dots 2.32$$

$$\text{and} \quad v_{\text{new}} = v_{\text{old}} + m \delta v \quad \dots 2.33$$

where  $\delta v$  is a conveniently chosen step length along the  $v$  axis. The values of  $m$  and  $\partial u / \partial v$  decide the manner in which the variables  $u$  and  $v$  are altered. Generally within the feasible space  $m$  is unity and  $\partial u / \partial v$  is calculated from equation (2.31), however situations arise when movement defined by these values is impossible. Such situations are shown diagrammatically in figure (2.6) where the feasible area in the  $u$ - $v$  plane of search is shown shaded. In these cases the feasible area is also bounded by maximum and minimum limits imposed on the variables. In figure (2.6a) the point A represents the optimum solution obtained from the last plane of search. Movement towards B is defined in the normal manner using equations (2.31), (2.32) and (2.33) with  $m$  having a value of unity. Once having attained B however movement in this direction is impossible without violating the upper bound imposed on variable  $v$  represented by the vertical line DE in the figure. In this case  $m$  is set to -1 and  $(\partial u / \partial v)$  is set to  $-1/R$ . This forces both variables to take lower values and the new direction of search, toward C, is at right angles to the objective function. A similar procedure is adopted should variable  $u$  reach its upper bound, which is illustrated in figure (2.6b).

The figures (2.6c) and (2.6d) show diagrammatically situations in which variables  $u$  and  $v$  have been driven to lower bound values. In the first case when  $u$  reaches its lower bound the current direction of search, FG, is bent toward H along the boundary of the feasible space so that  $u$

maintains its lower bound value. In the second case  $v$  is kept at its lower bound while  $u$  decreases further.

Once a new boundary point is located, such as points C, M, H and L in figures (2.6), the search procedure is continued with a new value of  $\partial u/\partial v$  calculated from equation (2.31).

On encountering a behaviour constraint smaller step lengths are taken from the most recent feasible point in the current direction of search. This process may be continued for any required accuracy being terminated when the following tolerance test is satisfied

$$\left. \begin{aligned} & \left| 1 - u_f/u_n \right| < t_1 \\ \text{and} \quad & \left| 1 - v_f/v_n \right| < t_1 \end{aligned} \right\} \dots 2.34$$

Where  $u_f$  and  $v_f$  are the latest feasible values of the variables,  $u_n$  and  $v_n$  are the most recent non-feasible values and  $t_1$  is a specified tolerance.

When such a point is established on the boundary of the feasible space, two tolerance tests are applied to determine whether the current solution is optimum within the current plane of search. The first of these tests is a tangency test that compares the slope  $\partial u/\partial v$  of the boundary of the feasible space with the slope  $-R$  of the objective function. For an optimum point to be confirmed it is necessary that these slopes are equal or within a specified tolerance  $t_2$ . This comparison is carried out in the form

$$\left| 1 - \left( \frac{\partial u}{\partial v} \right)_c / (-R) \right| < t_2 \quad \dots 2.35$$

For a true optimum to be obtained it is also necessary that the boundary of the feasible area, in the region of the point of tangency, must be convex. This is so when the second derivative  $\partial^2 u/\partial v^2 > 0$ , which is

also checked. Point D in figure (2.5) satisfied this test where it can be seen that no further reduction of the value of the objective function is possible due to the curvature of the boundary.

The second test to verify an optimum solution is called a nodal test. The current values of  $u_a$  and  $v_a$  at the boundary point a are compared with  $u_b$  and  $v_b$  at the previous boundary point b. This test is of a similar form to inequality (2.34) being

$$\left. \begin{array}{l} |1 - u_a/u_b| < t_3 \\ \text{and} \quad |1 - v_a/v_b| < t_3 \end{array} \right\} \quad \dots 2.36$$

where  $t_3$  is another specified tolerance. The purpose of this test is to establish that by moving from point a to b, the variables u and v have remained constant or have altered by very little indicating that the previous and current boundary points are adjacent. Generally this will be the case when the line of constant objective function corresponding to the current design is touching the feasible space at a node. With reference once again to figure (2.4) point C will satisfy this test.

A positive  $\partial^2 u / \partial v^2$  ensures optimality in the tangency test. If however the optimum solution is not obtained the sign of  $\partial^2 u / \partial v^2$  will indicate which of the two cases shown diagrammatically in figure (2.7) is developed. At point B in figure (2.7.a)  $\partial^2 u / \partial v^2$  is positive and care should be taken that the next step length is into the feasible area. In figure (2.7.b)  $\partial^2 u / \partial v^2$  at point B is negative. In this case the new direction of search is not evaluated by using equation (2.31) but by merely equating it to the slope of the boundary at this point. Due to the concavity of the constraint in figure (2.7.b) movement from B either towards C or C' will result in increased feasibility, however, only movement towards C reduces the value of the objective function. When

encountering a negative second derivative therefore search is continued by moving along the tangent in a direction of decreasing objective function.

It should be pointed out here that both the first and second derivatives are found numerically without explicit differentiation of the constraints. In figure (2.8) the variation of a function  $f$  against one variable such as  $v$ , for a constant value of  $u$  is shown. From this curve it is observed that

$$\partial f / \partial v = [f(v + e) - f(v - e)] / 2e \quad \dots 2.37$$

Similarly it can be shown that

$$\partial f / \partial u = [f(u + e) - f(u - e)] / 2e \quad \dots 2.38$$

and since

$$\partial u / \partial v = - \frac{\partial f}{\partial v} / \frac{\partial f}{\partial u} \quad \dots 2.39$$

It follows from these equations that

$$\partial u / \partial v = [f(v - e) - f(v + e)] / [f(u + e) - f(u - e)] \quad \dots 2.40$$

where  $e$  is a small incremental change in a function parameter.

At any stage the actual value of  $\partial^2 u / \partial v^2$  is not required but its sign is necessary for the tangency test and when deciding the direction of search. This sign is found by evaluating the constraint at a point adjacent to the current boundary point, along the tangent  $\partial u / \partial v$ . If this point is infeasible it indicates that the actual boundary line is convex and hence  $\partial^2 u / \partial v^2$  is positive.

A flow diagram for the computer program is shown in figure (2.9) where it is seen that once the data which defines the structural problem is input the first priority is the location of a feasible design from which to initiate the procedure.

It is assumed here that for normal structures a feasible design may be obtained from an infeasible design by an equal proportional increase of the design variables. This is achieved by first setting all the design variables at lower bound values and repeatedly employing the following formulae until a feasible design is at hand:

$$\left. \begin{aligned} u_{\text{new}} &= \lambda^{\Delta_u} u_{\text{old}} \\ v_{\text{new}} &= \lambda^{\Delta_v} v_{\text{old}} \\ w_{\text{new}} &= \lambda^{\Delta_w} w_{\text{old}} \end{aligned} \right\} \dots 2.41$$

etc.

where  $\lambda$  is a positive quantity greater than unity given by

$$\lambda = \min(u^{\Delta_u} u_{\text{old}} / u_{\text{old}}, v^{\Delta_v} v_{\text{old}} / v_{\text{old}}, w^{\Delta_w} w_{\text{old}} / w_{\text{old}}, \text{etc.}) \dots 2.42$$

and the terms  $\Delta_u, \Delta_v, \Delta_w$  etc. are Kronecker deltas which assume a value of +1 when the corresponding variable is below its upper bound value, and of zero when it is at its upper bound value. Use of equation (2.42) and equation (2.41) drives at least one of the variables to its upper bound. The Kronecker deltas ensure that in further moves variable bounds are not violated.

Having located a feasible solution the initial plane of search is selected and the first boundary solution is sought. This solution is stored and the search proper commences to find the optimum design in the current plane of search. Each successive feasible design obtained is stored, and the previous is discarded, as the value of the objective function is constantly reduced.

In the computer program facilities are available so that the direction of search can be altered in a dynamic manner. This is done when



a specific number of steps have been taken in a given direction without successfully reaching a boundary line. The method of selecting the new direction of search is the same as described above for the case when a boundary solution is at hand. In this manner computer time is saved by not pursuing a direction that does not lead to the optimum solution. It could be argued that the modified search direction should be of a steepest descent nature, however, this direction would only improve optimality whereas the direction actually used improves feasibility as well as optimality.

As can be seen from the flow diagram of figure (2.9), when a boundary is violated the variables are immediately returned to their previous stored values and the search is commenced from this point with the same direction vector but a reduced step size  $\lambda$ . For normal searching purposes a step size is conveniently selected beforehand and this value is input to the computer as an item of the data. A suitable value for  $\lambda$  was found to be one hundredth of the range of values over which the design parameters may vary. This value is reduced by a factor of 10 each time a non feasible solution is obtained and the design point has to be moved back, until finally the test for a boundary point given by inequalities (2.34) is satisfied. The original value of the step length is then restored before determining the new direction of search.

When the inequality tests of equations (2.35) and (2.36) indicate that an optimum has been achieved in the current plane of search, it is necessary to ascertain whether or not the overall optimum is also at this point. During the optimization procedure every possible combination of the variables into pairs is considered to represent a possible plane of search. As a result of this, before the overall optimum can be guaranteed, a complete round of sub-optimizations must have resulted in no significant

change in the values of the variables. The test takes the form of inequalities (2.36) where the suffices a and b now refer to the present and the previous round of sub-optimizations. This test is reproduced here for clarity and to introduce another tolerance  $t_4$

$$\left. \begin{array}{l} |1 - u_a/u_b| < t_4 \\ \text{and } |1 - v_a/v_b| < t_4 \end{array} \right\} \dots 2.43$$

For the optimum to be located this test must be satisfied for a complete round of suboptimizations.

## 2.5 Design Charts for Pitched Roof Frames

The method described in the last section was used to calculate the optimum design sections for a family of fixed based pitched roof frames subject to the deflexion constraints given by inequalities (2.25) and (2.26). These frames were considered to be component parts of a continuous portal shed as shown in figure (2.10) where the spacing between the frames is d. For loading purposes the shed is divided into segments of length d so that each individual frame lies at the centre of a section. The forces applied to each section are assumed to be totally carried by the corresponding central frame. As mentioned earlier the loading is of two types in combination, vertical roof loading and horizontal wind loading. These are initially expressed as uniform pressures which are then converted to conform to the idealized loading given in figures (2.2a) and (2.2b).

In CP3 Chapter V is a table from which the wind pressures imposed on buildings of various heights and of various degrees of wind exposure can be obtained. For wind velocities other than those defining the tabulated exposures the pressures may be obtained from the following formula

$$p_w = W^2 p_{72} / 5184 \dots 2.44$$

where  $p_w$  denotes the pressure corresponding to a velocity of  $W$  m.p.h.,  $W$  being the velocity at an effective height of 40 feet. The term  $p_{72}$  denotes the pressure corresponding to a velocity of 72 m.p.h., which is exposure D in CP3 Ch.V and may be obtained from

$$p_{72} = 8 + 0.2h \quad \dots 2.45$$

Here  $h$  is the height of the building in feet and lies between 10 ft and 60 ft. In equations (2.44) and (2.45) the units of  $p_w$  and  $p_{72}$  are lb/sq.ft and are converted to units of  $\text{kN/m}^2$  by multiplying by 0.04788. The horizontal uniformly distributed load,  $w_h$ , on each frame due to the section of shed cladding it supports is obtained by combining equations (2.44) and (2.45) with the frame spacing  $d$ , as

$$w_h = W^2 d(2.4384 + 0.2h_1 + 0.1 L \tan \phi) / 26050.42 \quad \dots 2.46$$

Here  $W$  is expressed in km/hr,  $h_1$  and  $L$  are expressed in metres and the angle of pitch  $\phi$  in degrees. The result is obtained in units of  $\text{kN/m run}$ .

The uniformly distributed load is assumed to be concentrated at the eaves of the frame as depicted in figure (2.2a) such that the horizontal force  $H$  and the moment  $M_h$  at the eaves is given by

$$H = 0.5 w_h (h_1 + h_2) \quad \dots 2.47$$

$$\text{and } M_h = w_h (-h_1^2 / 12 + h_2^2 / 2) \quad \dots 2.48$$

It can be seen by inspection of equation (2.48) that as the geometry of the frame alters the value of  $M_h$  changes sign and the moment reverses its direction.

To obtain the vertical uniformly distributed load acting on each frame the vertical loading density  $w_v$  is multiplied by the frame spacing. This is then replaced by vertical forces and fixed end moments acting at

the ends of each rafter so that the force  $V$  and the moment  $M_V$  depicted in figure (2.2.b) become

$$V = 0.5 w_v d L \quad \dots 2.49$$

$$\text{and} \quad M_V = w_v d L^2 / 48 \quad \dots 2.50$$

In producing the design charts a wind velocity of 100 kilometres per hour was adopted which is equivalent to exposure C in CP3 Chapter V (63 m.p.h.). The spacing between the frames  $d$  was taken as 8 metres and a roof loading  $w_v$  of 1.5 kilonewtons per square metre was adopted. The height of the columns  $h_1$  was varied between 3 metres and 15 metres, the pitch from  $0^\circ$  to  $40^\circ$  and the non-dimensional quantity  $q = L/h_1$  was altered between 1 and 8. An average of 0.6 seconds was required to produce each design.

In figure(2.11) typical graphs of the angle of pitch versus the second moment of area of the sections are shown for a constant  $h_1$  of 9 metres and different spans. For points to the left of the dotted line ab the vertical deflexion constraint dominates the design.

For designs lying to the right of line ef in figure (2.11) the horizontal deflexion constraint becomes increasingly dominant as the effective height of the frame increases.

In between the lines ab and ef both deflexion constraints are found to be equally dominant and both are critical in the minimum weight design. In this region the pitch of the frame is such that a balance is struck between the horizontal and vertical forces. These designs are those represented diagrammatically by point C in figure (2.4) when the objective function is not tangential to the feasible design space but touches it at a node. For a frame 9 metres high and given span and pitch, the optimum values of  $I_1$  and  $I_2$  can be directly read off the graphs of figure (2.11).

In figure (2.12) graphs of angle of pitch versus the optimum value of the objective function  $z$  is shown for a height of 9 metres and different values of span  $L$ . It is immediately noticeable from this figure that for a frame with a given ratio  $q = L/h_1$ , there is in fact an optimum pitch that makes the weight of the frame minimum. Points on the line  $cd$  represent the optimum pitch for each frame.

It is interesting to note that in figure (2.12) for small values of  $q$  the optimum pitch tends to decrease towards zero. This indicates that, under the loading conditions applied here, as  $q$  approaches unity it is indeed advantageous to build them rectangular. This demonstrates the vital importance of the geometry of a structure when designing for minimum weight. This aspect will be studied in greater detail later in this thesis.

The line  $cd$  of figure (2.12) is also plotted in figure (2.11) where it is noticed that, when the optimum pitch is selected for a frame, both deflexion constraints are equally effective. It can be seen from this that altering the geometry of the frame gives a result that is not over-designed with respect to one or other of the deflexion limitations.

In figure (2.13) the properties of curves such as  $cd$  of figures (2.11) and (2.12) are collected together so that for any frame of given  $q$  the optimum pitch may be found directly. It is noticed that for this wind velocity it is uneconomical to build frames of pitch greater than  $14^\circ$ . This quantity is seen to vary with the frame span however and for a span of 27 metres has reduced to  $12^\circ$ .

It is also interesting to note that for frames with large values of  $q$  the optimum angle of pitch once again tends toward zero. This is because for such frames a small increase in the pitch of the rafters necessitates a large increase in the length. The benefit gained by such an alteration of pitch as regards stiffness is therefore balanced by the increased volume necessary in the rafters.



In figure (2.12) graphs of angle of pitch versus the optimum value of the objective function  $z$  is shown for a height of 9 metres and different values of span  $L$ . It is immediately noticeable from this figure that for a frame with a given ratio  $q = L/h_1$ , there is in fact an optimum pitch that makes the weight of the frame minimum. Points on the line  $cd$  represent the optimum pitch for each frame.

It is interesting to note that in figure (2.12) for small values of  $q$  the optimum pitch tends to decrease towards zero. This indicates that, under the loading conditions applied here, as  $q$  approaches unity it is indeed advantageous to build them rectangular. This demonstrates the vital importance of the geometry of a structure when designing for minimum weight. This aspect will be studied in greater detail later in this thesis.

The line  $cd$  of figure (2.12) is also plotted in figure (2.11) where it is noticed that, when the optimum pitch is selected for a frame, both deflexion constraints are equally effective. It can be seen from this that altering the geometry of the frame gives a result that is not over-designed with respect to one or other of the deflexion limitations.

In figure (2.13) the properties of curves such as  $cd$  of figures (2.11) and (2.12) are collected together so that for any frame of given  $q$  the optimum pitch may be found directly. It is noticed that for this wind velocity it is uneconomical to build frames of pitch greater than  $14^\circ$ . This quantity is seen to vary with the frame span however and for a span of 27 metres has reduced to  $12^\circ$ .

It is also interesting to note that for frames with large values of  $q$  the optimum angle of pitch once again tends toward zero. This is because for such frames a small increase in the pitch of the rafters necessitates a large increase in the length. The benefit gained by such an alteration of pitch as regards stiffness is therefore balanced by the increased volume necessary in the rafters.

In figure (2.14) the values of optimum second moment of area for the columns and rafters are given for various values of span and column height. These correspond to the optimum pitch in each case. It is this figure and figure (2.13) that are used in conjunction to determine the sectional properties and the angle of pitch for frames of different dimensions. A prominent feature of these graphs is that each of the design curves has a discontinuity. These are the points of critical  $q$  when a rectangular frame becomes economical. Geometries which lie between the vertical axes and these discontinuities have pitched roofs whereas those lying away from the vertical axes are rectangular.

It should be stated here that figures (2.13) and (2.14) suggest values for  $I_1$  and  $I_2$  so that the weight of the frame is minimum. Nevertheless it is often found that the values obtained from these graphs are not available in the current safe load tables. To move up the table to sections with higher  $I$  values would detract from the advantages of the elaborate procedure of determining a minimum weight design. This is due to the fact that a continuous set of sections is not available in any safe load table.

The design charts in fact overcome this difficulty considerably. To explain this reference is made to figure (2.11). In this figure points along the line  $cd$  give the designs for optimum pitch. The corresponding values of  $I_1$  and  $I_2$  are obtained from the vertical axes of this figure. If these resulted in unavailable sections, the designer could then move along the line of constant span away from the line  $cd$  until available sections are obtained. In this manner the pitch of the frame is also altered but the final design is still optimal.

## 2.6 Design Examples

In order to design a frame of fixed geometry figure (2.11) may be used directly. For a frame of 21 metre span with a column height of 9 metres and a pitch of  $25^\circ$  this figure gives the sectional properties of the columns and rafters as

$$I_1 = 10.000 \times 10^8 \text{ mm}^4$$

$$I_2 = 9.211 \times 10^8 \text{ mm}^4$$

From the safe load tables the best sections that can be selected are 21 x 13 x 112 U.B. and 24 x 9 x 84 U.B. for the columns and the rafters respectively. These have second moments of area of  $10.911 \times 10^8 \text{ mm}^4$  and  $9.841 \times 10^8 \text{ mm}^4$  and are seen to be considerably higher than those required. These are the available optimum sections, however, for a pitch of  $25^\circ$  imposed by the design requirements giving a total structural weight of 5900 kgms.

If no restriction is imposed on the angle of pitch then figures (2.13) and (2.14) decide that the optimum pitch  $\phi = 11.18^\circ$  with

$$I_1 = 4.506 \times 10^8 \text{ mm}^4$$

$$I_2 = 6.147 \times 10^8 \text{ mm}^4$$

In this design both deflexion criteria dominate whereas in the former case only the horizontal deflexion was critical. It is also noticeable that previously the columns were of larger section than the rafters due in the main to the dominating horizontal displacement. In this second design however it is the rafters that require the greatest section due to the comparatively large span and the equally critical vertical deflexion.

The available sections taken from the safe load tables for the variable pitch design are  $21 \times 8\frac{1}{4} \times 55$  U.B. with an I value of  $4.736 \times 10^8 \text{ mm}^4$  for the columns and  $21 \times 8\frac{1}{4} \times 68$  U.B. with an I value of  $6.153 \times 10^8 \text{ mm}^4$  for the rafters. The total weight of this design is 3640 kgms which represents a 38% saving over the fixed geometry design. These figures indicate that in the minimum design the rafters have heavier sections than the columns, and for practical reasons this may not be desirable. It is also noticeable that the required I value necessary for the columns is less than that available in the safe load tables.

A better design with less weight than adopting the rafter section for the whole frame can be obtained by using figure (2.11) and once more altering the pitch of the frame. By moving along the line of constant span away from the optimum pitch the value of the sectional properties may be altered to

$$I_1 = 5.43 \times 10^8 \text{ mm}^4$$

$$I_2 = 5.522 \times 10^8 \text{ mm}^4$$

and  $\phi = 11.85^\circ$

Here the value of I for the rafters has been reduced to that of an available section  $21 \times 8\frac{1}{4} \times 62$  U.B. The second moment of area required for the columns does not differ significantly and therefore these may be fabricated from the same section as the rafters. The final weight of this design is 3633 kgms which is slightly less than the design utilizing available sections and optimum pitch. This is due to the fact that the actual sections employed in the former case did not fit the required optimal design sections as well as in the latter case. Altering the pitch in order to get a better fit has therefore saved weight even though the weight of the actual optimum design is increased.

## 2.7 Design of Pin Jointed Frame

In the case of a pin jointed frame the weight of the frame is proportional to its volume and the objective function is given by

$$z = \sum_i A_i l_i \quad \dots 2.51$$

As there is no bending action in the members the unknowns in the deflexion constraints for such a frame are the cross-sectional areas  $A$  of the members. For a pin jointed frame therefore the linear objective function of equation (2.51) involves no approximation.

The structure, shown in figure (2.15), is two degrees statically indeterminate. The members are placed in three groups. The cross-sectional area of members 2 and 4 is  $A_1$ , that of members 1, 3, 5 and 7 is  $A_2$ , and that of the four diagonals is  $A_3$ . The structure is to be designed so that the vertical deflexions  $y_A$  and  $y_B$  at joints A and B do not exceed 0.02" and 0.01" respectively. The matrix force method was used to derive the deflexion and compatibility equations taking the axial forces in members 9 and 10 as unknown redundants  $R_1$  and  $R_2$ . The non-linear programming problem representing the design thus became

$$\text{minimize } z = 200A_1 + 400A_2 + 400\sqrt{2} A_3$$

subject to

$$10(3/A_2 + 4\sqrt{2}/A_3) - \sqrt{2}R_1(0.5/A_2 + \sqrt{2}/A_3) \leq 0.01E/l$$

$$10(8/A_2 + 1/A_1 + 6\sqrt{2}/A_3) - \sqrt{2}(R_1 + R_2)(0.5/A_1 + 0.5/A_2 + \sqrt{2}/A_3) \leq 0.02E/l$$

$$10(1/A_1 + 2/A_2 + 4\sqrt{2}/A_3)/\sqrt{2} - R_1(0.5/A_1 + 1/A_2 + 2\sqrt{2}/A_3) - R_2(0.5/A_1) = 0$$

$$10(1/A_1 + 1/A_2 + 2\sqrt{2}/A_3)/\sqrt{2} - R_1(0.5/A_1 - R_2(1/A_1 + 1/A_2 + 2\sqrt{2}/A_3)) = 0$$

... 2.52



This problem is five dimensional as there are two unknown redundant forces  $R_1$  and  $R_2$ . These forces however are not independent and may be replaced by functions of the design parameters. To do this the equality constraints are solved simultaneously for the redundants and the resulting expressions substituted into the inequality constraints. This reduces the design space from five dimensions to three dimensions with a feasible design region within which the search for the optimum may proceed. This was not the case when equality constraints were present.

For the purposes of this design additional constraints were added in the form of lower and upper bounds imposed on the design parameters. These were respectively 5 sq.in. and 50 sq.in. The minimum weight design of the frame was found to be

$$A_1 = 5.00 \text{ sq.ins.}$$

$$A_2 = 50.29 \text{ sq.ins.}$$

$$A_3 = 35.70 \text{ sq.ins.}$$

$$\text{with } z = 41,311 \text{ cu.ins.}$$

A total of 27 sub-optimizations was required to reach this local optimum and the computer time required was 17 seconds. The tests of inequalities (2.36) and (2.43) were critical with  $t_3 = t_4 = 0.0001$  indicating that the optimum design lies at a node of the feasible design space.

The constraint on the deflexion at A was the limiting condition although the displacement of B was also very near its permissible value. These vertical displacements  $y_A$  and  $y_B$  in the final design were 0.0200 and 0.0096 inches respectively and the redundant forces  $R_1$  and  $R_2$  were 12.7279 and 2.8159 tons, both compressive forces.

## 2.8 Non-Linear Objective Function

In the design of rigid jointed sway frames the unknown sectional properties appearing in the constraints are the second moment of area of the members. It was stated earlier that a function representing the weight of such a frame in terms of these variables will be non-linear and has the form

$$z = \sum_i c_i l_i l_i^d \quad \dots 2.53$$

where  $c$  and  $d$  are constants.

The proposed algorithm may be used to solve such problems without linearisation of the objective function. This is done by replacing  $-R$  in equations (2.31) and (2.35) by the slope of the objective function at the current design point  $(\partial u / \partial v)_z$ . In this way the direction of search in the  $u-v$  plane is now given by

$$(\partial u / \partial v)_{BC} = 0.5 [(\partial u / \partial v)_c + (\partial u / \partial v)_z] \quad \dots 2.54$$

and the tangency test for the termination of successive sub-optimizations is given by

$$\left| 1 - \left( \frac{\partial u}{\partial v} \right)_c / \left( \frac{\partial u}{\partial v} \right)_z \right| < t_2 \quad \dots 2.55$$

The slope of the objective function is calculated numerically in the same way as the slopes of the constraints using equation (2.40).

The fact that a new direction of search is always between the tangents of the critical constraint and the objective function ensures that even with a non-linear objective function if a small enough step is taken then both the feasibility and the optimality of the solution will benefit. It becomes necessary however to test the objective function value after each successive step and if this should increase before a boundary is reached the search direction is recalculated using equation (2.54).

With particular reference to the portal frame shed design the non-linear objective function given by equation (2.19) may be simplified to

$$z = I_1^d + R I_2^d \quad \dots 2.56$$

and used instead of the linear objective function given by equation (2.23). This is the equation of a curve in  $I_1$  and  $I_2$  with a slope obtained by differentiation of

$$\frac{\partial I_1}{\partial I_2} = -R \left( \frac{I_2}{I_1} \right)^{d-1} \quad \dots 2.57$$

The slope of this curve is equal to that of the linear objective function when  $I_1 = I_2$ . When using universal beam sections for the columns and rafters of the frames the constant  $d$  may be assumed to have a value of 0.5.

The effect of using this objective function is to speed up the searching process due to the fact that the second derivative is positive. This means that the longer any direction of search can be pursued before a boundary is encountered the greater is the rate at which the optimality of the solution is improved. This is shown diagrammatically in figure (2.16) where it can be seen that as the linear direction of search from B to C is pursued the line of constant objective function  $z_1$  through B becomes more distant. The linearised line of constant objective function,  $z_2$ , is also shown passing through B and the direction of search obtained using this, from B to C, does not have such a beneficial effect.

The effect of incorporating a non-linear objective function into the proposed algorithm is demonstrated by re-designing a set of the portal frames dealt with earlier in this chapter. A column height of 9 metres is chosen and the span to height ratio  $q$  is fixed at 2.33. The angle of pitch of the roof is once again varied between  $0^\circ$  and  $40^\circ$ .

The graphs of figure (2.17) show the second moment of area required for the columns and rafters for the various angles of pitch when using the linear and non-linear objective functions. Curve a represents the non-linear design and curve b the linear. Once again these curves have three distinct segments. The first portion between  $0^\circ$  and approximately  $9^\circ$  represents designs in which the vertical deflexion constraint is critical. It is immediately noticeable that in this range when using a non-linear objective function the resulting designs have heavier sections for the rafters and lighter sections for the columns than when using a linear objective function. For a frame of pitch  $5^\circ$  the following results were obtained

	COLUMNS	RAFTERS	OBJECTIVE FUNCTION
Non-Linear	$3.899 \times 10^8 \text{ mm}^4$	$8.043 \times 10^8 \text{ mm}^4$	$5.296 \times 10^4 \text{ mm}^2$
Linear	$4.314 \times 10^8 \text{ mm}^4$	$7.657 \times 10^8 \text{ mm}^4$	$5.318 \times 10^4 \text{ mm}^2$

In this case the movement of weight into the rafters has resulted in an overall weight saving of 0.41% only.

The second portion of the curves a and b lies approximately between  $9^\circ$  and  $12.5^\circ$ . In this range both horizontal and vertical deflexion constraints are equally active and it is here that the optimum angle of pitch is to be found. Due to the fact that within this range the optimum design lies at a node of the feasible design space there is no difference between the design obtained using the linear or non-linear objection functions. This situation is illustrated diagrammatically in figure (2.4) which shows both the linear and non-linear objective functions.

The final portion of the curves is for angles of pitch greater than  $12.5^\circ$ . In this region it is the horizontal deflexion limitation which

dominates the design and use of the non-linear objective function is seen to reduce the moment of inertia required for the rafters while increasing that of the columns. For a frame of pitch  $25^{\circ}$  the following results were obtained

	COLUMNS	RAFTERS	OBJECTIVE FUNCTION
Non-Linear	$10.034 \times 10^8 \text{ mm}^4$	$9.191 \times 10^8 \text{ mm}^4$	$7.071 \times 10^4 \text{ mm}^2$
Linear	$10.000 \times 10^8 \text{ mm}^4$	$9.211 \times 10^8 \text{ mm}^4$	$7.071 \times 10^4 \text{ mm}^2$

The saving in weight is zero, indeed the alteration in the design sections is insignificant due to the fact that the ratio  $I_2/I_1$  is near unity having a value 0.919.

Figure (2.18) is a graph of the angle of pitch versus the value of the non-linear objective function of equation (2.56) corresponding to the linear and non-linear optimum designs. It is verified here that a small weight saving of about 0.4% is possible when the vertical deflexion dominates the design, however for pitches greater than about  $9^{\circ}$  the weights resulting from the linear and non-linear treatments are substantially the same.

## 2.9 Conclusions

The non-linear programming procedure proposed in this chapter has been useful in the optimum design of structures subject to deflexion limitations. In the designs carried out stress considerations were not considered. This aspect of design can be included without difficulty, however, and the necessary constraints may be constructed using either the matrix force or displacement methods. Such an addition to the design problem does not alter the proposed method of solution.



The method, however, would only seem to be practical for small problems due to the concept of sub-optimisation. Difficulties may also arise when large numbers of constraints are involved as only the most critical is considered when determining the new direction of search. Should several constraints be nearly critical simultaneously this direction may soon lead to an infeasible design. In such cases the most beneficial direction of search is probably in a hyper-space. This fact necessitates the simultaneous variation of several parameters and is treated in more detail in Chapter 4.

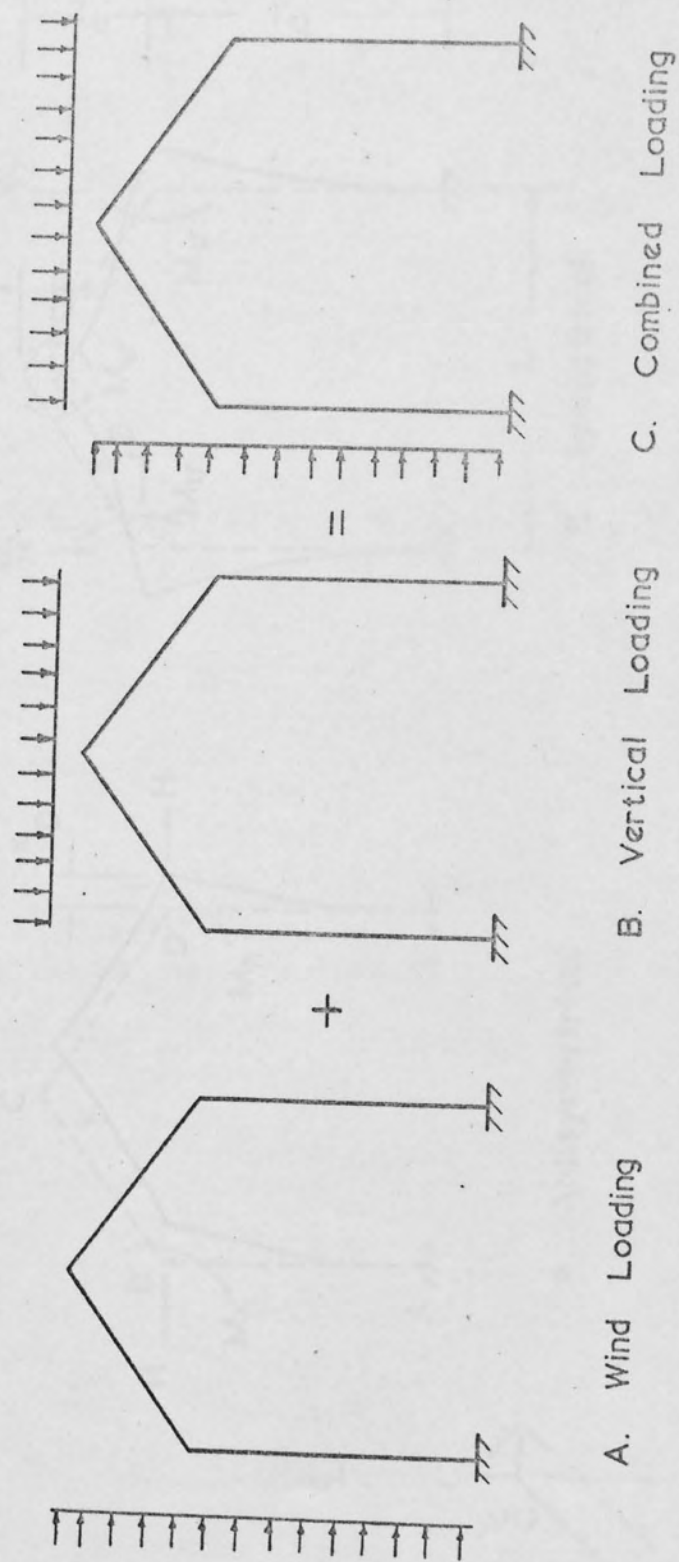


Figure 2.1. Frame Loading

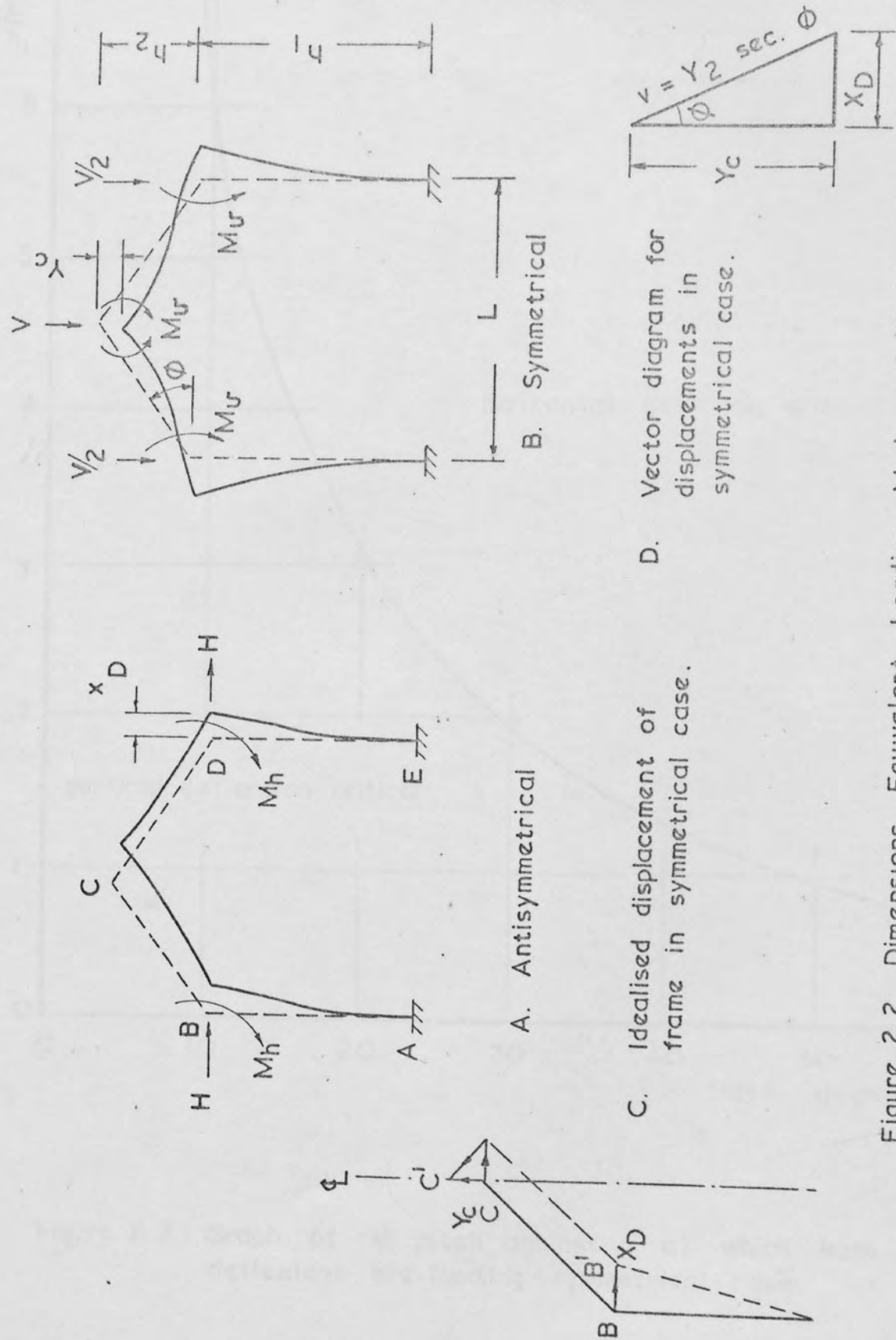


Figure 2.2. Dimensions, Equivalent Loading Modes of Deformation

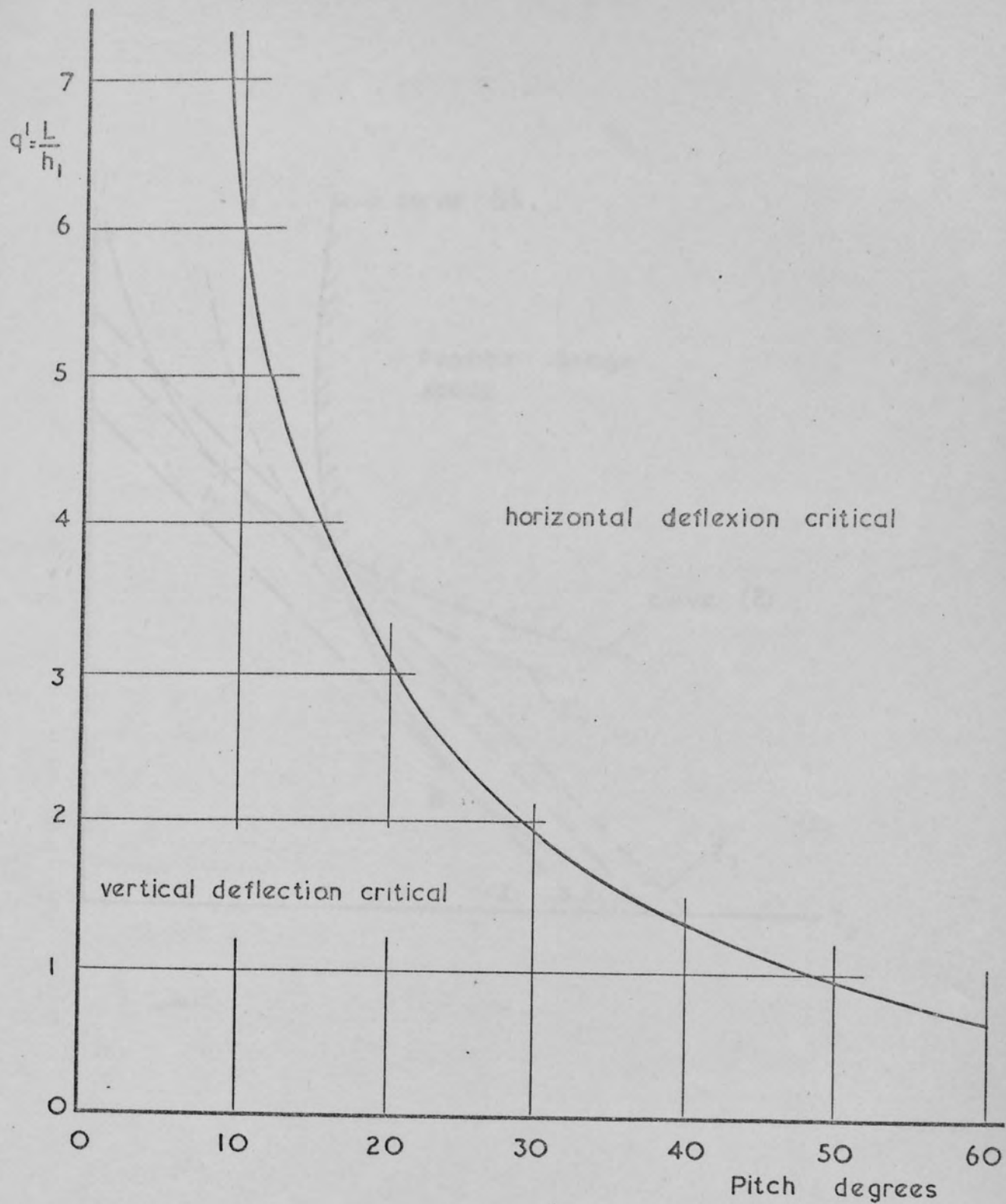


Figure 2.3. Graph of  $\phi$  pitch against  $q'$  at which both deflexions are limiting - symmetrical case.

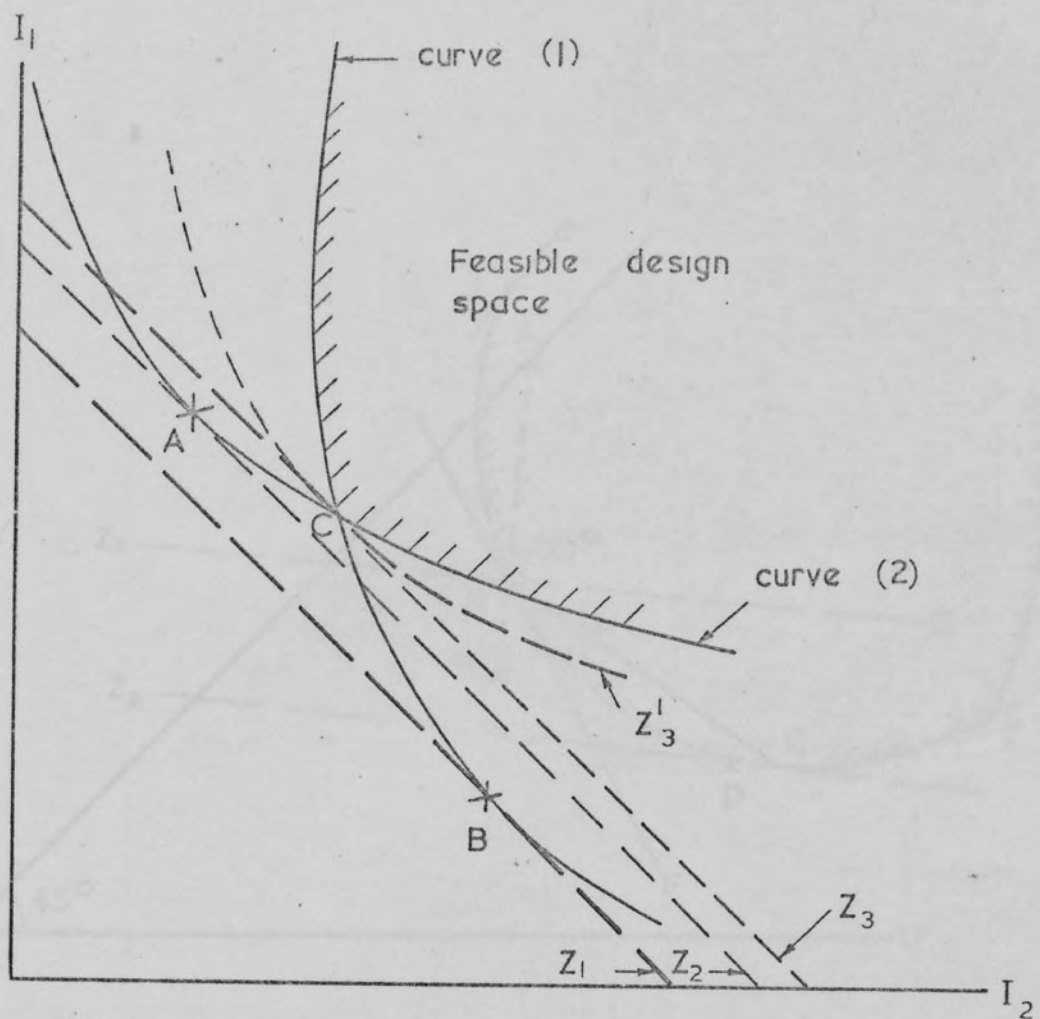


Figure 2.5. Aspects of design procedures

Figure 2.4. Aspects of optimum designs



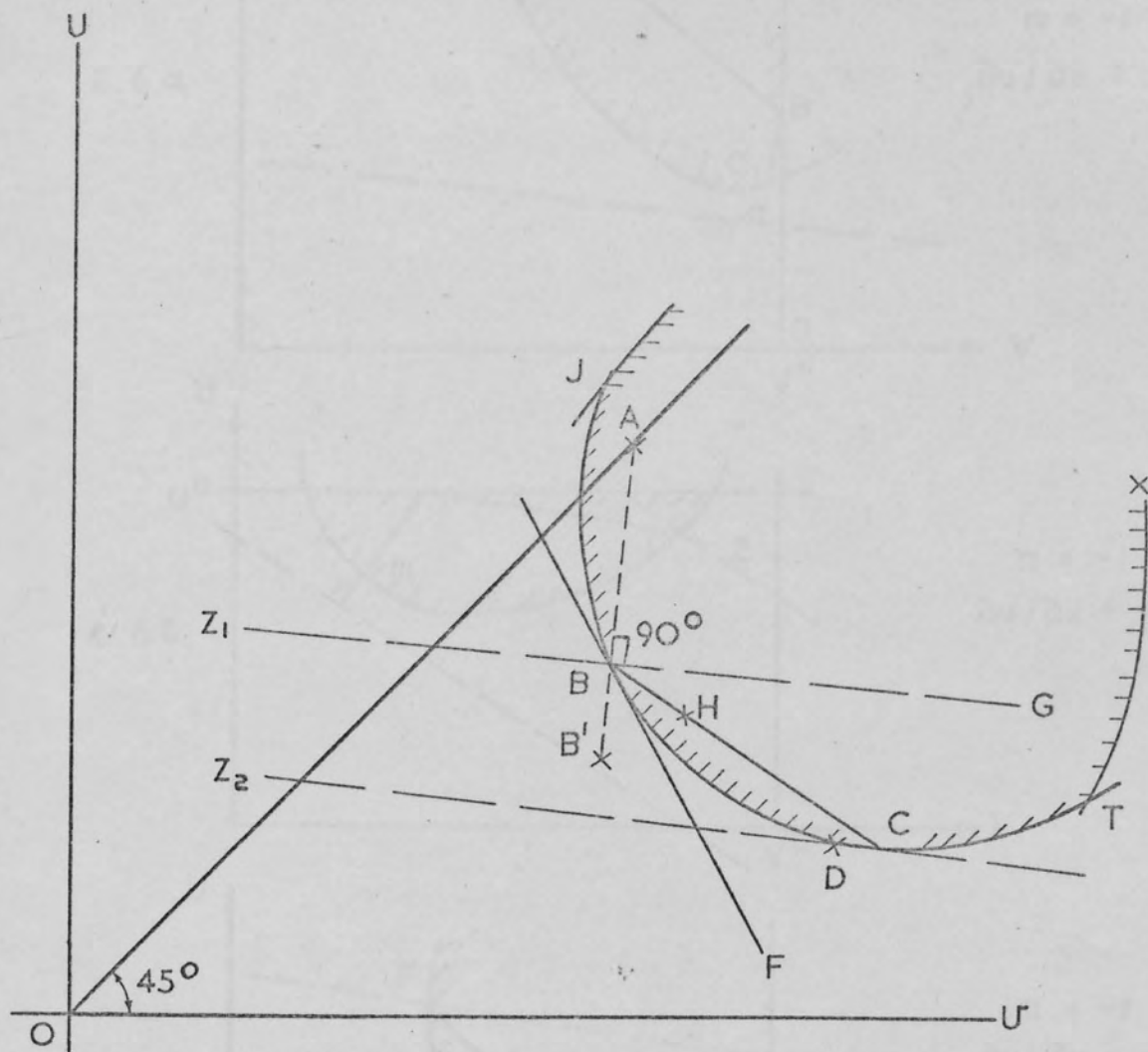
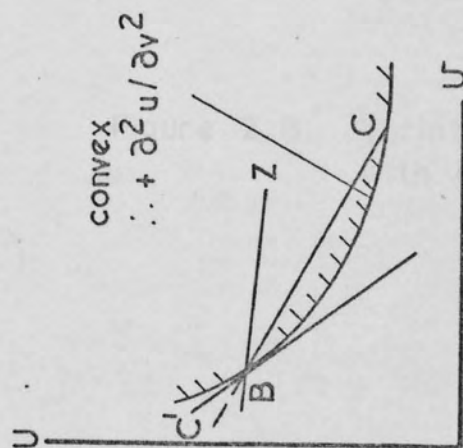
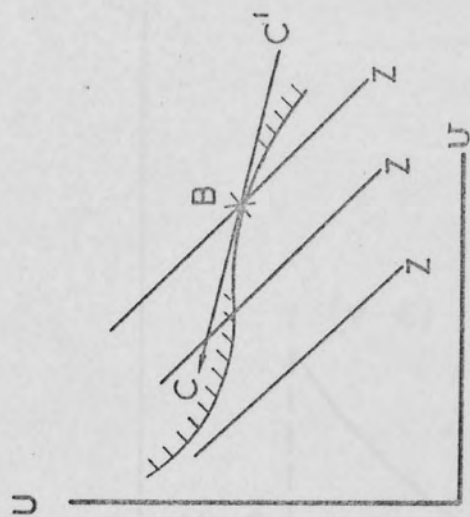


Figure 2.5. Aspects of design procedure





2.7a.  $\partial^2 u / \partial v^2$  is positive.  
 Search is continued  
 along  $BC$  not  $BC'$



2.7 b.  $\partial^2 u / \partial v^2$  is negative.  
 Search in direction of  
 decreasing  $v$  along  $BC$ .

Figure 2.7. Types of boundary solution possible

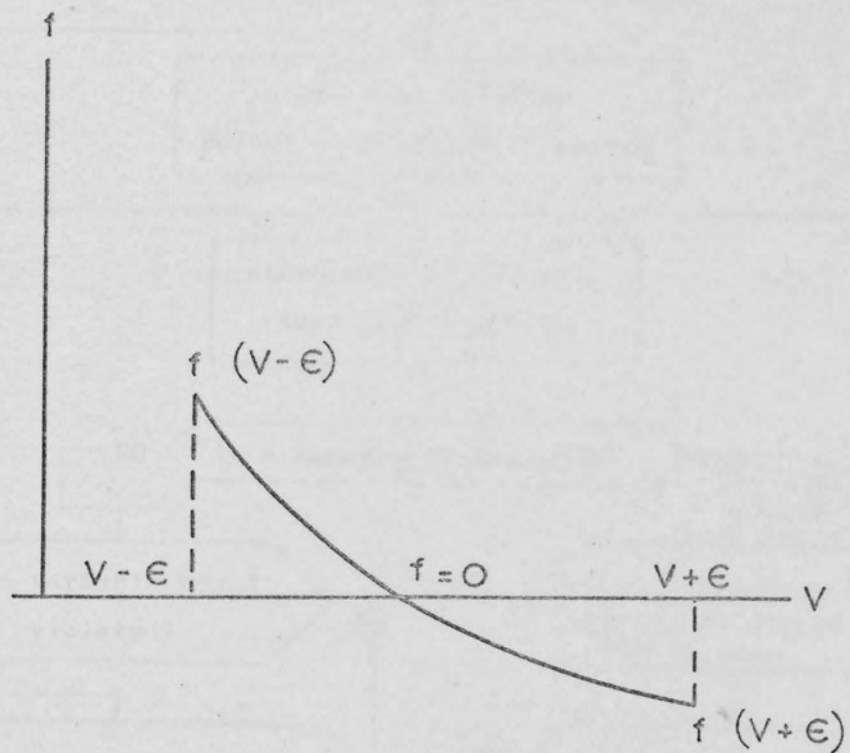


Figure 2.8. Variation of a constraint  $f$  with a variable  $V$ .

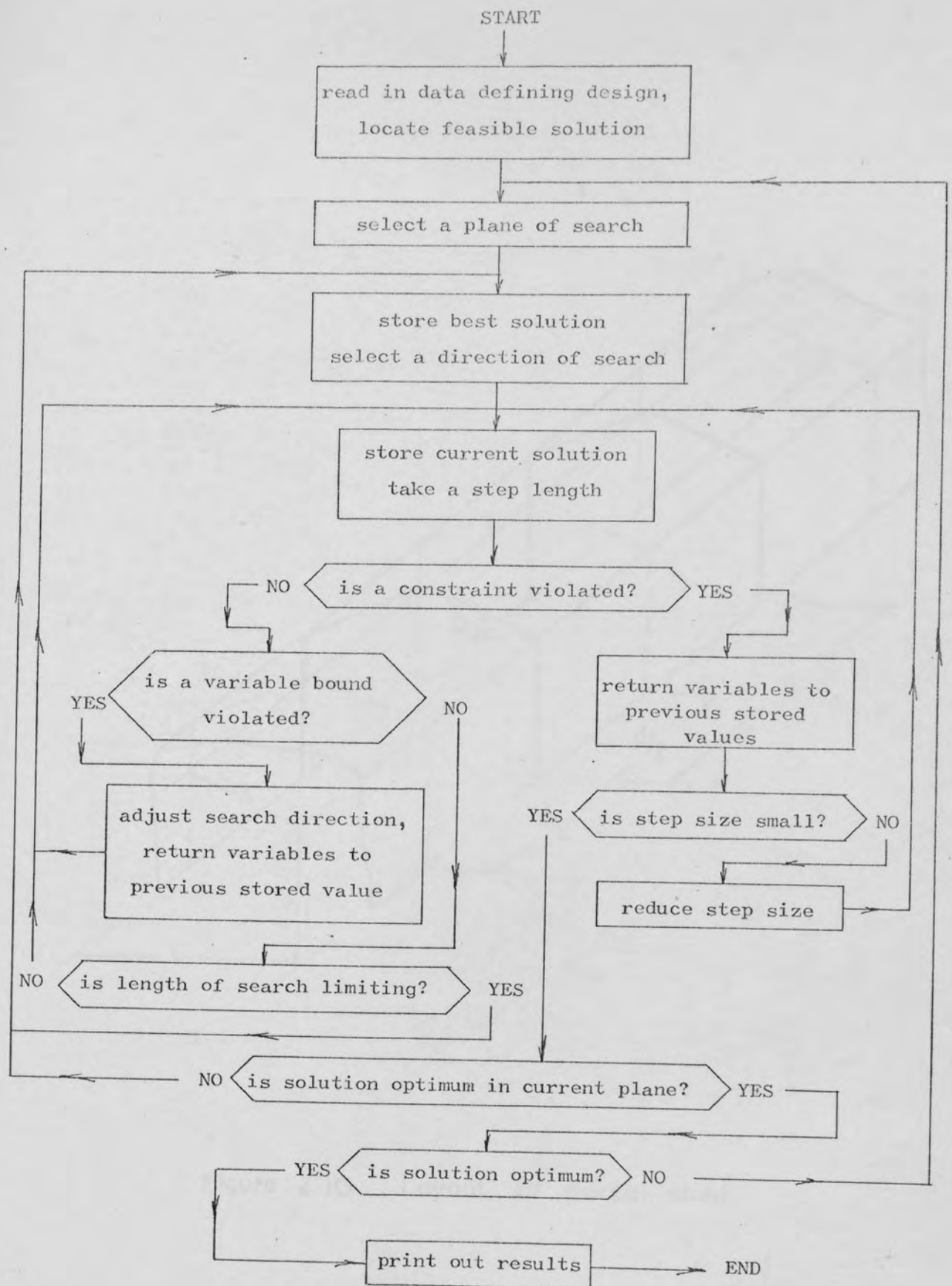


Figure 2.9 Flow Diagram of design procedure



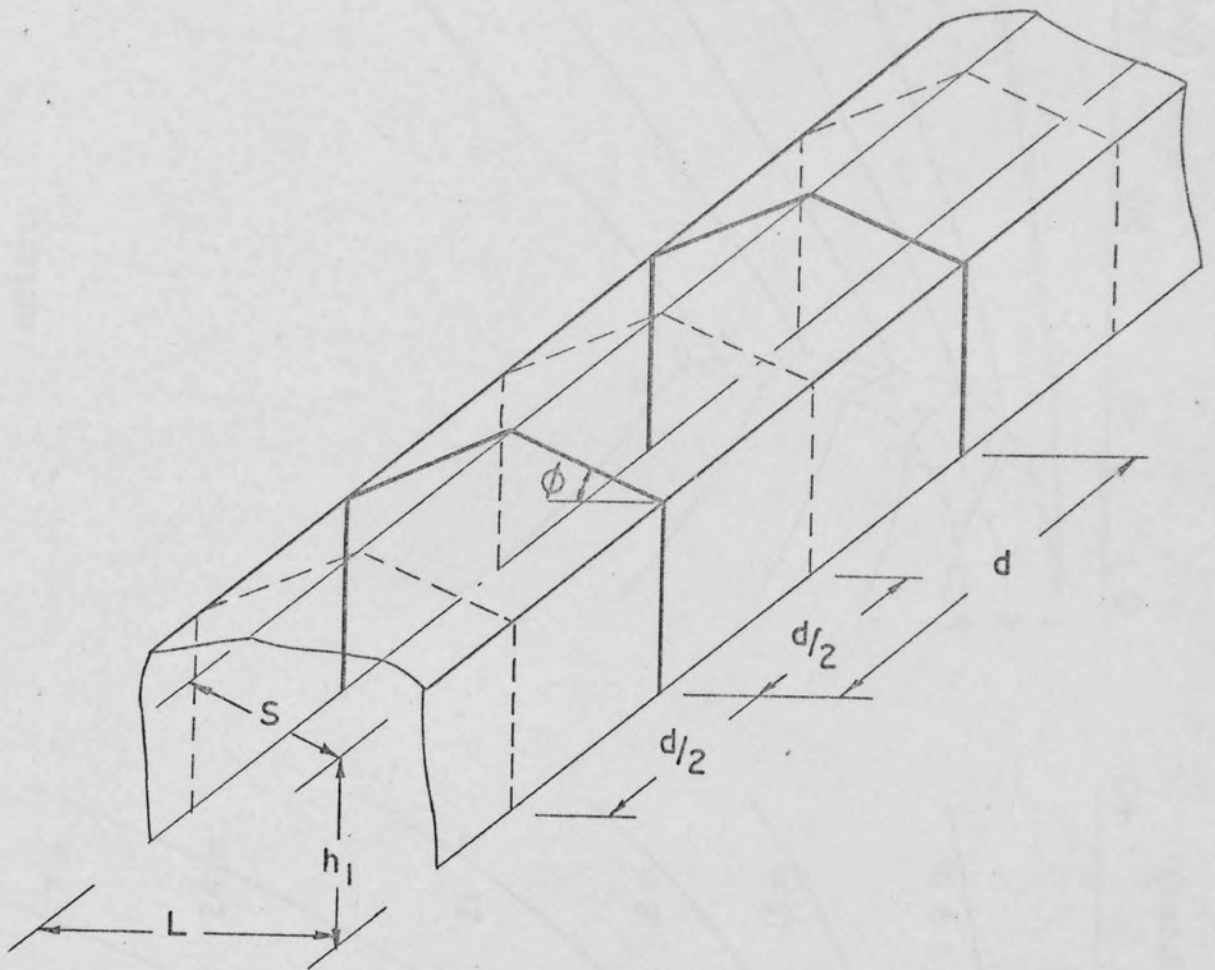
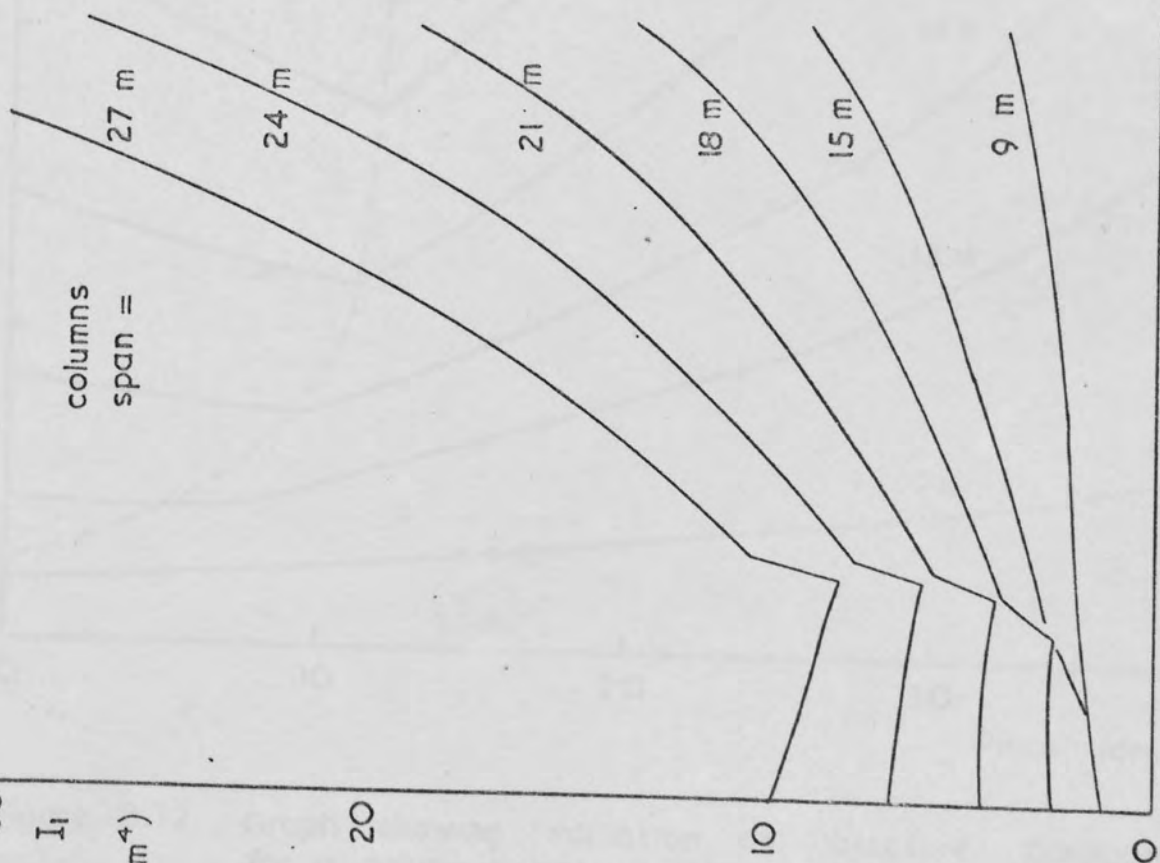


Figure 2.10 Layout of portal shed.

$I_1$   
( $\times 10^8 \text{ mm}^4$ )

columns  
span =



$I_2$   
( $\times 10^8 \text{ mm}^4$ )

rafters

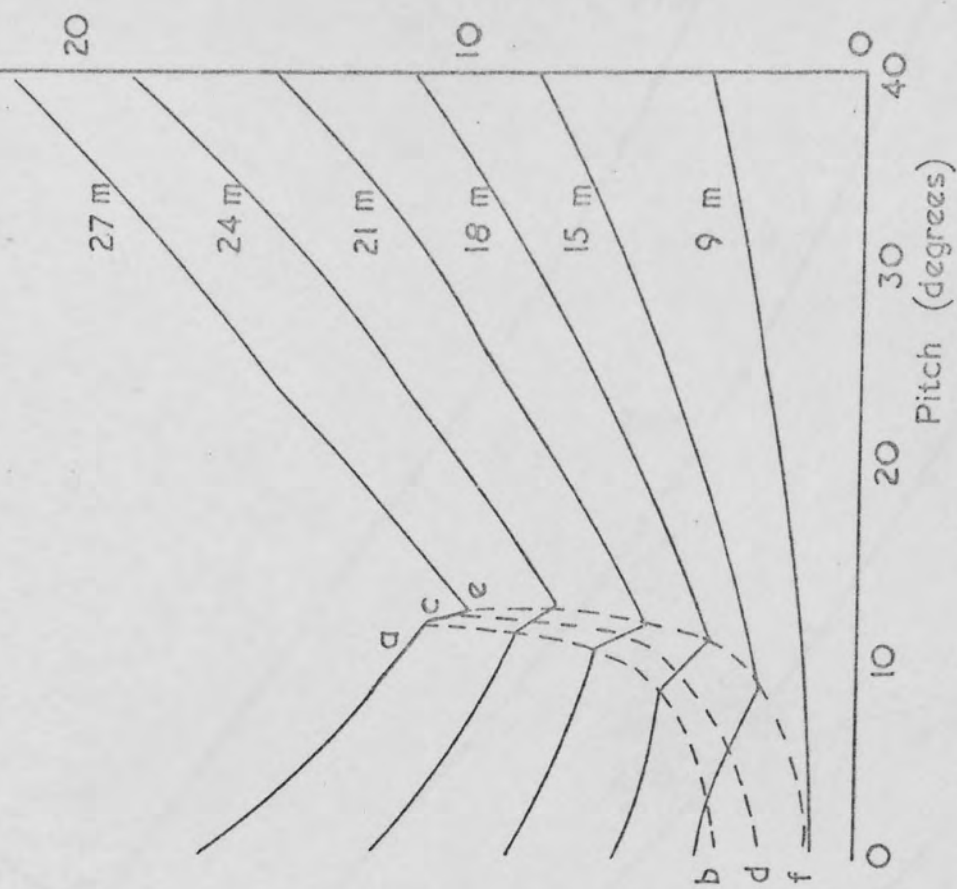


Figure 2.11. Design charts for column height of 9 metres (29.527 feet)

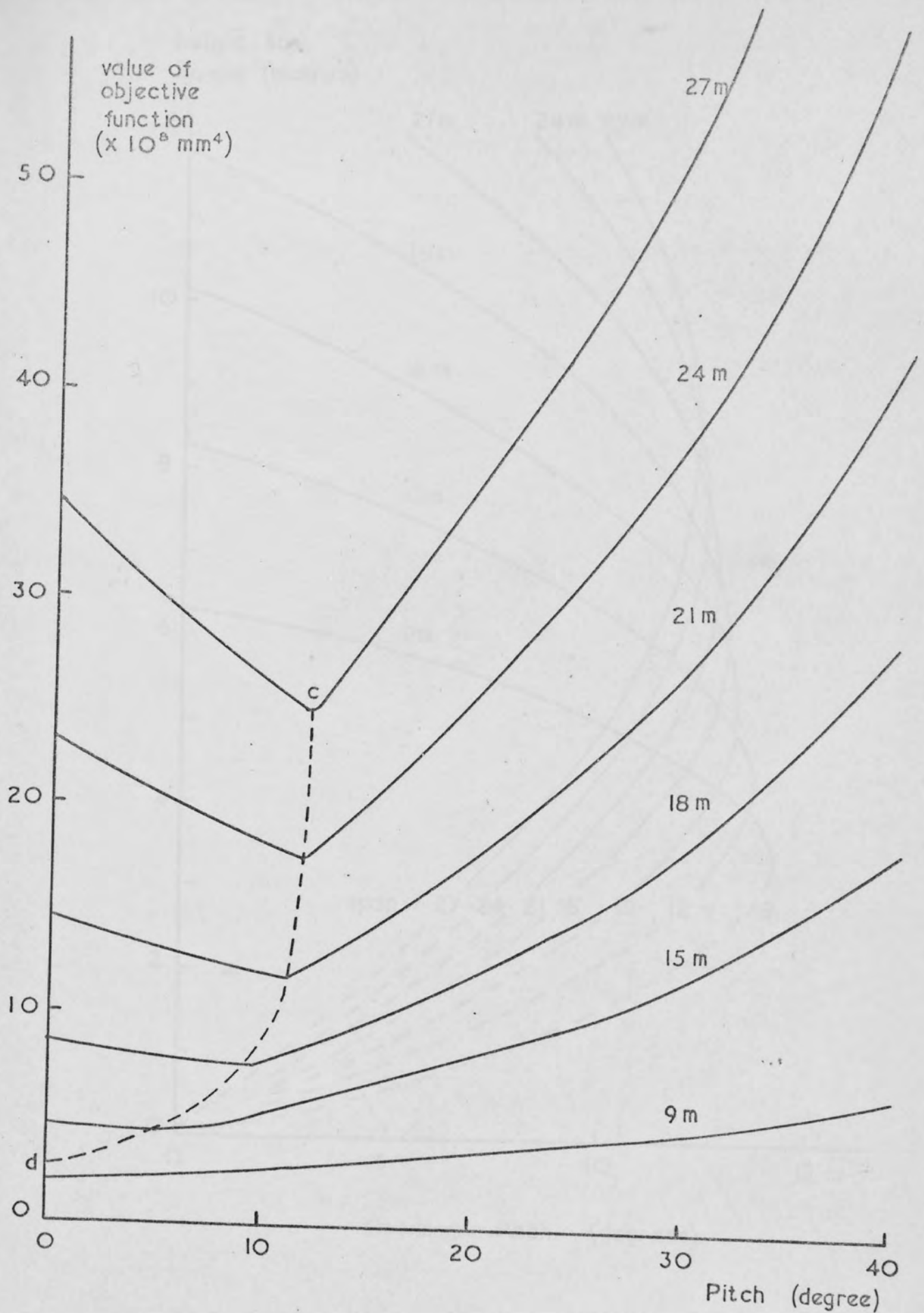


Figure 2.12. Graph showing variation of objective function for a column height of 9 metres (29.527 feet) with pitch and span

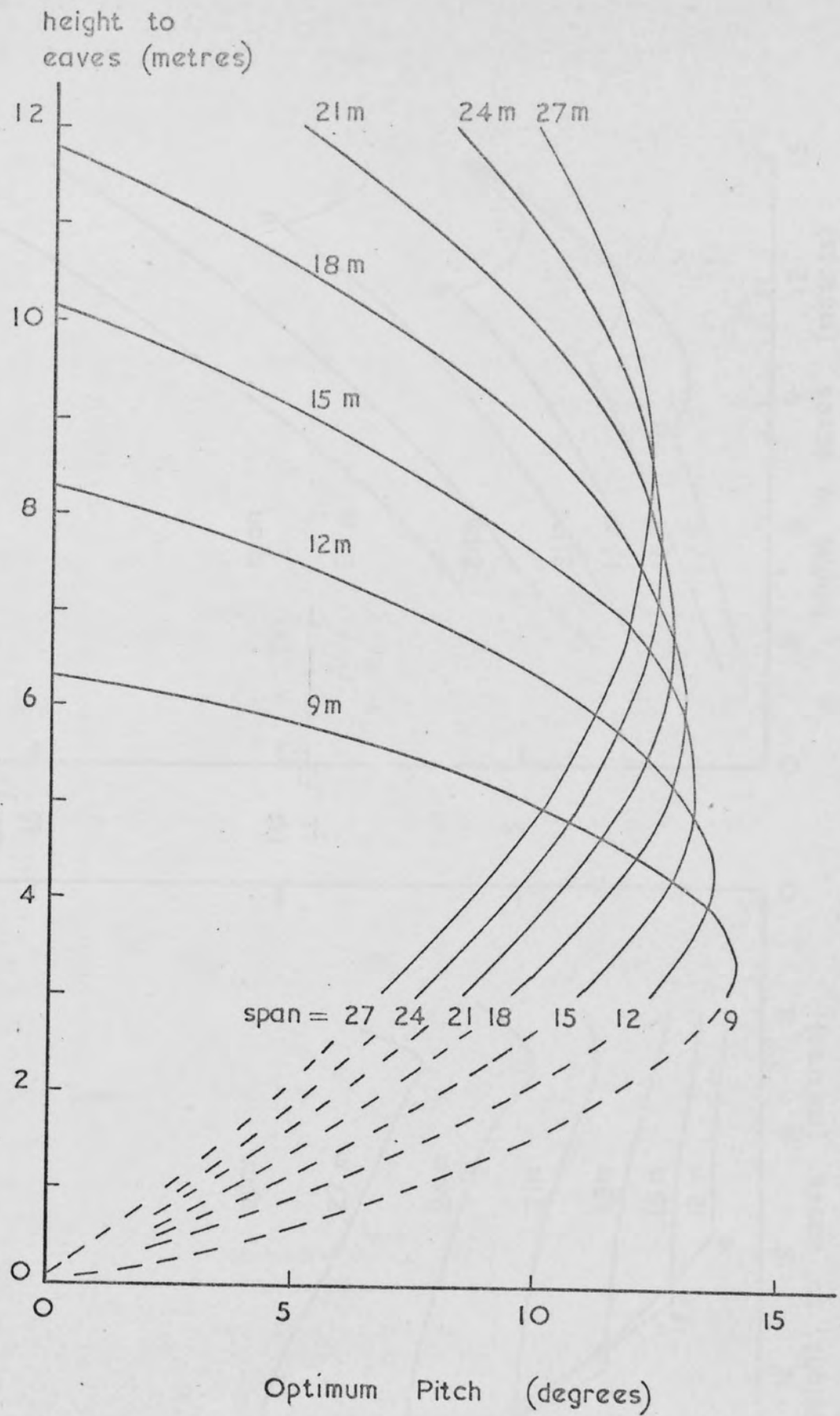


Figure 2.13. Design chart giving optimum pitch for portal frame of given height and span

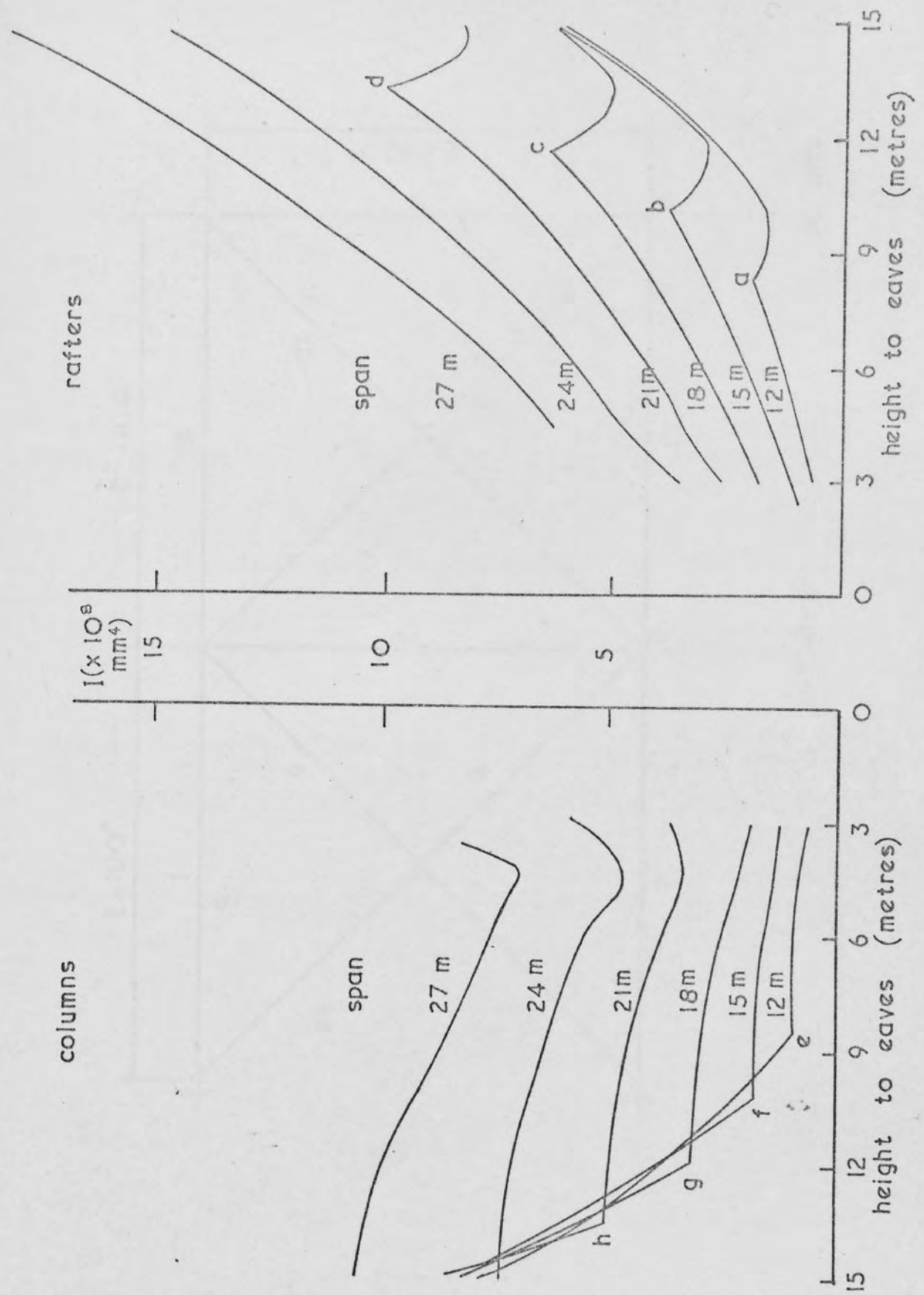


Figure 2.14. Design chart using optimum pitch for rafters



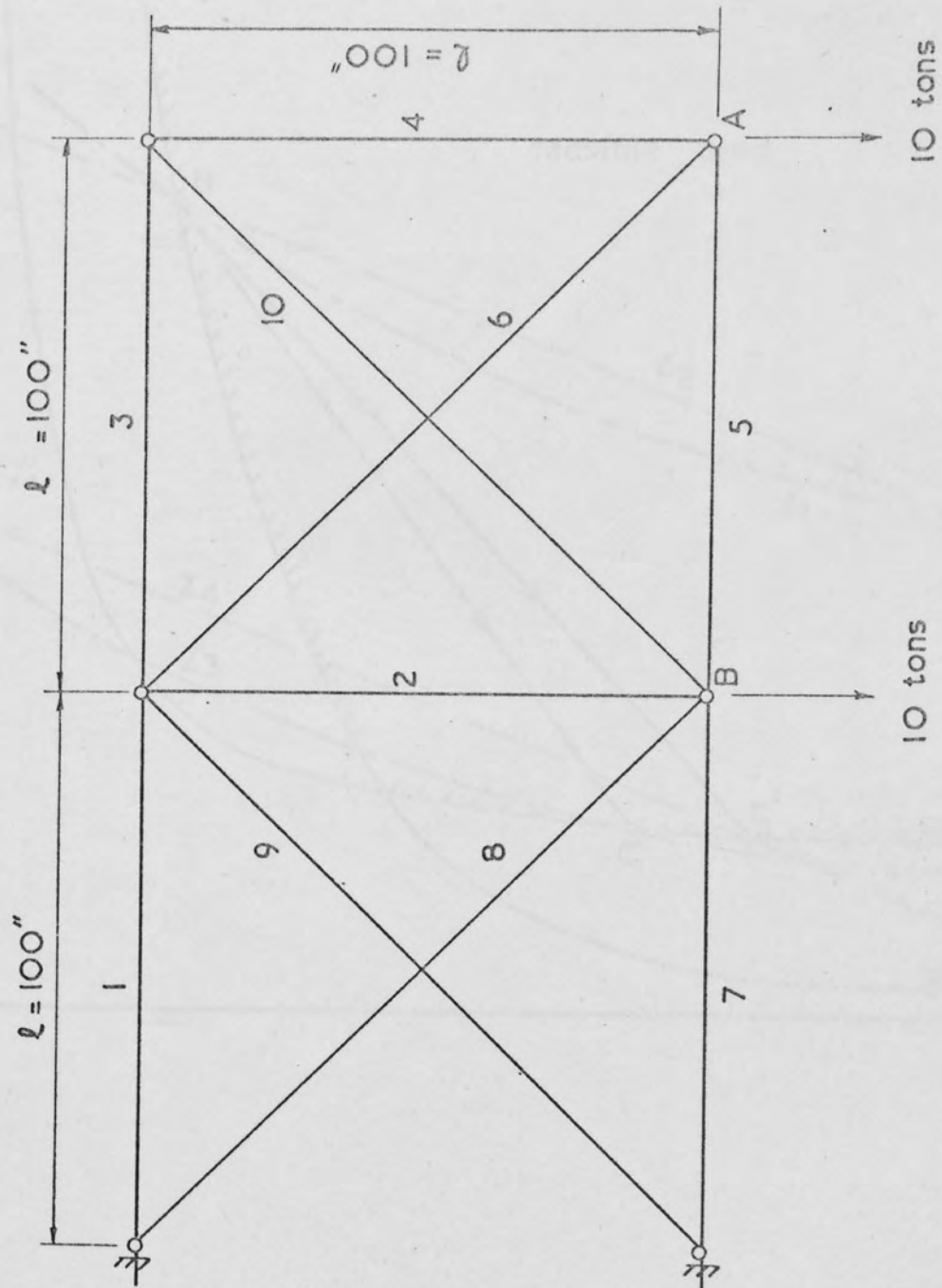


Figure 2.15. Pin jointed frame

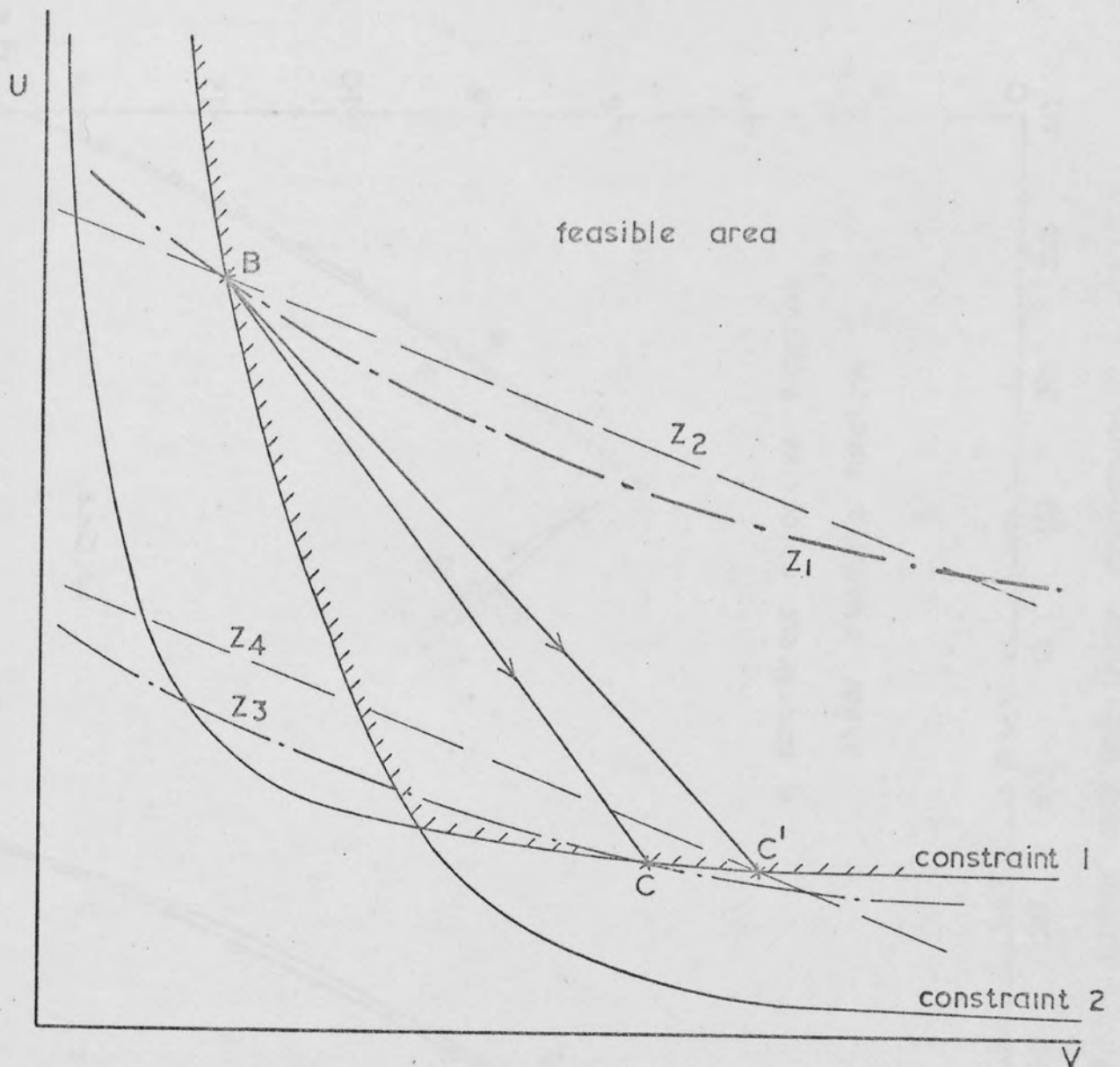


Figure 2.16. Effect of non-linear objective function on direction of search.

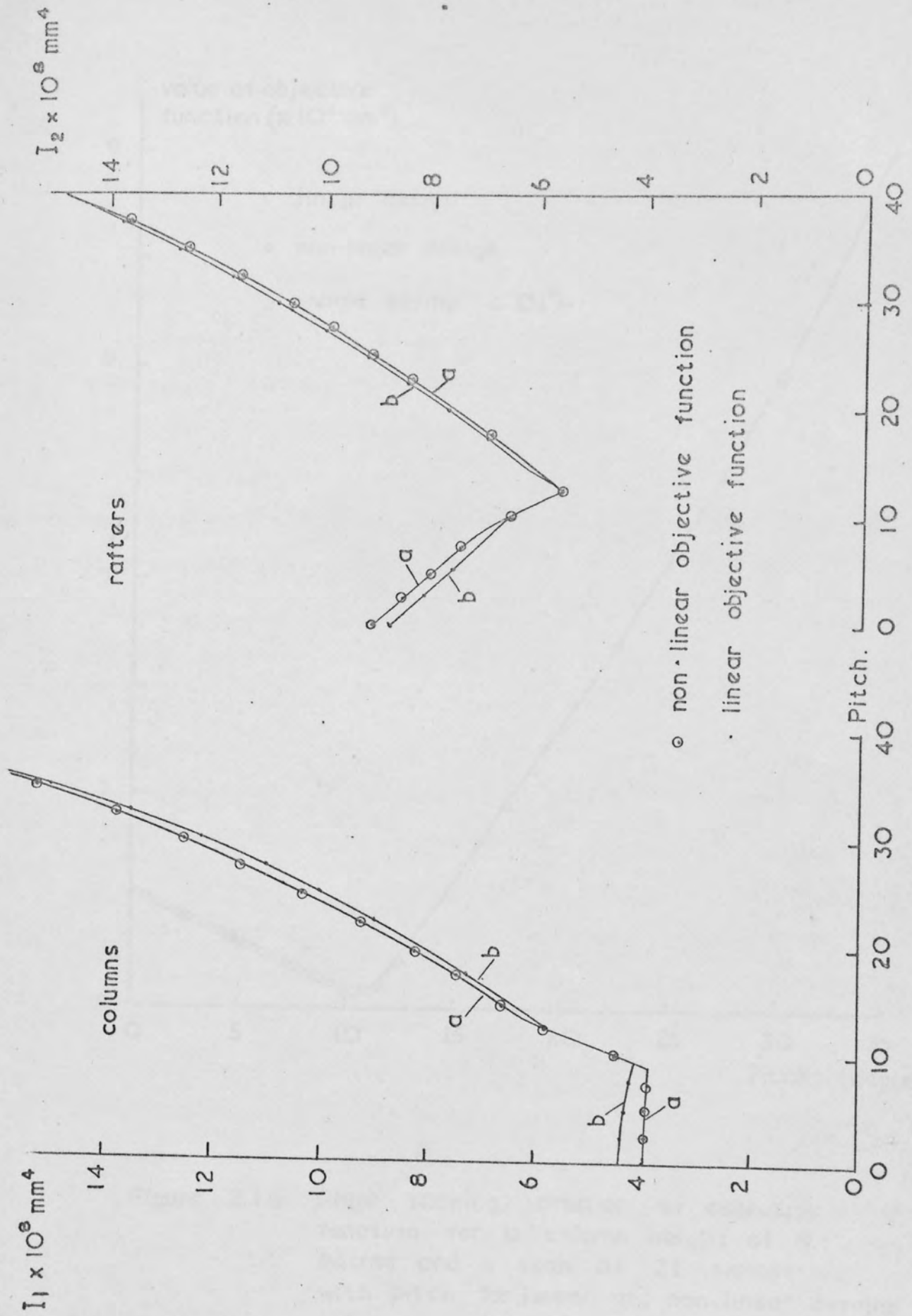


Figure 2.17 Linear and non-linear comparison

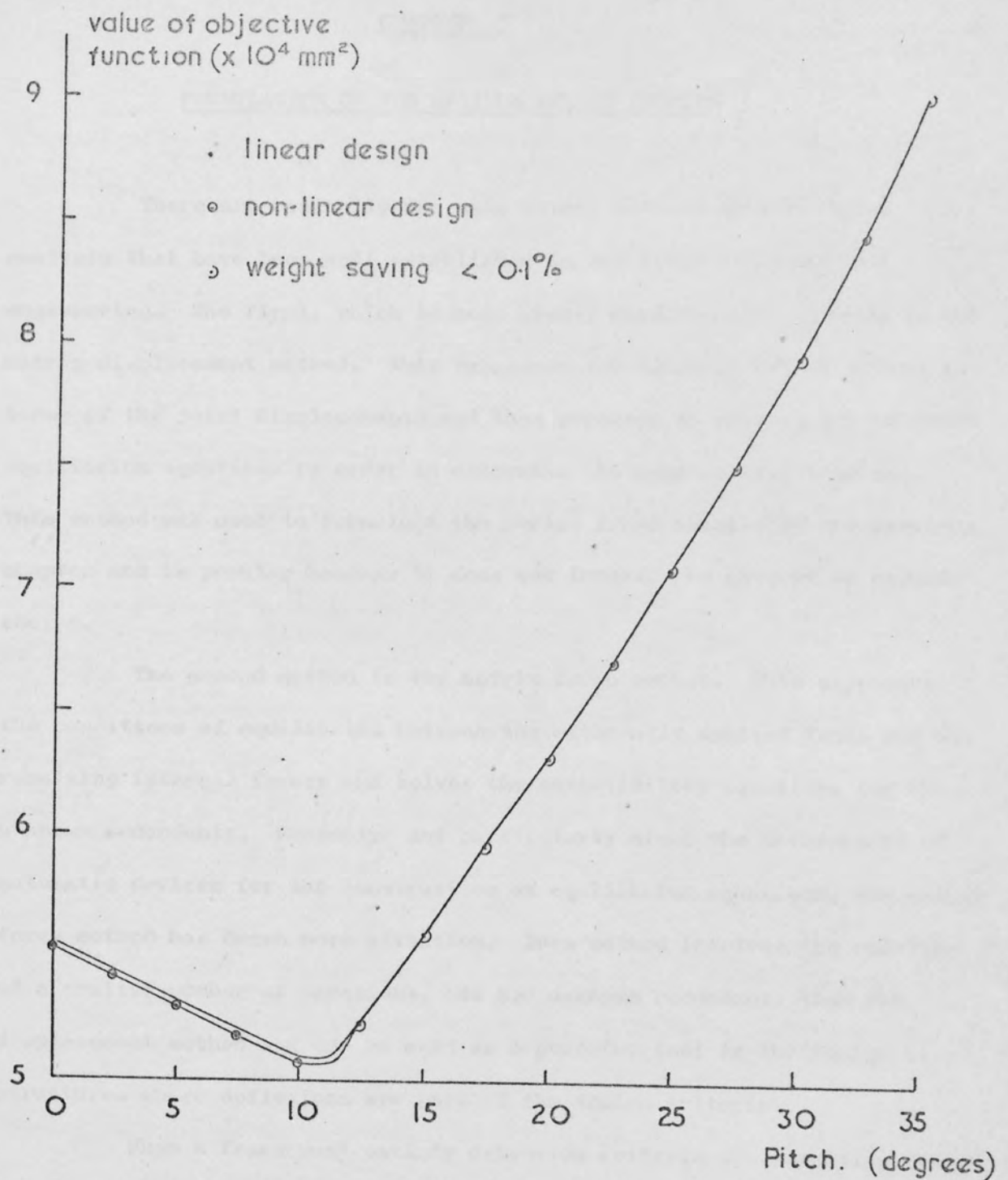


Figure 2.18. Graph showing variation of objective function for a column height of 9 metres and a span of 21 metres with pitch for linear and non-linear designs

CHAPTER 3FORMULATION OF THE OPTIMUM DESIGN PROBLEM

There are basically two main matrix methods of structural analysis that have been well established in the field of structural engineering. The first, which is more widely used than the second, is the matrix displacement method. This expresses the internal member forces in terms of the joint displacements and then proceeds to solve a set of joint equilibrium equations in order to determine the unknown displacements. This method was used to formulate the portal frame example of the previous chapter and is popular because it does not involve the concept of redundancies.

The second method is the matrix force method. This expresses the conditions of equilibrium between the externally applied loads and the resulting internal forces and solves the compatibility equations for the unknown redundants. Recently, and particularly since the development of automatic devices for the construction of equilibrium equations, the matrix force method has drawn more attention. This method involves the solution of a smaller number of equations, one per unknown redundant, than the displacement method and can be used as a powerful tool in the design of structures where deflexions are part of the design criteria.

When a frame must satisfy deflexion criteria the resulting design may be appreciably heavier than a design which satisfied only strength requirements. In such cases it is important to ensure that the structural material is used in the most efficient manner. This can be accomplished by adopting a minimum weight approach to design.



The problem is to design general statically indeterminate frames for minimum weight and to satisfy both deflexion and strength requirements. In particular, certain of the deflexions of the frame, the 'constrained deflexions', must not exceed specified permissible values until the working load level is exceeded. When formulating the design problem it is assumed that the behaviour of the frame is linear elastic. It is further assumed that a continuous range of sections is available and no attempt will be made to design directly in discrete sections.

The optimum design of structures may be carried out with reference to a number of its aspects. In Chapters 4 and 5 of this thesis the optimization is carried out with reference to structures of fixed geometry. Member sizes are selected so that the overall weight of the structure is minimized while a set of deflexion and stress limitations is satisfied.

The structures dealt with may be two or three dimensional having pinned joints. However, the method of formulation and the proposed method of solution is also applicable to rigidly jointed frames, provided that it can be assumed that the weight of a section is proportional to its second moment of area.

The design problem can be formulated using either the matrix displacement or the matrix force method. In the case of statically indeterminate structures with deflexion constraints, the matrix force method develops fewer constraints and therefore it is adopted here. The matrix force method can be modified to express all the constraints of the problem. In the case of hyperstatic structures these are of three types, namely the stress, the deflexion and the compatibility constraints.

### 3.1 The Matrix Force Method

For a member of a pin jointed structure the relationship between the axial force,  $p$ , and the extension of the member  $\delta$  can be obtained using

The problem is to design general statically indeterminate frames for minimum weight and to satisfy both deflexion and strength requirements. In particular, certain of the deflexions of the frame, the 'constrained deflexions', must not exceed specified permissible values until the working load level is exceeded. When formulating the design problem it is assumed that the behaviour of the frame is linear elastic. It is further assumed that a continuous range of sections is available and no attempt will be made to design directly in discrete sections.

The optimum design of structures may be carried out with reference to a number of its aspects. In Chapters 4 and 5 of this thesis the optimization is carried out with reference to structures of fixed geometry. Member sizes are selected so that the overall weight of the structure is minimized while a set of deflexion and stress limitations is satisfied.

The structures dealt with may be two or three dimensional having pinned joints. However, the method of formulation and the proposed method of solution is also applicable to rigidly jointed frames, provided that it can be assumed that the weight of a section is proportional to its second moment of area.

The design problem can be formulated using either the matrix displacement or the matrix force method. In the case of statically indeterminate structures with deflexion constraints, the matrix force method develops fewer constraints and therefore it is adopted here. The matrix force method can be modified to express all the constraints of the problem. In the case of hyperstatic structures these are of three types, namely the stress, the deflexion and the compatibility constraints.

### 3.1 The Matrix Force Method

For a member of a pin jointed structure the relationship between the axial force,  $p$ , and the extension of the member  $\delta$  can be obtained using

Hooke's law as

$$p = \frac{EA}{l} \delta \quad \dots 3.1$$

This equation may be rearranged so that the extension of the member is expressed in terms of the force; thus

$$\delta = \frac{1}{EA} p \quad \dots 3.2$$

Here  $1/EA$  is the flexibility of the member. For all the members of a structure similar equations can be written and expressed in matrix form as

$$\underline{Z} = \underline{f} \underline{p} \quad \dots 3.3$$

where  $\underline{f}$  is the member flexibility matrix for all the members, which relates the vector of member forces  $\underline{p}$  to the vector of corresponding member displacements  $\underline{Z}$ . It can be seen that the flexibility matrix  $\underline{f}$  includes the reciprocals of the section properties.

The equilibrium conditions between the externally applied loads  $\underline{L}$  on a structure and the resulting member forces  $\underline{p}$  may be expressed in matrix form as

$$\underline{p} = \underline{B} \underline{L} \quad \dots 3.4$$

Matrix  $\underline{B}$  is called the load transformation matrix and can be constructed from the equilibrium conditions in the structure.

In a statically indeterminate structure the applied load system is divided into two categories. These are the external loads  $\underline{L}_b$  acting on the basic statically determinate structure and a set of redundant reactions  $\underline{L}_r$ . The load vector therefore becomes  $\underline{L} = \{\underline{L}_b \underline{L}_r\}$  and is accompanied by a partitioning of the load transformation matrix such that  $\underline{B} = \{\underline{B}_b, \underline{B}_r\}$ . Equation (3.4) may now be re-written as

$$\underline{p} = \underline{B}_b \underline{L}_b + \underline{B}_r \underline{L}_r \quad \dots 3.5$$

From the definitions of  $\underline{B}_b$  and  $\underline{B}_r$  it can be seen that these matrices are determined from the frame geometry, the loading pattern and the positions of the selected redundants. These matrices therefore consist of constant terms being independent of the sectional properties of the structural members. Each row of  $\underline{B}_b$  and  $\underline{B}_r$  corresponds to a particular member force.

The column vector  $\underline{L}_b$  includes all the non-zero external loads acting upon the frame. The size of matrix  $\underline{B}_b$  depends upon this vector as each column corresponds to an externally applied load.

The relationship between the externally applied loads and the nodal displacements is obtained by means of the overall flexibility matrix of the structure. This relationship may be expressed in matrix form as follows

$$\begin{bmatrix} \underline{B}_b' \underline{f} \underline{B}_b & \underline{B}_b' \underline{f} \underline{B}_r \\ \underline{B}_r' \underline{f} \underline{B}_b & \underline{B}_r' \underline{f} \underline{B}_r \end{bmatrix} \begin{bmatrix} \underline{L}_b \\ \underline{L}_r \end{bmatrix} = \begin{bmatrix} \underline{X}_b \\ \underline{X}_r \end{bmatrix} \quad \dots 3.6$$

The displacements corresponding to  $\underline{L}_b$  and  $\underline{L}_r$  are  $\underline{X}_b$  and  $\underline{X}_r$  respectively. It is assumed that there is no lack of fit in the structure, and therefore  $\underline{X}_r$  is a null vector. Equations (3.6) give the deflexions at only those points at which an external load acts. Furthermore the displacement takes place along the line of action of the corresponding load. If any other deflexion is required it is necessary to include a corresponding zero term in the load vector.

Replacing  $\underline{B}' \underline{f} \underline{B}$  by the matrix  $\underline{F}$ , and using the same subscripts b and r, equations (3.6) can be written as

$$\underline{F}_{bb} \underline{L}_b + \underline{F}_{br} \underline{L}_r = \underline{X}_b \quad \dots 3.7$$

$$\underline{F}_{rb} \underline{L}_b + \underline{F}_{rr} \underline{L}_r = \underline{0} \quad \dots 3.8$$

In equation (3.8) the displacement vector  $\underline{X}_r$  has been replaced by a null vector  $\underline{0}$ . The matrices  $\underline{F}_{bb}$ ,  $\underline{F}_{br}$ ,  $\underline{F}_{rb}$  and  $\underline{F}_{rr}$  are the overall flexibility matrices of the structure and each element of these matrices includes the reciprocal of the section properties. The order of the square matrices  $\underline{F}_{bb}$  and  $\underline{F}_{rr}$  depends upon the number of external loads and the number of redundants respectively, whilst the orders of  $\underline{F}_{br}$  and  $\underline{F}_{rb}$  depends upon both.

When the structure is subjected to several independent sets of loads the vectors  $\underline{p}$ ,  $\underline{L}_b$ ,  $\underline{L}_r$ ,  $\underline{X}_b$  and  $\underline{X}_r$  become matrices. Each column of these matrices corresponds to a loading case, and the number of rows in matrices  $\underline{L}_b$  and  $\underline{X}_b$  depends upon the number of loads applied throughout all the loading conditions. The load transformation matrices and the overall flexibility matrices, however, remain unaltered.

For pin jointed frameworks the design problem can now be stated as the determination of the unknown section properties and redundant forces to

$$\text{minimize } z = \sum_j 1_j A_j \quad \dots 3.9$$

$$\text{subject to } \underline{F}_{bb} \underline{L}_b + \underline{F}_{br} \underline{L}_r \leq \underline{\Delta} \quad \dots 3.10$$

$$\underline{F}_{rb} \underline{L}_b + \underline{F}_{rr} \underline{L}_r = \underline{0} \quad \dots 3.11$$

$$\text{and } p_{ij}/(A_j \sigma_{ij}^*) \leq 1 \quad \dots 3.12$$

for  $i = 1, 2, \dots, nlc$  and  $j = 1, 2, \dots, nm$



Here  $n_{lc}$  and  $n_m$  are the number of loading cases and the number of members. The permissible stress in direct tension or compression for member  $j$  when load case  $i$  acts is  $\sigma_{ij}^*$  and the corresponding member force is  $p_{ij}$ . Both actual and permissible stresses have the same sign convention, and the permissible stresses are therefore given by positive or negative quantities as required. The matrix of permissible deflexions is denoted by  $\underline{\Delta}$ .

It is interesting to note that in the case of statically determinate structures the vector  $\underline{L}_r$  and the matrices  $\underline{F}_{br}$ ,  $\underline{F}_{rb}$  and  $\underline{F}_{rr}$  become null matrices. These render the compatibility constraints (3.11) superfluous and reduce the deflexion constraints (3.10) to

$$\underline{F}_{bb} \underline{L}_b \leq \underline{\Delta} \quad \dots 3.10a$$

In the case of minimum weight design using rigid plastic theory deflexions at collapse are neglected. This means the exclusion of constraints (3.10) from the problem. In this manner, when using the rigid plastic approach, only stress constraints are considered.

When dealing with rigidly jointed structures the stress constraints (3.12) become of the form

$$\left. \begin{aligned} \frac{p_{ij}}{A_j \sigma_{ij}^*} + \frac{M_{1ij} y_j}{I_j \sigma_{mij}} &\leq 1 \\ \frac{p_{ij}}{A_j \sigma_{ij}^*} + \frac{M_{2ij} y_j}{I_j \sigma_{mij}} &\leq 1 \end{aligned} \right\} \quad \dots 3.12a$$

for  $i = 1, 2, \dots, n_{lc}$  and  $j = 1, 2, \dots, n_m$

where  $y_j$  is the distance from the extreme fibre stress to the neutral axis of the section of member  $j$ ,  $I_j$  is the second moment of area, and  $\sigma_{mij}$  is

the permissible stress in bending.  $M_{1ij}$  and  $M_{2ij}$  are the moments at the first and second ends of member  $j$  when load case  $i$  acts.

In a design problem it is not usual to constrain the deflexion at every load point. For convenience it will be assumed that the set of constrained deflexions is the same for each loading case, and that these deflexions are  $ndc$  in number. The complete set of deflexion constraints (3.10) can therefore be replaced by the following set

$$\underline{F}_{bb}^T \underline{L}_b + \underline{F}_{br}^T \underline{L}_r \leq \underline{\Delta}^T \quad \dots 3.10b$$

$\underline{F}_{bb}^T$  and  $\underline{F}_{br}^T$  are obtained from  $\underline{F}_{bb}$  and  $\underline{F}_{br}$  by omitting the rows corresponding to the unconstrained deflexions.

It should be noted that if the design problem is formulated in terms of the matrix displacement method, then the constraints (3.10) and (3.11) must be replaced by a set of equations of the form

$$\underline{K}^{-1} \underline{L} \leq \underline{\Delta} \quad \dots 3.13$$

where  $\underline{K}$  is the overall stiffness matrix of the structure. As the number of these equations equals the number of degrees of freedom in the frame, the matrix force method may provide a more compact formulation of the problem than the displacement method. When using the matrix displacement method the stress constraints are still of the form given by equation (3.12) however the member forces  $p_{ij}$  are now obtained from the relationship.

$$\underline{P} = \underline{k} \underline{A} \underline{K}^{-1} \underline{L} \quad \dots 3.14$$

where matrix  $\underline{k}$  is the assemblage of member stiffnesses and  $\underline{A}$  is the displacement transformation matrix. When using either method to formulate the problem the objective function of equation (3.9) remains unaltered.

When the constraints of the design problem are stated in the form given by the matrix force method as summarized by equations (3.10), (3.11) and (3.12), it becomes a problem in non-linear programming. The non-linearity arises in the deflexion constraints (3.10), the compatibility equation (3.11) and the stress constraints (3.12).

For pin jointed frames the members can be assumed to deform in an axial manner only. As a result of this the structures of the overall flexibility matrices result in the constraints (3.10) and (3.11) including, as functions of the unknowns, the terms  $1/A_k$  and  $L_{r_{ic}}/A_k$ , where  $c = 1, 2, \dots, r$ , the number of redundant members.  $A_k$  is the  $k$ -th design variable and  $L_{r_{ic}}$  is the value of the  $c$ -th redundant force when the  $i$ -th load case acts. When the problem is formulated for rigid jointed structures further terms are introduced into the constraints of the type  $1/I_k$  and  $L_{r_{ic}}/I_k$ . The variables  $A_k$  and  $I_k$  are not independent of one another. One of these variables could therefore be removed from the problem by expressing one variable in terms of the other.

For the majority of cases, however, this would not prove to be necessary. This is because for a frame which is mainly rigidly jointed, such as a sway frame, the axial deformations are usually small when compared with those due to bending. In this case the constraints (3.10) and (3.11) only include such terms as  $1/I_k$  and  $L_{r_{ic}}/I_k$ .

Although the constraints may be obtained in terms of the second moments of area, the objective function of equation (3.9) is in terms of the member areas and therefore a relationship should be obtained between  $A$  and  $I$ . Strictly speaking the weight of a member is non-linearly related to its second moment of area. Clarkson (33), for instance, showed that for British Standard joints, the second moment of area is proportional to  $A^{2.65}$ . This is equivalent to the weight being proportional to  $I^{0.38}$ . Furthermore the

stress constraints (3.12a) require the distance,  $y$ , of the extreme fibre stress from the neutral axis which also becomes an unknown of the design problem. A further relationship between  $A$  and  $y$  is therefore required. These factors make the optimum design of rigid structures highly non-linear and difficult.

The non-linear programming algorithm of the next chapter requires a feasible design space in which to carry out a search for the optimum design. For this reason it is necessary to combine the deflexion constraints (3.10) and the compatibility equation (3.11). This is done to remove the equality constraints and increases further the non-linearity of the problem.

The values of the redundant forces  $\underline{L}_r$  may be obtained from equation (3.11) as

$$\underline{L}_r = - \underline{F}_{rr}^{-1} \underline{F}_{rb} \underline{L}_b \quad \dots 3.15$$

and the deflexion constraints (3.10) modified. The design problem may now be stated as determine the unknown sectional properties to

$$\text{minimize } z = \sum_j 1_j A_j \quad \dots 3.9$$

$$\text{subject to } (\underline{F}_{bb} - \underline{F}_{br} \underline{F}_{rr}^{-1} \underline{F}_{rb}) \underline{L}_b \leq \underline{\Delta} \quad \dots 3.16$$

$$p_{ij} / (A_j \sigma_{ij}^*) \leq 1 \quad \dots 3.12$$

$$\text{and } A_j^o \leq A_j \leq A_j^u \quad \dots 3.17$$

for  $i = 1, 2, \dots, nlc$  and  $j = 1, 2, \dots, nm$

Where  $A_j^o$  and  $A_j^u$  are respectively the lower and upper bound values imposed upon variable  $j$  so that realistic results are obtained.

The problem has now been stated in a non-linear programming form. The redundant variables have been replaced by functions of the variables

representing the sectional properties so that the remaining inequalities now determine a feasible hyperspace in a Euclidean space which is assumed to be connected. It should be stressed that the objective function  $z$  does not include the redundant variables and hence the elimination of these from the problem does not affect this function.

Many methods are available (34) to reach the optimum point by moving from one feasible point to another in some suitable direction. All these methods have common features being directly or indirectly based upon the principle of feasible directions. This entails starting with a feasible solution vector  $\underline{x}$  and determining a direction vector  $\underline{\delta x}$  which will improve the feasibility of the design without increasing its volume. This is termed a feasible direction. A step length to be taken in this direction is then determined and a new solution vector thus obtained. Proceeding in this manner the value of the objective function is successively reduced and the question arises under which conditions the process should be terminated having obtained the optimum point.

### 3.2 Automatic Construction of the Load Transformation Matrix

When considering the design of large general structures the construction of the load transformation matrix  $\underline{B}$  becomes rather cumbersome. This is particularly so when the matrix is required to be fed into a computer to carry out successive matrix force analyses of a structure. An automatic procedure for the formation of the load transformation matrix has been devised ( 35 ) and this can be readily programmed for a computer.

There exists a duality between the various matrices used in the force and displacement methods. Use can be made of this dual nature and particularly, in the present instance, of the two equations which relate the internal forces and the external loads of a structure, namely



$\underline{L} = \underline{A}' \underline{p}$  and  $\underline{p} = \underline{B} \underline{L}$ . Just as matrix  $\underline{B}$  was partitioned into  $\underline{B}_b \underline{B}_r$ , so matrix  $\underline{A}'$  can also be partitioned as

$$\underline{L}_b = \begin{bmatrix} \underline{A}'_b & \underline{A}'_r \end{bmatrix} \begin{bmatrix} \underline{p}_b \\ \underline{p}_r \end{bmatrix} \quad \dots 3.18$$

where  $\underline{p}_r$  are some of the member forces selected as internal redundants.  $\underline{A}'_r$  corresponds to  $\underline{p}_r$  in that it has the same number of columns as  $\underline{p}'_r$ , while  $\underline{A}'_b$  is square. This implies that the partitioning is carried out in such a manner as to make  $\underline{A}'_b$  have an equal number of rows as columns.

Rearranging equation (3.18) and extending the load vector to include the redundant forces gives the following set of equations

$$\begin{bmatrix} \underline{p}_b \\ \underline{p}_r \end{bmatrix} = \begin{bmatrix} (\underline{A}'_b)^{-1} & -(\underline{A}'_b)^{-1} \underline{A}'_r \\ \underline{0} & \underline{I} \end{bmatrix} \begin{bmatrix} \underline{L}_b \\ \underline{p}_r \end{bmatrix} \quad \dots 3.19$$

where  $\underline{0}$  is a null matrix that has the same number of rows as there are redundants, while the number of its columns is the same as the order of  $\underline{L}_b$ . Matrix  $\underline{I}$  is a unit matrix with order equal to the number of redundants.

It follows by comparison of equations (3.19) and (3.5) that

$$\underline{B}_b = \begin{bmatrix} (\underline{A}'_b)^{-1} \\ \underline{0} \end{bmatrix} \quad \text{and} \quad \underline{B}_r = \begin{bmatrix} -(\underline{A}'_b)^{-1} \underline{A}'_r \\ \underline{I} \end{bmatrix} \quad \dots 3.20$$

The construction of the displacement transformation matrix  $\underline{A}$ , used in the matrix displacement method, follows automatically from its derivation. However, care must be taken, when partitioning this matrix, so that suitable redundant members are selected and that, therefore, matrix  $\underline{A}'_b$  has an inverse.

## CHAPTER 4

### SOLUTION OF THE DESIGN PROBLEM

#### 4.1 Introduction

When the Dynamic Search algorithm of Chapter 2 is used to solve problems with an increasing number of variables it becomes laborious and inefficient. This is because to solve such problems it is necessary to permute the variables into pairs and to carry out an optimization in the plane of each pair. In the case of a problem with  $n$  variables this involves an optimization in  $n(n-1)/2$  different planes before all the permutations of the variables into pairs have been dealt with. Even when this is accomplished the optimum solution will probably not be obtained and further iterations of the process will be necessary.

This technique also becomes time consuming because much effort is spent in attempts to alter variables which do not yield much benefit to the structure, while maintaining more beneficial variables constant. For these reasons a general non-linear programming algorithm is put forward in this chapter to solve problems which involve many variables. In this algorithm a direction of search is used which incorporates the simultaneous variation of all the variables to better advantage.

#### 4.2 The Mathematical Problem

The optimum design problem described in Chapter 3 may be restated here in a more general mathematical form. This is done so that the method of solution may be developed more conveniently, and to indicate that the final algorithm may be applied to non-structural problems. The problem thus becomes

$$\text{minimize } z(x)$$

... 4.1

subject to

$$g_i(\underline{x}) \leq \quad , \quad \geq T_i \quad \dots 4.2$$

$$x_k^u \geq x_k \geq x_k^o \quad \dots 4.3$$

$$i = 1, 2, \dots M \quad k = 1, 2, \dots n$$

in which the objective function  $z$  and the behaviour functions  $g_i$  are differentiable functions of the  $n$ -component vector  $\underline{x}$  with continuous partial derivatives. There are a total of  $M$  behaviour functions which are constrained by the values of the  $M$ -component vector  $\underline{T}$ . Once again limits are imposed upon the design variables so that the upper and lower bounds of the  $k$ -th design variable are respectively  $x_k^u$  and  $x_k^o$ .

The method of solution proposed in this chapter is basically an alternate mode algorithm. The movement to the optimum solution is either within the feasible hyperplane of constant objective function, or in a direction orthogonal to this function so as to decrease the value of the objective function while maintaining feasibility. The method attempts to speed up the 'feasible directions' approach by obtaining a constant weight direction vector in which every constraint plays its part in accordance with its importance in the actual problem. In this way the more important a constraint is the more it influences the direction vector chosen. Thus the insignificant constraints have no influence on the direction of search while the nearly critical constraints are not violated within a short distance of travel.

To avoid the influence of local boundary conditions, once a point is obtained which lies on the boundary of the feasible region and a constant weight mode is embarked upon the total distance of travel is such that the movement is as far as possible into the feasible region away from

all the constraints. At this point the orthogonal mode of travel is adopted. This technique improves the possibility of obtaining a global optimum instead of being forces, by dominating local factors into a local optimum.

#### 4.3 Normalisation of the Constraints

When applying the method to structural engineering problems involving both stress and deflexion constraints, it has been found that the numerical values of the limits imposed on the constrained functions often hamper and falsify the weighting process necessary to produce the constant weight direction vector. To overcome this the following scaling of the constraints, termed normalisation, is carried out.

The inequalities in a given structural problem may be in either or both of the following two forms

$$g(x) \leq T \qquad T > 0 \qquad \dots 4.4$$

$$g(x) \geq T \qquad T < 0 \qquad \dots 4.5$$

The value of a constraint of the type given by inequality (4.4) is usually defined as

$$G = T - g(x) \geq 0 \qquad \dots 4.6$$

However for the purposes of this algorithm the normalised value of this constraint is defined as given by

$$G_N = d [1 - g(x)/T] \geq 0 \qquad \dots 4.6a$$

where  $d$  is a convenient positive scalar which is constant throughout. In a structural problem the limit imposed on a member stress is never zero, also that imposed on a particular nodal deflexion is extremely unlikely to be

zero and therefore equation (4.6a) always has a value.

The value of a constraint given by inequality (4.5) is usually defined as

$$G = g(x) - T \geq 0 \quad \dots 4.7$$

but the normalised form of this is also given by equation (4.6a).

It should be pointed out at this stage that a structural constraint is very likely to be of the following type

$$T_1 \leq g(x) \leq T_2 \quad \dots 4.8$$

where a behaviour function is bounded from below by  $T_1$ ,  $T_1 < 0$ , and from above by  $T_2$ ,  $T_2 > 0$ . This situation is dealt with by splitting the corresponding constraints into two, one of the type given by inequality (4.4), the other of the type given by inequality (4.5). Constraints of this type are therefore represented by two normalised constraints both of which must be non-negative for feasibility.

The non-linear programming problem may now be restated as

$$\begin{aligned} & \text{minimize } z(x) \\ & \text{subject to} \\ & G_{Ni}(x) = d[1 - g_j(x)/T_i] \geq 0 \\ & x_k^u \geq x_k \geq x_k^o \\ & d = \text{constant} > 0 \\ & i = 1, 2, \dots, m \\ & j = 1, 2, \dots, M \\ & M \leq m \\ & k = 1, 2, \dots, n \end{aligned} \quad \dots 4.9$$



where  $M$  is the total number of behaviour functions,  $m$  the total number of normalised constraints and  $n$  is once again the number of variables.

The advantage of dealing with normalised constraints may be shown with the aid of a simple example. Consider that there are three constraints of the following form

$$g_1(x) \leq 0.16$$

$$g_2(x) \geq -0.1$$

and 
$$g_3(x) \leq 3$$

For a given set of values for  $\underline{x}$ , the behaviour functions may have the values  $g_1(x) = 0.12$ ,  $g_2(x) = -0.07$ , and  $g_3(x) = 2.7$ . The values of these constraints are obtained from equations (4.6) and (4.7) as  $G_1 = 0.04$ ,  $G_2 = 0.03$  and  $G_3 = 0.3$ . These values give the appearance that the second constraint is nearest violation as  $g_2(x)$  is numerically nearest to its boundary value of  $-0.1$ . Normalising these constraints however with  $d = 1$  gives  $G_{N1} = 0.25$ ,  $G_{N2} = 0.3$  and  $G_{N3} = 0.1$ . These indicate that the third constraint, having the lowest normalised value is nearest violation and that the second constraint is in fact the least critical of the three.

#### 4.4 The Boundary Solution Vector

In common with other feasible direction algorithms the proposed method generates the  $(v + 1)$ th solution vector from the  $v$ -th solution vector in the following manner

$$\underline{x}_{v+1} = \underline{x}_v + \lambda \underline{\delta x} \quad \dots 4.10$$

Here  $\underline{x}_{v+1}$  is the vector of variables obtained from the latest step and

$\underline{x}_v$  is the vector of variables after the previous step. The direction of movement in space between the successive solutions is defined as  $\underline{\delta x}$  which is termed the direction vector. Finally  $\lambda$  is a positive scalar that defines the distance to be moved in this direction.

A solution vector that renders at least one of the normalised constraints critical by taking a zero or near zero value while the rest of the normalised constraints remain positive is said to be a boundary solution vector. It is at points defined by boundary solution vectors that a new direction of search is sought, until finally the vector containing the optimum solution is obtained. This is also a boundary solution vector.

A boundary solution vector may be obtained to any required accuracy by an iterative interpolation procedure, making use of the most recent feasible and non-feasible solution vectors. This procedure is initiated once equation (4.10) yields a non-feasible solution vector and consists of a successive averaging of feasible and non-feasible solutions until the condition that a boundary solution vector is obtained is verified. This condition is of two types, either

$$\left. \begin{array}{l} G_{Nj} < t_1 \\ j = 1, 2, \dots m \end{array} \right\} \dots 4.11a$$

for at least a single  $j$  or

$$\left. \begin{array}{l} \text{mod } (1 - x_i/y_i) < t_2 \\ i = 1, 2, \dots n \end{array} \right\} \dots 4.11b$$

must hold true. Both of these tests are only applied when the current solution vector is feasible, that is when  $G_{Nj} \geq 0$  for every normalised

constraint. The most recent non-feasible value of the  $i$ -th variable is denoted by  $y_i$  and the current feasible value is denoted by  $x_i$ . The quantities  $t_1$  and  $t_2$  are specified tolerances. The values of these quantities and hence the accuracy to which boundary solution vectors are required may be treated as variables. This is because in the early stages of a design synthesis it is wasteful to obtain exact boundary solution vectors merely to discard them once a direction vector is obtained. As the optimum solution is approached however boundary solution vectors are required to a greater accuracy since the optimum solution itself is such a vector.

#### 4.5 The Searching Procedure

The searching procedure to the optimum design is carried out in three basic stages. The object of the first stage is to locate the first boundary solution vector and is only carried out once. Having achieved this the other two stages are operated successively until the optimum solution vector is obtained to within a specified tolerance. Stage 2 of the algorithm is the constant volume mode of travel within the design space and stage 3 aims at reducing the structural volume.

Stage 1: To locate the first boundary solution vector, each variable is initially equated to its lower bound value. The resulting solution, unless optimum, is non-feasible and the volume of the structure must be increased to achieve feasibility. The linear objective function is of the form

$$z(x) = \sum_{i=1}^n c_i x_i \quad \dots 4.12$$

and the rate of change of the objective function with the  $i$ -th variable is

obtained by partial differentiation as

$$\frac{\partial z}{\partial x_i} = c_i \quad \dots 4.13$$

Movement orthogonal to the hyperplane of constant objective function to increase the value of the objective function can be achieved by forming the elements of the direction vector  $\underline{\delta x}$  from

$$\delta x_i = c_i \quad \dots 4.14$$

$$i = 1, 2, \dots n$$

Such a choice of direction vector, however, will increase the values of the expensive variables more than the cheaper variables. In accordance with equation (4.10) the new value of the  $i$ -th variable is given by  $x_i'$  where

$$x_i' = x_i^0 + \lambda c_i \quad \dots 4.15$$

The contribution of the  $i$ -th variable in increasing  $z$  is therefore given by

$$\delta z_i = c_i (x_i' - x_i^0) = \lambda c_i^2 \quad \dots 4.16$$

and is seen to be proportional to the square of the corresponding coefficient in the objective function. This direction vector is therefore not chosen as the initial direction of search since the expensive variables should not be encouraged to take large values, unless this would benefit the structure as a whole by making it possible to reduce many cheap variables later. As no evidence is available at this stage to support this the initial direction of search is chosen by forming the elements of the direction vector from

$$\delta x_i = + 1/c_i \quad \dots 4.17$$

$$i = 1, 2, \dots n$$

By choosing this direction vector the more expensive variables, with large objective function coefficients, will increase less than the cheaper ones so that the contribution of each variable in altering  $z$  is the same. The new value of the  $i$ -th variable after a single step is now obtained from equation (4.10) as

$$x_i' = x_i^0 + \lambda/c_i \quad \dots 4.18$$

and the increase in the objective function due to this variable as

$$\delta z_i = c_i (x_i' - x_i^0) = \lambda \quad \dots 4.19$$

This is seen to be entirely independent of the objective function coefficients and numerically equal to the chosen step length.

In the actual algorithm the step length scalar  $\lambda$  is selected so that at least one variable will be at its upper bound after a single alteration of the variables. This is achieved by selecting  $\lambda$  from:

$$\lambda = \min_{i, \Delta_i \neq 0} [c_i (x_i^u - x_i)] \quad \dots 4.20$$

with the corresponding direction vector  $\underline{\delta x}$  formed by

$$\delta x_i = + \Delta_i/c_i \quad \dots 4.21$$

where  $\Delta_i$  is the Kronecker delta, given by

$$\begin{aligned} \Delta_i &= 1 \quad \text{when } x_i^u \neq x_i \\ \Delta_i &= 0 \quad \text{when } x_i^u = x_i \end{aligned} \quad \dots 4.22$$



Initially  $x_i$  is equal to  $x_i^0$  and equations (4.10), (4.20) and (4.21) for the governing variable  $i$  in equation (4.20), drives  $x_i$  to  $x_i^u$ . The remaining variables have values which range between their upper and lower bounds and the new solution is not always feasible. It may therefore be necessary to drive one or more other variables to their upper bounds. This is accomplished by further applications of equations (4.10), (4.20) and (4.21).

Stage 2: At this stage the direction vector is recalculated so that it points into the feasible space away from the active constraints in the hyperplane of constant objective function. The purpose of this stage is to obtain a design point so that the feasibility of the design is improved as much as possible. By doing this more advantage will be reaped in the next stage, when reducing the value of the objective function, than if merely a small step away from the active constraints were taken.

The best constant weight direction vector is that which permits the greatest travel before encountering another constraint. For large problems however, it is not advantageous to test several directions and therefore only one of the infinite number of possible direction vectors is generated. The new direction vector must have the merit of helping the normalised constraints, particularly the active ones, increase their values.

Stage three of the algorithm may bring about a condition where some of the expensive variables have been driven, artificially, to their lower bounds. The optimum solution may not require this and at stage two therefore it is necessary to make it possible for these variables to increase their values. This is provided that this action does not decrease the values of the critical normalised constraints.

The detailed calculation of the direction vector is given later.

Once this is decided upon, step lengths  $\lambda$  are taken in accordance with equation (4.10) until a constraint is encountered. The determination of  $\lambda$  is also given later.

Stage 3: As stated earlier the aim of this stage is to reduce the value of the objective function by moving in an orthogonal direction. The starting position of this movement is at a point which is midway between the two most recent boundary solutions that have the same objective function value. That is, the solutions that commenced and terminated the previous stage. Each value of the new direction vector is formed by simply equating it to minus the coefficient of the corresponding variable in the objective function

$$\text{i.e.} \quad \delta x_i = -c_i$$

$$i = 1, 2, \dots n$$

... 4.23

A direction vector of this type will decrease the expensive variables at a greater rate than the cheaper variables.

A step size  $\lambda$  is then determined and equation (4.10) together with the tests given by inequalities (4.11a) and (4.11b) are utilized to locate a further boundary solution vector. Stages 2 and 3 are employed repeatedly until an optimum solution vector is obtained. This is checked by a tolerance test which is carried out at the end of stage three of each cycle. This test is of the form

$$|1 - x'_{bi}/x_{bi}| < t_3$$

$$i = 1, 2, \dots n$$

... 4.24

where  $x_{bi}$  is the current boundary value of variable  $i$  and  $x'_{bi}$  is the value of the same variable at the end of the previous cycle.

An alternative test for termination may be carried out on the successive objective function values obtained at the ends of each stage three. This involves the following single test

$$|1 - z/z'| < t_4 \quad \dots 4.25$$

where  $z$  and  $z'$  are the current and the previous values of the objective functions respectively, ( $z < z'$ ).

This test terminates the procedure when the benefit reaped by the objective function on successive iterations becomes insignificant.

It should be pointed out here that the tests of equations (4.24) and (4.25) may not be sufficient to verify even a local optimum. For instance if the feasible design space is highly irregular the optimum point may lie at the bottom of a very narrow and steep sided valley. In this case movement in the constant weight plane will be restricted by the small feasible area of this plane and movement to reduce the weight soon founders unless the axis of the valley is parallel to the line of steepest descent. In either case variation of the variables is restricted and the tests of equations (4.24) and (4.25) may be positive if  $t_3$  and  $t_4$  are sufficiently large. For the purposes of the proposed algorithm situations of this type were assumed to be uncommon in structural problems.

#### 4.6 The Constant Weight Direction Vector

The evaluation of the elements of the constant weight direction vector used in stage 2 is an important part of the proposed algorithm. A well chosen direction vector here will lead to a significant reduction of the objective function value in the next stage. To evaluate this vector it is convenient to define a slope matrix  $\underline{S}$ , that plays an important role

in determining the direction vector as

$$\underline{S} = \begin{bmatrix} s_{11} & s_{12} & \dots & s_{1j} & \dots & s_{1m} \\ s_{21} & s_{22} & \dots & s_{2j} & \dots & s_{2m} \\ \vdots & \vdots & & \vdots & & \vdots \\ s_{i1} & s_{i2} & \dots & s_{ij} & \dots & s_{im} \\ \vdots & \vdots & & \vdots & & \vdots \\ s_{n1} & s_{n2} & \dots & s_{nj} & \dots & s_{nm} \end{bmatrix} \quad \dots 4.26$$

$$\text{with } s_{ij} = \partial G_{Nj} / \partial x_i$$

The slope matrix contains the rate of change of each normalised constraint  $j$  with respect to each variable  $i$ . These partial derivatives are obtained by numerical differentiation as follows

$$\partial G_{Nj} / \partial x_i = s_{ij} = (G'_{Nj} - G_{Nj}) / \varepsilon \quad \dots 4.27$$

$$j = 1, 2, \dots m$$

$$i = 1, 2, \dots n$$

where  $G_{Nj}$  is the value of the  $j$ -th normalised constraint when the  $i$ -th variable has a value  $x_i$  and  $G'_{Nj}$  is the value of this same constraint when the value of the  $i$ -th variable is increased by an increment  $\varepsilon$  to become  $x_i + \varepsilon$

By using this slope matrix the elements of a direction vector may be obtained by adding all the elements of a whole row of the slope matrix. This is expressed in matrix notation as

$$\underline{\delta x} = \underline{S} \underline{i} \quad \dots 4.28$$

where  $\underline{i}$  is a unit column vector of order  $m$ . Such a direction vector suffers from the fact that it does not preserve the constant value of  $z$ . However, by virtue of equation (4.26) the elements of  $\underline{\delta x}$  indicate the manner in which each variable should be altered so that all the constraints are best affected.

At the commencement of this stage the design point lies on or near a boundary of the feasible space. The initial concern of this stage is therefore to increase the value of the most critical constraints so as to move into the feasible space. With the present direction vector however, equal care is taken to see that the non-critical constraints are also increased in value. Due to the straightforward summation technique used to form this vector non-critical constraints which demand a reduction of a particular variable may overwhelm the effect of a critical constraint requiring this same variable to be increased. In this way the direction vector produced by equation (4.28) when using the current slope matrix  $\underline{S}$  may well be infeasible.

To avoid this situation it is necessary to adjust the contribution of each constraint to the slope matrix so that critical and near critical constraints are preponderant. This will ensure that the direction vector is feasible and will not lead to the violation of a near critical constraint after a short distance of travel. The improved direction vector is therefore obtained by factoring each element  $s_{ij}$  so that as  $G_{Nj} \rightarrow 0$ ,  $\partial G_{Nj} / \partial x_i$  will have a more significant effect. This is achieved by multiplying the denominator in equation (4.27) by  $(1 + G_{Nj})$ , to become

$$s_{ij}^* = (G_{Nj}^i - G_{Nj}) / \epsilon (1 + G_{Nj}) \quad \dots 4.29$$



The modified slope matrix therefore becomes

$$\underline{S}^* = \begin{bmatrix} * & * & \dots & * & \dots & * \\ s_{11} & s_{12} & & s_{1j} & & s_{1m} \\ * & * & \dots & * & \dots & * \\ s_{21} & s_{22} & & s_{2j} & & s_{2m} \\ \cdot & \cdot & & \cdot & & \cdot \\ \cdot & \cdot & & \cdot & & \cdot \\ * & * & \dots & * & \dots & * \\ s_{i1} & s_{i2} & & s_{ij} & & s_{im} \\ \cdot & \cdot & & \cdot & & \cdot \\ \cdot & \cdot & & \cdot & & \cdot \\ * & * & \dots & * & \dots & * \\ s_{n1} & s_{n2} & & s_{nj} & & s_{nm} \end{bmatrix} \quad \dots 4.30$$

and the direction vector is now obtained from

$$\underline{\delta x} = \underline{S}^* \underline{i} \quad \dots 4.31$$

Furthermore, once a given  $G_{Nj}$  is more than a prescribed percentage of its maximum value  $d$ , which is defined in equation (4.6a), it is possible to neglect this constraint entirely by setting all the elements of the corresponding column of the modified slope matrix  $\underline{S}^*$  to zero. In equation (4.29) it is noticed that as  $G_{Nj} \rightarrow 0$ ,  $s_{ij}^* \rightarrow s_{ij}$  and as a result only constraints that are fully satisfied contribute fully to the direction vector. It is this weighting process that requires the concept of constraint normalisation so that it is possible to gauge easily the criticality of the various constraints.

The latest direction vector still suffers from the fact that the value of objective function is not maintained constant. The increase in the value of the objective function after having taken a step length  $\lambda$  is given by

$$\sum_{i=1}^n \delta z_i = \lambda \sum_{i=1}^n c_i \delta x_i \quad \dots 4.32$$

In order to maintain constant  $z$  conditions it is necessary to ensure that this is equal to zero

$$\text{i.e.} \quad \lambda \sum_{i=1}^n c_i x_i = \sum_{i=1}^n c_i x_i = 0 \quad \dots 4.33$$

having removed the constant scalar quantity  $\lambda$ . This condition is satisfied later in the final step of the formation of the direction vector by weighting the elements of the vector according to the corresponding objective function coefficients. To counter the otherwise detrimental effects of this weighting the elements of the current direction vector are modified at this stage by setting

$$\begin{aligned} \delta x_i^* &= c_i \delta x_i \\ i &= 1, 2, \dots, n \end{aligned} \quad \dots 4.34$$

The vector  $\underline{\delta x}^*$  thus obtained is used as the basis from which the actual vector is formed. This final vector will not only preserve the value of the objective function constant but also ensure that the variable bounds are not violated. At this juncture it is convenient to introduce two new vectors  $\underline{\alpha}$  and  $\underline{\beta}$ . An element  $\alpha_i$  of  $\underline{\alpha}$  is given by

$$\alpha_i = \frac{\delta x_i^* - \delta x_{\min}^*}{\delta x_{\max}^* - \delta x_{\min}^*} \quad \dots 4.35a$$

while that of  $\underline{\beta}$  is given by

$$\beta_i = \frac{\delta x_{\max}^* - \delta x_i^*}{\delta x_{\max}^* - \delta x_{\min}^*} \quad \dots 4.35b$$

$$i = 1, 2, \dots, n$$

where  $\delta x_{\max}^*$  and  $\delta x_{\min}^*$  are the largest and the smallest elements in the vector  $\delta x^*$ . It is noticeable that equations (4.35a) and (4.35b) have the following properties

$$\left. \begin{aligned} 0 &\leq \alpha_i \leq 1 \\ 0 &\leq \beta_i \leq 1 \\ \beta_i &= 1 - \alpha_i \end{aligned} \right\} \dots 4.36$$

At least one variable  $i$  has its  $\alpha_i = 0$  and at least one other variable  $k$  has  $\alpha_k = 1$ ;  $i \neq k$ .

Equations (4.35a) and (4.35b) have the merit that the actual value of  $\alpha_i$  or  $\beta_i$  indicates how best to alter a variable  $i$ , for the bigger the values of  $\alpha$  the more the corresponding variable should be increased. It follows that variables with high values of  $\alpha$  will increase the values of the normalised constraints and particularly the critical ones.

It should be emphasised here, however, that it is possible for a variable to be at its upper bound and to have an  $\alpha$  value of unity. Such a variable cannot be increased in spite of the value of  $\alpha$ . It is also possible for a variable near its lower bound to have a value for  $\alpha$  near zero or alternatively a  $\beta$  value near unity. Such a variable must not be decreased in value drastically. These eventualities are accommodated by introducing two further vectors  $\underline{k}$  and  $\underline{k}'$  where the  $i$ -th elements  $k_i$  and  $k_i'$  are given by

$$\left. \begin{aligned} k_i &= \alpha_i (x_i^u - x_i) \\ k_i' &= \beta_i (x_i - x_i^o) \\ i &= 1, 2, \dots, n \end{aligned} \right\} \dots 4.37$$

It is noticed that when both  $\alpha_i$  and  $(x_i^u - x_i)$  are large,  $k_i$  is large, indicating that a variable should be increased and can be increased. Alternatively if  $k_i'$  is large then the corresponding variable should be reduced in value.

Each variable has an associated value for  $k$  and  $k'$  representing how that variable can best be changed. The final direction vector contains a combination of the pair, the elements being calculated from

$$\delta x_i = \frac{C_T}{c_i} \left( \frac{k_i}{K} - \frac{k_i'}{K'} \right)$$

where

$$K = \sum_{i=1}^n k_i$$

$$K' = \sum_{i=1}^n k_i'$$

and

$$C_T = \sum_{i=1}^n c_i$$

... 4.38

The value of  $C_T$  is constant for a particular problem being the summation of the objective function coefficients. The factor  $C_T/c_i$  is the weighting factor mentioned earlier and preserves the constant value of the objective function by relatively scaling down the expensive variables and scaling up the cheaper ones. In this way the constant objective function condition of equation (4.33) is satisfied.

The sign of any element of the direction vector is decided by the term  $(k/K - k'/K')$ . A variable with a high  $k/K$  and a low  $k'/K'$  will make this term large and positive, indicating that the variable will be increased. On the other hand, any variable with a low  $k/K$  and a large  $k'/K'$  will be decreased.

It should be pointed out that it is possible for  $K'$  to vanish indicating that it is impossible to decrease any variable without violating either a normalised constraint or the lower bound of a variable. In this case it is impossible to move in any feasible direction without increasing the value of the objective function.

As an example of the formation of the constant weight direction vector consider the following non-linear programming problem.

$$\text{Minimize } z = 4x_1 + 3x_2 + 2x_3 + x_4$$

subject to

$$g_1(x) = \frac{16}{x_1} + \frac{28}{x_2} + \frac{12}{x_3} + \frac{35}{x_4} \leq 20.5$$

$$g_2(x) = \frac{15}{x_1} - \frac{22}{x_2} + \frac{5}{x_3} + \frac{20}{x_4} \leq 6$$

$$2 \leq x_i \leq 10$$

$$i = 1, 2, 3, 4.$$

This is a non-structural problem but the behaviour functions are similar to those encountered when dealing with such problems and will provide a useful illustration. Taking the scalar quantity  $d = 10$  the normalised constraints become

$$G_{N1} = 10 \left[ 1 - \left( \frac{16}{x_1} + \frac{28}{x_2} + \frac{12}{x_3} + \frac{35}{x_4} \right) / 20.5 \right] \geq 0$$

$$G_{N2} = 10 \left[ 1 - \left( \frac{15}{x_1} - \frac{22}{x_2} + \frac{5}{x_3} + \frac{20}{x_4} \right) / 6 \right] \geq 0$$

A boundary solution vector is available given by

$$\{x_1 \quad x_2 \quad x_3 \quad x_4\} = \{2 \quad 4 \quad 6 \quad 10\}$$



with an objective function value of  $z = 42$ . The normalised constraints have the values  $G_{N1} = 0$  and  $G_{N2} = 1.9444$ .

The slope matrix of equation (4.26) is constructed taking a value for the increment  $\epsilon$  of unity. The values of  $G'_{N1}$  and  $G'_{N2}$  are calculated by altering each element of  $\underline{x}$  in turn in the normalised constraints. On increasing the value of the first variable from 2 to 3 the new value of the first normalised constraint becomes 1.3008 and equation (4.27) gives the value of  $s_{11}$  as

$$s_{11} = (1.3008 - 0)/1 = 1.3008$$

The new value of the second normalised constraint becomes 6.1111 and equation (4.27) gives the value of  $s_{12}$  as

$$s_{12} = (6.1111 - 1.9444)/1 = 4.1667$$

This is repeated for the three remaining variables and the slope matrix  $\underline{S}$  becomes

$$\underline{S} = \begin{bmatrix} 1.3008 & 4.1667 \\ 0.6829 & -1.8333 \\ 0.1394 & 0.1985 \\ 0.1552 & 0.3031 \end{bmatrix}$$

The modified slope matrix  $\underline{S}^*$  is obtained using equation (4.29) to form the elements. In this case when considering the first variable and the second constraint the corresponding element is now given by

$$s_{12}^* = (6.1111 - 1.9444)/(1 + 1.9444) = 1.4135$$

and the modified slope matrix of equation (4.30) becomes

$$\underline{S}^* = \begin{bmatrix} 1.3008 & 1.4135 \\ 0.6829 & -0.6226 \\ 0.1394 & 0.0674 \\ 0.1552 & 0.1029 \end{bmatrix}$$

It is noticed how the elements of the second non-critical column, have a smaller influence on each row compared to the elements of the second column of  $\underline{S}$ .

Two direction vectors may now be formed using the elements of these two matrices in equations (4.28) and (4.31). That obtained from the slope matrix  $\underline{S}$  being

$$\underline{\delta x} = \{5.4675, -1.1504, 0.3379, 0.4583\}$$

and that from the modified slope matrix  $\underline{S}^*$  being

$$\underline{\delta x} = \{2.7143, 0.0603, 0.2068, 0.2581\}$$

It is immediately noticeable that the element corresponding to the second variable in these vectors has changed sign. This is because this second constraint benefits by a reduction in the value of the second variable and the first constraint benefits by an increase in this variable. The benefit to be gained by the second constraint dominates in the formation of the first of the above direction vectors. The detrimental effect of decreasing the second variable on the critical constraint however, is allowed for when forming the second vector from the modified slope matrix.

Equations (4.34) and (4.35) can now be used to construct vectors  $\underline{\alpha}$  and  $\underline{\beta}$ . These, together with the upper and lower bound values, imposed on the variables, are then used in equation (4.37) to obtain the values of the elements of vectors  $\underline{k}$  and  $\underline{k}'$ . The results of these

calculations can be summarised as

$$[ \underline{a} \ \underline{\beta} \ \underline{k} \ \underline{k}' ] = \begin{bmatrix} 1.0000 & 0 & 8.0000 & 0 \\ 0 & 1.0000 & 0 & 2.0000 \\ 0.0218 & 0.9782 & 0.0872 & 3.9128 \\ 0.0072 & 0.9928 & 0 & 7.9424 \end{bmatrix}$$

The elements of  $\underline{a}$  indicate that the constraints benefit most when the first variable increases as the element which corresponds to this variable is unity. The three remaining variables will result in relatively little benefit to the constraints when increased. Indeed the values of  $\underline{\beta}$  suggest that these variables should be reduced.

The vector  $\underline{k}$  considers also the relative positions of the variables between their bound values and emphasises that the first variable should be increased by having a large element corresponding to this variable. This vector also indicates that it is impossible to increase the fourth variable, by having a corresponding zero element, due to the fact that  $x_4$  is already at its upper bound.

Vector  $\underline{k}'$  indicates that there is more scope for the reduction of the fourth variable than of the second, this being near its lower bound, by having a relatively large element corresponding to  $x_4$ . The significance of this is that although there is little difference between these two variables as far as benefit to the behavioural constraints is concerned, the fourth variable should be reduced by a greater amount than the second. This will move the solution away from the upper bound constraint of the fourth variable without quickly violating the lower bound limitation on the second variable by an unnecessary drastic reduction.

The actual constant weight direction vector is constructed using equation (4.38). Summation of the elements  $\underline{k}$  and  $\underline{k}'$  gives  $K = 8.0872$

and  $K' = 13.8552$ . With  $C_T = 10$ , therefore, the first element of the direction vector becomes

$$\delta x_1 = \frac{10}{4} \left( \frac{8}{8.0872} - \frac{0}{13.8552} \right) = 2.4730$$

Considering all the variables in turn, the constant weight direction vector becomes

$$\underline{\delta x} = \{ 2.4730, -0.4810, -1.3585, -5.7340 \}$$

which exactly satisfies the constant objective function condition of equation (4.33).

This direction vector is now used in equation (4.10) with a small step length  $\lambda = 0.1$  to generate a new solution vector

$$\{ x_1 \quad x_2 \quad x_3 \quad x_4 \} = \{ 2.2469, \quad 3.9518, \quad 5.8652, \quad 9.4266 \}$$

The objective function has maintained a value of 42 but the normalised constraints have both increased in value becoming  $G_{N1} = 0.2620$  and  $G_{N2} = 3.1960$ . The solution is not only more feasible in this respect, but also because the solution is away from the lower bound limit of the first variable and the upper bound limit of the fourth which were both active prior to this move.

#### 4.7 The Determination of the Step Size

The ideal step size in any stage is that which will yield a boundary solution vector after one step length has been taken. To obtain this is an extremely difficult if not impossible task as it involves the solution of many non-linear equations involving several variables. Each constraint has to be solved independently to find at which point the current direction of

search will intersect it. This is because no information is available to ascertain beforehand which of the constraints will be violated first.

It has been found, therefore, that in the general case it is impossible to predict an ideal value for the step size. In order to determine a value, use is made of the fact that as the optimum solution is approached the possible distance of travel between constraints reduces until it becomes equal to zero. At each stage a step length is selected based on the distance  $D$  moved in the stage immediately previous to the current stage. It is easy to show that the value of  $D$  is given by

$$D = \sqrt{\left( \sum_{i=1}^n (x_i - x_{pi})^2 \right)} \quad \dots 4.39$$

where  $x_{pi}$  is the commencing value of variable  $i$  in the previous stage.

Now since each variable  $x_i$  is altered by an amount  $\lambda \delta x_i$  in a single step and it is required to move a total distance  $D$ , then the following expression must be satisfied

$$D = \lambda \sqrt{\left( \sum_{i=1}^n (\delta x_i)^2 \right)} \quad \dots 4.40$$

The required step size  $\lambda$  is therefore obtained by eliminating  $D$  from equations (4.39) and (4.40) giving

$$\lambda = \sqrt{\left( \sum_{i=1}^n (x_i - x_{pi})^2 / \sum_{i=1}^n (\delta x_i)^2 \right)} \quad \dots 4.41$$

Care must be taken that the value of  $\lambda$  calculated in this manner does not cause a variable to violate its limiting values. It is therefore necessary to ascertain that the following conditions involving the amount by



which each variable is altered are satisfied

$$x_i^o - x_i \leq \lambda \delta x_i \leq x_i - x_i^u \quad \dots 4.42$$

To ensure this an upper bound  $\lambda_i$  is imposed by each variable  $i$  on  $\lambda$ . This is given by

$$\left. \begin{aligned} \lambda_i &= (x_i^u - x_i) / \delta x_i \\ \text{for } \delta x_i &> 0 \\ \text{or } \lambda_i &= (x_i^o - x_i) / \delta x_i \\ \text{for } \delta x_i &< 0 \\ i &= 1, 2, \dots, n \end{aligned} \right\} \quad \dots 4.43$$

The minimum value of  $\lambda$  given by equations (4.41) and all the equations (4.43) is selected as the step length.

#### 4.8 The Non-Linear Programming Algorithm

Two algorithms have been produced to solve non-linear structural design problems in a general fashion. Both of these algorithms are based on the three stages described in the previous sections and each will now be described in turn.

A flow diagram for the first algorithm is given in figure (4.1). This shows the path that the computer takes through the various stages, commencing with stage 1 and then alternating between stages 2 and 3 until the optimum solution is reached. A characteristic of this algorithm is that to terminate any stage a boundary solution vector must be obtained to within a prescribed tolerance.

A flow diagram for stage 1 is given in figure (4.2). The aim of this stage is to locate the first boundary solution vector by driving successive variables to their upper bound values. Should the situation arise where all the variables are at their upper bounds and no feasible solution has been located the process is terminated. This does not necessarily mean that a feasible solution is not available. However, in a normal structural problem, as the sectional properties of the members increase so the nodal displacements and the member stresses throughout the structure tend to decrease. The greatest obstacle to locating the first feasible solution is envisaged when unusual deflexion constraints are included in the problem. This is when deflexions are not merely restricted numerically but when the various deflexions must be restricted in relation to each other. In this case the constraints are independent of the numerical values of the deflexions and hence the probability that these deflexions will decrease as the sectional properties increase may not improve feasibility.

Having located the first boundary solution vector, stage 2 is initiated. A flow diagram for this stage is given in figure (4.3). The first time this stage is entered the step length is evaluated such that at least a single variable is driven to a bound. This is necessary because to evaluate a step length using equation (4.41) requires a previous boundary solution vector. On subsequent entries to this stage both equations (4.41) and (4.43) are used to evaluate the distance to be travelled.

Stage 2 of the search procedure may be terminated in two ways. The first of these is on locating a boundary solution vector, however, it is possible for the quantities  $K$  and  $K'$  to assume a zero value in which case it is impossible to form a constant weight direction vector which does not merely retrace the previously defined search path. A solution which has

these properties is treated as a boundary solution vector.

The flow diagram for stage 3 is given in figure (4.4). This mode of travel reduces the value of the objective function and includes the tests necessary to terminate the procedure.

The algorithm presented above expends some effort to locate an accurate boundary solution vector. This is because each feasibility check demands a re-analysis of the structure, and once a boundary solution vector is available all the information obtained from these analyses is discarded. Furthermore, for large problems some of the assumptions made become less reliable and an elaborate process to obtain an accurate intermediate solution becomes unnecessary. A second algorithm is therefore proposed here which has the added advantage that it reduces the number of times the slope matrix is constructed. The time taken in producing a slope matrix is primarily dependent on the number of unknown variables in the problem. For instance, in an  $n$  dimensional problem the constraints are evaluated  $n$  times. Care should be taken, therefore, to reduce the construction of new slope matrices to the necessary minimum.

The main flow diagram for the amended algorithm is given in figure (4.5) where it can be seen that the formation of the constant weight direction vector has been removed from stage 2. Between stages 1 and 2 the slope matrix is evaluated and the initial constant weight direction vector is based upon it. Between stages 3 and 2 however the constant weight direction vector is only based upon a newly formed slope matrix if a required number of cycles have employed the current slope matrix or if it is impossible to obtain a feasible direction vector using the current slope matrix.

A new modified slope matrix however is required at each cycle. The terms of this modified slope matrix are dependent upon the criticality of the various constraints as well as the corresponding terms in the current

slope matrix. It is noticed that an element  $s_{ij}^*$  of the modified slope matrix is given by

$$s_{ij}^* = s_{ij} / (1 + G_{Nj}) \quad \dots 4.44$$

$$i = 1, 2, \dots n$$

$$j = 1, 2, \dots n$$

where both  $G_{Nj}$  and  $s_{ij}$  are available and therefore a modified slope matrix is formed without any additional evaluation of the constraints.

The modified flow diagram for stage 1 is shown in figure (4.6). This is much the same as that for the previous algorithm, the only difference being that the quest for a boundary solution vector is terminated once a feasible solution that is away from upper bound constraints is obtained. This is done so that some weight saving over an upper bound solution is achieved but, most important, because at this stage the first slope matrix is formed and the constant weight direction vector that is produced from it should be relatively unaffected by variable bound influences. In this way the best direction vector is achieved when the slope matrix is most meaningful.

Figure (4.7) gives the modified flow diagram for stage 2. This stage now produces successive solutions until an infeasible solution is obtained whereupon the last feasible solution terminates the stage.

The solution vector which initiates stage 3 is once again taken as the average of those which commenced and terminated the previous stage. The flow diagram for the modified stage 3 is given in figure (4.8). When the first generated solution is feasible further step lengths are taken until an infeasible solution is obtained, whereupon the previous feasible solution terminates the stage. On the other hand if the first step should yield an infeasible solution the averaging procedure is adopted until a feasible

solution is located to terminate the stage.

At this point in the algorithm the tests that ascertain whether or not the optimum is at hand are applied. Should these prove positive and if the most recent constant weight direction vector was based on a new slope matrix the final solution is obtained. On the other hand if the tests are positive but the current slope matrix is not new a new slope matrix is evaluated. Stage 2 is then entered once more so that the optimum may be verified, or otherwise, by a further cycle.

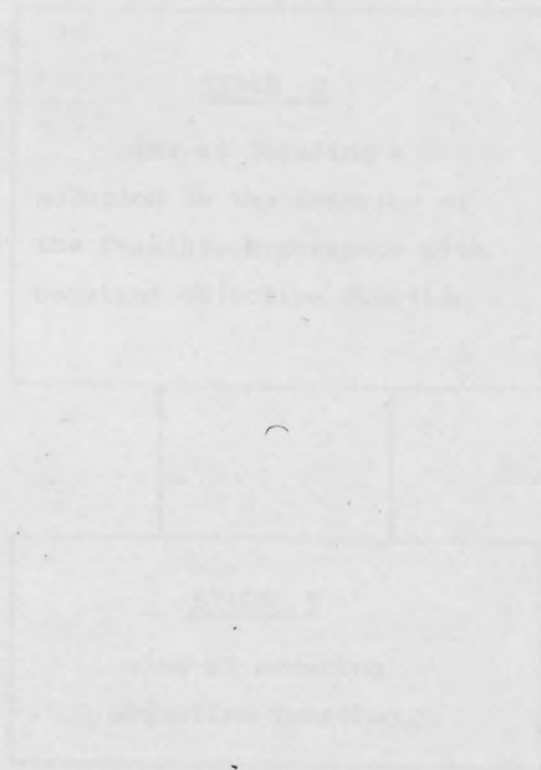


Figure 4.1. Flowchart of the algorithm.



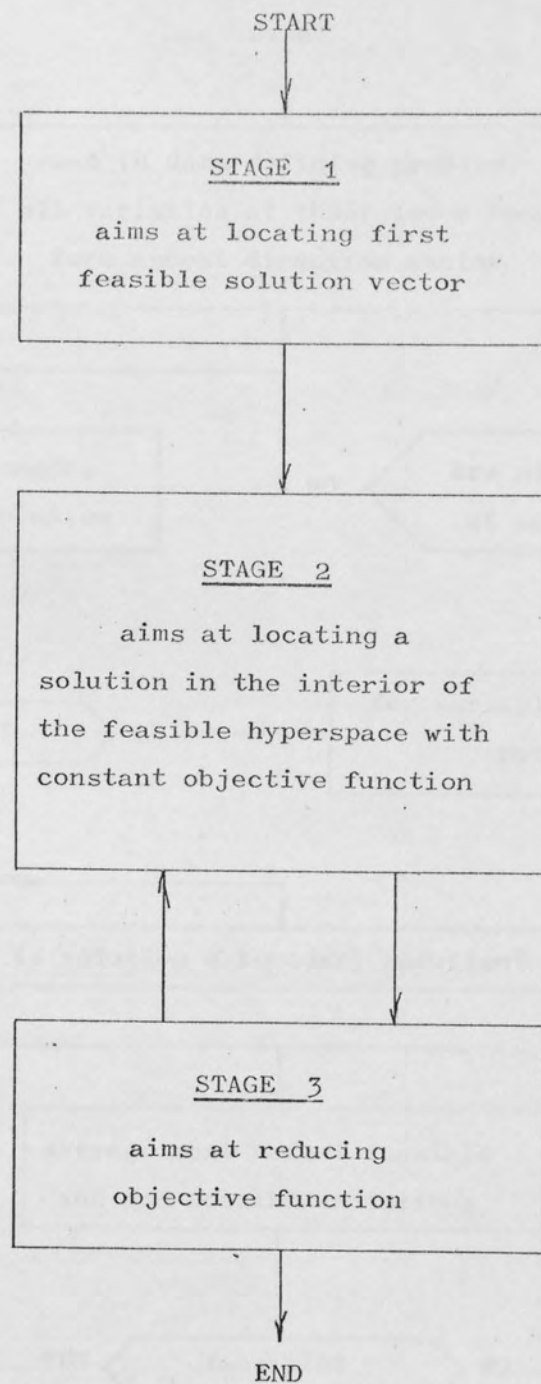


Figure 4.1 Master flow diagram of 1st algorithm

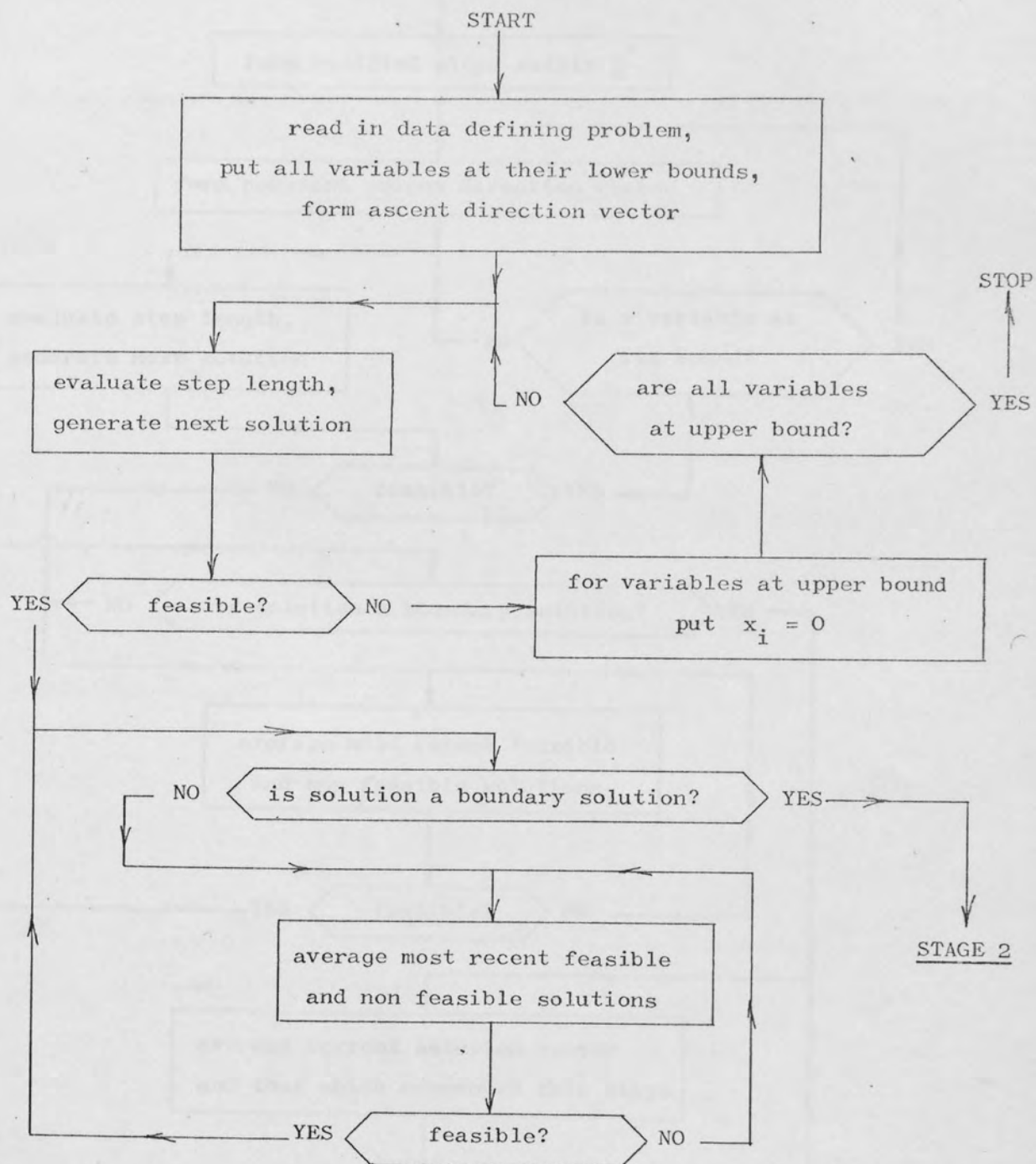


Figure 4.2 Stage 1 flow diagram

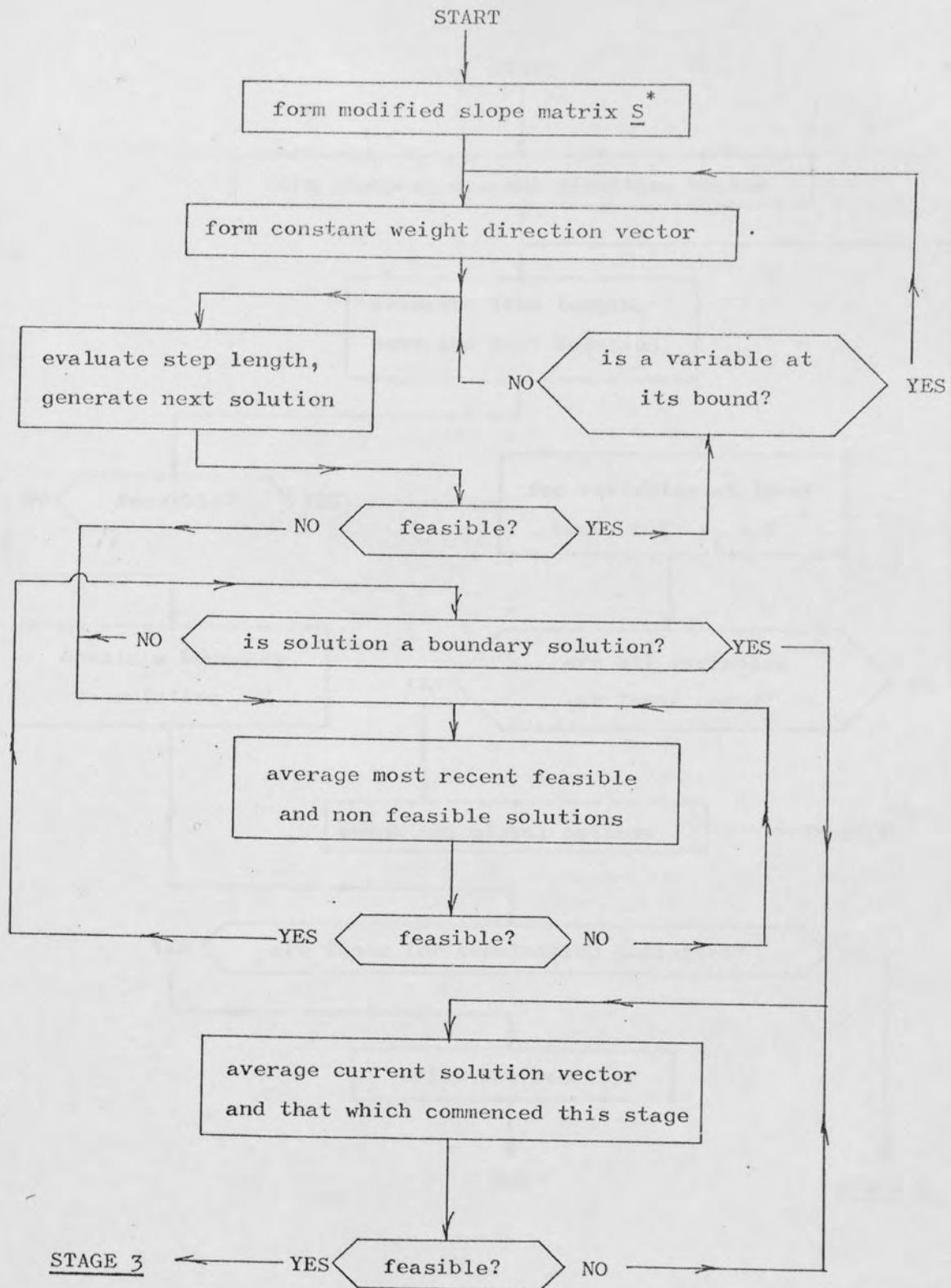


Figure 4.3 Stage 2 flow diagram

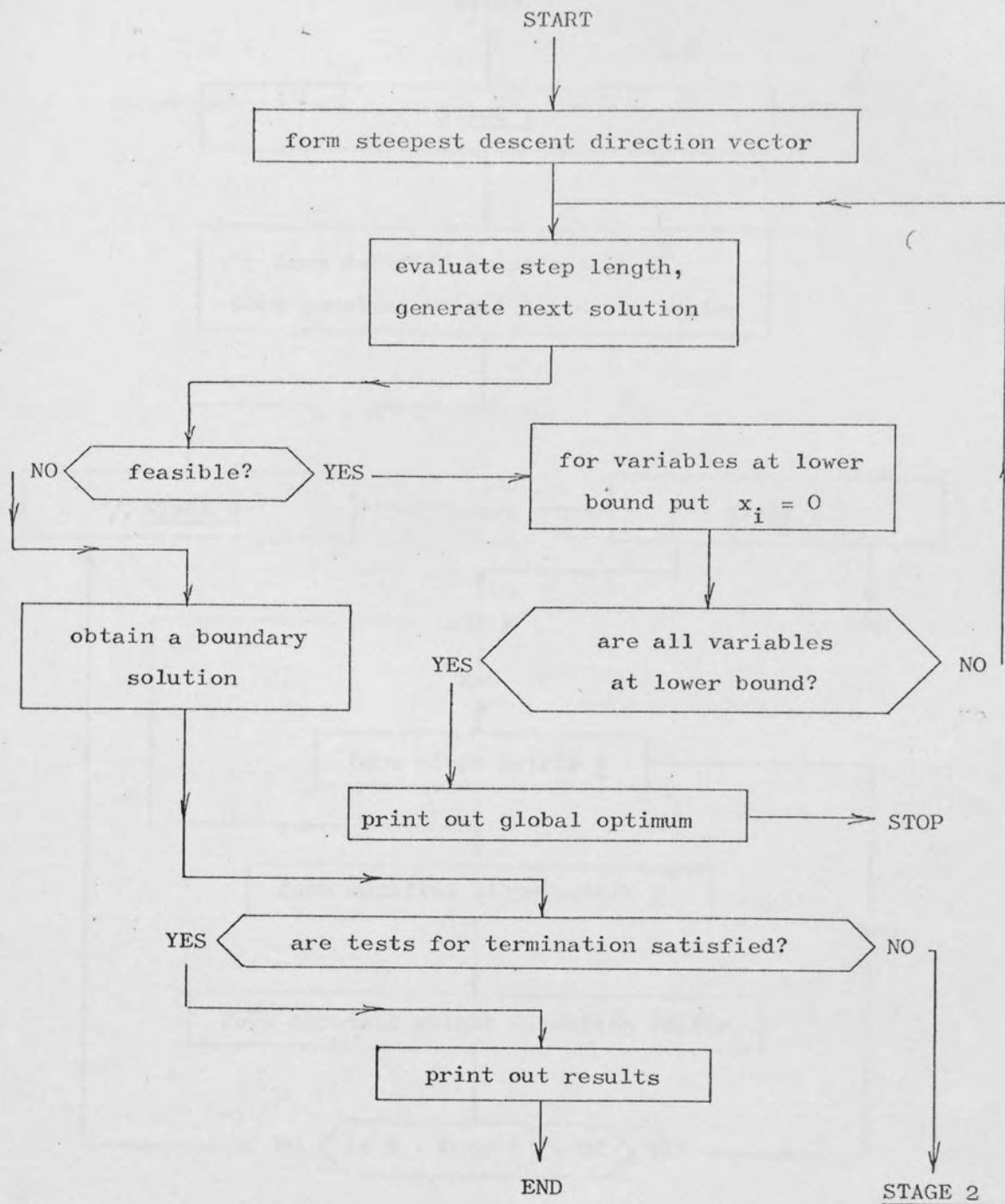


Figure 4.4 Stage 3 flow diagram

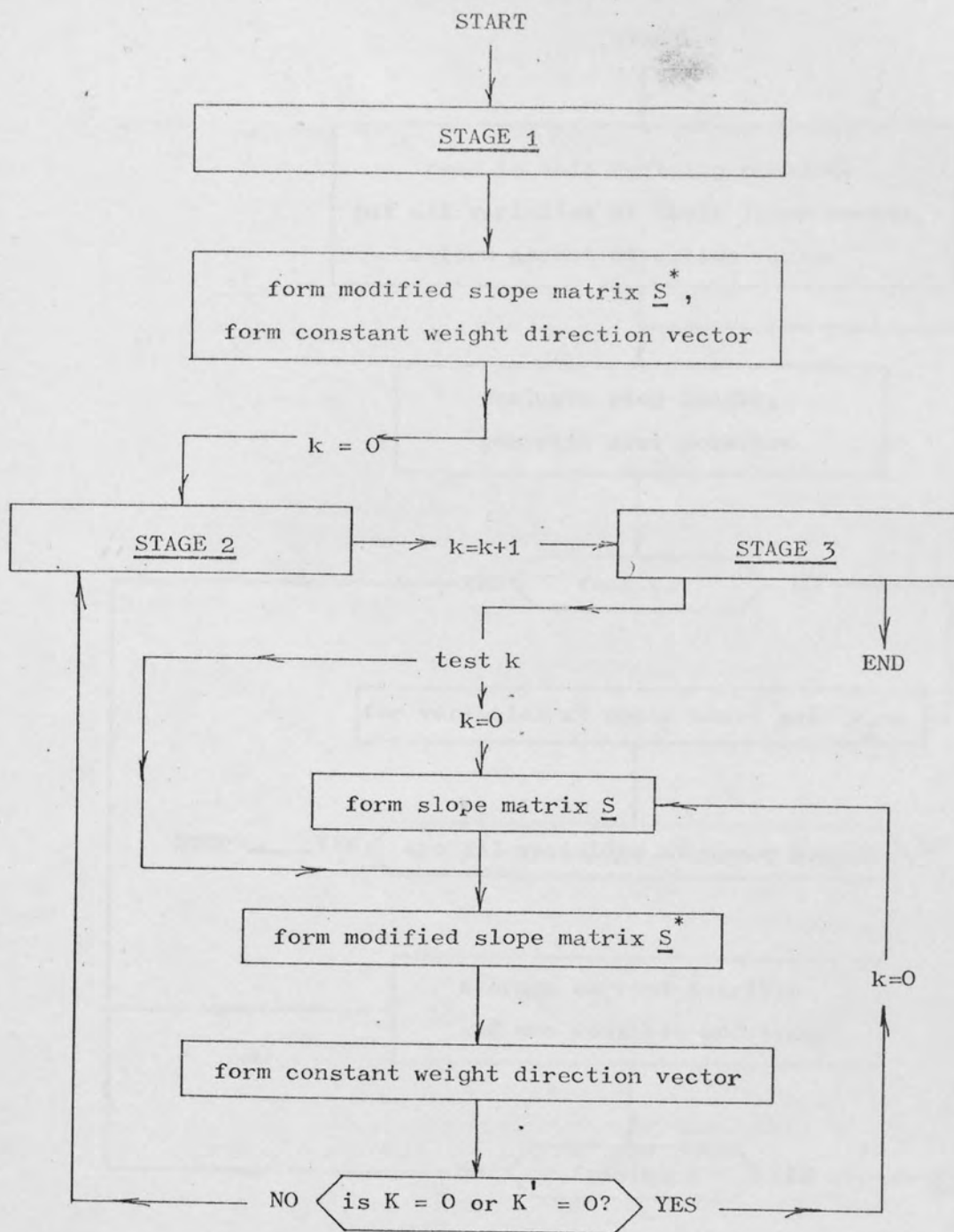


Figure 4.5 Modified main flow diagram



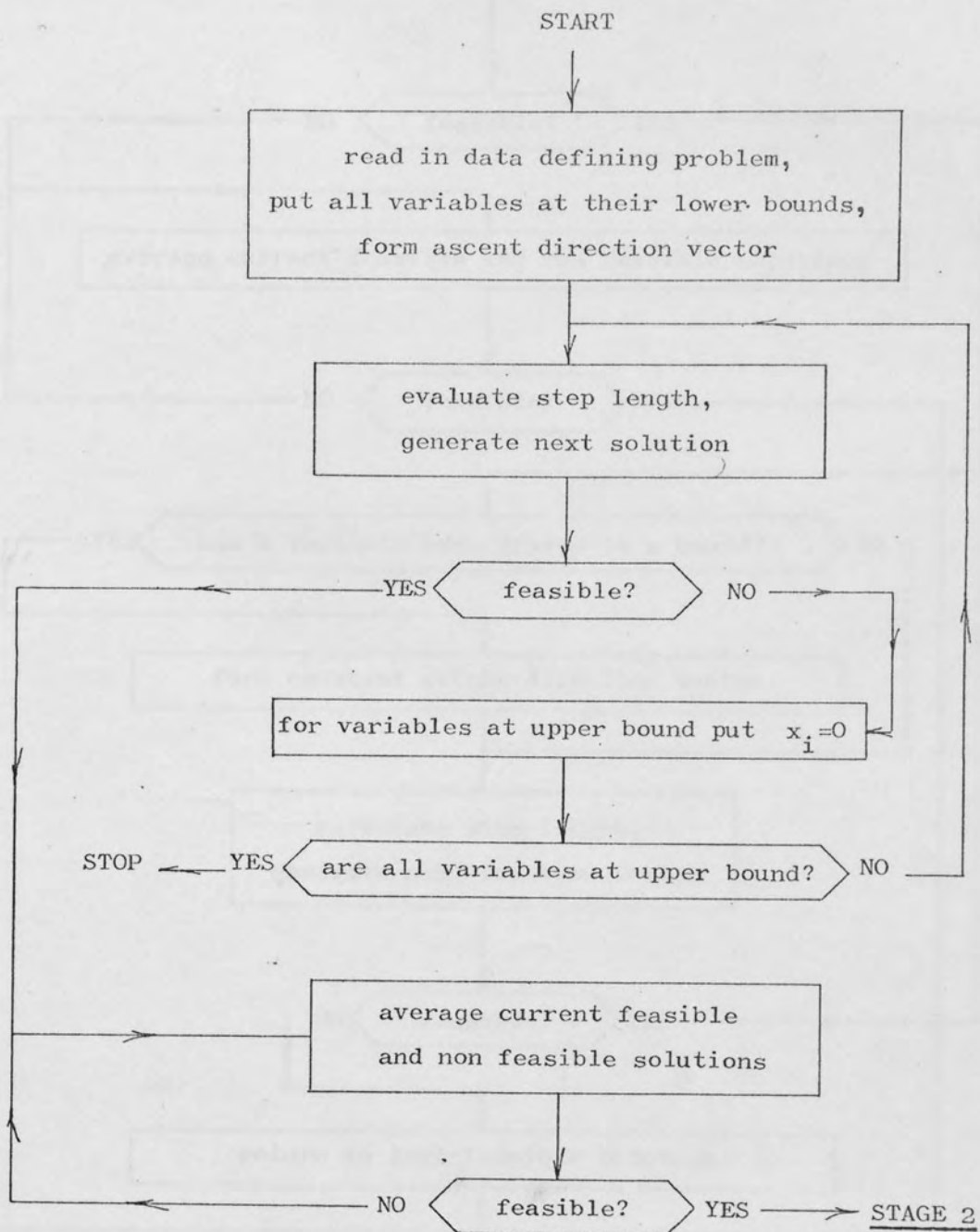


Figure 4.6 Modified stage 1 flow diagram

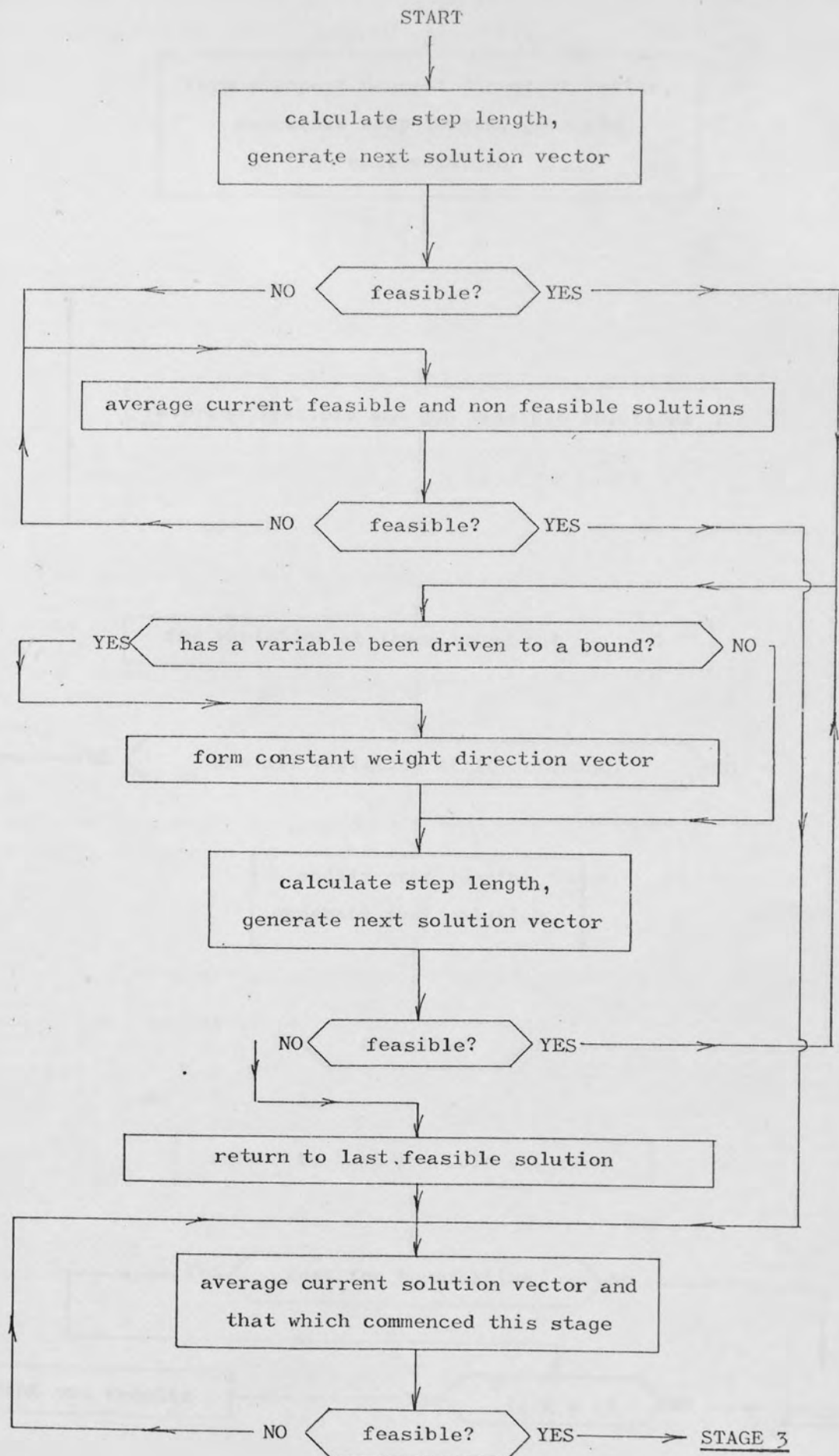


Figure 4.7 Modified stage 2 flow diagram

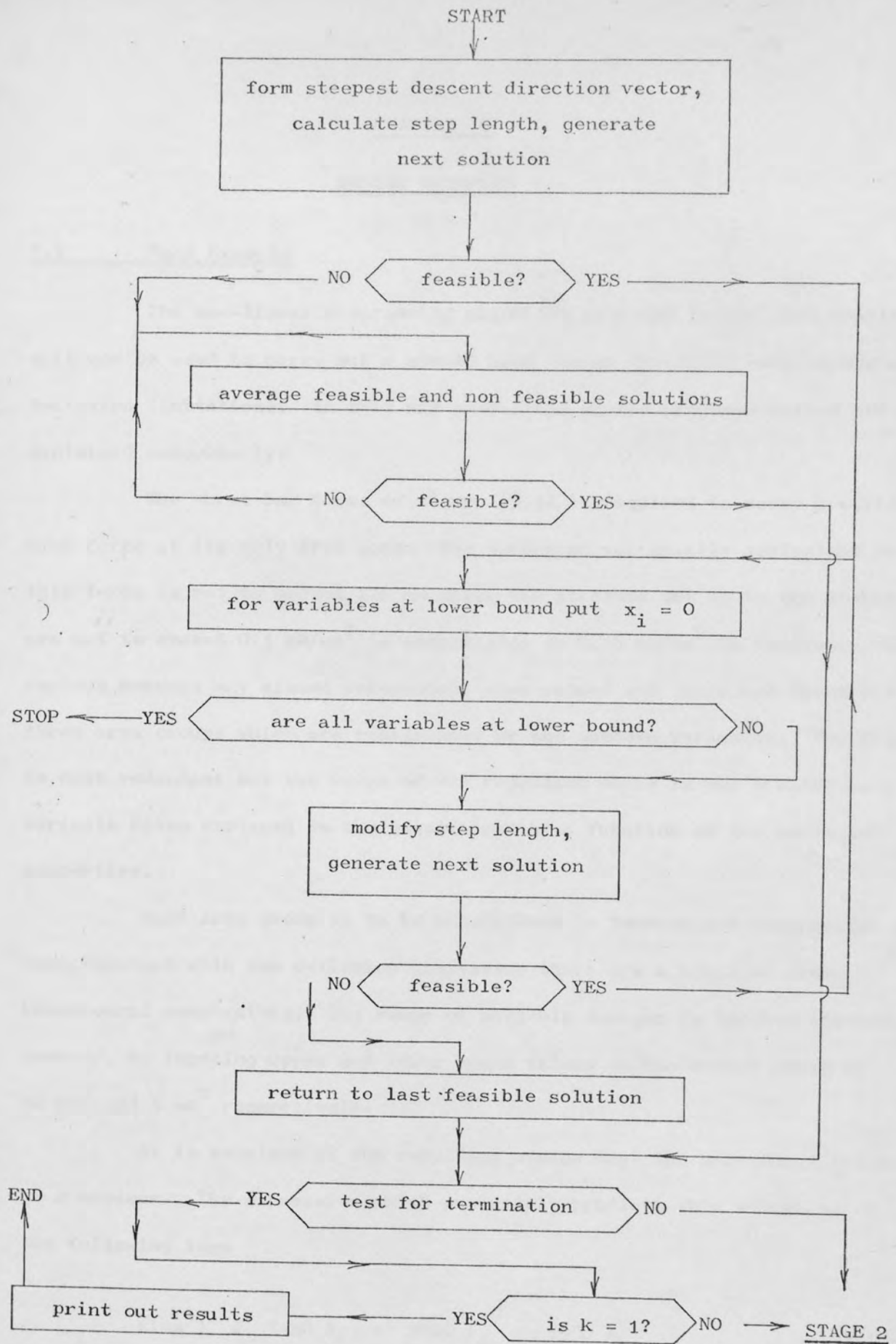


Figure 4.8 Modified stage 3 flow diagram

## CHAPTER 5

DESIGN EXAMPLES5.1 Hand Example

The non-linear programming algorithm proposed in the last chapter will now be used to carry out a simple hand design involving both stress and deflexion limitations. In this way some steps of the proposed method are explained numerically.

The three bar truss of figure (5.1) is required to carry a vertical 4 kN force at its only free node. The deflexion vectorially equivalent to this force is not to exceed 1.2 mm while the stresses set up in the members are not to exceed  $0.1 \text{ kN/mm}^2$  in compression or  $0.16 \text{ kN/mm}^2$  in tension. The various members may assume independent area values and there are therefore three area groups which are represented by the unknown variables. The frame is once redundant but the value of the redundant force is not treated as a variable being replaced in the constraints by a function of the sectional properties.

Each area group is to be constrained in tension and compression so that together with the deflexion limitation there are a total of seven behavioural constraints. The range of possible designs is further limited, however, by imposing upper and lower bound values on the member areas of  $50 \text{ mm}^2$  and  $5 \text{ mm}^2$  respectively.

It is required of the resulting design that the structural volume be a minimum. The expression which accurately predicts this volume is of the following form

$$z(\text{mm}^3) = 3120 A_1 + 2000 A_2 + 1500 A_3 \quad \dots 5.1$$

where  $A_1$ ,  $A_2$  and  $A_3$  are the areas of members 1, 2 and 3 respectively. For numerical convenience this will be divided throughout by 1000.

The constraints are formulated using the matrix force method of structural analysis and the design problem is seen to be one of

$$\text{minimizing } z = 3.13 A_1 + 2 A_2 + 1.5 A_3$$

subject to

$$0.16 \geq [1.79 + (12.05A_1 - 9.21A_2)A_3 / (5.16A_2A_3 + 5.66A_1A_3 + 7.14A_1A_2)] / A_1 \\ \geq -0.1$$

$$0.16 \geq [-2.79 + (15.76A_1 - 12.05A_2)A_3 / (5.16A_2A_3 + 5.66A_1A_3 + 7.14A_1A_2)] / A_2 \\ \geq -0.1$$

$$0.16 \geq (-20.45A_1 + 15.63A_2) / (5.16A_2A_3 + 5.66A_1A_3 + 7.14A_1A_2) \geq -0.1$$

$$[18.48A_1 + 11.84A_2 - (61.11A_2^2 + 104.52A_1^2 - 159.84A_1A_2)A_3 / (5.16A_2A_3 + 5.66A_1A_3 + 7.14A_1A_2)] / A_1A_2 \leq 1.2$$

$$\text{and } 50 \geq A_i \geq 5$$

where  $i = 1, 2, 3$

The tolerances required for the various tests are to be  $t_1 = 0.3$ ,  $t_2 = 0.01$ ,  $t_3 = 0.01$ , and  $t_4 = 0.0075$ .

Stage 1 of the solution is commenced by placing the variables at their lower bound values of 5. Then since  $\{c_1 \ c_2 \ c_3\} = \{3.12 \ 2 \ 1.5\}$  equation (4.17) gives the initial direction of search as

$$\underline{\delta x} = \{0.3205 \quad 0.5 \quad 0.6667\}$$



Equations (4.20) and (4.22) can now be used to calculate a step size  $\lambda$ . The upper bound limitation on the variables is 50, for the first variable therefore, equation (4.20) gives

$$\lambda_1 = 3.12 (50 - 5) = 140.4$$

Similarly the value of  $\lambda_2 = 90$  and  $\lambda_3 = 67.5$ . The least value of  $\lambda$  is therefore 67.5. Using this value in equation (4.10) gives the first generated solution vector as

$$\begin{bmatrix} A_1 \\ A_2 \\ A_3 \end{bmatrix} = \begin{bmatrix} 5 \\ 5 \\ 5 \end{bmatrix} + 67.5 \begin{bmatrix} 0.3205 \\ 0.5 \\ 0.6667 \end{bmatrix} = \begin{bmatrix} 26.6337 \\ 38.7500 \\ 50.0000 \end{bmatrix}$$

The first three constraints of this problem are seen to be of the type given by equation (4.8) and are therefore represented by two normalised constraints. By substituting the current values of the variables into the first constraint the stress in member 1 is found to be  $0.0643 \text{ kN/mm}^2$ , a tensile stress lying within the required range. Substitution into equation (4.6a), with a value for  $d$  of 10, gives the values of the normalised constraints corresponding to the stress in this member as  $G_{N1}^T = 5.9820$  and  $G_{N1}^C = 16.43$ . Here the superscripts T and C refer to the tensile and compressive normalised constraints respectively.

It is noticeable from these results that should the value of any normalised stress constraint exceed that of  $d$  the associated member does not act in the corresponding manner. Similar operations for the remaining stress constraints and the single deflexion constraint reveal that the current design is feasible.

The averaging procedure to locate a boundary solution vector is now commenced. At this stage the most recent non-feasible value for the first variable is 5 and its current feasible value is 26.6337. The average

of these two values gives a new value of  $A_1$  as 15.8168. This process is carried out for all the variables and the resulting solution vector is found to be non-feasible. Repeated interpolation of this type is carried out for all the variables simultaneously and the first boundary solution vector is found to be

$$\{A_1 \quad A_2 \quad A_3\} = \{21.2252 \quad 30.3125 \quad 38.75\}$$

at which point the deflexion limitation dominates the design.

It is now possible to construct the modified slope matrix  $\underline{S}^*$  and a constant weight direction vector. The current values of the normalised constraints are found to be

$$\begin{array}{lcl} \text{member 1} \left\{ \begin{array}{l} G_{N1}^T \\ G_{N1}^C \end{array} \right. & = & \begin{array}{l} 4.919 \\ > 10 \end{array} \\ \text{member 2} \left\{ \begin{array}{l} G_{N2}^T \\ G_{N2}^C \end{array} \right. & & \begin{array}{l} > 10 \\ 0.560 \end{array} \\ \text{member 3} \left\{ \begin{array}{l} G_{N3}^T \\ G_{N3}^C \end{array} \right. & & \begin{array}{l} 9.838 \\ > 10 \end{array} \\ \text{deflexion} & G_{ND} & 0.286 \end{array}$$

from which it can be seen that apart from the deflexion constraint only the compressive limitation of member 2 is near violation. For this reason the new constant weight direction vector will be influenced only by these constraints, and the columns of the modified slope matrix which correspond to the rest will have only zero elements. Subject to this condition the elements of the modified slope matrix are obtained from equation (4.29) giving

$$\underline{S}^* = \begin{bmatrix} 0 & 0 & 0 & 0.0833 & 0 & 0 & 0.1555 \\ 0 & 0 & 0 & 0.1346 & 0 & 0 & 0.1329 \\ 0 & 0 & 0 & 0.0001 & 0 & 0 & 0.0001 \end{bmatrix}$$

Equations (4.34) and (4.35) are now used to construct vectors  $\underline{\alpha}$  and  $\underline{\beta}$ . These together with upper and lower bounds imposed on the variables, are then used in equation (4.37) to obtain the vectors  $\underline{k}$  and  $\underline{k}'$ . The results of these calculations are summarised as

$$[\underline{\alpha} \quad \underline{\beta} \quad \underline{k} \quad \underline{k}'] = \begin{bmatrix} 1 & 0 & 28.7748 & 0 \\ 0.7181 & 0.2819 & 14.1375 & 5.5499 \\ 0 & 1 & 0 & 11.2500 \end{bmatrix}$$

Summing the last two columns gives  $K = 8.0872$  and  $K' = 13.8552$ . The new direction vector is now evaluated using equation (4.38) and found to be

$$\underline{\delta x} = \{ 1.4227 \quad -0.0029 \quad -2.9553 \}$$

It is interesting to note here that the most expensive variable is to be increased in value and the least expensive decreased.

Equations (4.43) are now used to obtain a new step length. The value of  $\lambda$  necessary to drive  $A_1$  to its upper bound is found to be

$$\lambda_1 = (50 - 21.2252)/1.4227 = 20.2254$$

Step lengths  $\lambda_2$  and  $\lambda_3$  required to drive variables  $A_2$  and  $A_3$  to their lower bounds are similarly found to be 8728.4482 and 11.4201 respectively. To prevent a variable bound violation the least of these values is used in equation (4.10) to generate a further solution vector which is found to be

$$\{A_1 \quad A_2 \quad A_3\} = \{37.4725 \quad 30.2794 \quad 5.0000\}$$

This solution is feasible and the corresponding values of the normalised constraints are

$$\begin{array}{lcl} \text{member 1} \left\{ \begin{array}{l} G_{N1}^T \\ G_{N1}^C \end{array} \right. & = & \begin{array}{l} 6.882 \\ >10 \end{array} \\ \text{member 2} \left\{ \begin{array}{l} G_{N2}^T \\ G_{N2}^C \end{array} \right. & & \begin{array}{l} >10 \\ 1.180 \end{array} \\ \text{member 3} \left\{ \begin{array}{l} G_{N3}^T \\ G_{N3}^C \end{array} \right. & & \begin{array}{l} >10 \\ 7.060 \end{array} \\ \text{deflexion} & G_{ND} & 2.362 \end{array}$$

By comparing these values with those obtained from the previous boundary solution vector it is immediately noticeable that the two most critical constraints have increased in value. The constant weight direction of search has therefore been away from the critical constraints. In the current solution  $A_3$  is at its lower bound value and before commencing stage 3 of the algorithm  $\delta x_3$  is set to zero. The steepest descent vector is otherwise formulated from equation (4.23) and found to be

$$\underline{\delta x} = \{-3.12 \quad -2 \quad 0\}$$

Equation (4.41) gives the value of the step length required to travel a distance equal to that travelled in stage 2 as  $\lambda = 32.01$ . This step length cannot be employed however as equation (4.43) reveals that a step length of  $\lambda = 10.4078$  is all that is required to drive the first variable to its upper bound.

Use of equation (4.10) followed by the averaging procedure leads to a new boundary solution vector of

$$\{A_1 \quad A_2 \quad A_3\} = \{32.3986 \quad 27.0269 \quad 5\}$$

This represents a reduction in the objective function from the 184.972, of the last boundary solution vector, to 162.637. At this point the most critical constraint is that which limits the compressive force in member 2 indicating that in moving from the first boundary solution vector, where deflexion was most critical, to the second the design space has been crossed.

Stages 2 and 3 are now repeatedly employed and in five cycles a solution is obtained satisfying the conditions for termination defined by equations (4.24) and (4.25). This solution represents a final design of

$$A_1 = 20.2698 \text{ mm}^2$$

$$A_2 = 29.9501 \text{ mm}^2$$

$$A_3 = 5.0000 \text{ mm}^2$$

with a structural volume of  $130,642 \text{ mm}^3$ . The penultimate boundary solution obtained was

$$\{A_1 \quad A_2 \quad A_3\} = \{20.1218 \quad 30.2164 \quad 5.0000\}$$

with an objective function value of 130.712 as opposed to the 130.642 of the final design. Comparison of these solutions is found to satisfy both of the termination tests simultaneously. In this case the most altered variable, the area of member 2, has changed by 0.89% and the objective function has reduced by only 0.06%.

The analysis of the final optimum design reveals that the stresses



in members 1, 2, and 3 are 0.0867, -0.0992 and 0.0094 kN/mm<sup>2</sup> respectively, and that the vertical deflexion at the free node is 1.1998 mm. From these results it can be seen that not only is the deflexion critical but so too is the compressive stress of the second member.

It is noticed that during the design procedure once the area of member 3 has been driven to its lower bound it remains there in spite of the fact that this is the cheapest variable. For this reason, following the second boundary solution vector obtained, the route to the optimum can be shown as a two-dimensional graph. This is done in figure (5.2) on which are also plotted the only two constraints that become critical during the search for the optimum, namely, the deflexion constraint and the compressive stress constraint of member 2. It is noticed that as the optimum is approached the movement is practically along the boundary surface of the feasible design region, and the actual distance between boundary solution vectors becomes smaller. This latter fact supports the notion that as the optimum is approached so the initial step size taken in any stage should reduce. This graph also shows that the feasible space to be searched decreases as the solution proceeds.

Figure (5.3) shows the variation of the numerical values of the member areas in successive boundary solution vectors. Following initial drastic variation due to the transversing of the feasible area the variables are seen to converge gently toward their final values. This is emphasised in figure (5.4) where the percentage changes in the values of the variables are shown in successive cycles. Here the dotted line indicates the variation in the most affected variable, where it is noticed that as the optimum solution is approached  $A_2$  becomes the most affected variable, and its value tends to stabilise until finally its alteration is less than the 1% required.

Curve a of figure (5.5) is a plot of the percentage decrease in the objective function from that resulting after the previous cycle. Curve b in the same figure is a plot of the objective function values corresponding to each boundary solution vector expressed as a percentage of that of the first boundary solution vector. This is seen to be a gentle curve, and both curves show that as the final result is approached so the changes in the objective function become insignificant.

Figure (5.6) indicates the variation in the value of the redundant force as the design proceeds. It is interesting to note that initially the force becomes alternatively tensile and compressive. However, over the last three cycles it converges gently towards its final tensile value of 0.0472 kN.

## 5.2 2-Dimensional Braced Truss

The structure of figure (5.7) is a practical frame commonly used in structural engineering as a Truss Bridge. This structure was originally designed for minimum weight by Toakley (36) using a trial and error method. The structure has 22 members grouped together, with some members made out of the same section, so that there are 16 groups. The member, and group numbering is indicated in the figure. There are 6 redundant members, i.e. the structure is hyperstatic to the sixth order. Two separate loads of 498.375 kN and 299.025 kN are applied independently at A and B as shown in the figure. The vertical deflexions at these points were limited to 12.7 mm. The working stresses in the members were limited to  $0.147 \text{ kN/mm}^2$  in both tension and compression. Youngs modulus of the material was  $207 \text{ kN/mm}^2$ .

Altogether there are 32 stress constraints, 2 deflexion constraints and 6 compatibility equations to deal with the redundant forces. In addition

to these upper and lower bound limitations were imposed upon the design variables of  $1290.3 \text{ mm}^2$  and  $6451.6 \text{ mm}^2$  respectively.

The programs written for all the design problems to be discussed in this chapter are in Atlas Autocode to operate on the Atlas 1 computer at Chilton. The general method of solution is similar in all cases being based upon the flow diagrams of the previous chapter, where the details of the optimization procedure have been described.

The braced frame now under consideration was designed for various values of the tolerance  $t_3$  required for the termination test of equation (4.24). The variation in the volume of the structure with respect to this tolerance is shown in figure (5.8). It is noticed that the reduction in the volume becomes insignificant once the tolerance is reduced below  $10^{-4}$ . In the same figure the variation of the computer time is also shown. It is clear from this graph that imposing a small tolerance on the problem increases the computer time without much loss in weight of the final design.

Using the first of the two proposed algorithms, and a tolerance on the objective function of 0.0001% the final areas obtained are tabulated in table (5.1). The final volume obtained was  $2.5036 \times 10^8 \text{ mm}^3$  as compared to  $2.47 \times 10^8 \text{ mm}^3$  obtained by Toakley. This indicates a close agreement between the direct solution used by the proposed method and that obtained by Toakley.

When designing hyperstatic frames the forces throughout the structure continually change as the design progresses. This is illustrated in connection with this example in table (5.2) where the initial and final forces due to both the load cases are tabulated. In the final design both deflexion criteria are critical, that at A when the first loading case is applied and that at B when the second is applied.

### 5.3 Schwedler Dome Design

The Schwedler Dome shown in plan in figure (5.9) and in elevation in figure (5.10) was designed under two independent load systems. The first load system consisted of a 99.675 kN load acting vertically downwards at each joint. The vertical deflexions of points A and B shown in figure (5.9) were not to exceed 5.08 mm and 2.54 mm respectively when this load case was acting. The second load system was a single 498.375 kN load acting horizontally and to the right at joint A. Under this load system the horizontal deflexions at nodes A and B were not to exceed 20.32 mm and 10.16 mm respectively.

Youngs modulus for the material was  $207 \text{ kN/mm}^2$  and the stresses in the members were once again limited in both tension and compression to  $0.147 \text{ kN/mm}^2$ . The 54 members of the dome were collected together into 9 area groups as tabulated in figure (5.10). The design problem was therefore one of 9 variables, the values of which were limited by upper and lower bounds of  $6451.60 \text{ mm}^2$  and  $1290.32 \text{ mm}^2$ .

The final design was obtained using the first algorithm with values of  $t_2 = 0.001$  and  $t_3 = 0.0001$ , and is given in table (5.3). The value of the weight function corresponding to this design was found to be  $8.2925 \times 10^8 \text{ mm}^3$  and was achieved after 20 iterations of the optimization procedure.

### 5.4 Buckling of Members

In all the previously described examples no allowance is made for the possibility of the buckling of compression members in the final designs obtained. Short structural members in compression fail by crushing or yielding of the material, however, slender structural members in compression

yield by buckling before the crushing stress has been reached. For a given cross-sectional area the longer such a strut is the lower will be the load necessary to cause buckling.

This presents no real difficulty when dealing with the design of statically determinate structures. In practical situations the framework members will consist of sections selected from the safe load tables. It is observed that if the designer is restricted to using only those sections for which the radius of gyration increases, or retains substantially the same value as the area increases, there will be negligible loss in economy. Thus a solution is obtained to the optimization problem by restricting slightly the choice of sections and taking a lower bound on the area of compression members as the area required to carry safely the known axial compression. If the area has to be increased above this value to satisfy a deflexion constraint, the allowable stress will not be less than the value originally assumed due to the isostatic properties.

When dealing with statically indeterminate structures member stresses vary with changes in member areas and therefore a lower bound area technique is no longer practical. In this case should an area be increased to satisfy a deflexion constraint the allowable stress of the corresponding member or any other member may well decrease making any initially selected lower bound area un-economical. It therefore becomes necessary to recalculate allowable compressive stresses at each solution vector in order to evaluate the corresponding normalised constraints.

A theoretical formula, from which buckling may be predicted was produced by Euler for an ideal axially loaded strut. In practice however struts depart from ideal behaviour due to imperfections in the material, friction in the pinned ends, initial curvature etc. As a result of this



more practical formulae have been put forward including that by Rankine-Gordon.

A practical formula used in structural engineering is the Perry-Robertson formula. This allows for non-ideal conditions by assuming an initial curvature in the strut. The formula is as follows

$$\sigma_c^* = \frac{\sigma_t^* + (\eta + 1)\sigma_e}{2} - \sqrt{\left\{\left(\frac{\sigma_t^* + (\eta + 1)\sigma_e}{2}\right)^2 - \sigma_t^* \sigma_e\right\}} \quad \dots 5.2$$

where  $\sigma_e$  is the Euler critical stress given by

$$\sigma_e = E \pi^2 r^2 / l^2 \quad \dots 5.3$$

In these equations  $\sigma_c^*$  and  $\sigma_t^*$  are the allowable member stresses in compression and tension,  $E$  is Young's modulus of the material and  $l$  and  $r$  are respectively the length and radius of gyration of the member under consideration. The symbol  $\eta$  is a number embodying the initial curvature of the strut and the geometrical shape of the section. This formula is used to form Table 17 of B.S.449, which deals with allowable compressive stresses, using a factor of safety of 1.7 and a value of  $\eta$  given by

$$\eta = 0.3(1/100r)^2 \quad \dots 5.4$$

The shapes of the curves obtained when relating allowable stress with slenderness ratio ( $= l/r$ ) are plotted in figure (5.11) for the Euler, Rankine-Gordon, and Perry-Robertson equations. The Perry-Robertson formula is found to best fit reality and is employed in the computer program when evaluating the compressive stress constraints of the area groups.

At any stage during the optimization procedure the only member properties available are the cross-sectional areas. It is therefore

necessary to obtain a relationship between the minimum radius of gyration and the cross-sectional area. The minimum radius of gyration is chosen because it is this that will yield the largest value of slenderness ratio and it is about the corresponding axis that buckling will occur.

Figure (5.12) shows a plot of the radius of gyration against the cross-sectional area of selected mild steel equal angle sections from the safe load tables. Figure (5.13) shows a similar plot for selected standard mild steel channels and universal beams. The result is a scatter of points through which any number of lines and curves can be fitted to give a continuous relationship between area and radius of gyration. For use in the computer program the following linear relationships were utilised

$$\begin{array}{ll}
 r = 0.00991667 A & \dots 5.5 \\
 \text{if } 0 < A \leq 2253.9 \text{ mm}^2 & \left. \vphantom{\begin{array}{l} r = 0.00991667 A \\ \text{if } 0 < A \leq 2253.9 \text{ mm}^2 \end{array}} \right] \\
 \text{or } r = 18 + 0.0019307 A & \left. \vphantom{\begin{array}{l} r = 18 + 0.0019307 A \\ \text{if } 2253.9 < A \leq 12500 \end{array}} \right] \\
 \text{if } 2253.9 < A \leq 12500 & \dots 5.6
 \end{array}$$

When the final design is obtained each area group is associated with a corresponding minimum value for the radius of gyration. When selecting actual discrete sections it is desirable if possible to choose sections which lie near to the straight line relationships between  $r$  and  $A$  which are represented in figures (5.12) and (5.13) by the lines  $ab$  and  $bc$ . The flexible nature of the proposed method makes it possible to replace the linear relationships of equations (5.5) and (5.6) with any other desired relationship with the minimum of effort.

### 5.5 Tower Design

The tower structure shown in figure (5.14) has a total of 19 joints and 54 members of which 9 are redundant members. This structure was designed so as to satisfy stress and deflexion limitations under two separate loading cases. The components of the loading cases are shown in figure (5.15) where the vertical and horizontal forces are separated. The first load case consisted of a vertical force acting at each joint of the structure to simulate self weight. Additional forces were applied at the ends of the cantilevers to simulate the weight of the transmission cables. The second load case consisted of these forces together with horizontal forces applied at each level in the structure. In this load case additional horizontal forces were also applied at the ends of the cantilever arms to represent sway of the transmission cable.

The horizontal sway of the tower was limited to 4.6 mm and the member stresses throughout the structure were limited to  $0.16 \text{ kN/mm}^2$  in tension. The stresses in the compression members were not to exceed the allowable values obtained from the Perry-Robertson formula of equation (5.2) when using the relationship of equations (5.5) and (5.6) to relate member area and radius of gyration.

The members of the structure were grouped into 10 area groups, as indicated in figure (5.14) and the design was further limited by imposing upper and lower bound values on these area groups of  $500 \text{ mm}^2$  and  $10000 \text{ mm}^2$  respectively.

The design was carried out once again using the first of the two proposed algorithms. The decrease in the volume of successive boundary solutions is shown in figure (5.16), where the volume of the first boundary solution is taken as 100%. It can be seen from this graph that initially the volume decreases rapidly. However, the curve gradually becomes less

steep as the number of iterations increases and the final result is approached. This result is obtained with a value of  $t_4 = 0.005$ .

The percentage change in the most affected variable between successive boundary solutions is shown in figure (5.17). In the early stages of the design there is a considerable alteration of the variables due to the traversing of the feasible design space. In certain iterations of the design process all the variables are altered by a similar amount. In others, however, a major alteration occurs in one of the variables and the remainder are only slightly affected. This explains the irregular nature of the graph, of figure (5.17), with the valleys corresponding to the former case and the peaks to the latter case. As the final design is approached this graph is seen to become less irregular and converges to a value of less than 1%.

The values of the variables at each of the boundary solutions obtained are plotted in the graph of figure (5.18). Once again it is noticed that there is a considerable variation in the initial stages of the design. Eventually however the curves become less irregular and the variables settle down about their final values.

The final design obtained is given in table (5.4) and corresponds to a structural volume of  $5.20 \times 10^8 \text{ mm}^3$ . This table gives the sectional areas required for the various groups together with the corresponding minimum radius of gyration. This table also gives the first boundary solution obtained. In the final design both buckling and deflexion criteria were active, the vertical deflexion at the top of the tower being 4.596 mm, very close to its permissible value of 4.6 mm.

## 5.6 Cantilever Designs

In order to investigate the computer time and storage requirements of the proposed methods when applied to designs of increasing size and

complexity, a series of three-dimensional cantilever structures were considered. The first of these is shown in figure (5.19) and consists of 12 joints and 28 members of which 4 are redundants. The members of this structure are divided into 7 area groups which are also indicated in the figure.

The second cantilever is shown in figure (5.20) and is an extension of the first. The span has been increased from 6.25 metres to 11.5 metres by the addition of a further 8 joints and 28 members. The second cantilever is therefore 8 times redundant and has an additional 7 area groups which are also indicated in the figure.

The third cantilever is a similar extension of the second with a span of 15.75 metres. This structure is shown in figure (5.21) and now has 28 joints, 84 members of which 12 are redundant, and 21 area groups. The fourth and fifth cantilever structures are obtained in an identical fashion. These have spans of 19 metres and 21.25 metres respectively and are shown in figures (5.21) and (5.22). The fourth cantilever has 36 joints, 112 members of which 16 are redundants, and 28 area groups. Finally the fifth cantilever has 44 joints, 140 members of which 20 are redundants, and 35 area groups.

Each of these cantilevers was subjected to two independent loading cases so as to deflect the structure in a vertical plane and also to twist the structure. To conveniently describe this loading arrangement the overall structure may be divided into 10 sections numbered from 1 to 10 in figures (5.19) to (5.23). Forces are applied to each of these sections in an identical manner, only the magnitude of the forces varying from section to section. This loading is indicated in figure (5.24) where it can be seen that the first load case consists of two equal vertical forces applied at nodes such as A and B along the upper surface of the cantilever. The magnitudes of these forces when applied to the various sections are given in



the second column of the table of figure (5.24) and represent a vertical uniformly distributed load of 30 kN/metre run.

The second loading case is also given in this figure and consists of a vertical force applied at nodes such as B along the upper surface of the cantilever together with a horizontal force at nodes such as C along the soffit of the cantilever. This load case has the effect of twisting the cantilever and the values of the forces corresponding to the various cross-sections are given in the third and fourth columns of the table.

The design criteria to be satisfied by the final minimum weight designs included both deflexion and stress considerations. The deflexion at any cross-section was not to exceed  $1/325$  of the distance of that cross-section from the supports. The stress criteria were of two types, the stress of each member in tension being restricted to  $0.16 \text{ kN/mm}^2$  but that in compression being dependent upon the buckling considerations mentioned earlier. Young's modulus of the material was taken as  $207 \text{ kN/mm}^2$  and values of the tolerances were  $t_1 = t_2 = 0.001$  and  $t_3 = t_4 = 0.0001$ .

The cantilever designs described above represent a range of designs with increasing complexity. The first is a problem with 7 design variables, 14 stress constraints and 4 deflexion constraints. The fifth is a problem with 35 design variables, 70 stress constraints and 20 deflexion constraints.

The progress of each design is given in graphical form in figures (5.25) to (5.29). Curve a of these figures represents the decrease in the structural volume at successive boundary solutions, where the volume of the first boundary solution is taken as 100%. In common with the previous design examples these curves become less steep as the final result approaches. Curve b in figures (5.25) to (5.29) represent the percentage change of the values of the most affected variables between one boundary solution and the

next. These curves are seen to be irregular but are similar to those obtained in other designs.

In all five cantilever designs it is noticeable that in the first few cycles of the process the percentage change of the most affected variable is large. This is due to the geometry of the structure and the grouping of the members. Each successive stage of the overall cantilever contributes an additional 7 area groups to the design problem. The additional span to the cantilever due to each stage becomes progressively less, however, and as a result the overall length of corresponding area groups in successive stages is less. In this way group number 30 of the fifth cantilever is less expensive than group number 2. The initial iterations of the design process attempt to gain advantage from this fact by allocating more weight to the less expensive area groups although in the final design it is obvious that the more expensive area groups should have larger cross-sections. This fact soon becomes apparent in the design process and weight is transferred from the cheaper end of the structure to the more expensive but structurally effective end of the structure.

This observation could have been utilized before commencement of the design process by the allocation of varying upper bound limits to the various area groups. In the present designs a lower bound of  $400 \text{ mm}^2$  and an upper bound of  $12000 \text{ mm}^2$  was imposed on all the area groups. However if this upper limit were successively reduced for the additional stages of the cantilever then the cheaper area groups at the free end of the structure would be prevented from taking unnecessarily large values in the early part of the design.

Cantilevers 1, 2 and 3 were designed using the first of the two proposed algorithms. This entailed the evaluation of a slope matrix at each boundary solution. In an attempt to reduce computer time the remaining cantilevers, 4 and 5, having respectively 28 and 35 unknown variables, were

designed using the second of the proposed algorithms. This algorithm does not require the evaluation of so many slope matrices or the accurate location of the boundary of the feasible space. In this manner during the design of the fourth cantilever only 4 slope matrices were produced and for the fifth cantilever, 7, whereas for the first three designs 16, 18 and 29 slope matrices were required before the final result was obtained.

In figures (5.28) and (5.29) the boundary solutions at which a new slope matrix was evaluated are shown by the triangulated points on curve a. Following the production of a new slope matrix this curve becomes more steep. This indicates that a better direction of search is being pursued resulting in a greater weight saving. This is especially so in figure (5.29) and is accompanied by a jump in curve b which indicates that the new direction of search is once again pointing into the feasible design space.

In figure (5.30) the curve a from each of the figures (5.25) to (5.29) is plotted. It can be seen from this figure that the volume of the final design expressed as a percentage of the volume of the first boundary solution varies for each design. This, however, is more a measure of the efficiency of the initially selected feasible solution than it is of the final design. For the first two cantilevers the buckling stress conditions of the members dominated the design throughout and for the third cantilever the deflexion criteria were on the verge of violation in the final design. It is evident from figure (5.30) that the initial feasible solutions selected for these designs become increasingly inefficient as the final designs obtained had volumes of 54.5%, 42.5% and 36.3% of the respective initial volume.

This increasing inefficiency is due to the initial allocation of large sectional properties to the cheaper area groups toward the ends of the

cantilevers. When deflexion criteria are not dominant this is unnecessary due to the relatively lighter loads carried by these members. In the designs of cantilevers 4 and 5 the deflexion criteria become more dominant due to the increasing span of the cantilevers as well as the additional loading. The efficiency of the initial designs selected for these cases shows an immediate improvement, the volumes of the final designs being respectively 45.2% and 43.5% of the initial designs.

The deflected shape of the fifth cantilever is plotted in figure (5.31) at various stages of its design. After 5 iterations of the design process the deflected shape is given by curve a in the figure. This is seen to be well within the desired limits and at this stage the stress criteria dominate the design. After 3 more iterations the volume of the structure has reduced to 60.2% of the initially selected volume and the transfer of volume from the end of the cantilever toward the supports has resulted in the deflexion at cross-section 10 reaching its permissible upper bound value.

The deflected shape of the structure is now given by curve b in the figure. Once the deflexion becomes critical the design process redistributes the structural material in such a way as to decrease the volume while at the same time decreasing the maximum deflexion. The effect of this is shown in the figure by curves c and d which represent the deflected shape after 12 and 17 iterations when the volume of the cantilever was 52.8% and 48.7% of the initially selected volume. At both of these stages of the design it is the stress criteria which are critical, however, after 22 iterations the deflexion at the end of the cantilever is once again at its maximum value. The deflected shape of this final design is given by curve e in the figure and the structure now has a volume 43.5% of that of the first feasible design.

The final volumes of the five cantilevers designed are plotted in

figure (5.32). Assuming the density of the material to be  $7.69 \times 10^{-8} \text{ kN/mm}^3$  the actual weights of the five designs vary between 1,428 kg of the first cantilever and 15,370 kg of the fifth cantilever.

The computer time required to obtain these final designs is plotted in figure (5.33). Without prior knowledge of the likely behaviour of any particular design it is not possible to make an accurate estimate of the computer time that will be required to carry out a design. Furthermore due to the size of a design problem it may be impossible to complete a design in the maximum time available for one run on the computer.

Facilities which write and read the current information concerning the design to and from a magnetic tape were therefore included in the computer programme. When embarking upon a design the first priority is to form the load transformation matrices of the structure which remains unaltered throughout the design. These are then dumped onto magnetic tape and are immediately available for any further runs necessary to continue the design from a current best solution. This enables wastage of computer time to be avoided.

The total time graph of figure (5.33) indicates that the computer time required increases rapidly as does the number of variables involved and the size of the structure being designed. Curve 1 of this figure covers the designs of the first three cantilevers which used the first of the two proposed non-linear programming algorithms. Curve 2 covers the designs of cantilevers 4 and 5 which employed the second algorithm. It is noticeable from comparison of these two curves that the second algorithm represents a saving of computer time over the first algorithm.

This fact is substantiated in the graph of figure (5.34) where the time per iterations of the design process is plotted for each of the

designs. Here again curve 1 represents the first of the proposed algorithms and curve 2 the second. It is also noticeable from this graph that the second algorithm is more efficient in terms of computer time.

Finally the computer storage requirements for the five designs are plotted in figure (5.35). From this figure it can be seen that, in common with the time requirements, the storage requirements increase at a greater rate as the complexity of the design increases. In this figure curve a represents the storage requirements when the design is initially entered into the computer and the load transformation matrices are formed. On the other hand curve b represent the computer storage requirements of successive runs when information concerning the design is already stored on magnetic tape.

The final designs obtained for the five cantilevers are tabulated in tables (5.5) and (5.6).

## 5.7 Conclusions

For the specific optimization problems defined in chapter 3 the proposed method makes use of the special features of these problems to improve the process of obtaining the final result. The application of the method is general. However its use in the minimum weight design of static and hyperstatic structures directly has shown to be promising.

The method may be extended to deal with rigidly jointed structures having non-linear objective functions. This can be achieved by considering the objective function coefficients to be variable quantities equal to the instantaneous partial derivatives of the objective function with respect to the corresponding design variables. Since, as described in Chapter 2, the non-linear objective function is convex toward the origin, the use of such



a function will accelerate the progress of the design.

It is not possible to determine with any certainty how closely the solutions to the non-linear design problems posed in this chapter approach local optima. If the solution of a particular problem was commenced from several widely different initial feasible solutions, and the same final solution was obtained each time, it could probably be concluded that a global optimum had been attained. This procedure has not, however, been used in the present work. It is felt that this technique is of very limited application as it obviously results in a great increase in computer time.

Group No.	Area (mm <sup>2</sup> )
1	3447.4124
2	3546.6380
3	3171.6065
4	1290.9651
5	1304.5715
6	1306.5135
7	1290.7716
8	1291.3522
9	1328.7715
10	1291.3522
11	1291.5458
12	1291.4167
13	1290.9651
14	1308.3844
15	1298.0619
16	4516.0554

Table 5.1 : FINAL SOLUTION VECTOR

Member No.	MEMBER FORCES (kN)			
	INITIAL DESIGN		FINAL DESIGN	
	Load System 1	Load System 2	Load System 1	Load System 2
1	-334.44	-617.39	-196.69	-406.92
2	-186.81	-476.51	-142.02	-399.62
3	-427.29	-455.12	-329.85	-319.51
4	-84.36	87.71	-77.61	129.68
5	-283.06	-226.02	-185.69	-145.12
6	47.34	-75.89	123.35	34.71
7	-153.09	-127.68	-127.03	-105.98
8	31.09	35.70	73.60	70.93
9	76.90	182.47	122.96	261.59
10	48.59	353.03	92.90	403.80
11	90.07	102.18	234.30	328.97
12	41.15	-139.56	122.81	-65.60
13	111.93	118.06	227.39	216.81
14	-61.85	-46.95	-60.74	-43.11
15	111.58	92.89	138.39	115.21
16	-37.54	-31.11	-83.55	-69.42
17	21.97	71.71	-57.07	-64.05
18	244.05	218.04	86.72	-7.34
19	63.17	248.01	-26.99	84.25
20	54.31	19.34	-22.70	-49.10
21	215.41	162.40	94.33	61.88

Table 5.2 : VARIATION OF MEMBER FORCES

Group No.	Area (mm <sup>2</sup> )
1	1290.32
2	1290.32
3	1290.32
4	5009.15
5	5442.89
6	3271.15
7	5008.85
8	6042.96
9	5863.90

Table 5.3 : SCHWEDLER DOME DESIGN

Group No.	Area (mm <sup>2</sup> )		Final Minimum Radius of Gyration (mm)
	1st Feasible Solution	Final Result	
1	3052.19	3300.94	24.37
2	4152.86	1791.17	17.76
3	2396.09	2877.81	23.55
4	5984.37	1275.70	12.65
5	2645.88	2449.72	22.73
6	2708.83	2262.81	22.37
7	5044.76	732.18	7.26
8	3016.80	2131.84	21.14
9	5428.28	1266.91	12.54
10	640.62	500.00	4.96

Table 5.4 : TOWER DESIGN SECTIONAL PROPERTIES

Final Value of Area Groups (mm <sup>2</sup> )			
Cantilever No.			
Group No.	1	2	3
1	760	1381	3455
2	2904	4262	5968
3	1114	1549	2429
4	2598	3165	3428
5	704	1435	2073
6	1766	2131	5739
7	1030	2453	1508
8	-	839	1756
9	-	2387	4023
10	-	1129	1805
11	-	1579	2121
12	-	869	1821
13	-	1056	2278
14	-	926	867
15	-	-	849
16	-	-	1655
17	-	-	1084
18	-	-	1017
19	-	-	581
20	-	-	750
21	-	-	438

Table 5.5 : FINAL RESULT OF CANTILEVERS 1, 2 and 3



		Final Area (mm <sup>2</sup> )				Final Area (mm <sup>2</sup> )	
Group No.	Cantilever No.		Group No.	Cantilever No.			
	4	5		4	5		
1	7604	10473	22	1337	6683		
2	7675	11072	23	1072	6711		
3	4790	3204	24	1642	5088		
4	5145	3864	25	1492	6093		
5	4545	2931	26	728	5587		
6	4829	3173	27	1421	6337		
7	1944	1769	28	964	5558		
8	5549	8429	29	-	4384		
9	8690	9173	30	-	4381		
10	2492	2417	31	-	5178		
11	4124	4449	32	-	5657		
12	3651	4259	33	-	5459		
13	3314	5768	34	-	5774		
14	1978	4592	35	-	4857		
15	2201	6955					
16	4966	7289					
17	2682	4584					
18	2541	6036					
19	2567	5367					
20	2477	6732					
21	1095	5962					

Table 5.6 : FINAL RESULT OF CANTILEVERS 4 and 5

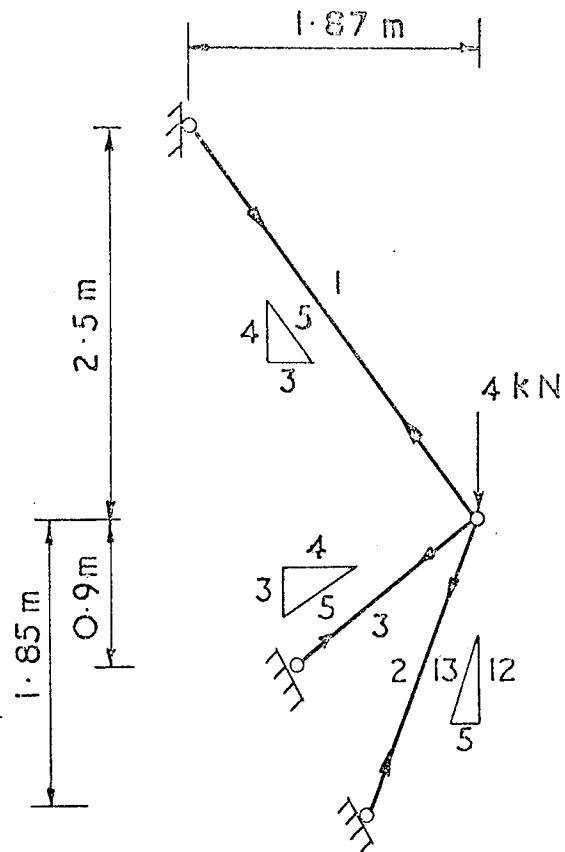


Figure 5.1. 2 Dimensional frame with a single redundant

constraint governing compression in member 2

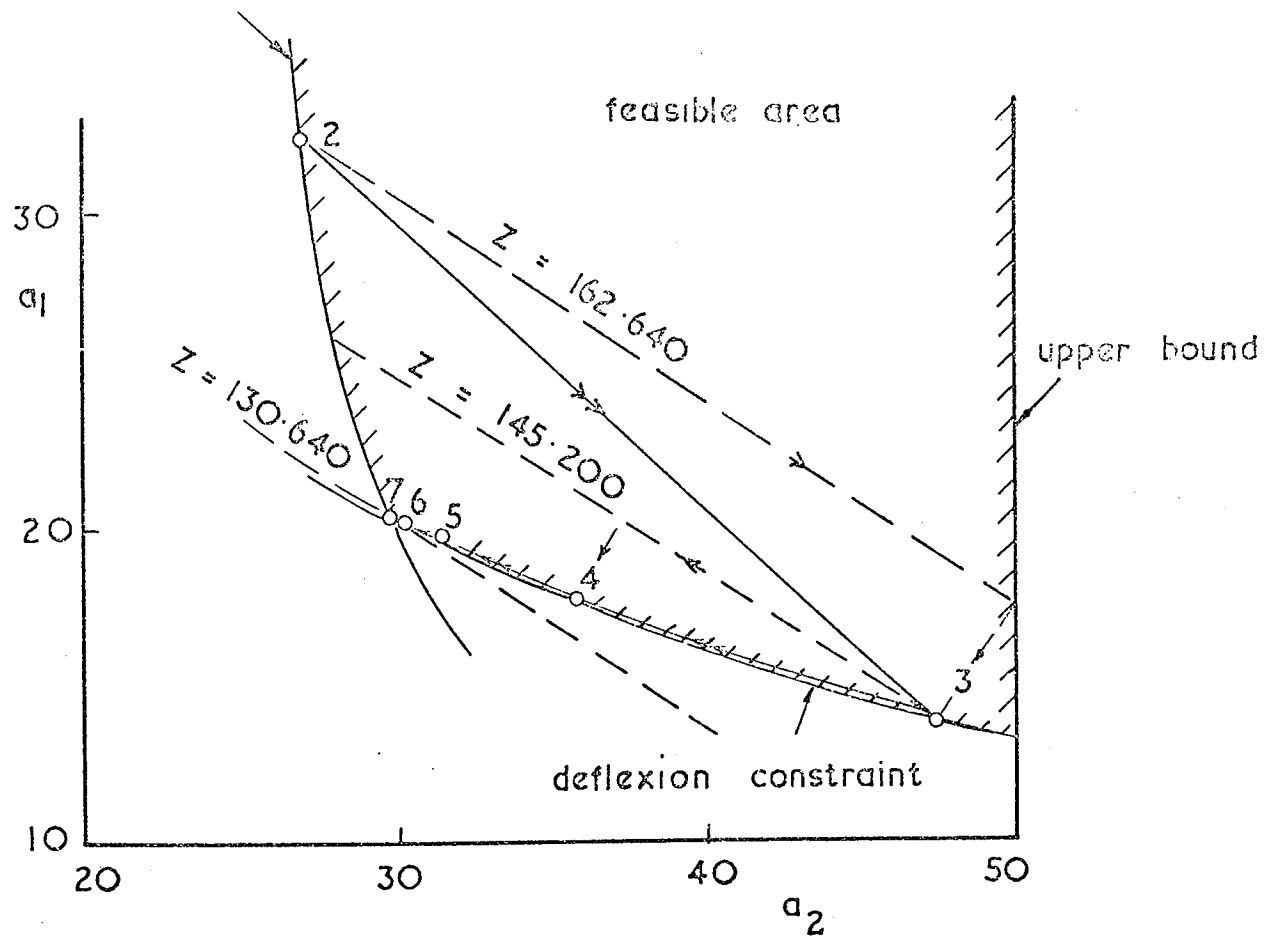


Figure 5.2 Path to the optimum with  $a_3 = \text{constant} = 5$

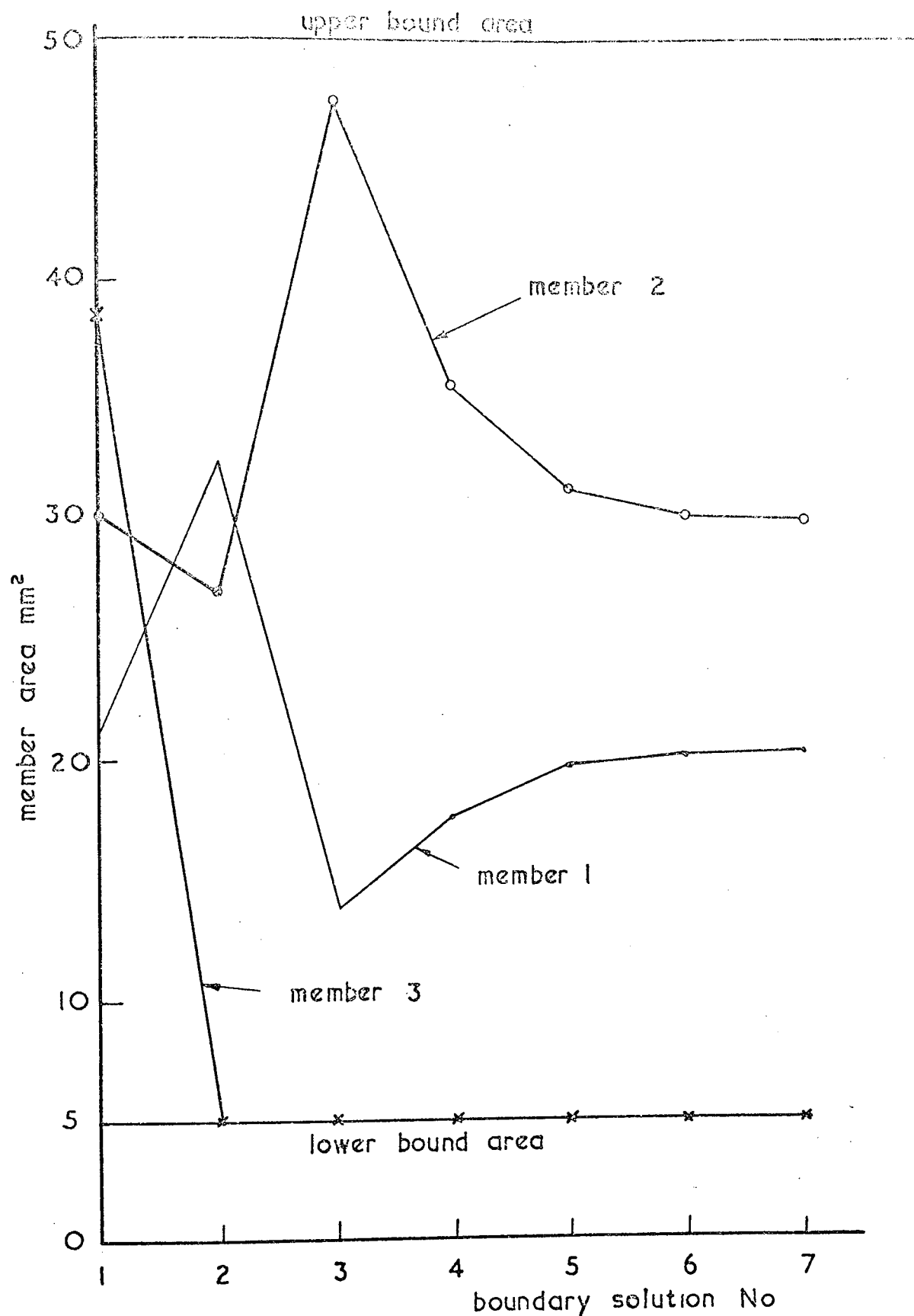


Figure 5.3. Variation of member areas

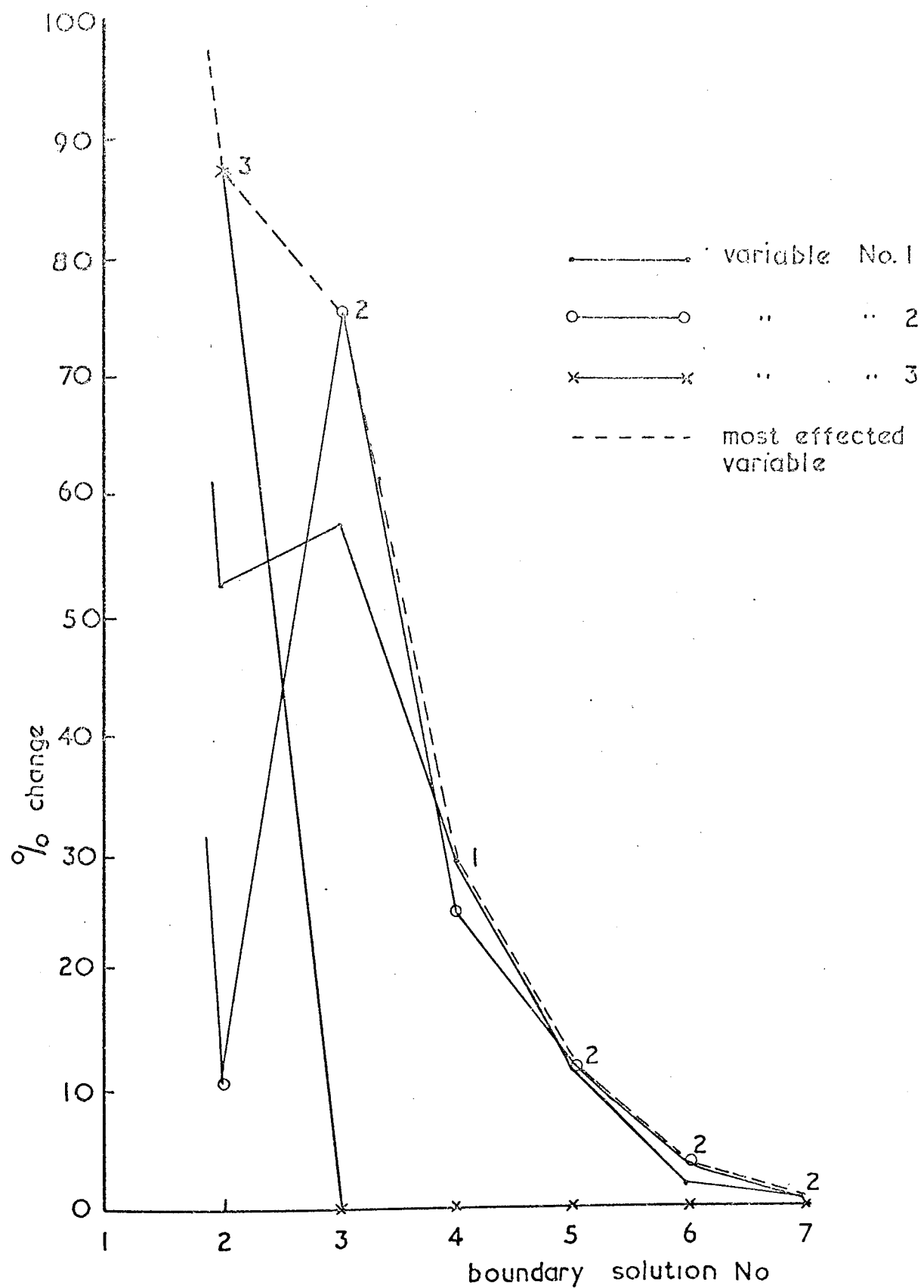


Figure 5.4 % change in variables between boundary solutions

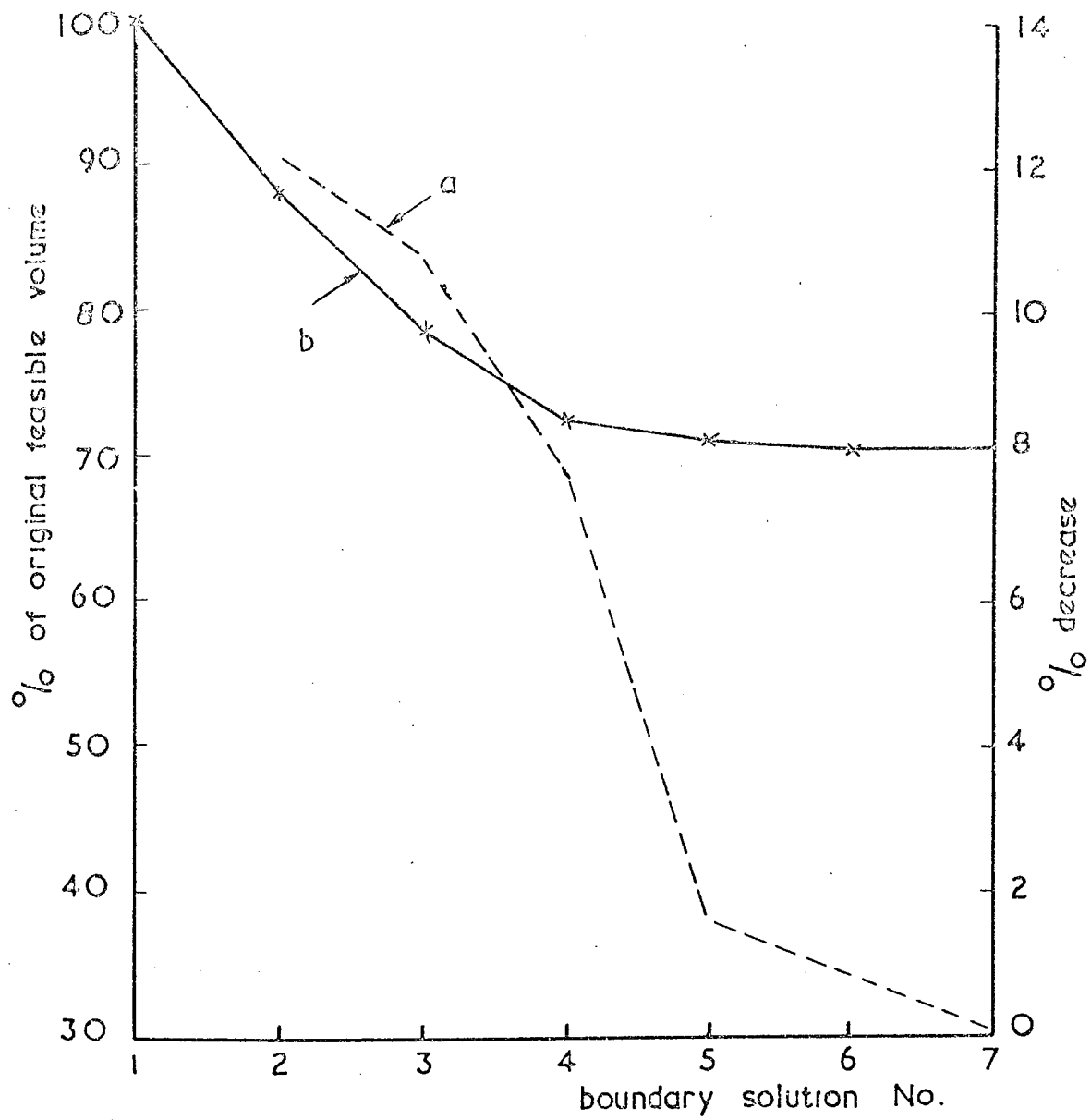


Figure 5.5. Variation in the objective function



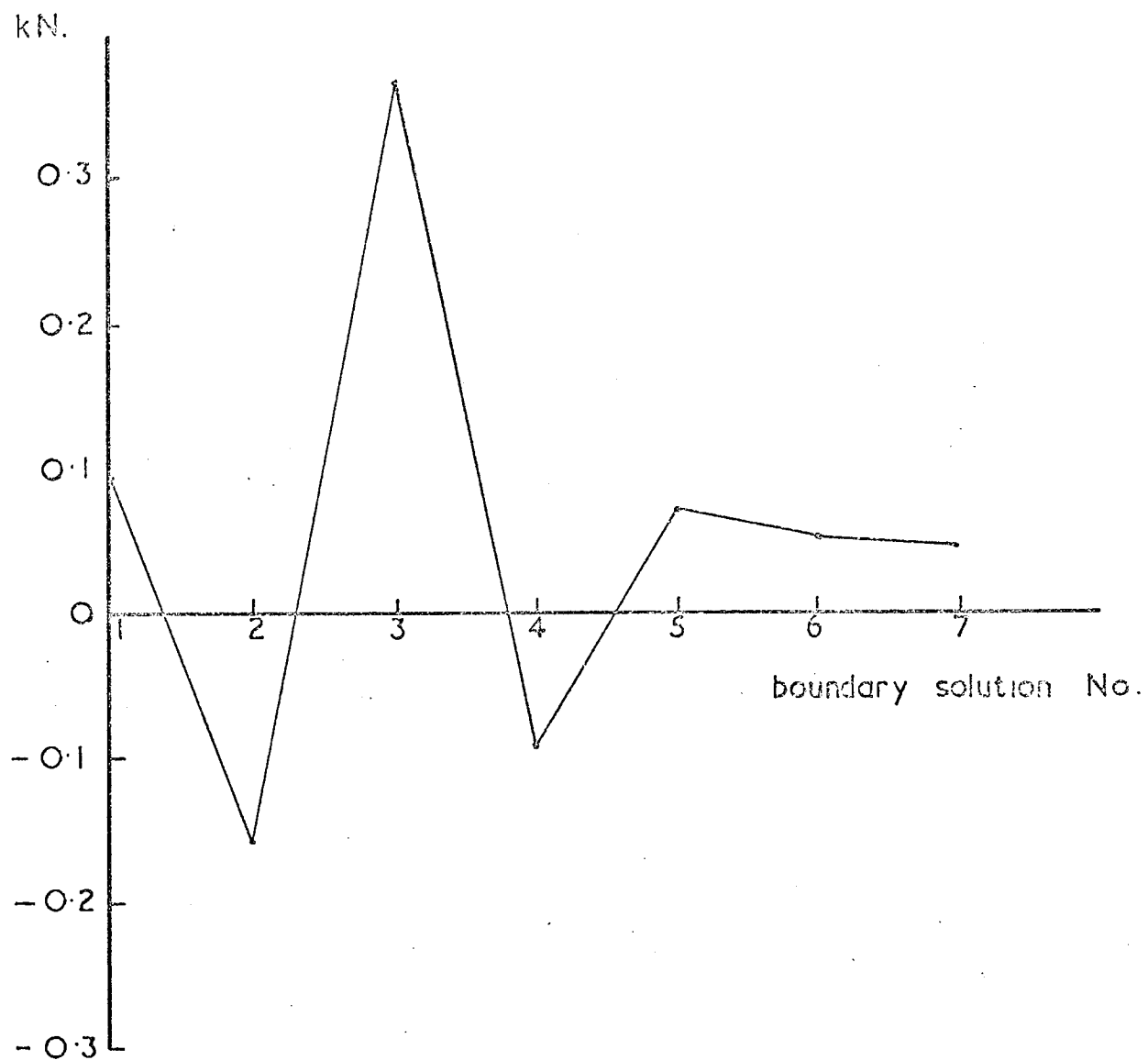
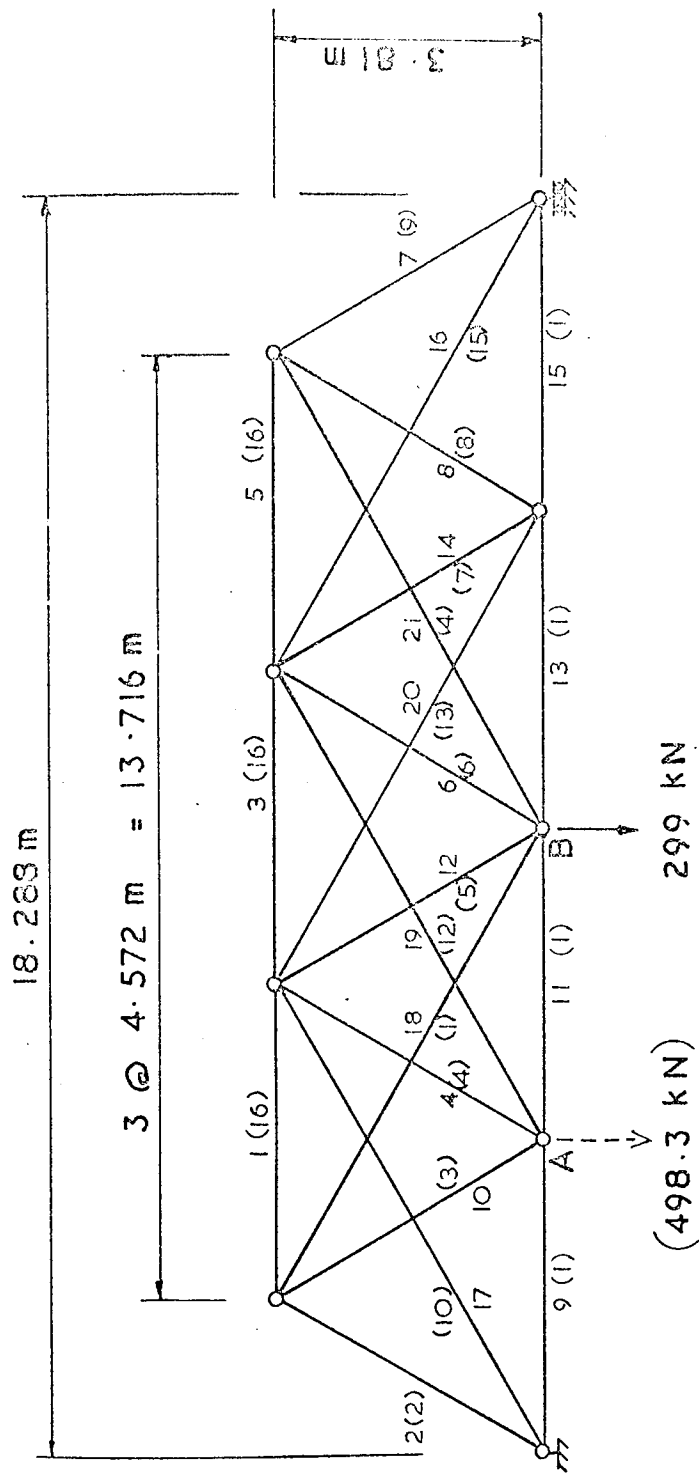


Figure 5. 6. Vairation of redundant force.



Numbers inside brackets indicate area groupings the remainder are member numbers.

Figure 5.7. 2 Dimensional braced framework.

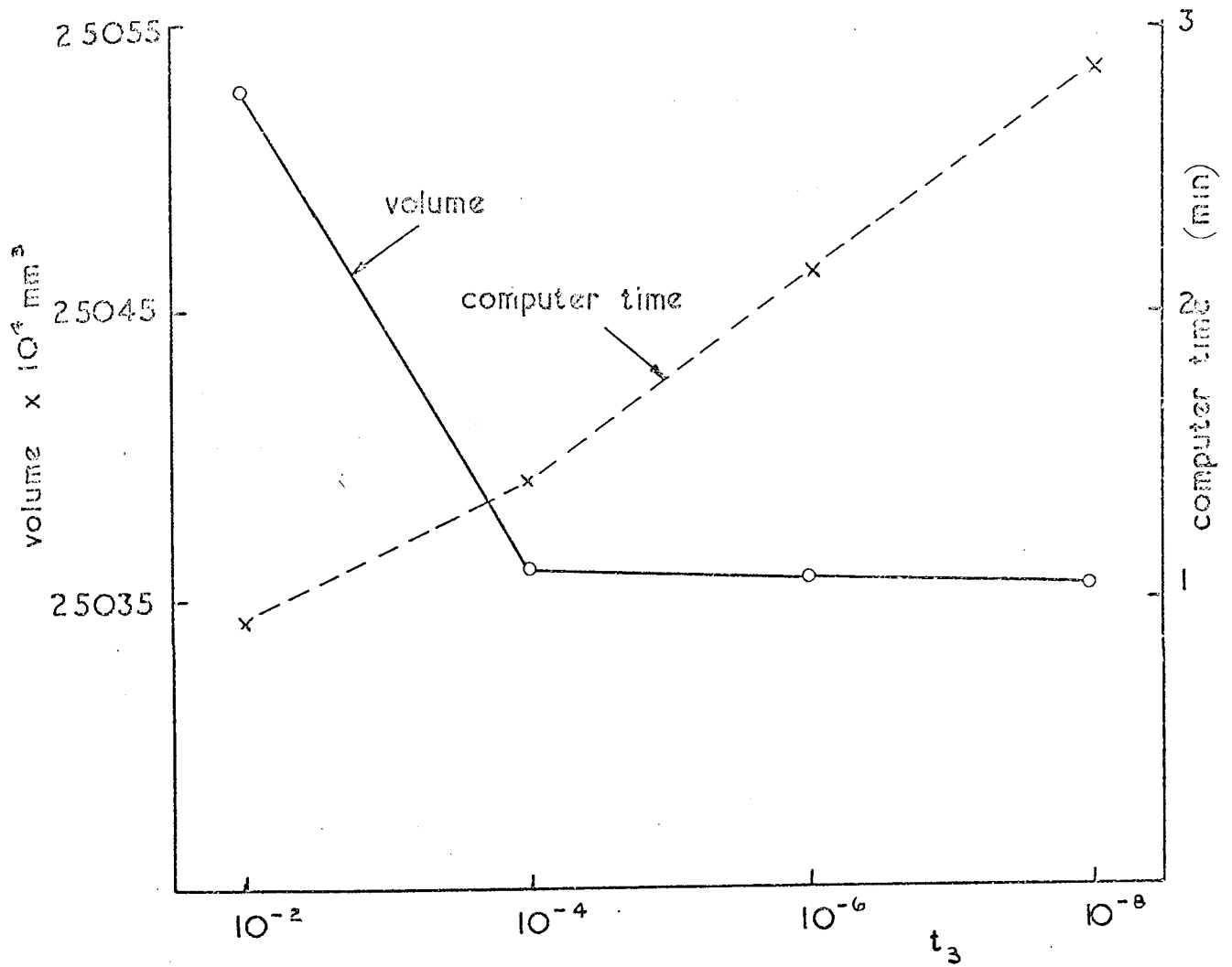
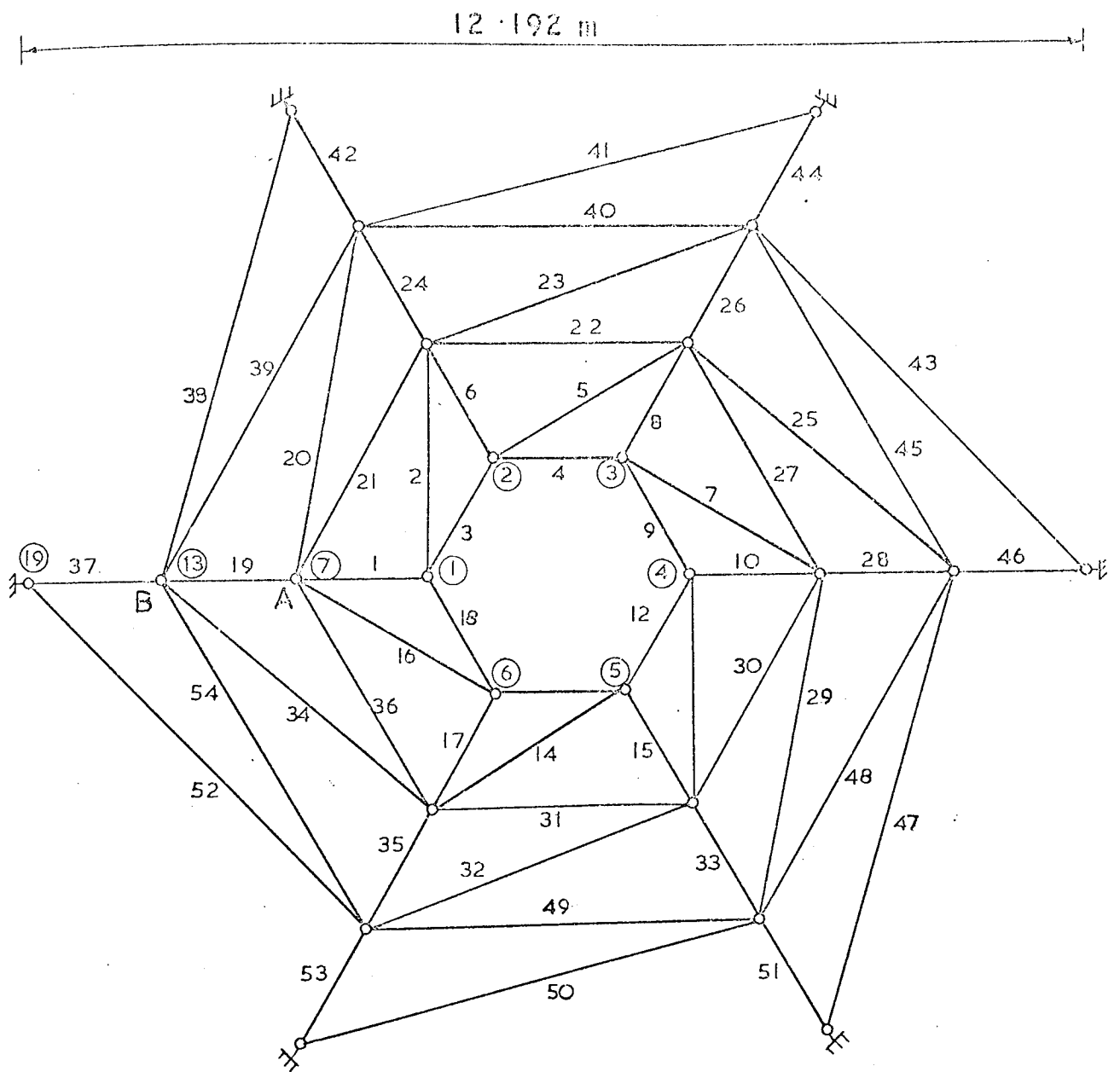
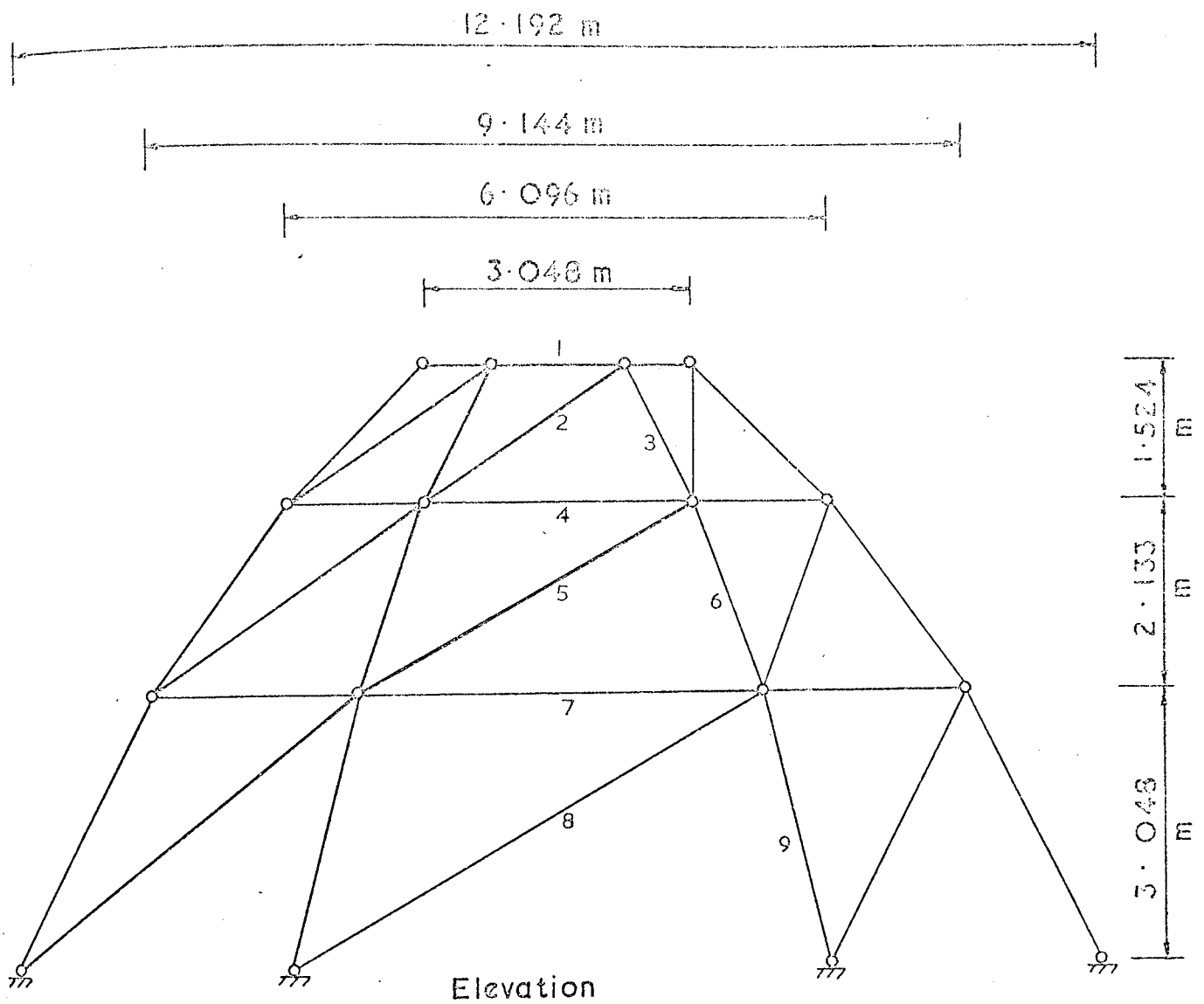


Figure 5.8. Effect of decreasing tolerance  $t_3$ .



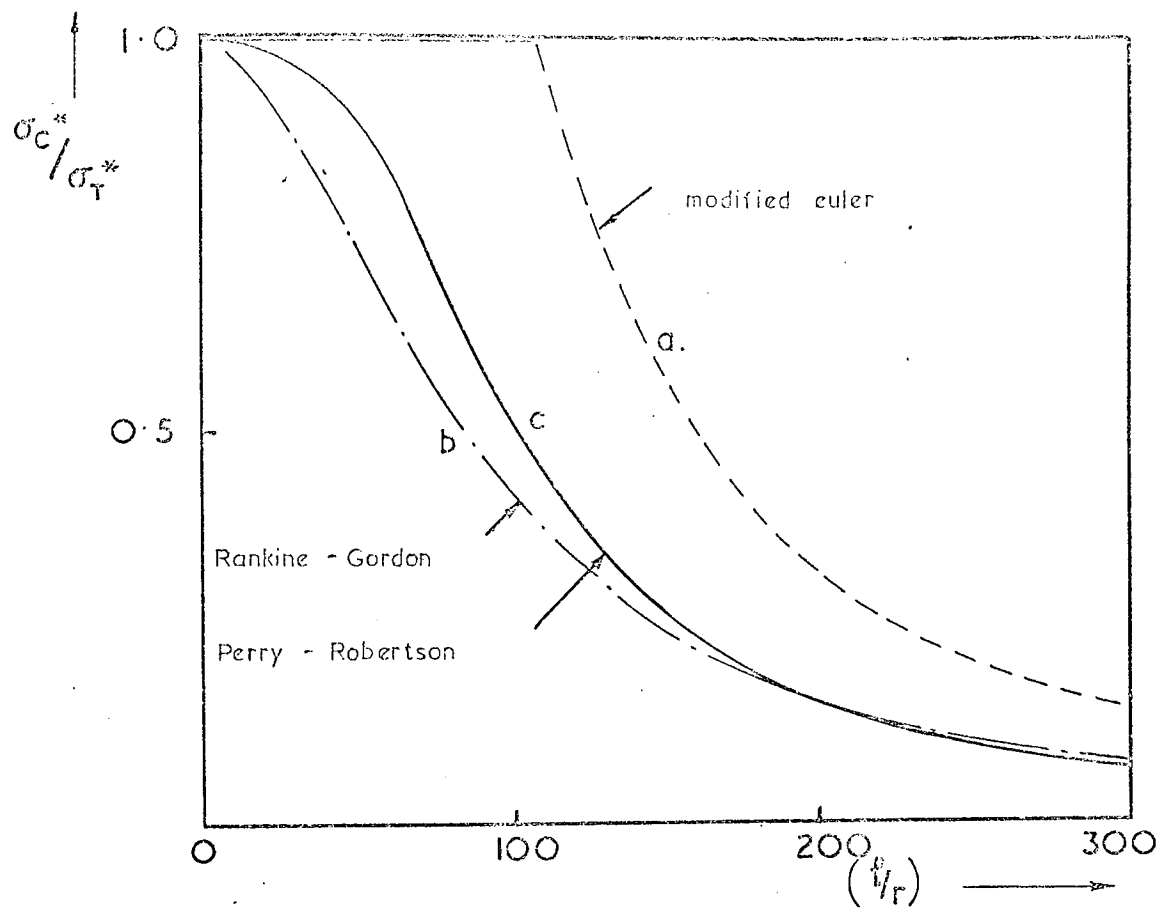
Plan indicating member numbering and joint numbering

Figure 5.9. Schwedler dome.



area.	group	no.	1	comprises	members	3	4	9	12	13	18
"	"	2	"	"	"	2	5	7	11	14	16
"	"	3	"	"	"	1	6	8	10	15	17
"	"	4	"	"	"	21	22	27	30	31	36
"	"	5	"	"	"	20	23	25	29	32	34
"	"	6	"	"	"	19	24	26	28	33	35
"	"	7	"	"	"	39	40	45	48	49	54
"	"	8	"	"	"	38	41	43	49	50	52
"	"	9	"	"	"	37	42	44	46	51	53

Figure 5.10. Schwedler dome



$$a. \quad \sigma_c^* = \sigma_E = E \pi^2 / (l/r)^2$$

$$b. \quad \sigma_c^* = \sigma_T^* / \left( 1 + \frac{1}{7500} (l/r)^2 \right)$$

$$c. \quad \sigma_c^* = \frac{1}{1.7} \left[ \frac{\sigma_T^* + (\eta + 1) \sigma_E}{2} - \sqrt{\left\{ \left( \frac{\sigma_T^* + (\eta + 1) \sigma_E}{2} \right)^2 - \sigma_T^* \sigma_E \right\}} \right]$$

$$\eta = 0.3 (l/100r)^2$$

Figure 5.11 Comparison of formulae



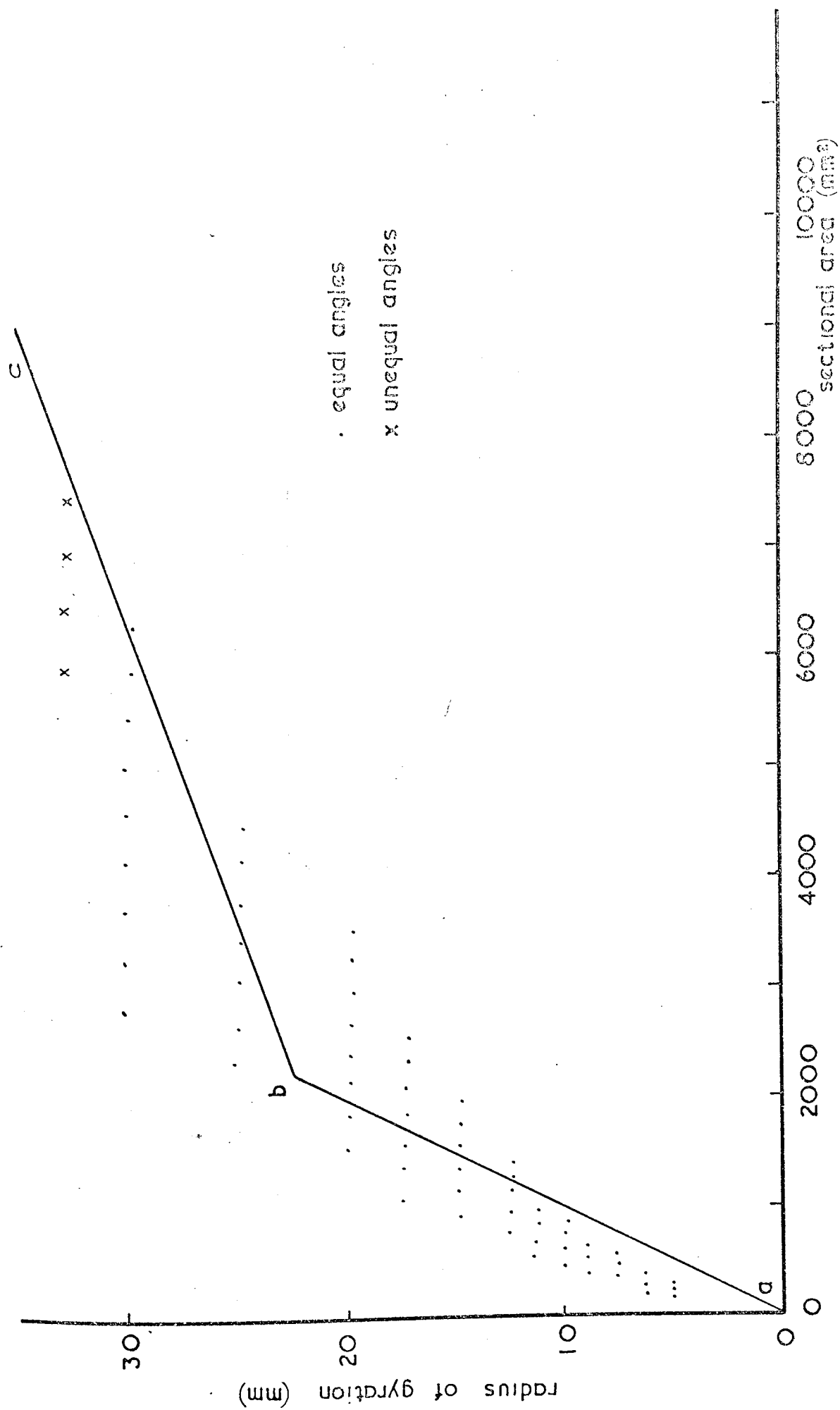


Figure 5.12. Radius of gyration versus cross sectional area for angle sections

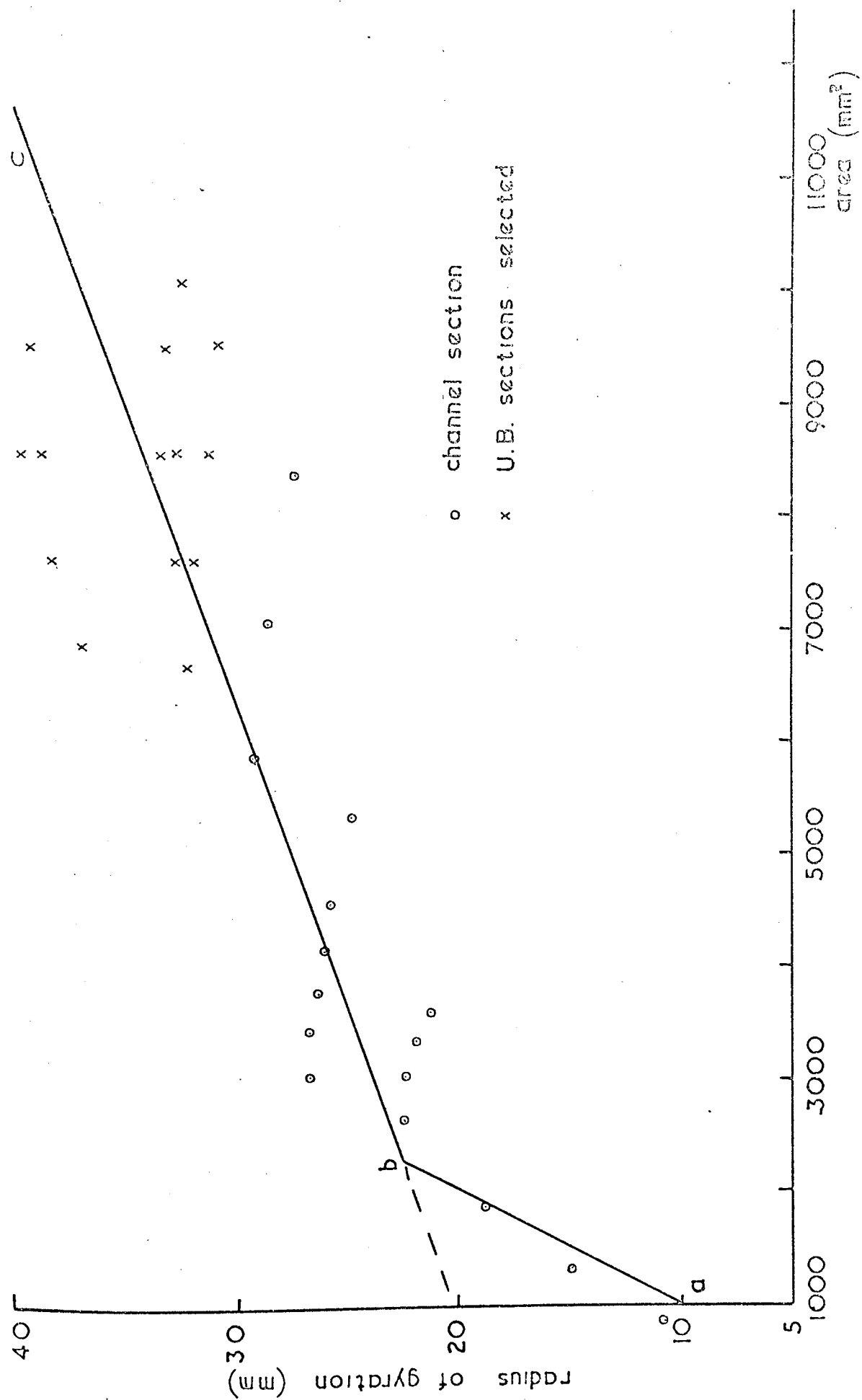


Figure 5.13 Radius of gyration versus cross sectional area for beams and channels

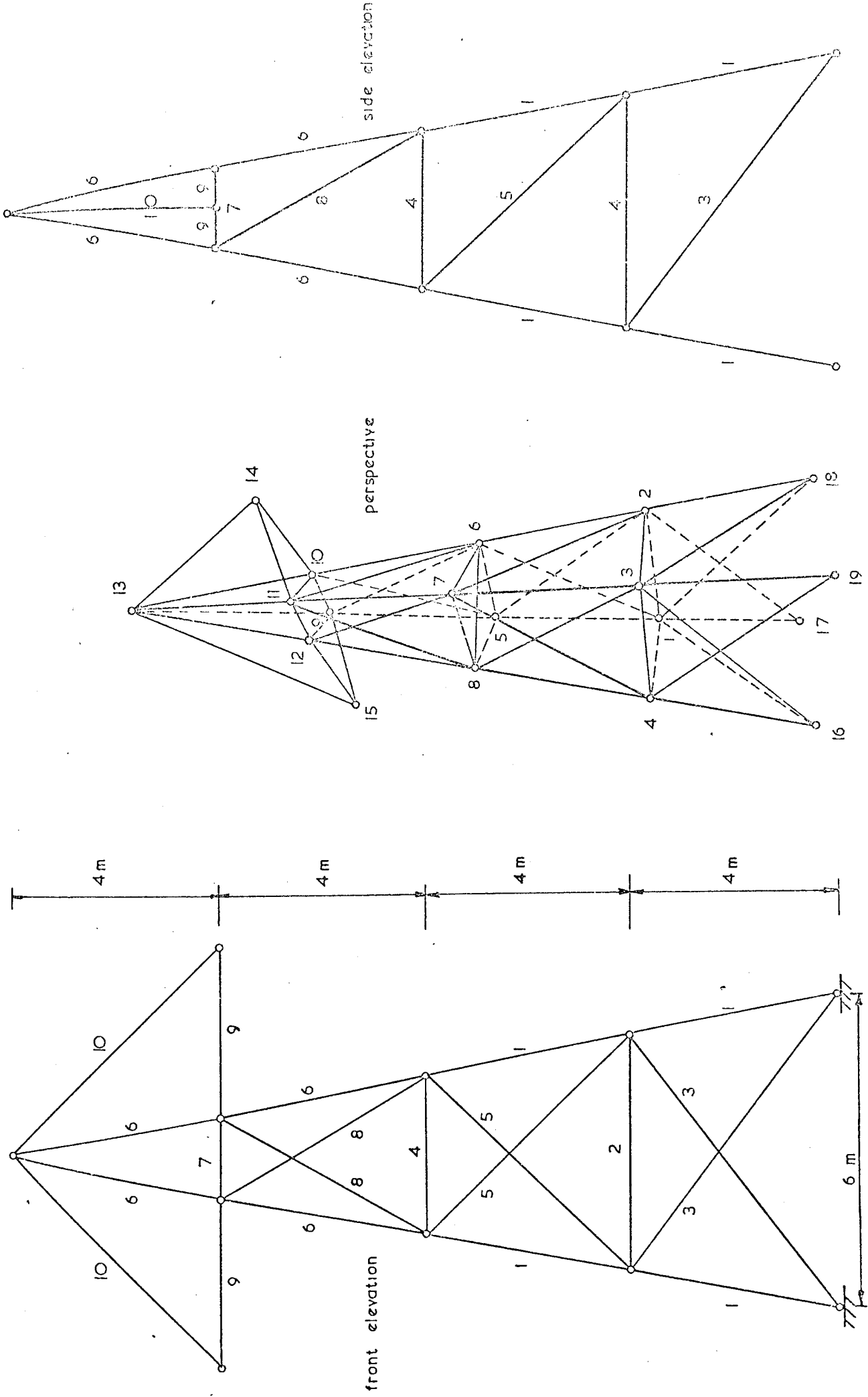


Figure 5.14 Tower structure (area groups and joint numbering indicated)

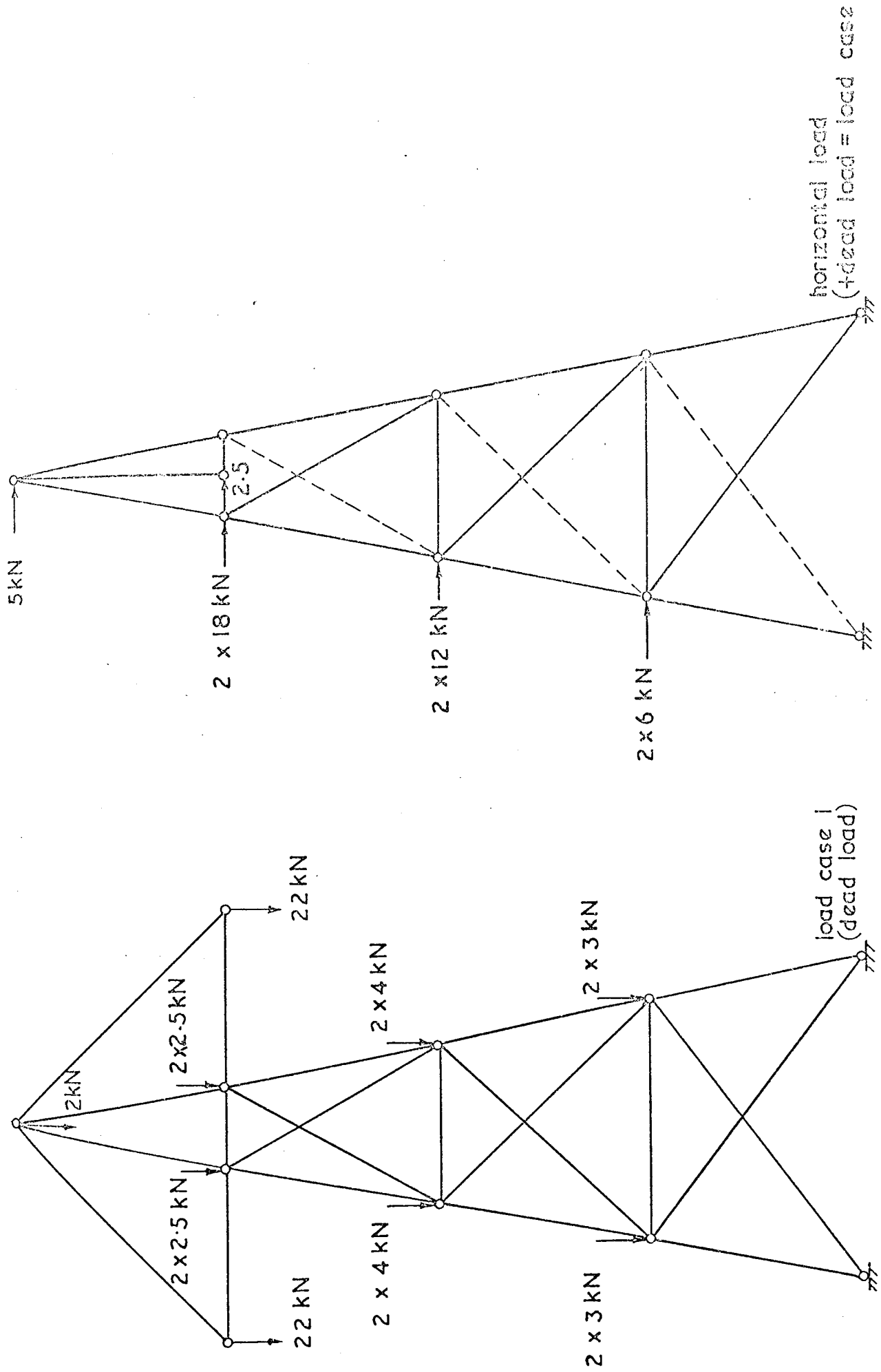


Figure 5.15. Loading of tower structure

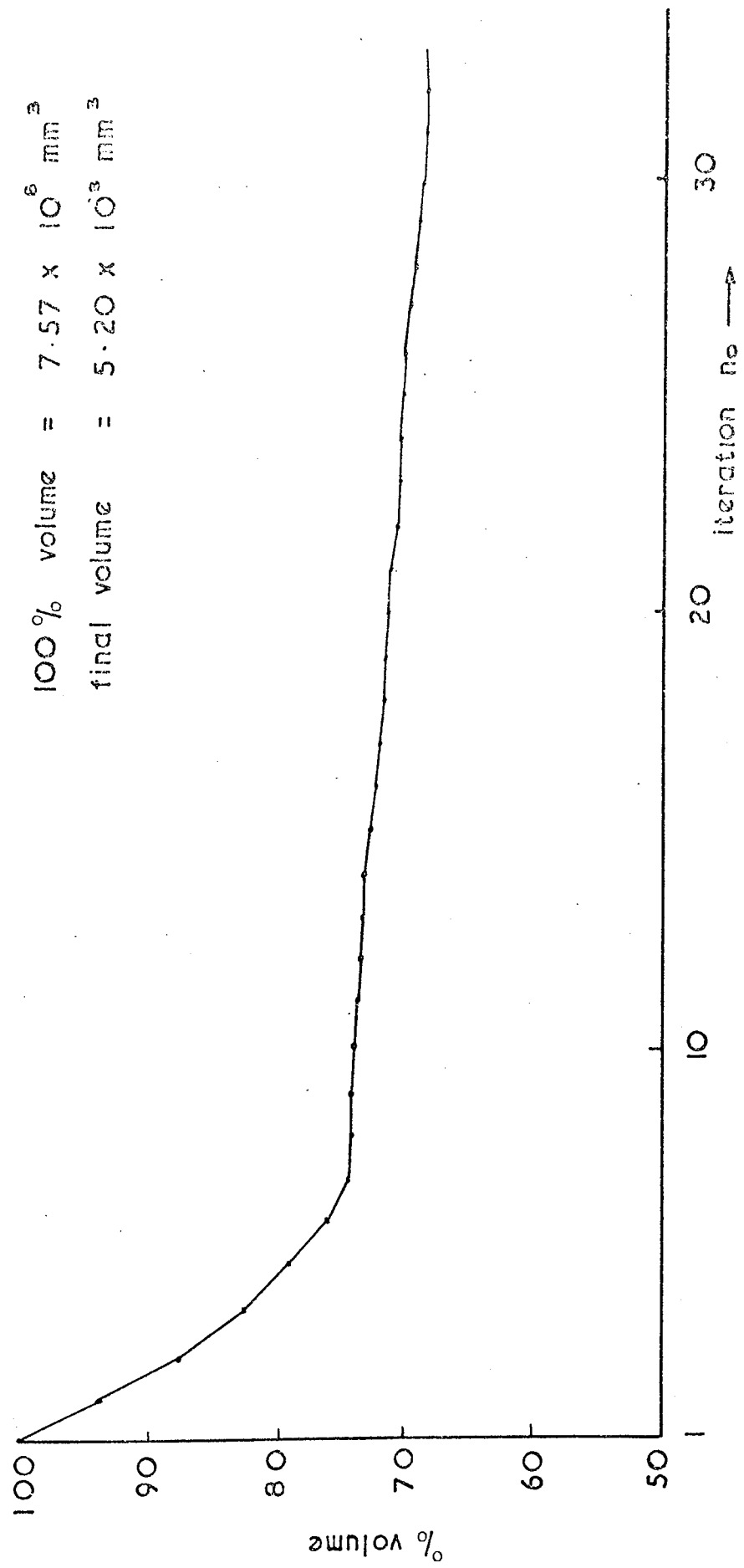


Figure 5. 16 Volumetric decrease

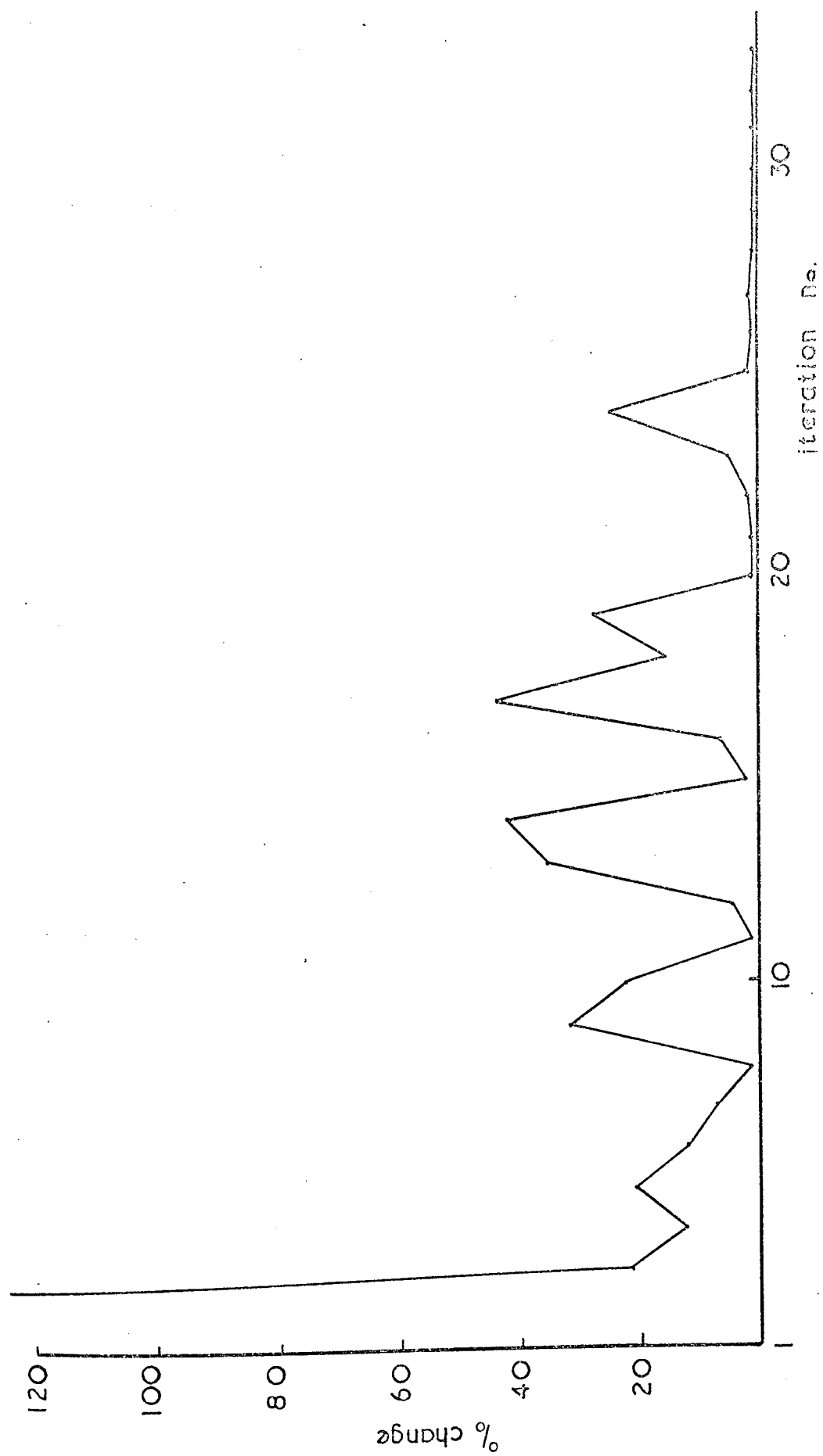


Figure 5.17 Percentage change of most effected variable



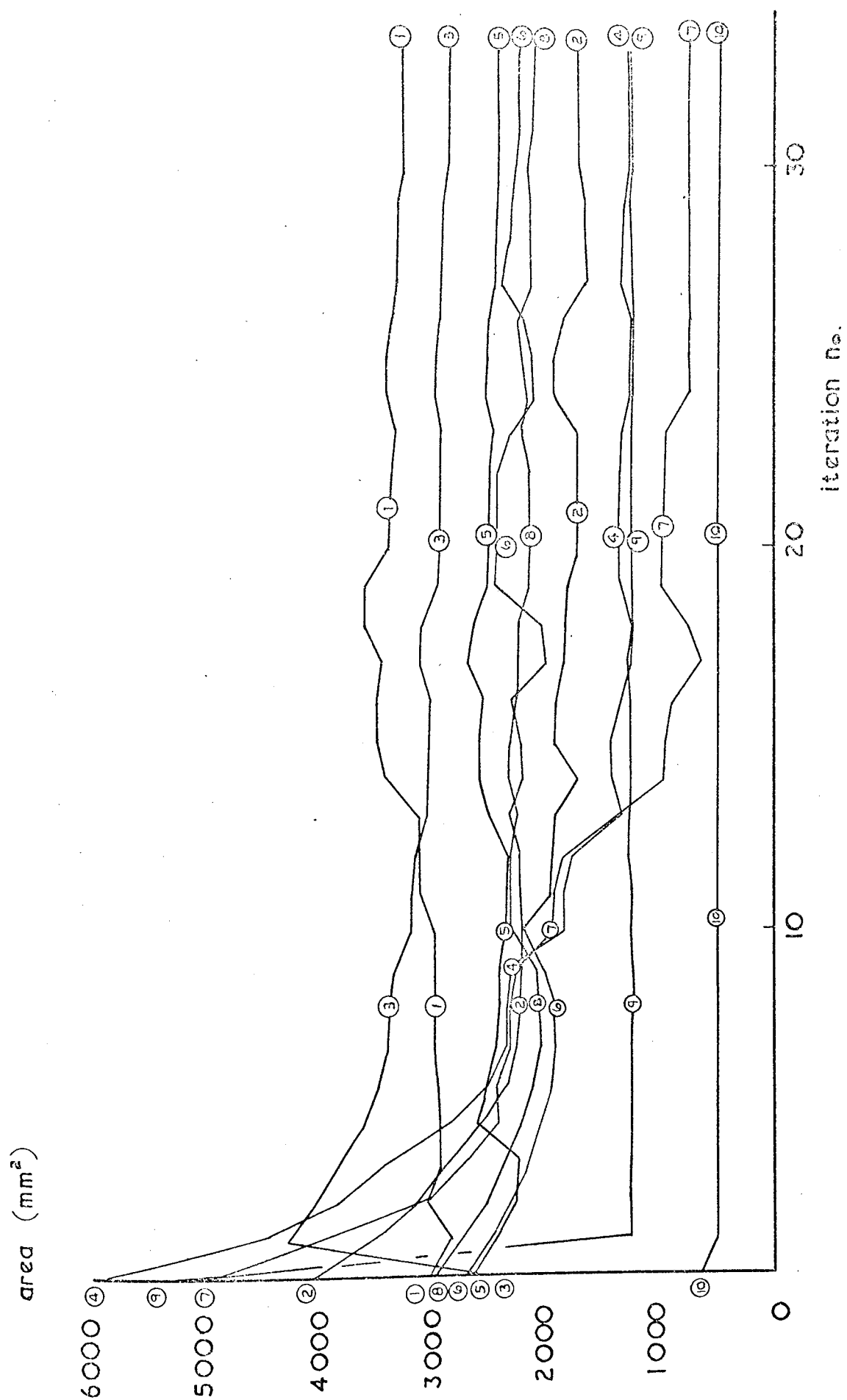
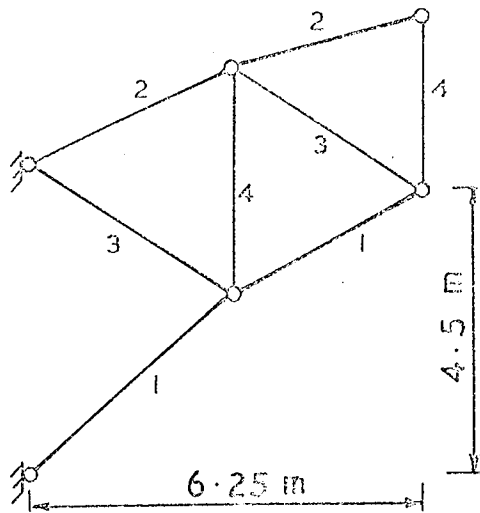


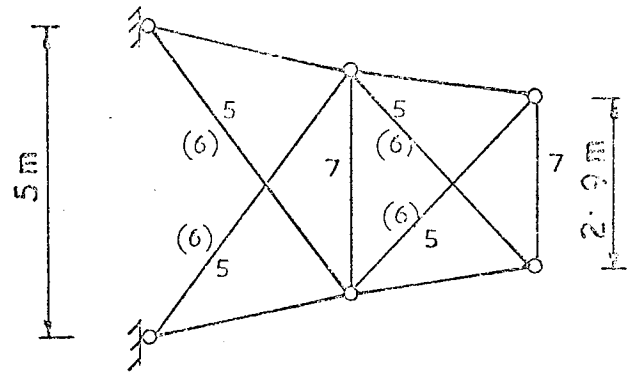
Figure 5.18 Successive alteration of variables

Cross section No.

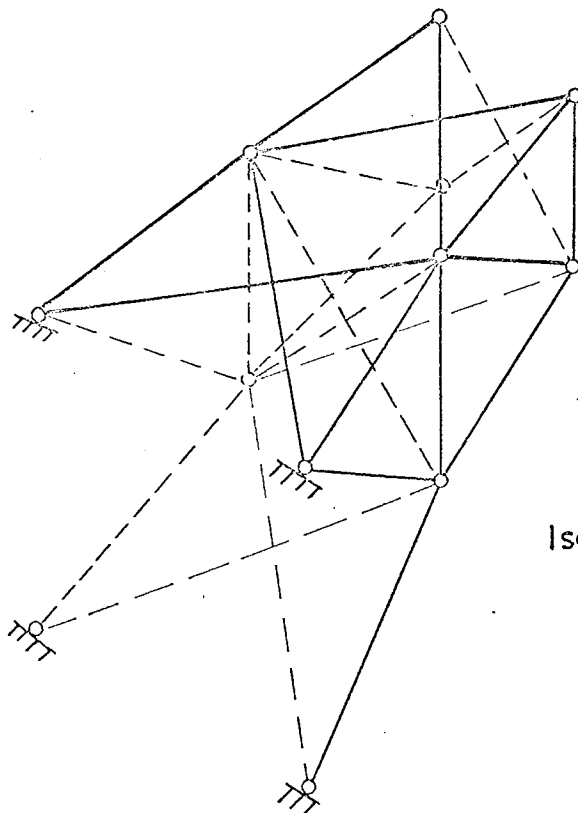
1                      2



Side elevation



Top and bottom plans

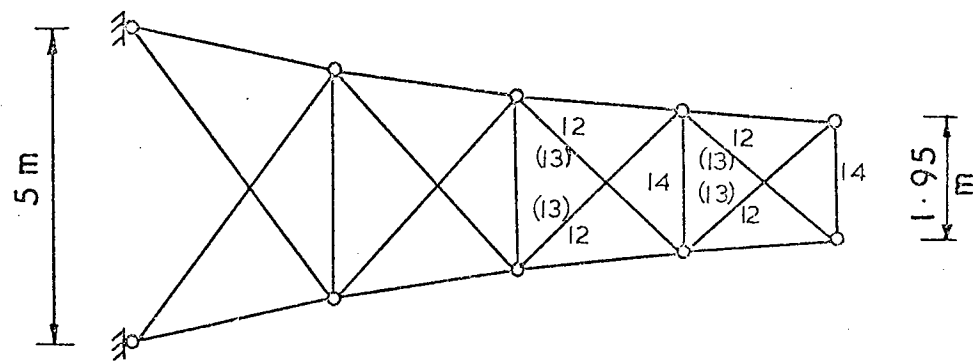
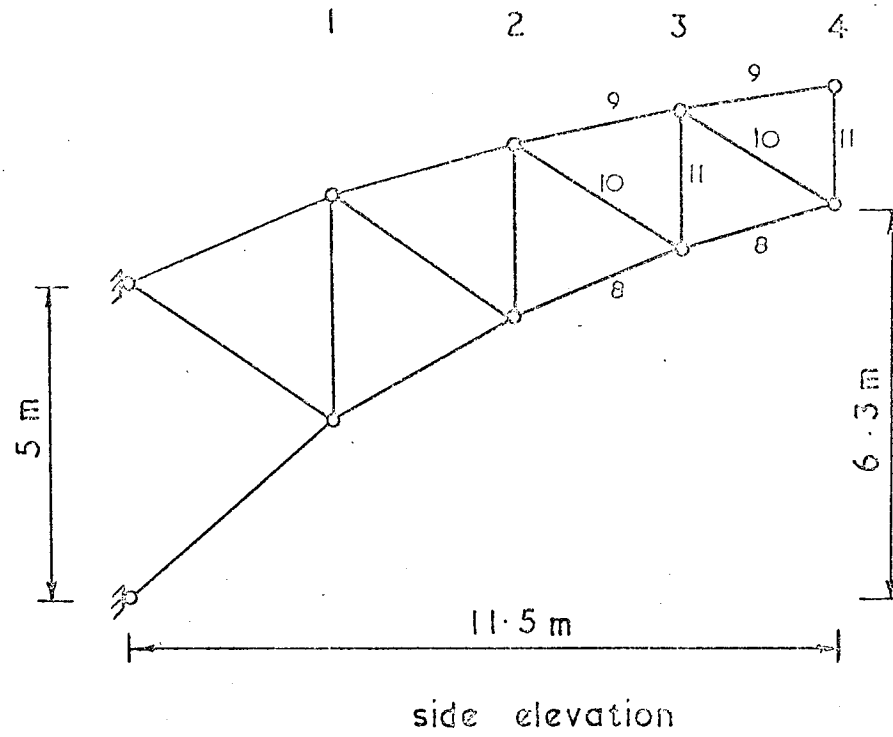


Isometric

area groupings shown,  
brackets indicating where  
top and bottom differ.

Figure 5.19 Cantilever 1

cross section no.



top and bottom plans

additional area groupings  
only are indicated.

Figure 5.20. Cantilever 2



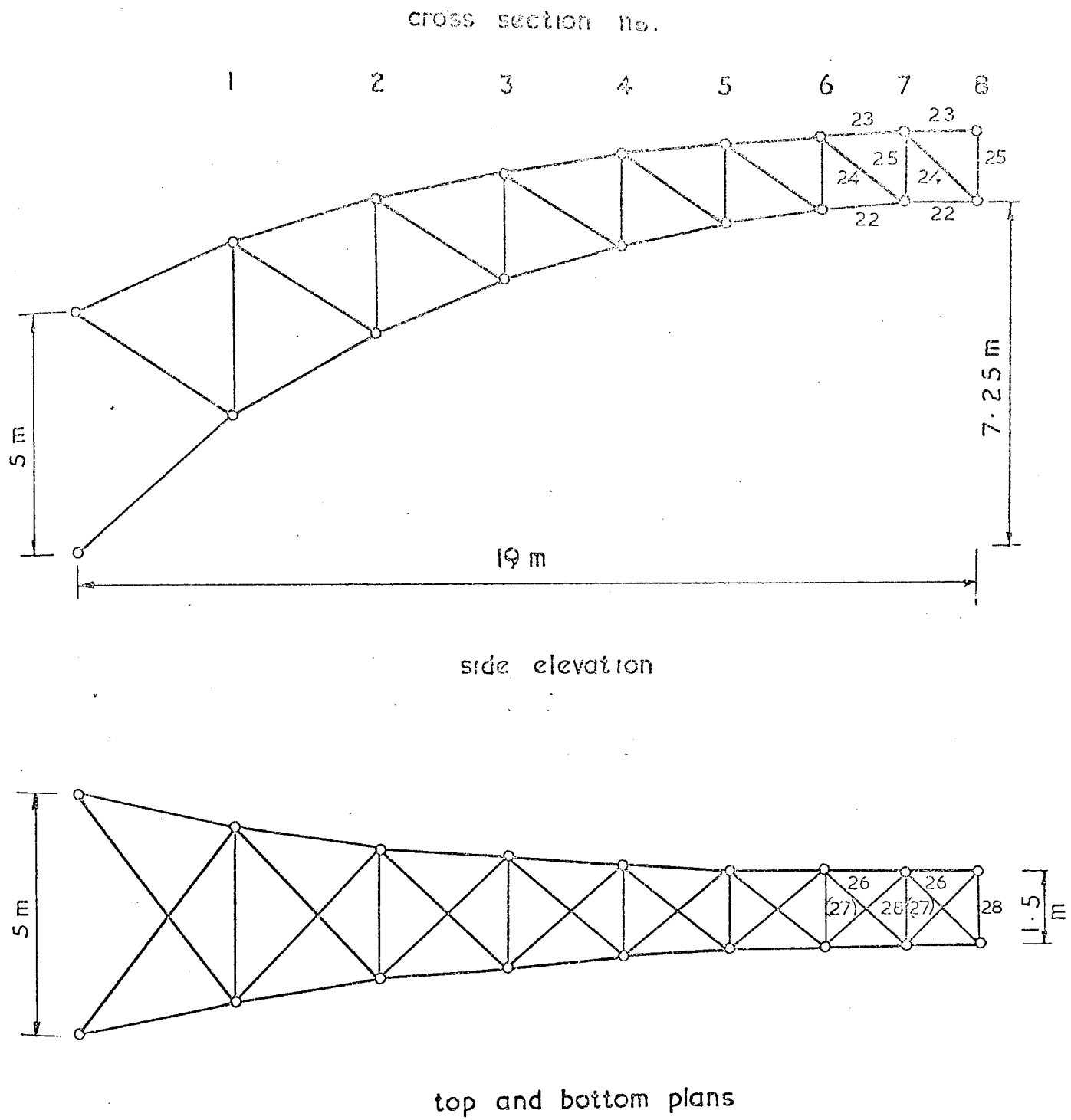
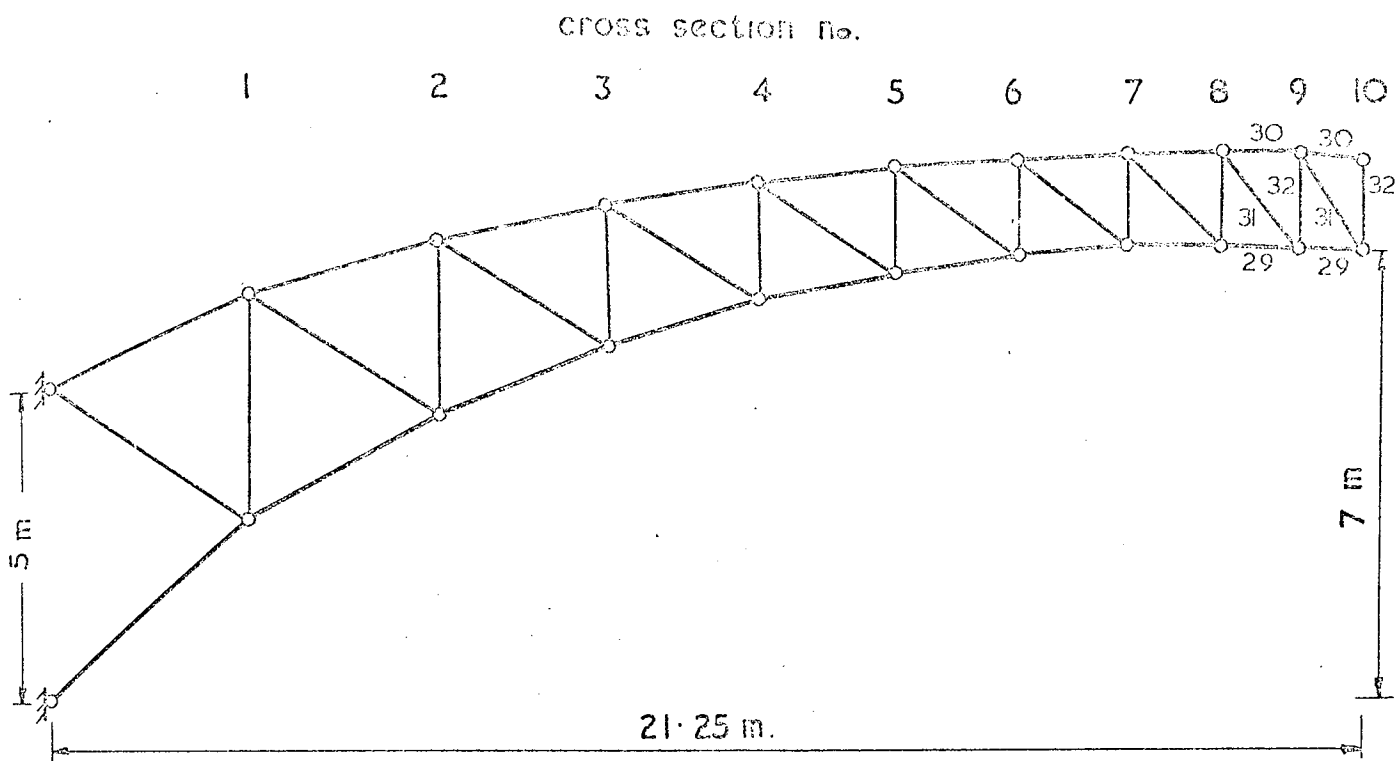
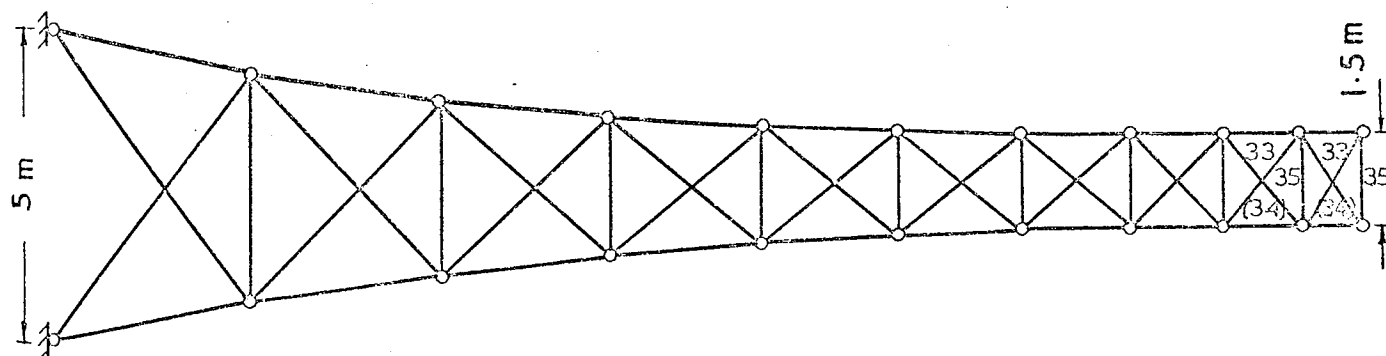


Figure 5.22 Cantilever 4



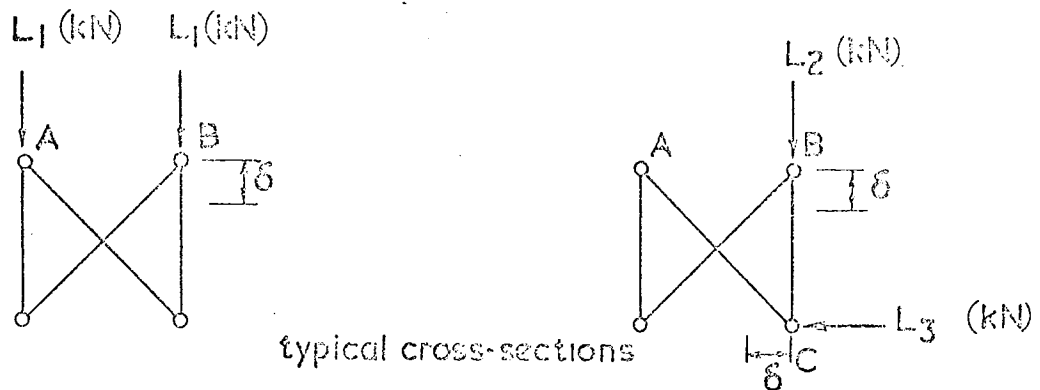
side elevation



top and bottom plans

Figure 5.23. Cantilever 5





load case 1 = 30 kN/m.rum.

load case 2

C.S. No.	$L_1$ (kN)	$L_2$ (kN)	$L_3$ (kN)	$\delta_{max} = \frac{\text{span}}{325}$ (mm)
1	48.75	60.93	24.37	10.00
2	45.00	56.25	22.50	19.23
3	41.25	51.56	20.62	21.69
4	37.50	46.67	18.75	35.39
5	33.75	42.18	16.87	42.31
6	30.00	37.50	15.00	48.47
7	26.25	32.81	13.12	53.84
8	22.50	28.12	11.25	58.47
9	18.75	23.43	9.37	62.31
10	15.00	18.75	7.50	65.39

Figure 5.24. Loading arrangements

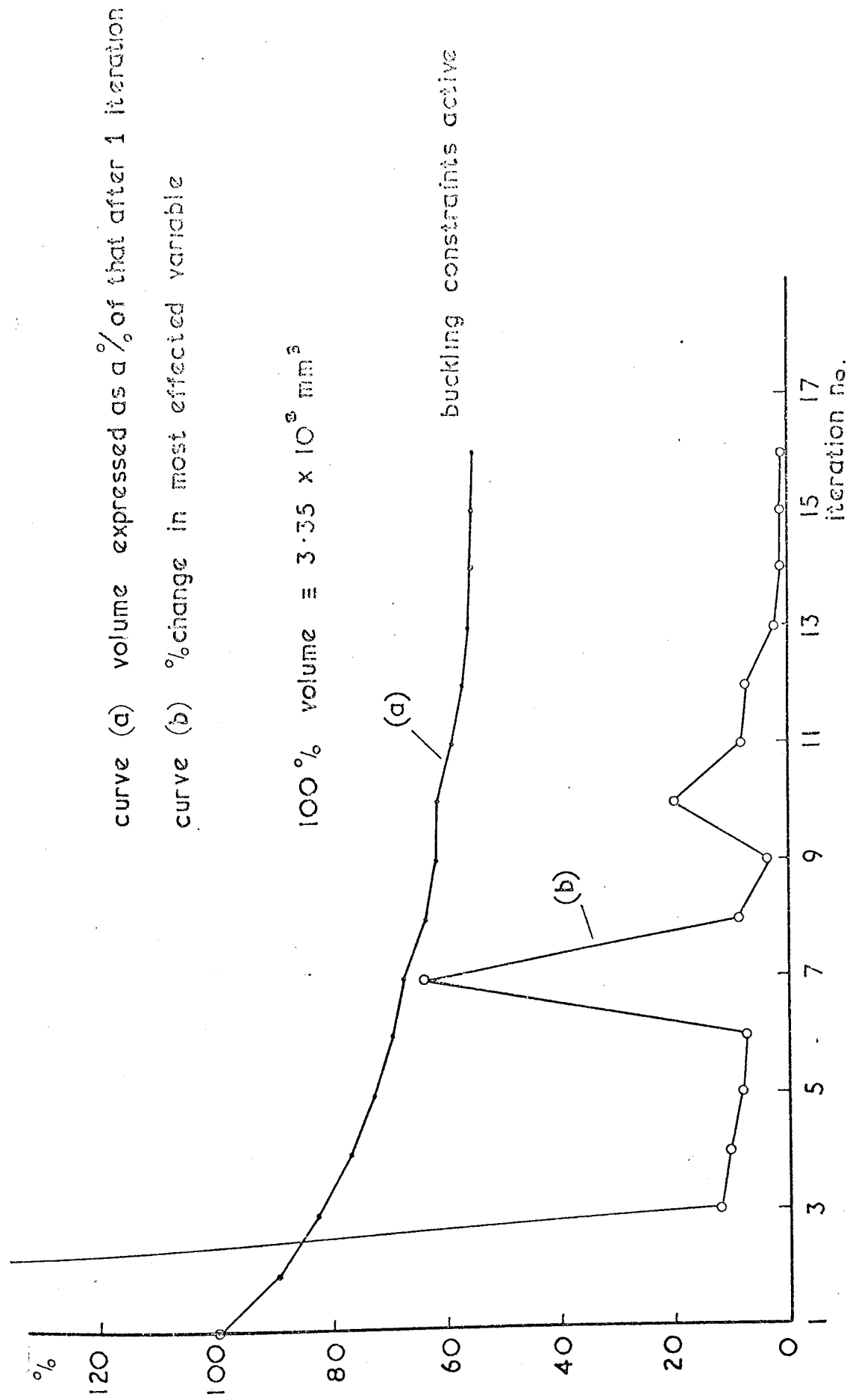


Figure 5.25 Progress of design cantilever I

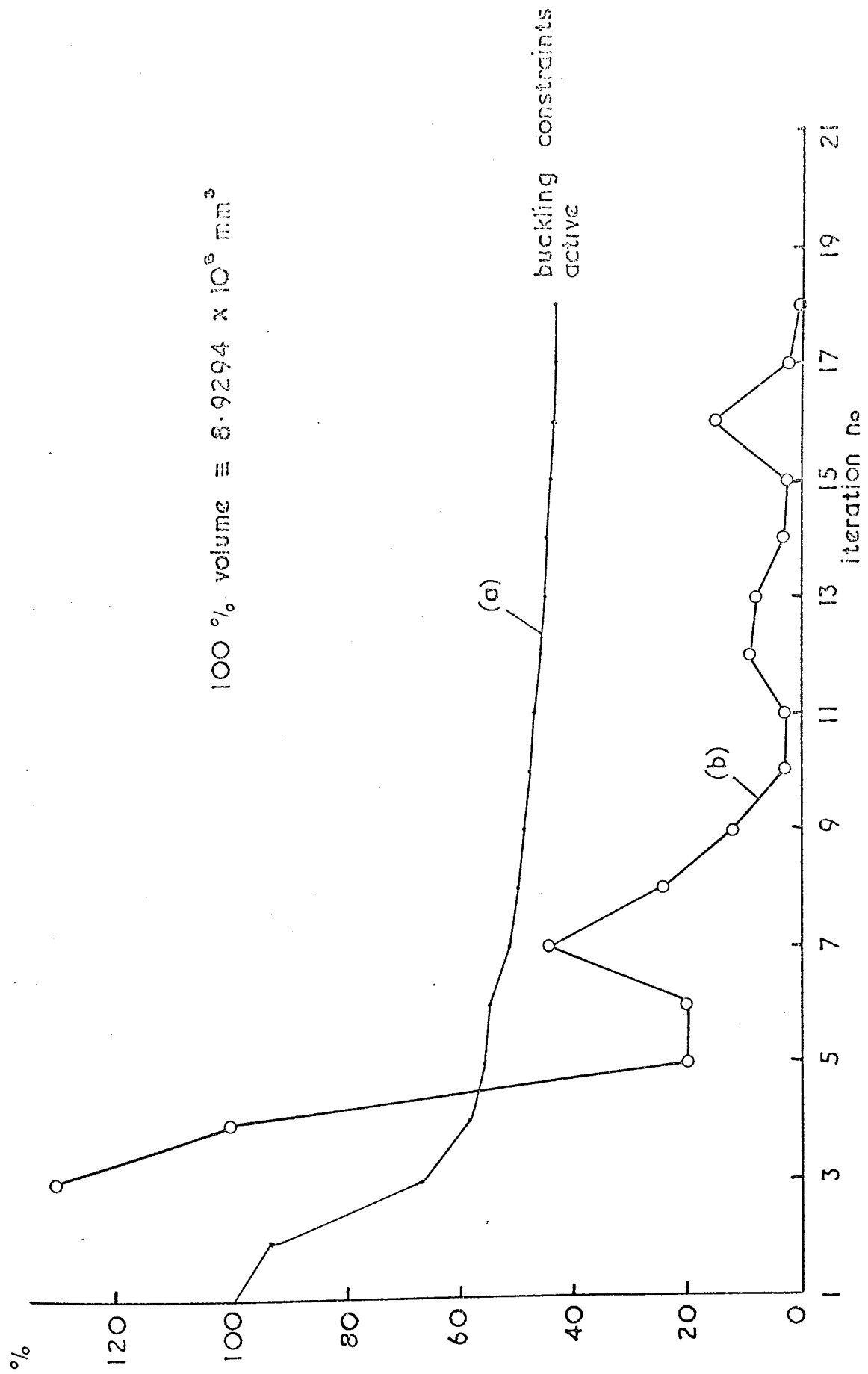


Figure 5. 26 Progress of design cantilever 2

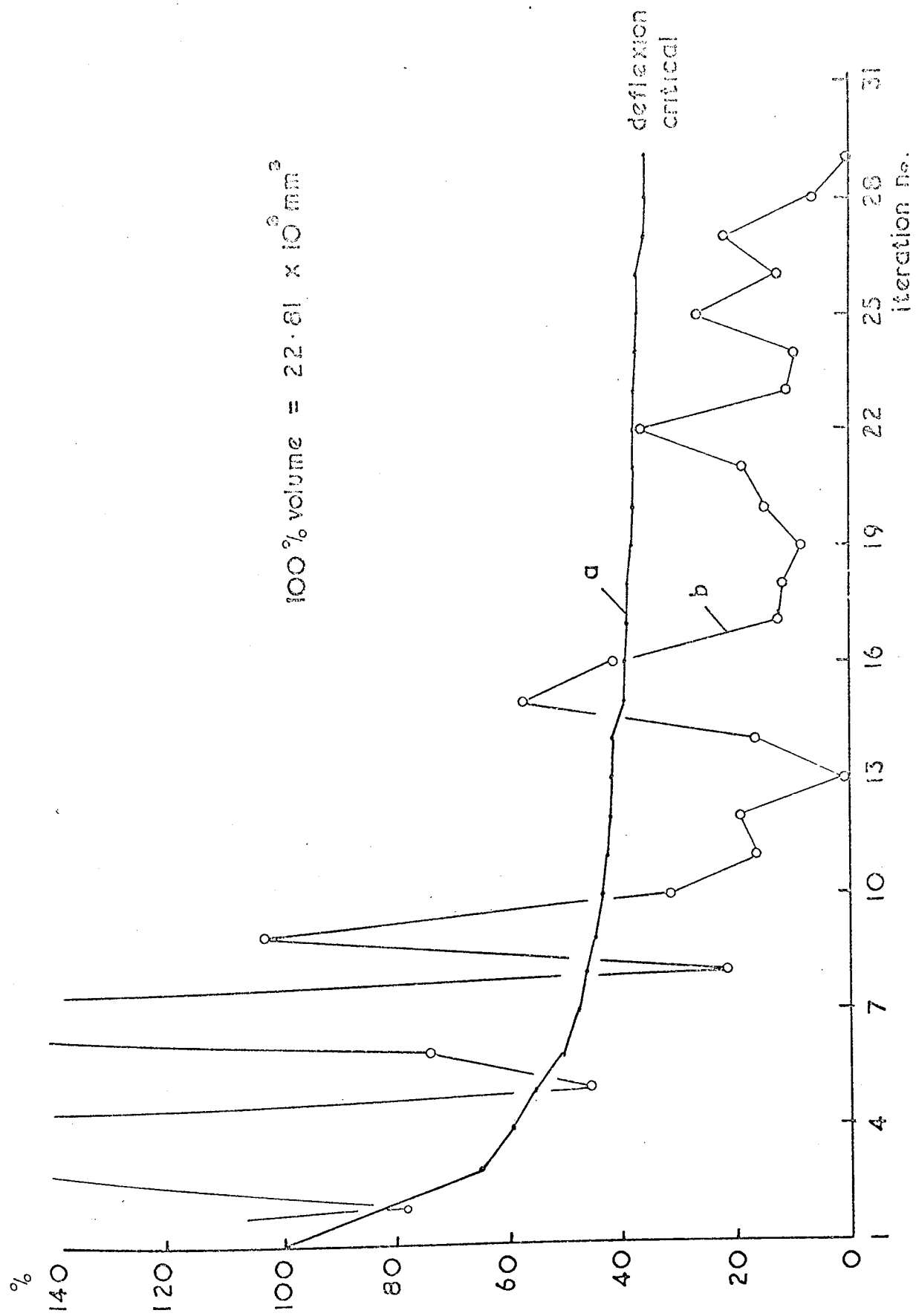


Figure 5.27 Progress of design - cantilever 3

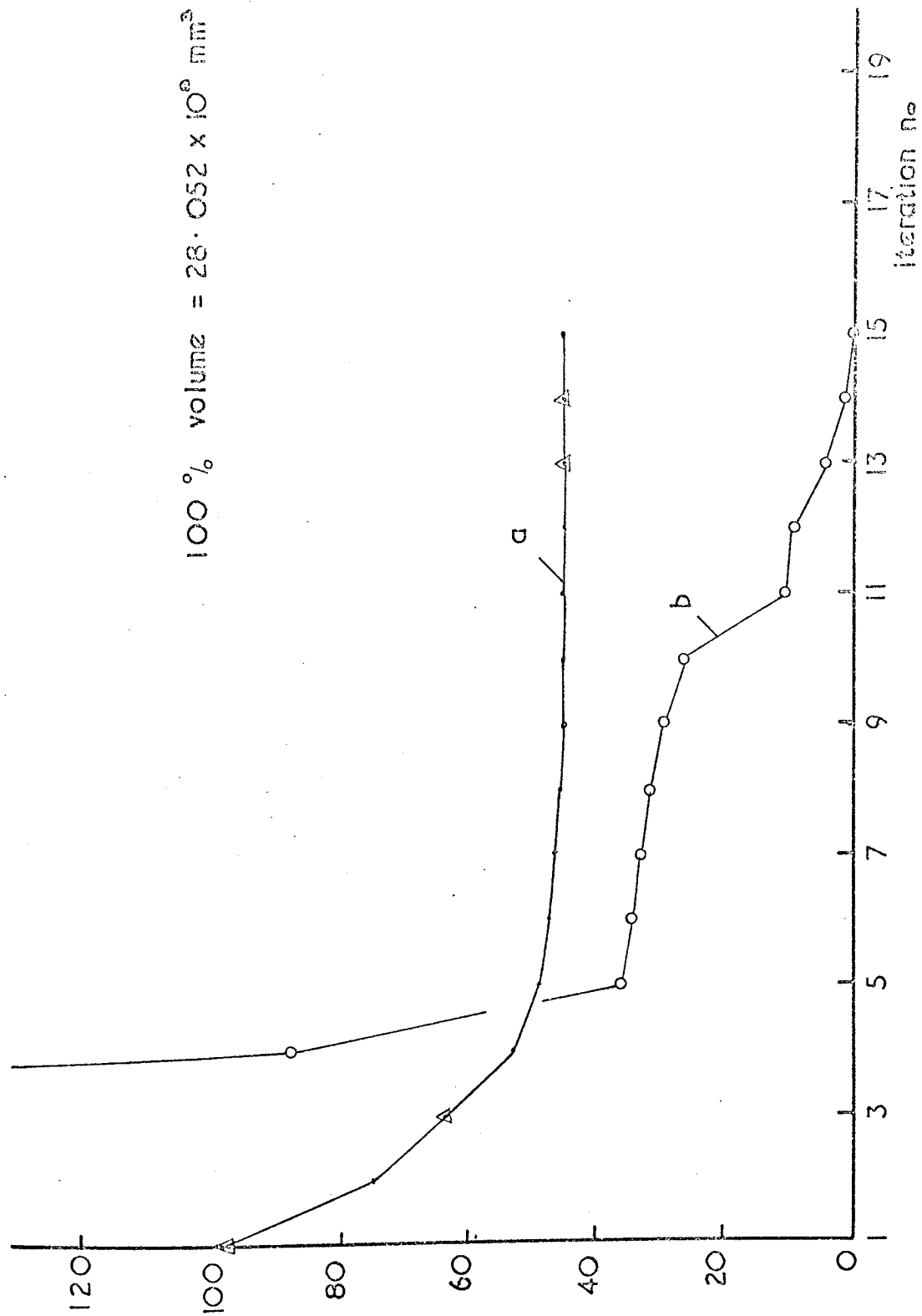


Figure 5.28. Progress of design - cantilever 4

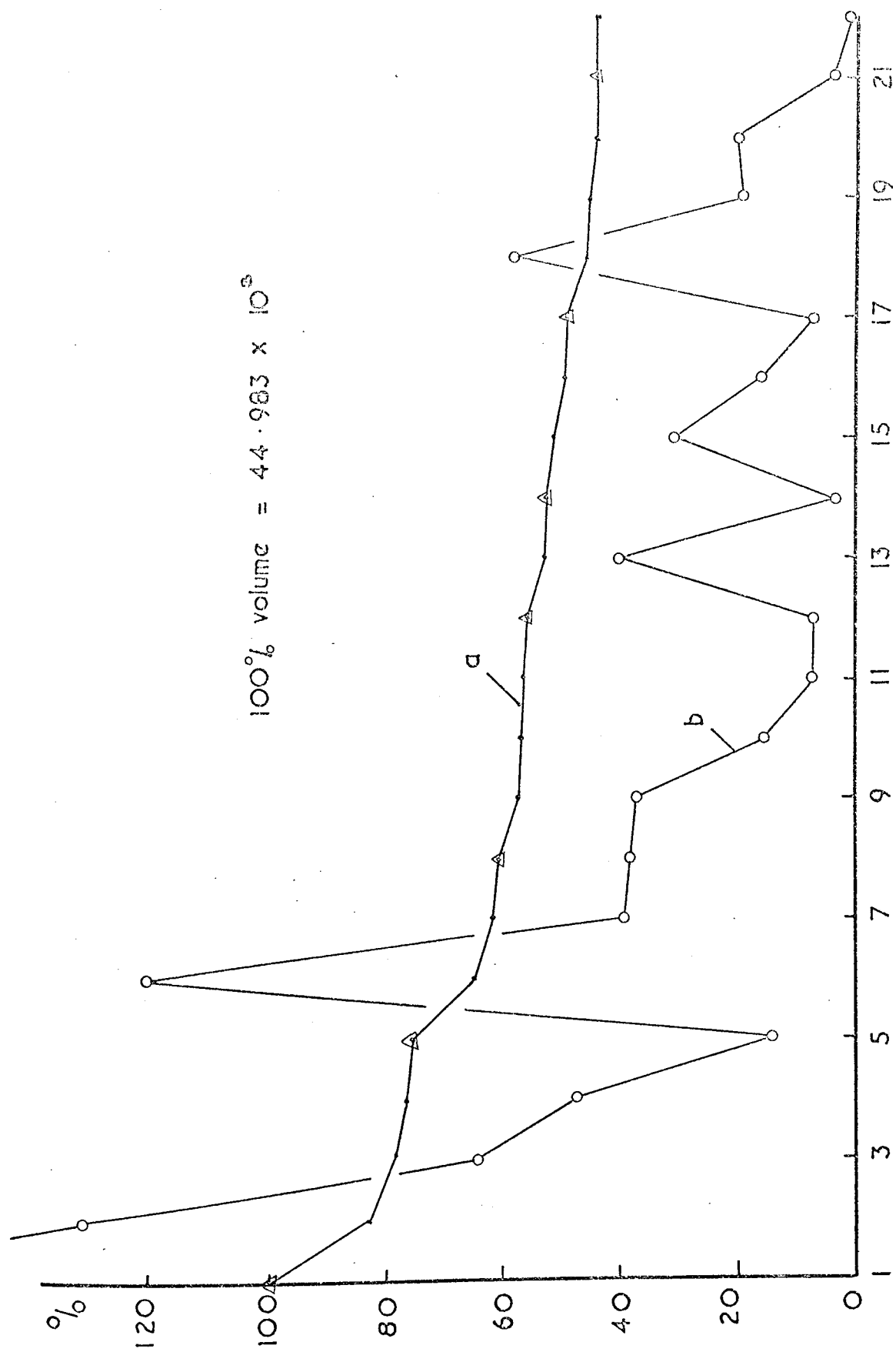


Figure 5.29. Progress of design - cantilever 5.



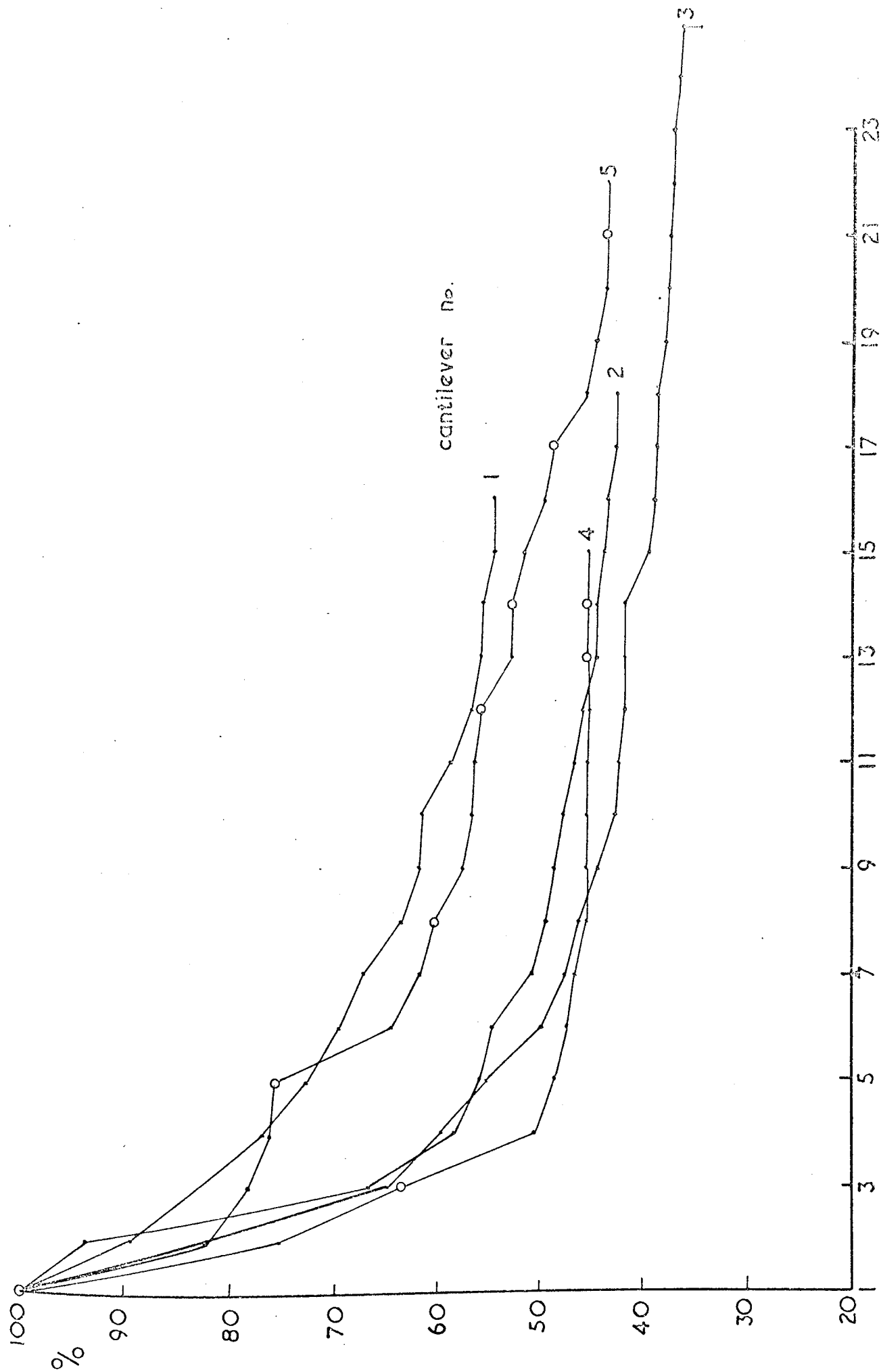
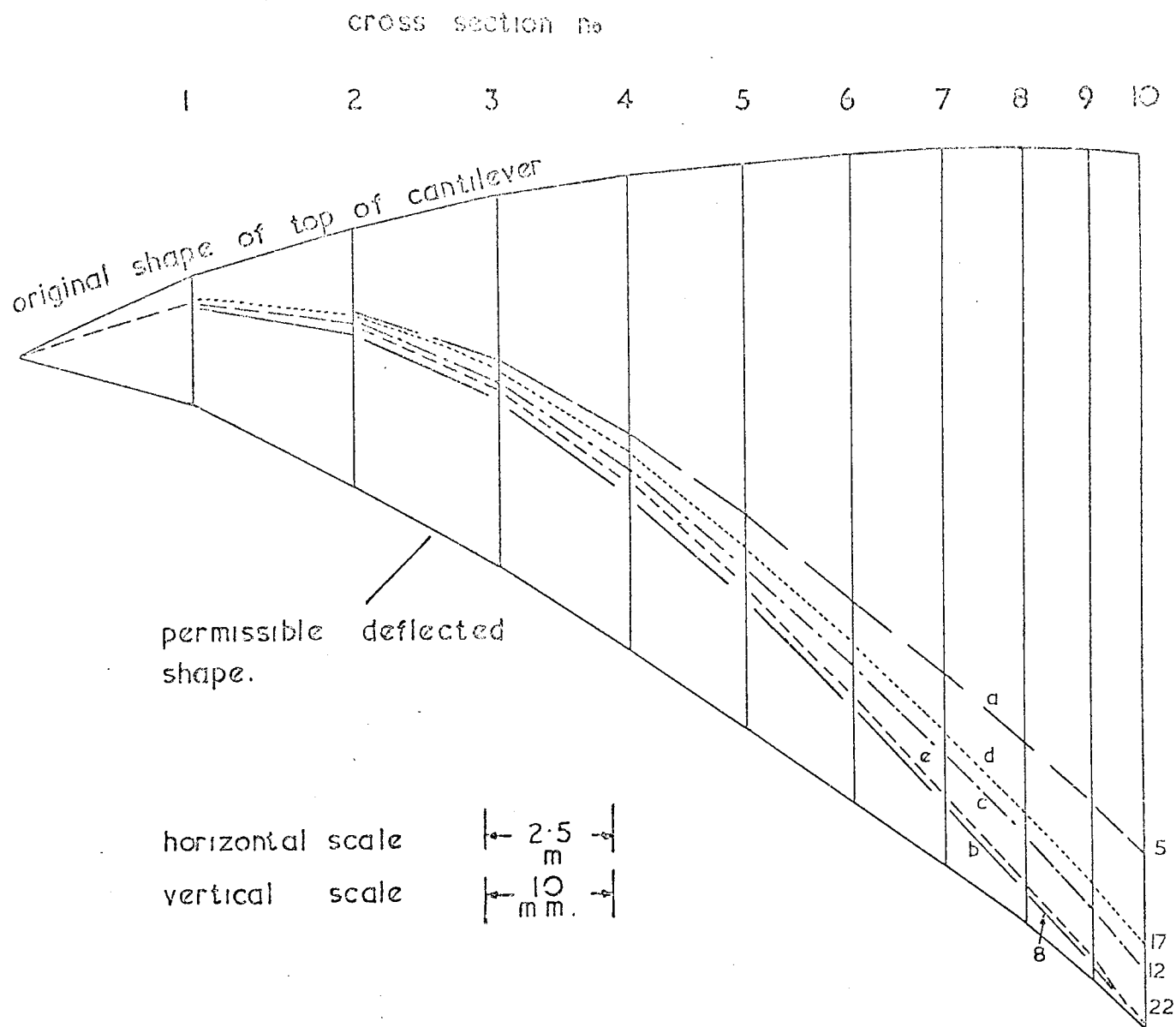


Figure 5.30. Comparison of designs.



a.	— — —	shape after	5	iterations	vol = 75.6%
b	— — —	" "	8	"	" = 60.2%
c	— . — . —	" "	12	"	" = 52.8%
d	.....	" "	17	"	" = 48.7%
e	-----	" "	22	"	" = 43.5%

Figure 5.31. Deflected shape of stage 5 at various stages due to load case 1

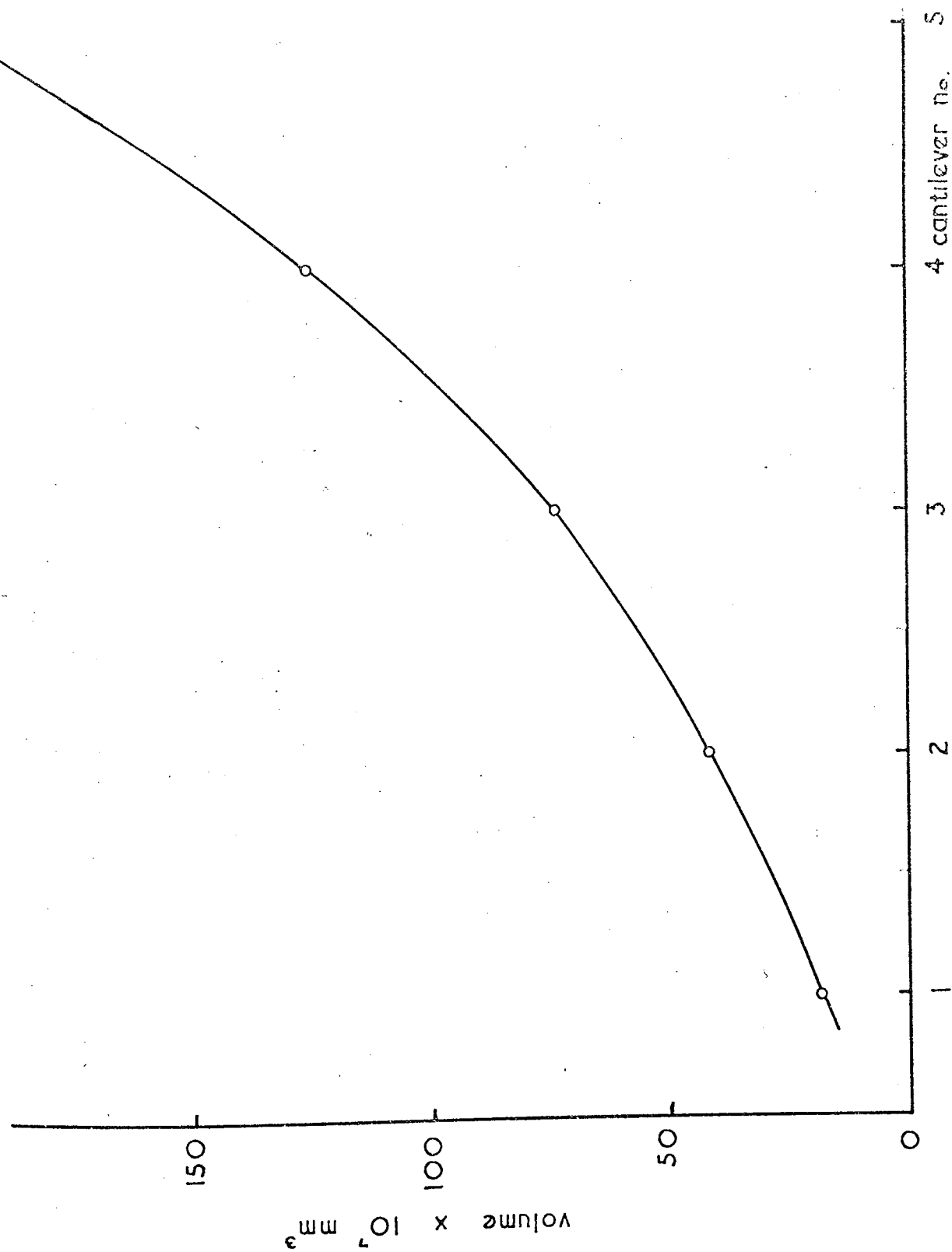


Figure 5.32. Final volumes obtained

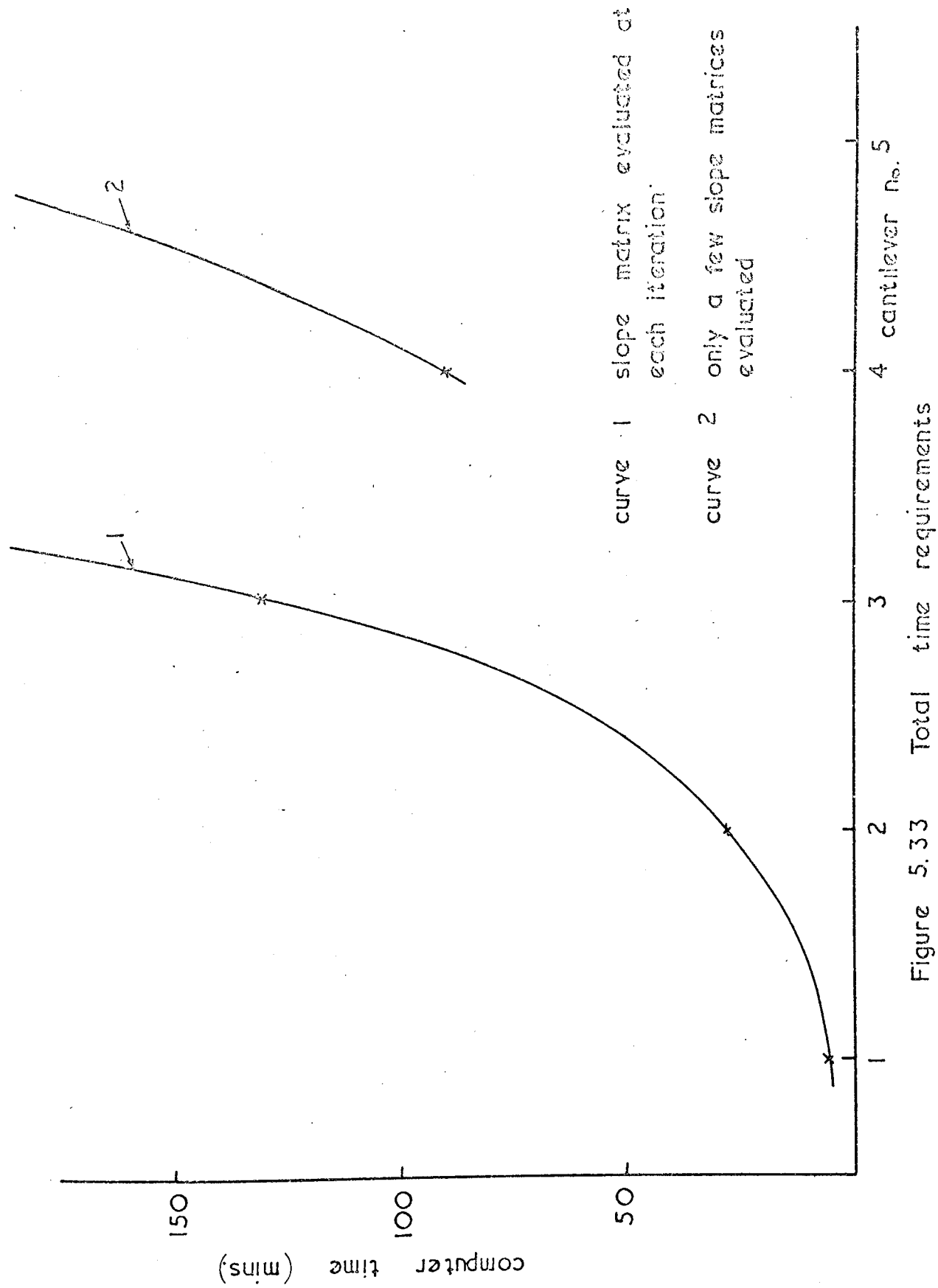


Figure 5.33 Total time requirements

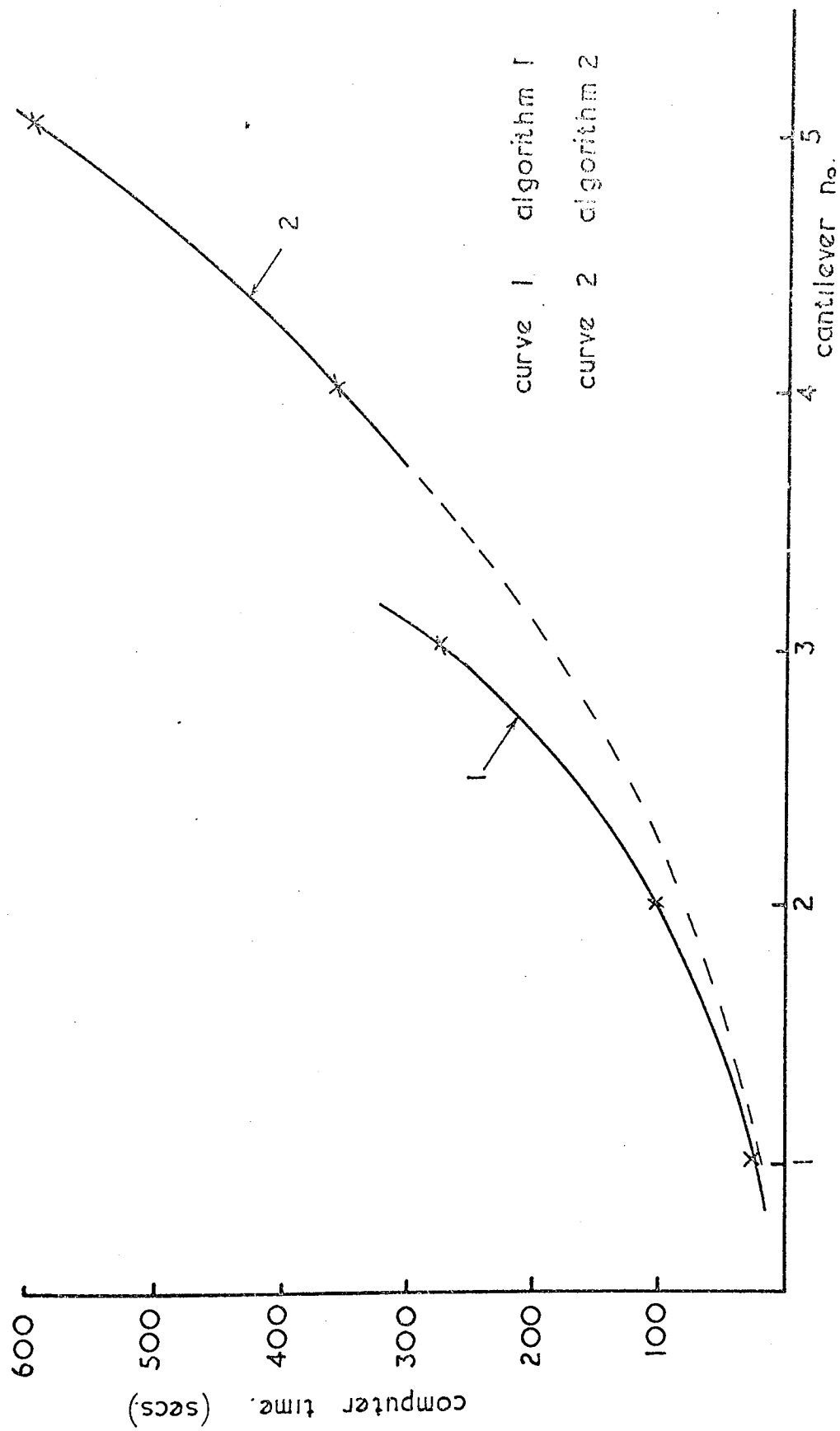


Figure 5. 34. Time required per iteration of design process

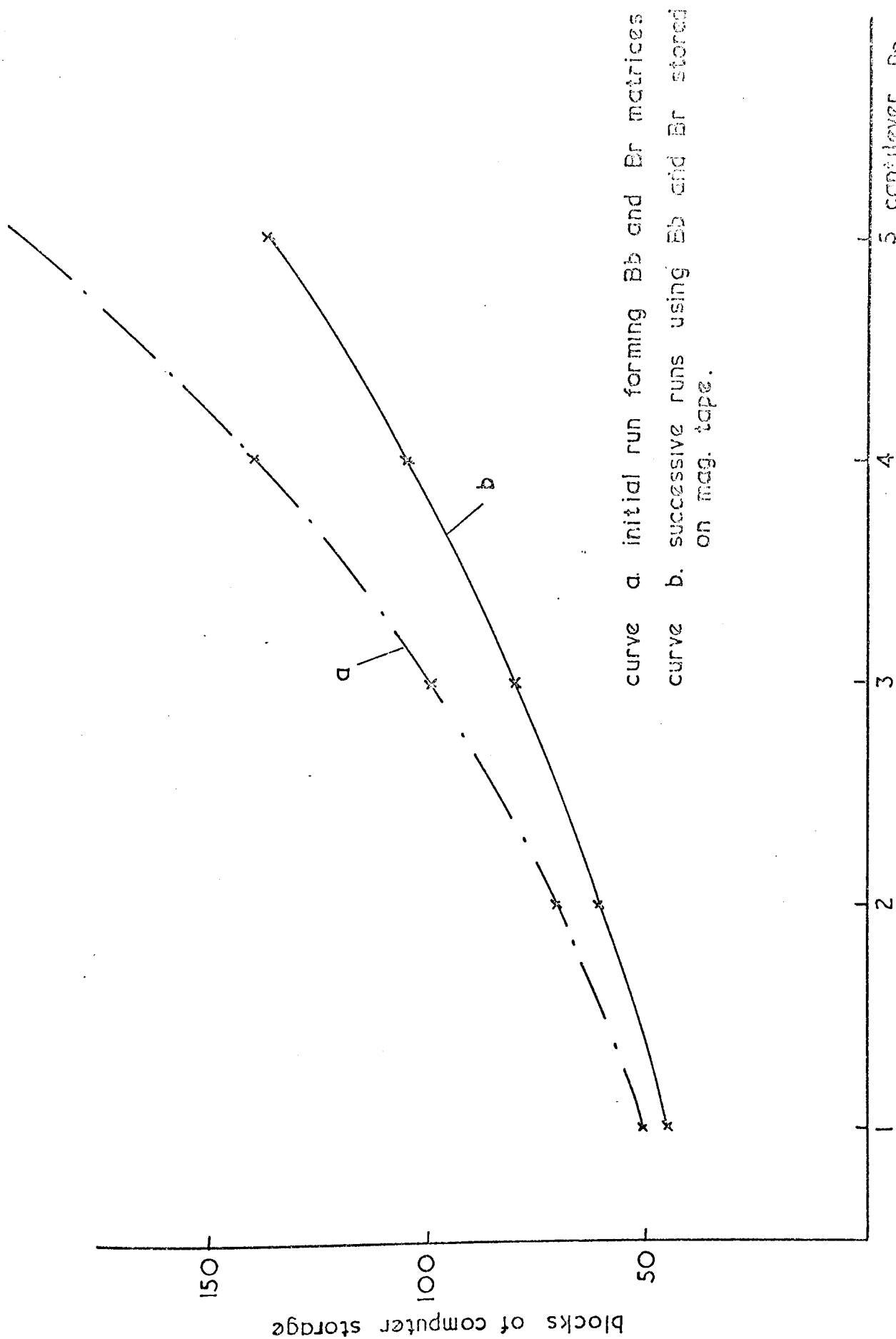


Figure 5.35. Computer storage requirements.



## CHAPTER 6

THEOREMS OF STRUCTURAL VARIATIONS6.1 Introduction

A complete analysis of a structure involves the determination of all the nodal displacements and the member forces. In the case of a first order hyperstatic structure, the force  $\pi_i$  in a given member  $i$  is evaluated from

$$\pi_i = p_i + r^* f_i \quad \dots 6.1$$

where  $p_i$  is the force in the member of a corresponding basic statically determinate structure with the redundant member removed. The force in the redundant member is  $r^*$  and  $f_i$  is the force in member  $i$  produced by unit equal and opposite forces acting instead of the redundant member.

Equation (6.1) can be generalised to several redundants and then used to analyse general hyperstatic structures. To do this the redundant members are removed and the resulting basic structure is analysed under two systems of loads. The first is the actual externally applied load system while the second consists of pairs of equal and opposite unit forces. Compatibility conditions are then utilized to derive the values of the redundants. Once these are obtained, the actual forces in all the members and the nodal deflexions are evaluated. This is in fact the basis of the compatibility method - generally referred to as the matrix force method, which can be stated mathematically as

Evaluate:

$$P = \frac{B}{b} \frac{L}{b} + \frac{B}{r} \frac{L}{r}, \quad \dots 6.2$$

and

$$\underline{X}_b = \underline{F}_{bb} \underline{L}_b + \underline{F}_{br} \underline{L}_r \quad \dots 6.3$$

from the condition that

$$\underline{0} = \underline{F}_{rb} \underline{L}_b + \underline{F}_{rr} \underline{L}_r \quad \dots 6.4$$

where  $\underline{p}$  is the vector of member forces,  $\underline{L}$  is the applied load vector or matrix that corresponds to the nodal displacements  $\underline{X}$ . The force transformation matrix is  $\underline{B}$  while  $\underline{F}$  is the overall flexibility matrix. Suffix b refers to the basic statically determinate structure while suffix r refers to the redundants. The manner in which matrix force method was formulated indicated that, from the beginning, its originators realised that hyperstatic structures form an extension to statically determinate ones.

Major contributions to the fundamental theories of structural analysis were made during the last century. Notably Mohr (37) and Castigliano (38) discovered that the forces and displacements of a structure can be derived by considering the strain energy of the structure. Earlier, Maxwell (39) carried out deflexion calculations of structures by removing a member of the structure and replacing it with a pair of equal and opposite forces. It was found later that this work and that of Mohr was, in fact, a special approach to a more general one due to Muller-Breslau (40), who was the first to enunciate the compatibility method fully.

The dual approach, often known as the equilibrium method or the matrix displacement method, was also derived using the contributions referred to above. This method can be stated mathematically as

Solve

$$\underline{X} = \underline{K}^{-1} \underline{L} = (\underline{A}^T \underline{K} \underline{A})^{-1} \underline{L} \quad \dots 6.5$$

to calculate

$$\underline{p} = \underline{k} \underline{A} \underline{X} \quad \dots 6.6$$

where  $\underline{A}$  is the displacement transformation matrix,  $\underline{k}$  is the assemblage of member stiffness submatrices and  $\underline{K}$  is the overall stiffness matrix.

The equilibrium and the compatibility methods are the only two distinct basic methods for the analysis of hyperstatic structures. Nearly every contribution made to structural theory in the 20th century can be recognised as an application of these two basic methods. An interesting genealogy of these was given by Matheson (41) who also showed the inter-connecting relationships of the various methods.

Historical requirements forced the classical theorists of the last century to concentrate upon the analysis of hyperstatic structures by inserting 'redundant' members into a more elementary structure. However, the work of Maxwell, Mohr and Muller-Breslau clearly indicates that they indeed understood that there is a hierarchy of structures in which the analysis of complex structures can be obtained from the more elementary ones. Perhaps they only partially recognised the significance of this hierarchy.

The reverse process that predicts the exact behaviour of elementary structures from more general ones has been less obvious and has attracted less attention. This is one concern of this chapter and gives rise to the development of the theorems in structural variations. In the second half of this century matrix methods have been utilized to produce general computer techniques for the analysis of complex structures (Livesley, Jennings and Majid, etc.). Once such an analysis is carried out, the proposed theorems can be applied to analyse a multitude of derived structures, without further resort to either of the basic methods. These theorems can also be used to predict the behaviour of a structure from the

results of another which has the same shape but with different material and cross-sectional properties. The significance of the theorems becomes more apparent when they are employed to design structures and particularly when the geometry and the topology of the structure constitute the basic design variables.

## 6.2 The Theorems of Structural Variations

These theorems predict:

- (i) The forces and the deflexions throughout a structure when the cross-sectional properties of all the members are varied proportionally;
- (ii) The forces and the deflexions throughout a structure when the cross-sectional properties of one or more members are altered independently;
- (iii) Consequently it becomes possible to predict the forces and the displacements throughout a resulting, derived structure when one or more members of a parent structure are totally removed, while the cross-sectional properties of the remaining members are altered independently.

### 6.2.1 Assumptions

It is assumed that the stress-strain relationship of the material of the structure is linear elastic and obeys Hooke's law. Furthermore it is assumed that no gross deformation takes place in the structure and thus frame instability is ruled out. This implies that the load deflexion relationship is also assumed to be linear and that the principle of superposition is valid.

Throughout this paper only pin-jointed frames are considered. However, the fundamental principles expounded here do not change qualitatively.

ively if they were generalised so that they may also cover rigidly jointed structures. For pin-jointed structures, members and joints are subjected to direct loads while the areas of the members are considered to be basic variables. The extension of the present work to include rigid structures requires the inclusion of the second moment of areas of the members as further basic variables. The members and the joints are then considered to sustain forces as well as moments and undergo translations as well as rotations.

#### 6.2.2 The Unit Load Matrix

The influence of the variation in the area of any member on the rest of a structure can be predicted by first applying a pair of equal and opposite unit loads to the structure so that they act axially at the ends of that member. An analysis of the structure under this pair of loads makes it possible to study the effect of that member on the rest of the structure. To study the independent effect of every member requires the application of pairs of unit loads to each member. For convenience these forces can be resolved so that their components may act parallel to the overall reference, X, Y, Z axes of the structure. A matrix consisting of all these components is hereinafter called the unit load matrix.

The sign conventions are shown in Figure (6.1) where the local member axes P, Q, R of a member ab are also indicated. End a of the member is considered as the first end and an arrow on the member, pointing to the second end b, indicates the direction of positive P axis. Applying external positive loads  $W_a$  and  $W_b$  at a and b respectively, the components of these forces can be readily expressed in terms of the direction cosines of the

member as

$$\begin{bmatrix} w_{aX} \\ w_{aY} \\ w_{aZ} \\ w_{bX} \\ w_{bY} \\ w_{bZ} \end{bmatrix} = \begin{bmatrix} l_P & 0 \\ m_P & 0 \\ n_P & 0 \\ 0 & l_P \\ 0 & m_P \\ 0 & n_P \end{bmatrix} \begin{bmatrix} W_a \\ W_b \end{bmatrix} \quad \dots 6.7$$

where  $w_X$ ,  $w_Y$  and  $w_Z$  are the components of  $W$  in  $X$ ,  $Y$  and  $Z$  directions respectively and  $l_P$ ,  $m_P$  and  $n_P$  are the direction cosines of the  $P$  axis of the member.

For  $W_a = -1$  and  $W_b = -1$ , equations (6.7) reduce to

$$\{ w_{aX} \ w_{aY} \ w_{aZ} \ w_{bX} \ w_{bY} \ w_{bZ} \} = \{ -l_P \ -m_P \ -n_P \ l_P \ m_P \ n_P \} \quad \dots 6.8$$

These components are indicated in Figure (6.1). The components of the unit external loads at the ends of the other members are similar and once these are collected together, they can be expressed as a matrix  $\underline{C}$  which is the unit load matrix.

Suppose a member  $g$  is connected to joint  $i$  at its first end and joint  $j$  at its second end, while another member  $h$  is similarly connected to  $s$  and  $t$ . A part of matrix  $\underline{C}$  with the contributions of these members is of the form

$$\begin{aligned}
 \underline{C} = & \left[ \begin{array}{cc}
 \cdot & \cdot \\
 \cdot & \cdot \\
 \cdot & \cdot \\
 \cdot & \cdot \\
 -l_{Pg} & 0 \\
 -m_{Pg} & 0 \\
 -n_{Pg} & 0 \\
 \cdot & \cdot \\
 \cdot & \cdot \\
 \cdot & \cdot \\
 0 & -l_{Ph} \\
 0 & -m_{Ph} \\
 0 & -n_{Ph} \\
 \cdot & \cdot \\
 \cdot & \cdot \\
 \cdot & \cdot \\
 +l_{Pg} & 0 \\
 +m_{Pg} & 0 \\
 +n_{Pg} & 0 \\
 \cdot & \cdot \\
 \cdot & \cdot \\
 \cdot & \cdot \\
 0 & +l_{Ph} \\
 0 & +m_{Ph} \\
 0 & +n_{Ph} \\
 \cdot & \cdot \\
 \cdot & \cdot \\
 \cdot & \cdot \\
 \cdot & \cdot
 \end{array} \right] \begin{array}{l} \\ \\ \\ \\ \left. \begin{array}{l} \text{at } i \end{array} \right\} \\ \\ \\ \\ \left. \begin{array}{l} \text{at } s \end{array} \right\} \\ \\ \\ \\ \left. \begin{array}{l} \text{at } j \end{array} \right\} \\ \\ \\ \\ \left. \begin{array}{l} \text{at } t \end{array} \right\} \\ \\ \\ \\
\end{array}
\end{aligned}$$

... 6.9

It can be readily observed that the unit load matrix  $\underline{C}$  is the transpose of the well-known displacement transformation matrix  $\underline{A}$  mentioned earlier. The formal construction of  $\underline{A}$  and hence  $\underline{C}$  automatically is given elsewhere (Majid 35).



### 6.2.3 Analysis Under Unit Loads

While analysing a structure under the actual external loads  $\underline{L}$ , it is now possible at the same time to evaluate the joint displacements  $\underline{\chi}$  and the member forces  $\underline{f}$  due to the unit load matrix. This is particularly convenient because instead of constructing  $\underline{C}$ , its transpose  $\underline{A}$ , which has in any case to be constructed, can be used in the analysis. Compounding  $\underline{L}$  and  $\underline{A}^T$ , an inverse transformation of the form given by equations (6.5) results in the joint displacements, thus

$$[\underline{\chi} \quad \underline{\chi}] = \underline{K}^{-1} [\underline{L} \quad \underline{A}^T] \quad \dots 6.10$$

Premultiplying  $[\underline{\chi} \quad \underline{\chi}]$  by  $\underline{kA}$ , yields the member forces, thus

$$[\underline{p} \quad \underline{f}] = \underline{kA} [\underline{\chi} \quad \underline{\chi}] \quad \dots 6.11$$

Alternatively if  $\underline{p}$  and  $\underline{\chi}$  are known or when  $\underline{L}$  is a null vector,  $\underline{\chi}$  and  $\underline{f}$  can be obtained from

$$\underline{\chi} = \underline{K}^{-1} \underline{A}^T$$

and

$$\underline{f} = \underline{kA} \underline{\chi}$$

... 6.12

The solution of  $\underline{L} = \underline{KX}$  when  $\underline{L}$  is a rectangular matrix of an order less than  $\underline{K}$ , does not require the inversion of  $\underline{K}$ . However when loads  $\underline{C}$  are also applied,  $[\underline{L} \quad \underline{A}^T]$  has an order higher than  $\underline{K}$  and it is more economical to invert  $\underline{K}$ .

### 6.2.4 Variation of Forces with Those of Member Areas

The first theorem of structural variation predicts the forces in the members of a structure when the area of a given member (or members) is

being varied. To derive an expression for the new force in any member, let the original area of the given member be  $A$ , while the change in its area be  $\delta A$ . When  $\delta A$  is positive the member size increases and defining  $\alpha$  as  $\delta A/A$ , it follows that  $\alpha$  is also positive. On the other hand, for decreasing area,  $\delta A$  is negative and so is  $\alpha$ . If  $A'$  is the remaining new area of the decreasing member then

$$\left. \begin{aligned} A' &= A - \delta A, \\ \alpha &= -\delta A/A \end{aligned} \right\} \dots 6.13$$

and hence  $A' = (1 + \alpha)A$

In particular for the total removal of a member

$$A - \delta A = 0 \text{ and } \alpha = -1.$$

Consider now a general three-dimensional pin-jointed hyperstatic structure such as that shown in Figure (6.2). The structure is subject to a general set of external loads

$$\underline{L} = [L_1 \quad L_2 \quad \dots \quad L_d]$$

where  $d$  is the total degrees of freedom. There are  $n$  members in the structure and the resulting tensile forces in these are

$$\underline{p} = [p_1 \quad p_2 \quad \dots \quad p_n]$$

Consider that the area of member  $i$  is being varied from  $A_i$  to  $A'_i$  by an amount of  $\delta A_i$ . This member, which is shown to be connected to joints  $a$  and  $b$ , can be split into two new members of areas  $A'_i$  and  $\delta A_i$ . The corresponding forces would be  $p'_i$  and  $p''_i$  respectively. This is possible provided

that

$$p_i = p_i' + p_i''$$

and

$$p_i / \Delta_i = p_i' / \Delta_i = p_i'' / \delta \Delta_i = \sigma$$

... 6.14

where  $\sigma$  is the stress in member  $i$  as well as in each part of that member.

It follows from equations (6.13) and (6.14) that

$$p_i'' = -\alpha p_i$$

$$p_i' = (1 + \alpha)p_i$$

... 6.15

Any member of this structure, such as the new member joining  $ab$ , with area  $\delta \Delta_i$  and force  $p_i''$ , can be removed without altering the member forces elsewhere, provided that the member is replaced by two equal and opposite external forces  $p_i''$ , acting at  $a$  and  $b$  and in the same direction as the member. This is shown in figure (6.2b) where, for clarity, a part of the structure is shown isolated. However, the case to be considered is the total removal of this member without compensation by external forces, i.e. with the net external force  $p_i'' = 0$ .

In figure (6.2c) the original structure is shown subject to a second external system of only two equal and opposite unit loads at  $a$  and  $b$  acting axially to  $ab$ . The resulting member forces due to these are given as

$$\underline{f}_i = \{f_{1i} \quad f_{2i} \quad \dots \quad f_{ii} \quad \dots \quad f_{ni}\}$$

where  $f_{1i}$  is the force in member 1 due to unit loads acting axially to member  $i$ . Since member  $i$  is split into two members, the forces  $f_{ii}'$  and  $f_{ii}''$ , shown in the figure are given as

$$f_{ii}'' = -\alpha f_{ii}$$

and

$$f_{ii}' = (1 + \alpha)f_{ii}$$

... 6.16

Under these unit loads the member with area  $\delta A_i$  and force  $f_{ii}''$  can be removed provided it is compensated by equal and opposite forces  $f_{ii}''$  at a and b. The total external forces now acting at these points will therefore be  $1 - f_{ii}''$  as shown in figure (6.2d).

The magnitude of the unit loads can always be increased by a factor  $r_\alpha$  and the resulting member forces become  $\{r_\alpha f_{1i} \quad r_\alpha f_{2i} \quad \dots \quad r_\alpha f_{ni}\}$ . The two parts of member i will then sustain forces  $r_\alpha f_{ii}''$  by  $\delta A_i$  and  $r_\alpha f_{ii}'$  by  $A_i'$ . The removal of  $\delta A_i$  will therefore require compensation of  $r_\alpha f_{ii}''$  and the net externally applied loads at a and b become  $r_\alpha - r_\alpha f_{ii}''$ . It follows that, under the actual external loads  $\underline{L}$ , if  $\delta A_i$  is removed without compensation then

$$r_\alpha - r_\alpha f_{ii}'' - p_i'' = 0 \quad \dots 6.17$$

This, together with equations (6.15) and (6.16) give

$$r_\alpha = -\alpha p_i' / (1 + \alpha f_{ii}') \quad \dots 6.18$$

In the remaining member, which has an area  $A_i'$ , the force due to the actual external loads is  $p_i'$ , while the change in this force was shown to be  $r_\alpha f_{ii}'$ . The final force  $\pi_i$  is therefore given by

$$\pi_i = p_i' + r_\alpha f_{ii}' \quad \dots 6.19$$

Using equations (6.15), (6.16), (6.18) and (6.19) it follows that

$$\pi_i = p_i' (1 + \alpha) / (1 + \alpha f_{ii}') \quad \dots 6.20$$

The force in any other member  $j$  is also found by the superposition of  $p_j$  and  $r_{\alpha} f_{ji}$ . In general the final force in member  $j$  due to the variation of the area of member  $i$  is given by

$$\pi_j = p_j + r_{\alpha i} f_{ji} \quad \dots 6.21$$

The factor  $r_{\alpha}$  is hereinafter called the variation factor. Comparing equation (6.21) and (6.1), it is immediately evident that the variation in the area of a member has the same effect on the forces of the other members as its complete removal. In fact when a member  $i$  is completely removed then  $\alpha_i = -1$  and equation (6.18) gives the removal factor  $r_i$  as

$$r_i = p_i / (1 - f_{ii}) \quad \dots 6.22$$

More generally, considering the structure as a whole and varying every member independently, the forces  $\pi$  in all the members, due to the variation of any member can be expressed in matrix form as

$$\underline{\pi} = \underline{P} + \underline{R} \underline{\lambda} \quad \dots 6.23$$

The vectors  $\underline{\pi}$ ,  $\underline{P}$  and  $\underline{\lambda}$  and the matrix  $\underline{R}$  are best defined by first expanding equation (6.23). This takes the form

$$\begin{bmatrix} \pi_1 \\ \pi_2 \\ \vdots \\ \pi_j \\ \vdots \\ \pi_n \end{bmatrix} = \begin{bmatrix} p \\ p \\ \vdots \\ p \\ \vdots \\ p \end{bmatrix} + \begin{bmatrix} R_1 & 0 & \dots & 0 \\ 0 & R_2 & & \vdots \\ & \ddots & R_j & \vdots \\ 0 & \dots & 0 & R_n \end{bmatrix} \begin{bmatrix} \lambda_1 \\ \lambda_2 \\ \vdots \\ \lambda_j \\ \vdots \\ \lambda_n \end{bmatrix} \quad \dots 6.24$$

In these equations  $j$  is a typical member, vectors  $\underline{\pi}$ ,  $\underline{p}$  and  $\underline{\lambda}$  are of order  $n^2 \times 1$  while matrix  $\underline{R}$  is of order  $n^2 \times n^2$ . Each subvector  $\underline{p}$  of equations (6.24) consists of the member forces throughout the structure due to the external loads only. The subvector  $\underline{\lambda}_j$  contains the forces in all the members due to the application of unit equal and opposite tensile forces at the ends of member  $j$ , thus

$$\underline{\lambda}_j = \{f_{1j} \quad f_{2j} \quad \dots \quad f_{jj} \quad \dots \quad f_{nj}\} \quad \dots 6.25$$

On the other hand  $\underline{\pi}_j$  defines the forces in the members due to the external loads, while member  $j$  is also altered. Hence

$$\underline{\pi}_j = \{\delta_i \pi_{ij}\} \quad \dots 6.26$$

where  $\pi_{ij}$  is the force in member  $i$  due to the external loads, while member  $j$  is changing. The Kronecker  $\delta_i$  is defined as

$$\left. \begin{aligned} \delta_i &= 1, \text{ for } i \neq j, \\ \delta_i &= 0, \text{ for } i = j \end{aligned} \right\} \quad \dots 6.27$$

For instance vector  $\underline{\pi}_3$  is

$$\underline{\pi}_3 = \{\pi_{1,3} \quad \pi_{2,3} \quad 0 \quad \pi_{4,3} \quad \dots \quad \pi_{n,3}\} \quad \dots 6.28$$

The matrix  $\underline{R}$  is diagonal in which each submatrix  $\underline{R}_j$  is also diagonal. A non-zero element  $r_{kk}$  of  $\underline{R}_j$  is given by

$$\left. \begin{aligned} r_{kk} &= r_j(1 - \delta_k) - \delta_k p_j / f_{jj} \\ \text{where } k &= 1, 2, 3, \dots n; \\ \delta_k &= 1, \text{ for } k = j; \\ \text{and } \delta_k &= 0, \text{ for } k \neq j; \end{aligned} \right\} \quad \dots 6.29$$

It is noticed that when  $k = j$ ,  $\delta_k = 1$  and  $r_j(1 - \delta_k)$  vanishes. The first of equations (6.29) therefore reduces to

$$r_{kk} = -p_j/f_{jj} \quad \dots 6.30$$

Substituting this in equation (6.24) reduces  $\pi_{jj}$  in member  $j$  to zero as shown in equation (6.28). As an illustration the submatrix  $\underline{R}_3$  of order  $n \times n$  is derived by using equations (6.29) and (6.30) as

$$\underline{R}_3 = \begin{bmatrix} r_3 & 0 & 0 & 0 & \dots & 0 \\ 0 & r_3 & 0 & 0 & & \vdots \\ 0 & 0 & -p_3/f_{33} & 0 & & \vdots \\ 0 & 0 & 0 & r_3 & & \vdots \\ \vdots & & & & \ddots & 0 \\ 0 & \dots & & 0 & & r_3 \end{bmatrix} \quad \dots 6.31$$

#### 6.2.5 Variation of Deflexions with Proportional Changes in Areas

The second theorem predicts the deflexions throughout the structure when all the members of the structure are varied proportionally. Consider the set of stiffness equations (6.5) which gives the deflexions of the structure with fixed areas. An element  $K_{uv}$  of the overall stiffness matrix consists of accumulative stiffnesses of the form  $A\mu$  contributed by the members. For each member the area  $A$  is to be varied while  $\mu$  is kept constant, depending on the length, Young's modulus and direction cosines of the member.

Thus

$$K_{uv} = \sum_{j=1}^J A_j \mu_j \quad \dots 6.32$$



The summation covers  $J$  members, such as  $j$ , connected to a given joint. In most cases only one member contributes to  $K_{uv}$  and in the case of pin-jointed structures only the elements on the loading diagonal of  $\underline{K}$  receive contributions from more than one member.

Consider that every area in the structure is varied proportionally so that  $\alpha (= \delta A/A)$ , is kept constant for all the members. At a given instant, the area  $A_k^*$  for member  $k$  is given by

$$A_k^* = A_k (1 + \alpha) \quad \dots 6.33$$

The new element  $K_{uv}^*$ , of the stiffness matrix, now becomes

$$K_{uv}^* = \sum_{j=1}^J A_j^* \mu_j = (1 + \alpha) \sum_{j=1}^J A_j \mu_j \quad \dots 6.34$$

In this manner the entire overall stiffness matrix changes to

$$\underline{K}^* = (1 + \alpha) \underline{K} \quad \dots 6.35$$

where  $(1 + \alpha)$  is a scalar quantity. The new deflexions  $\underline{X}^*$  may be obtained by solving  $\underline{L} = \underline{K}^* \underline{X}^*$ , which, using equation (6.35) may be written as

$$\underline{X}^* = \frac{1}{1 + \alpha} \underline{K}^{-1} \underline{L} \quad \dots 6.36$$

But from equations (6.5),  $\underline{K}^{-1} \underline{L} = \underline{X}$ , it follows that

$$\underline{X}^* = \frac{1}{1 + \alpha} \underline{X} \quad \dots 6.37$$

Equations (6.37) indicate that once the original structure is analysed under the external loads for  $\underline{X}$ , the new structure need not be re-analysed. For a given degree of freedom  $e$ , dividing the corresponding elements of  $\underline{X}$  and  $\underline{X}^*$

by  $x_e$ , which is the deflexion before any member variations, it follows that

$$y = x_e^*/x_e = 1/(1 + \alpha) \quad \dots 6.38$$

which is the equation of a hyperbola. It is noticed that when  $\alpha = 0$ , i.e. before any variations in the areas, the non-dimensional deflexion  $y = x^*/x$  is unity. It is also interesting to note that the slope of the hyperbole at  $\alpha = 0$ ,  $y = 1$  is  $-1$ , indicating that for any structure the curve cuts the  $y$  axis at an angle of  $45^\circ$ .

#### 6.2.6 Variation of Deflexions with Individual Areas

This theorem of structural variations predicts the deflexions throughout the structure when the area of one (or more) member is varied independently or when they are totally removed, thus resulting in a new structure.

Consider a hyperstatic structure with a total of  $t$  redundant members. From equations (6.3) and (6.4) the flexibility equations for this structure for  $m$  loading points become

$$\begin{bmatrix} x_1 \\ x_2 \\ \vdots \\ x_j \\ \vdots \\ x_m \\ \dots \\ 0 \\ \vdots \\ 0 \end{bmatrix} = \begin{bmatrix} & & & F_{1,k} & \dots & F_{1,\gamma} \\ & & & \vdots & & \vdots \\ & & F_{bb} & \vdots & & \vdots \\ & & & \vdots & & \vdots \\ & & & F_{m,k} & \dots & F_{m,\gamma} \\ \dots & \dots & \dots & \dots & \dots & \dots \\ 0 & F_{k,1} & \dots & F_{k,m} & F_{k,k} & \dots & F_{k,\gamma} \\ \vdots & \vdots & & & \vdots & & \\ & & & & & & \\ \vdots & \vdots & & & \vdots & & \\ 0 & F_{\gamma,1} & \dots & F_{\gamma,m} & F_{\gamma,k} & \dots & F_{\gamma,\gamma} \end{bmatrix} \begin{bmatrix} L_1 \\ L_2 \\ \vdots \\ L_j \\ \vdots \\ L_m \\ \dots \\ \pi_1 \\ \pi_2 \\ \vdots \\ \pi_i \\ \vdots \\ \pi_t \end{bmatrix} \quad \dots 6.39$$

where, for convenience,  $k = m + 1$  and  $\gamma = m + t$ .

Consider the case when the area of any, say the last, redundant member is varied. The force  $\pi_i$  in any other redundant member  $i$  will be given by equation (6.21), which becomes

$$\pi_i = p_i + r_{at} f_{it}$$

Each redundant member can be removed from the structure provided that equal and opposite axial forces  $\pi_i$  are applied to the structure instead of the member. Equations (6.39) can then be written, treating the forces  $\pi$  as

external forces, as

$$\begin{bmatrix} \psi_1 \\ \psi_2 \\ \vdots \\ \psi_j \\ \vdots \\ \psi_m \\ \dots \\ 0 \\ \vdots \\ \vdots \\ 0 \\ 0 \end{bmatrix} = \begin{bmatrix} & & & F_{1,k} & \dots & F_{1,\gamma-1} & F_{1,\gamma} \\ & & & \vdots & & \vdots & \\ & & & \vdots & & \vdots & \\ & & & \vdots & & \vdots & \\ & & & & & & \\ & & & F_{m,k} & \dots & F_{m,\gamma-1} & F_{m,\gamma} \\ \dots & \dots & \dots & \dots & \dots & \dots & \dots \\ F_{k,1} & \dots & F_{k,m} & F_{k,k} & \dots & F_{k,\gamma-1} & F_{k,\gamma} \\ \vdots & & \vdots & \vdots & & \vdots & \vdots \\ \vdots & & \vdots & \vdots & & \vdots & \vdots \\ F_{\gamma-1,1} & \dots & F_{\gamma-1,m} & F_{\gamma-1,k} & \dots & F_{\gamma-1,\gamma-1} & F_{\gamma-1,\gamma} \\ F_{\gamma,1} & \dots & F_{\gamma,m} & F_{\gamma,k} & \dots & F_{\gamma,\gamma-1} & F_{\gamma,\gamma} \end{bmatrix} \begin{bmatrix} L_1 \\ L_2 \\ \vdots \\ L_j \\ \vdots \\ L_m \\ \dots \\ p_1 + r_{at} f_{1t} \\ \vdots \\ p_i + r_{at} f_{it} \\ \vdots \\ p_{t-1} + r_{at} f_{t-1,t} \\ \pi_t \end{bmatrix} \quad \dots 6.40$$

In these equations  $\pi_t$  is variable because the area of member  $t$  is being varied. Hence both  $\alpha_t$  and  $r_{at}$  are variables. Similarly the joint deflexions are also variables and for this reason they are denoted, in equations (6.40), by  $\psi$  to differentiate them from the initial deflexions  $x$ . On the other hand although each  $\pi_i$  is changing, the forces  $p_i$  for  $i = 1, 2, \dots, t$ , are constants and predetermined before varying member  $t$ .

Each element of the entire matrix  $\underline{F}$  in equation (6.40) is of the form

$$F = \phi + \theta / A_t' \quad \dots 6.41$$

where  $\phi$  and  $\theta$  are constants while the new area  $\Lambda'_t$  is a variable. The quantity  $r_{at}^{f_{it}}$  is dependent on  $\Lambda'_t$  and has the form  $\rho \Lambda'_t$  where  $\rho$  is also a constant. Hence a displacement  $\psi_j$ , evaluated from equation (6.40), has the form

$$\psi_j = \phi + \theta / \Lambda'_t + \rho \Lambda'_t + (\phi + \theta / \Lambda'_t) \pi_t \quad \dots 6.42$$

The quantities  $\phi$ ,  $\theta$  and  $\rho$  are all constants, obtained by multiplying a row of  $\underline{F}$  by the column on the right hand side of equation (6.40) and then collecting the terms.

Furthermore, the last equation, in (6.40) is of the form

$$0 = \phi + \theta / \Lambda'_t + \rho \Lambda'_t + (\phi + \theta / \Lambda'_t) \pi_t$$

which gives  $\pi_t$  in the form

$$\pi_t = -(\phi + \rho \Lambda'_t + \nu \Lambda'^2_t) / (\phi + \rho \Lambda'_t) \quad \dots 6.43$$

where  $\nu$  is also a constant. It should be stressed that the constants  $\phi$ ,  $\theta$  and  $\rho$  in the numerator and denominator of equation (6.43) are all different from each other and from those of equation (6.42).

Substituting for  $\pi_t$ , from equation (6.43) into equation (6.42) and collecting the similar terms, it is found that

$$\varepsilon_1 + \varepsilon_2 \Lambda'_t + \varepsilon_3 \Lambda'^2_t + \varepsilon_4 \Lambda'^3_t + \varepsilon_5 \Lambda'_t \psi_j + \varepsilon_6 \Lambda'^2_t \psi_j = 0 \quad \dots 6.44$$

where  $\varepsilon_1, \varepsilon_2, \dots, \varepsilon_6$  are arbitrary constants. Now when  $\Lambda'_t = 0$ , i.e. when member  $t$  is removed, equation (6.44) remains true for all values of  $\psi_j$ , i.e. when  $\Lambda'_t = 0$ ,  $|\psi_j| > 0$  and therefore equation (6.44) gives  $\varepsilon_1 = 0$ , thus

$$\varepsilon_2 \Lambda'_t + \varepsilon_3 \Lambda'^2_t + \varepsilon_4 \Lambda'^3_t + \varepsilon_5 \Lambda'_t \psi_j + \varepsilon_6 \Lambda'^2_t \psi_j = 0$$

Dividing through by  $A_t'$ , we obtain

$$\varepsilon_2 + \varepsilon_3 A_t' + \varepsilon_4 A_t'^2 + \varepsilon_5 \psi_j + \varepsilon_6 A_t' \psi_j = 0 \quad \dots 6.45$$

This formally proves that the variation of any displacement  $\psi_j$  with changes in the area of any one redundant member  $t$  is hyperbolic.

The constants  $\varepsilon$  can be obtained from the boundary conditions. However, the equation of the hyperbola can be explicitly derived more elegantly as follows

Let  $\chi_{ji}$  be the deflexion at  $j$  due to a unit force at the ends of member  $i$ . Increasing this unit load by a factor  $r_{\alpha i}$ , the displacement at  $j$  becomes  $r_{\alpha i} \chi_{ji}$ . Using the principle of superposition to add the displacements  $r_{\alpha i} \chi_{ji}$  and  $x_j$  which is due to the actual loading, we obtain

$$\psi_j = x_j + r_{\alpha i} \chi_{ji} \quad \dots 6.46$$

The factor  $r_{\alpha}$  is the variation factor given by equation (6.18). The non-dimensional deflexion  $y'$  is thus given by

$$y' = \psi_j / x_j = 1 + r_{\alpha i} \chi_{ji} / x_j = 1 + c_{\alpha i} \quad \dots 6.47$$

where, using equation (6.18) for  $r_{\alpha}$

$$c_{\alpha i} = -\alpha_i p_i \chi_{ji} / [x_j (1 + \alpha_i f_{ii})] \quad \dots 6.48$$

Denoting the constant  $D$  as  $p_i \chi_{ji} / x_j$  equation (6.48) becomes

$$c_{\alpha i} = -\alpha_i D / (1 + \alpha_i f_{ii}) \quad \dots 6.49$$

But from equation (6.47),  $y' = 1 + c_{\alpha i}$  and using this with equation (6.49), it follows that





$$\text{i.e. } \psi_j = \phi + \theta / A_k'$$

which is a special case of equation (6.42).

Equations (6.46) and (6.47) may be applied to statically determinate structures. However, care must be taken that a member is not totally removed, thus leading to the formation of a mechanism. When this is the case, as  $f_{kk}$  is equal to unity, the value of  $y^*$  obtained from equation (6.51) is infinite.

It is advantageous to generalise equation (6.46), in a manner similar to equations (6.23) and (6.24). In this case, if  $\underline{X}$  is the displacement vector corresponding to  $\underline{L}$ ,  $\underline{\chi}$  is the vector of displacements due to unit loads,  $\underline{\psi}$  is the final displacement vector and  $\underline{R}^*$  is the matrix of variation factors, then equation (6.46) is generalised to become

$$\underline{\psi} = \underline{X} + \underline{R}^* \underline{\chi} \quad \dots 6.53$$

In its expanded form, these equations have the form

$$\begin{bmatrix} \psi_1 \\ \psi_2 \\ \vdots \\ \psi_j \\ \vdots \\ \psi_n \end{bmatrix} = \begin{bmatrix} \underline{x} \\ \underline{x} \\ \vdots \\ \underline{x} \\ \vdots \\ \underline{x} \end{bmatrix} + \begin{bmatrix} \underline{R}_1^* & 0 & \dots & 0 \\ 0 & \underline{R}_2^* & \dots & 0 \\ \vdots & 0 & \ddots & \vdots \\ \vdots & 0 & \dots & \underline{R}_j^* & \dots & 0 \\ \vdots & \vdots & \vdots & 0 & \ddots & 0 \\ \vdots & \vdots & \vdots & \vdots & \vdots & \underline{R}_n^* \\ 0 & \dots & 0 & \dots & 0 & \dots & 0 \end{bmatrix} \begin{bmatrix} \chi_1 \\ \chi_2 \\ \vdots \\ \chi_j \\ \vdots \\ \chi_n \end{bmatrix} \quad \dots 6.54$$

where  $j$  is a typical member, vectors  $\underline{\psi}$ ,  $\underline{X}$  and  $\underline{\chi}$  are of order  $n.d \times 1$ , while  $\underline{R}^*$  is a diagonal matrix of order  $n.d \times n.d$ . The subvector  $\underline{x}$  consists of the nodal displacements due to the external loads. The subvector  $\underline{\chi}_j$  contains the nodal displacements due to unit loads at the ends of member  $j$ , thus

$$\underline{\chi}_j = \{ \chi_{1j} \quad \chi_{2j} \quad \dots \quad \chi_{ij} \quad \dots \quad \chi_{dj} \} \quad \dots 6.55$$

Similarly for  $\psi_j$ . The submatrix  $\underline{R}_j^*$  is of the form

$$\underline{R}_j^* = r_{\alpha j} \cdot \underline{I}, \quad \dots 6.56$$

in which  $r_{\alpha j}$  is the variation factor for member  $j$ . The identity matrix  $\underline{I}$  and  $\underline{R}_j^*$  are of order  $d \times d$ .

In the case when more than one member is being varied independently, it is first necessary to alter one of these by the required amount and evaluate the resulting forces and displacements, before proceeding to alter the next member. In the case of rigidly jointed structures where axial and flexural stiffnesses are significant, it is necessary to change the area and the second moment of area of a varying member independently, and not simultaneously.

In most cases, and particularly when structures are being designed, it is often necessary to study the effect of varying one or a few members, on a number of deflexions or forces. In these cases the first and the third theorems become particularly useful. The second theorem is used when all the members are being altered. This theorem becomes specially useful when the design parameter is the topology or the shape of the structure. In these cases, it is often required to evaluate the weight of the remaining structure when one or more members are being totally removed.

### 6.3 Application to a Plane Frame

The simple hyperstatic frame shown in figure (6.3a) is selected as an example to illustrate the efficacy of the theorems. The frame has two redundant members and may be analysed by any of the two basic methods. The

theorems of structural variations can then be used to predict the behaviour of any one of the nine derivatives shown in figures (6.3b) to (6.3j). Every member of the ten frames shown may have a different cross-section from every other member.

For instance consider the case when the area of each member of the frame in figure (6.3a) is first reduced by a factor of 0.4 ( $\alpha = -0.4$ ) and then the vertical member is removed resulting in the frame shown in figure (6.3b). In the original frame members (1) and (2) have an area  $A_{g1}$  of 7.312 square inches while members (3) and (4) have area  $A_{g2} = 8.5670$  square inches, the distance  $l$  is 100 inches and the modulus of elasticity is  $13.4 \times 10^3$  tons per square inch. The frame is subject to a horizontal load of 10 tons at the common joint B. Using matrix displacement method (equations (6.10) and (6.11)) to analyse the frame, it is found that  $x_B = 97.50 \times 10^{-4}$  inch,  $v_B = -17.60 \times 10^{-4}$  inch,  $\chi_{B3} = 1.77 \times 10^{-4}$  inch,  $f_{33} = 0.546$  tons and  $p_3 = 2.020$  tons, where  $x_B$  and  $v_B$  are the horizontal and vertical deflexions at joint B under the actual load of 10 tons. With  $\alpha = -0.4$  and the above values of  $x_B$  and  $\chi_{B3}$ , equation (6.38) gives  $y$  as 1.6700,  $x_B^*$  as  $162.50 \times 10^{-4}$  inch and  $\chi_{B3}^*$  as  $2.95 \times 10^{-4}$  inch. The value of  $p_3$  and  $f_{33}$  on the other hand do not change due to an all round alteration of member areas. This follows from the fact that

$$\underline{k}^* = (1 + \alpha)\underline{k} \quad \dots 6.57$$

and hence using equation (6.37) it follows that

$$\underline{p} = \underline{k} \underline{A} \underline{X} = \frac{1}{1 + \alpha} \underline{k}^* \underline{A} (1 + \alpha) \underline{X}^* = \underline{k}^* \underline{A} \underline{X}^* \quad \dots 6.58$$

where  $\underline{k}^*$  is the new member stiffness matrix. The constant  $D$ , therefore, also remains unaltered at a value of 0.0365. From equation (6.51), the value

of  $y^*$  is calculated to be 1.804.

In figure (6.4) the variation of  $y$  with  $\alpha$  for the frame of figure (6.3a) is shown as curve (1). Curve (2) shows the manner in which  $y^*$ , for the horizontal deflexion at B, varies with the area of member 3. Curve (3) to curve (6) gives the variation of  $y$  at different values of  $\alpha_3$ , each curve also being hyperbolic. From these curves and curve (7), for instance, it is found that if only half the area of member 3 is removed while the other members are intact, then  $y_B$  for the horizontal deflexion at B will be 1.024, giving  $x_B$  as  $99.74 \times 10^{-4}$  inch. From these curves it is noticed that to obtain the frame of figure (6.3b) it is possible to move from A to E on curve (7) then move vertically to D. However, a better route is to move to B on curve (1), followed by a movement to D on curve (2). This route involves less calculations since movement to B does not change the member forces.

The frame of figure (6.3c) is derived from that of figure (6.3a) in a similar manner. One way of achieving this aim is to double the areas of all the members first, then remove members 1 and 4 and finally reduce the area of member 3 to half its original value.

When doubling the member areas  $\alpha$  is equal to 1 and equation (6.38) is used to calculate the new value of  $x_B$  as  $48.78 \times 10^{-4}$  inches. This equation is also used to calculate the new matrix  $\underline{\chi}$ , however, the matrix  $\underline{f}$  containing the member forces due to the dummy load matrix remains unaltered. To remove member 1 the removal factor  $r_1$  is calculated from equation (6.18) with a value of  $\alpha_1 = -1$ . The removal factor thus obtained has a different value under each set of loads applied to the structure. Using this set of values, the deflexions and forces throughout the resulting structure as well as the behaviour under the dummy load matrix may be predicted using equations (6.21) and (6.46). In this way it is found that the horizontal deflexion of

B increases to  $110.11 \times 10^{-4}$  inches. An exactly similar procedure is adopted to remove member 4 which further increases the horizontal deflexion of B to  $188.11 \times 10^{-4}$  inches.

The structure is now statically determinate and matrix  $\underline{f}$  obtained after the removal of member 4 is a unit matrix. Any further alteration of member areas must be with a value of  $\alpha$  less than -1 to avoid obtaining an infinite removal factor from equation (6.18). Such an alteration with  $\alpha = -1$  would lead to the formation of a mechanism.

To reduce the area of member 3 to half its original value  $\alpha_3$  is set to -0.75 and equations (6.18) and (6.21) give the required horizontal deflexion at B as  $318.86 \times 10^{-4}$  inches.

#### 6.4 General Applications of the Theorems

A significant use of the theorems is in the analysis of a number of large structures that are all derivatives of a more general parent structure. The latter can be first analysed on a large computer and its results can be kept on the backing store of the same computer, or more conveniently, of that of a smaller computer. These results may then be used repeatedly at different future dates to analyse one of the derived structures. A further use of the theorems is to satisfy the new structural design code (recommended following the Ronan point disaster). A requirement of this code is the safety of the structure, both from stress and deflexion points of view, when any one member of the structure is removed as a result of an accident or for repair. The theorems can be conveniently used to analyse all these different derived structures.

The shape of a structure, both its topology and geometry, is of prime importance from the engineering point of view. Hitherto this has been decided upon by intuition, where experience has been the main factor.

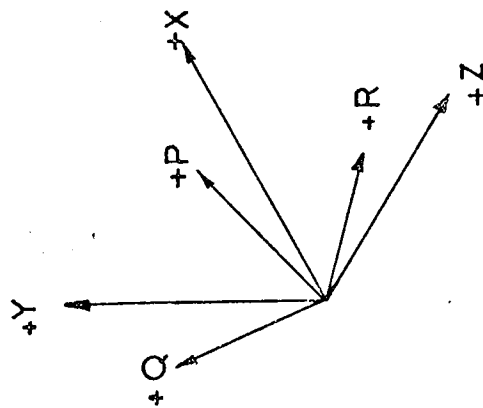
The theorems of structural variations may play a significant part in deciding the shape of a structure. There are two methods to achieve this aim. The first method is to arrange a network of possible nodes to cover the feasible space and then develop a 'ground structure' by joining every node to every other node. The actual shape of the structure is then obtained by removing those members and joints from the ground structure that do not have a significant function. The second, and more modest, method is to combine several candidate topologies to form the initial ground structure. The theorems of structural variations become useful with both these methods in selecting the final shape from the ground structure.

## 6.5 Conclusions

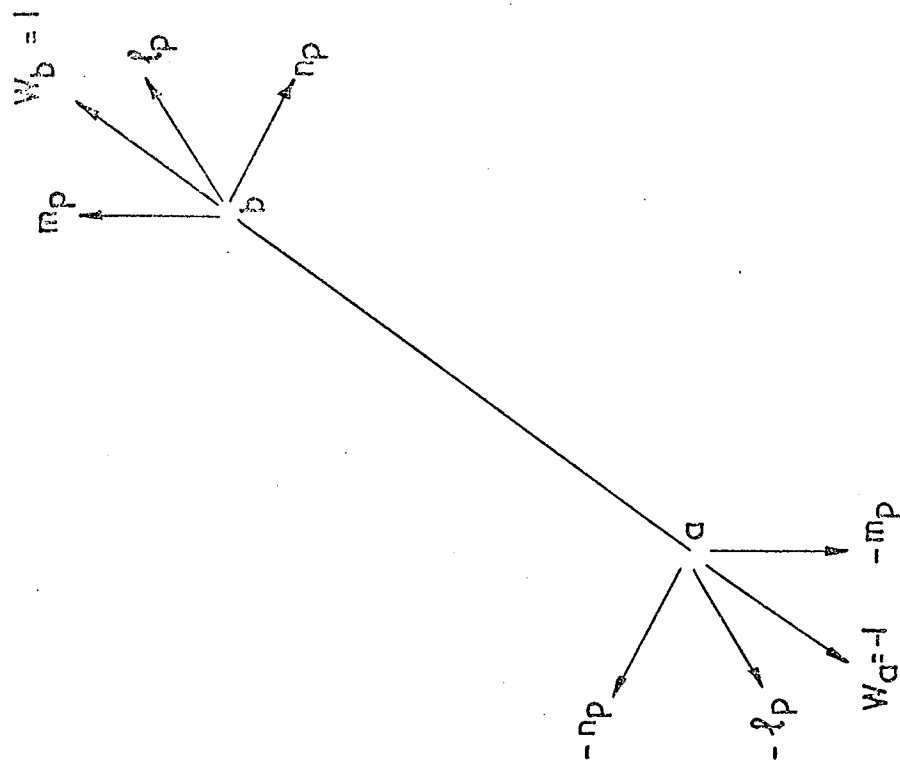
The theorems of structural variations, that were proved in this chapter, confirm that structures are closely related to each other. Thus the analysis of a general structure can be used to predict the behaviour of a variety of other derived structures. These theorems also suggest that the results of analysing a structure can be preserved for future use in the analysis of other derived structures.

The theorems enable the prediction of the behaviour of a structure after the total removal of some of its members while changing the areas of the other members independently. From a definition of the stiffness of a member,  $k = EA/l$  or  $k = EI/l$ , it is evident that the theorems are equally true when the moduli of elasticity  $E$  of the members are varying. Hence the theorems can also be applied in the analysis of one structure from the results of a different structure made out of a different material.

It is demonstrated how the theorems can be used in satisfying the newly recommended codes and for the design of structures where the geometry and the topology are fundamental design parameters. It is these latter aspects that are discussed in more detail in the following chapter.



a. sign conventions



b. components of unit loads

Figure 6.1. Sign conventions



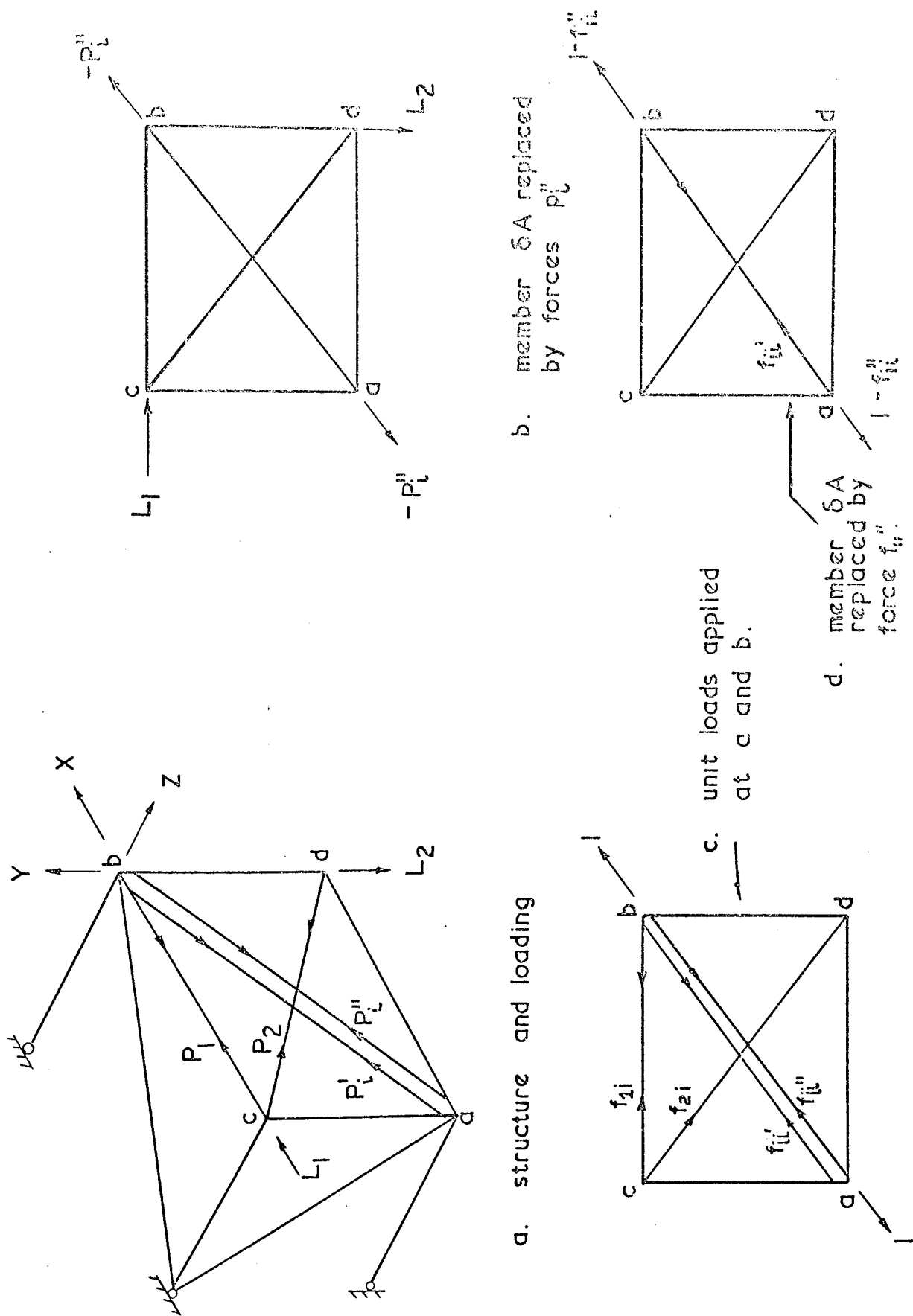


Figure 6.2 A general structure

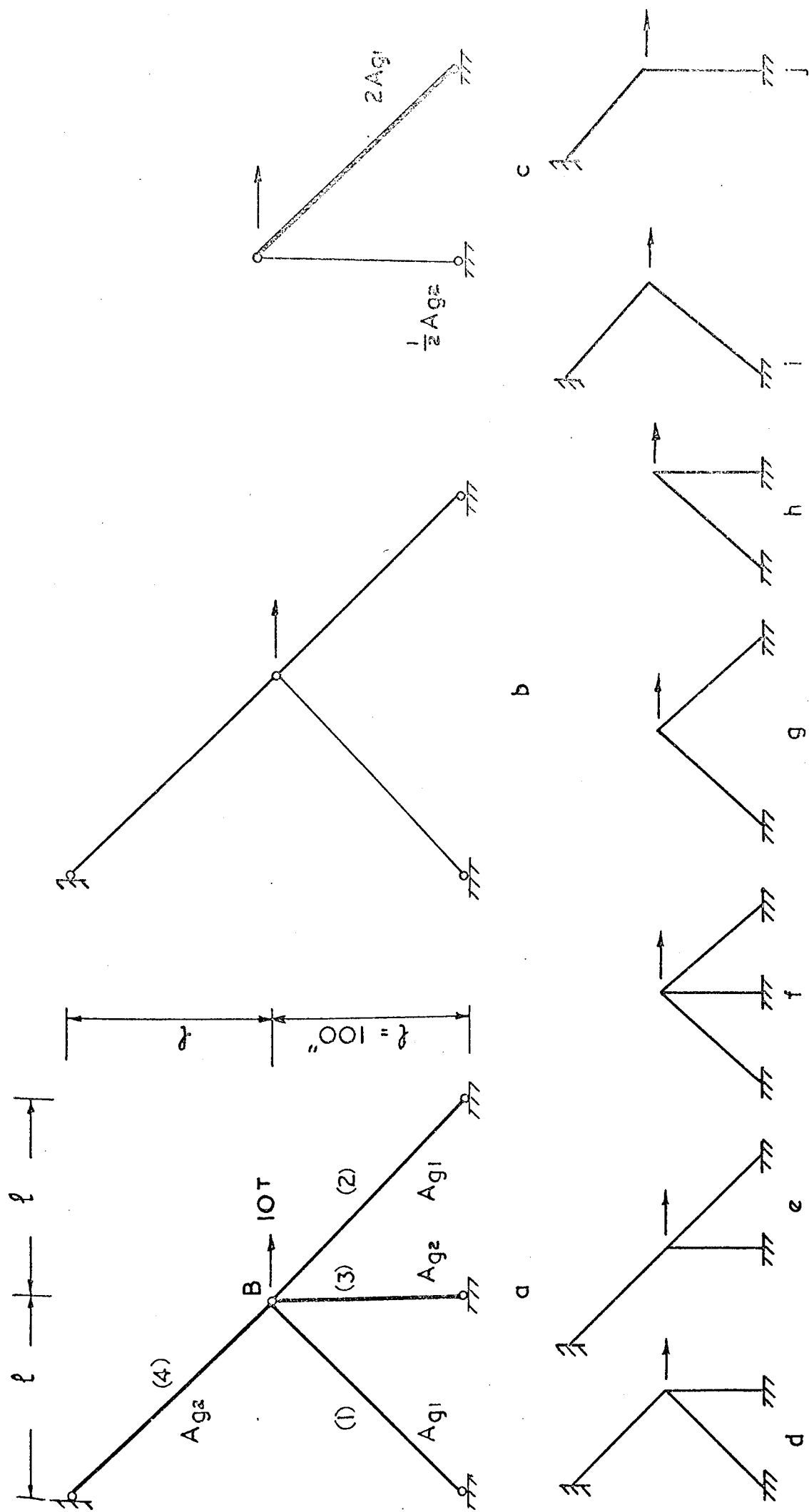


Figure 6.3. Derivatives of a hyperstatic structure

a. the structure and dimensions. b. to j. the derivatives

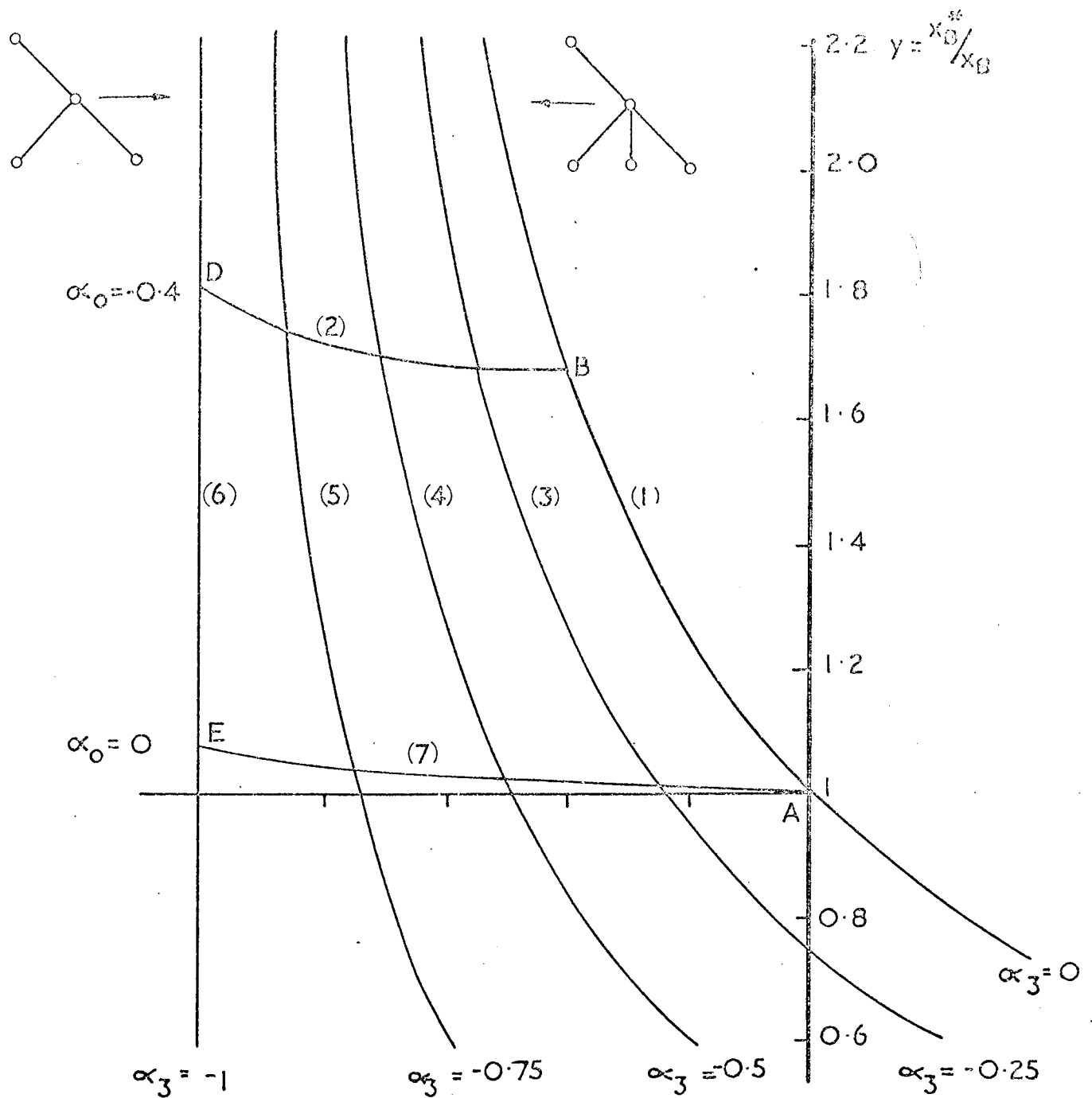


Figure 6.4. Variations of horizontal deflexion at joint B of the frame in figure 6.3a. with member areas.

- curve (1) variation of  $y$  with  $\alpha$  for the whole structure
- curve (2) variation of  $y^*$  with  $\alpha_3$
- curves (3) to (6) variation of  $y$  at different values of  $\alpha_3$
- curve (7) variation of  $y^*$  with  $\alpha_3$ , other areas remaining at initial values.

## CHAPTER 7

### SHAPE AS A DESIGN PARAMETER

#### 7.1 Introduction

There are a number of constraints that combine to determine the final design of a structure, including factors affecting shape. The more significant of these constraints are

(i) Functional constraints that affect the geometry of the structure, including the existence or the removal of elements or joints that detract from the efficacy of the structure.

(ii) Aesthetic or architectural constraints that affect significantly the appearance of the structure as well as the shape or size of its components.

(iii) Stress constraints which are imposed as safety requirements and

(iv) Deflexion constraints which may constitute functional, geometrical or safety requirements. These prevent the structural components from separating.

These constraints often interact. For instance in hyperstatic structures, compatibility constraints must also be satisfied when stress or deflexions are to be restricted.

There are a variety of methods to satisfy the above constraints and these result in the selection of structures of different shape. Although all of these are adequate only one can claim the merit of being optimal.

The design synthesis itself invariably consists of at least the following three steps

(i) Deciding upon the distribution of structural joints and the manner in which these are linked together, i.e. the topology of the structure.

(ii) The geometry associated with a given topology may be varied until the position of the joints and the inclination of the members are defined.

(iii) The selection of member properties to satisfy the design requirements.

This chapter is concerned with all three of these steps and attempts to select the various aspects so that an objective function, which relates to the structural volume, is minimized. Hitherto the appearance of a structure is often derived by intuition where experience is the main factor. For this reason theoretical procedures are proposed here to decide the geometry and the topology of structures.

## 7.2 Design for Optimum Shape

The method to be put forward here is to design pin-jointed structures for minimum weight, where topology as well as geometry are fundamental design variables. The functional requirements for the existence of any member or joint are the satisfaction, under several load vectors, of stress and deflexion constraints. In the proposed method it is possible to form the ground structure, from which the synthesis commences, by covering the design space with a network of nodes in the manner suggested by Dorn, Gomory and Greenberg (30). To reduce computation however, it is suggested that several candidate topologies are combined to form the initial ground structure. In this respect engineering experience is utilized with advantage. However during the design procedure, nodes or members are removed in a manner dictated by the design requirements, thus obtaining new shapes for the structure.

The proposed design method makes use of the theorems of structural variation given in detail in Chapter 6 of this thesis. It is convenient

however to restate them briefly at this stage.

These theorems suggest that it is possible, without prior analysis of a derived structure, to exactly forecast

(i) The forces in the members of a derived structure, when the area of a member (or members) of a parent structure is being varied; or totally removed. If  $p_i$  and  $p_j$  are the forces in members  $i$  and  $j$  due to the external loads and  $\pi_i$  and  $\pi_j$  are these forces when the area of member  $i$  is altered, without altering the external loads, then the first theorem of structural variation states that

$$\pi_i = p_i (1 + \alpha_i) / (1 + \alpha_i f_{ii}) \quad \dots 7.1$$

and

$$\pi_j = p_j + r_{\alpha i} f_{ji} \quad \dots 7.2$$

where  $\alpha_i$  is the ratio of the change in the area of member  $i$ ,  $\delta a_i$  to the original area  $a_i$ . The quantities  $f_{ii}$  and  $f_{ji}$  are the forces in members  $i$  and  $j$  when unit loads are applied at the ends of member  $i$ . Finally  $r_{\alpha i}$  is given by

$$r_{\alpha i} = -\alpha_i p_i / (1 + \alpha_i f_{ii}) \quad \dots 7.3$$

(ii) The deflexions throughout the structure may also be exactly predicted when all the members of the structure are varied proportionally. If  $\underline{X}$  is the vector of joint deflexions in the structure and  $\underline{X}^*$  are the resulting deflexions when every member is varied by a constant ratio  $\alpha$ , then the second theorem states that

$$\underline{X}^* = \frac{1}{1 + \alpha} \underline{X} \quad \dots 7.4$$

where  $1/(1 + \alpha)$  is a scalar quantity. Such a change of the member areas does not affect the member forces.

(iii) Finally the variation in the deflexions throughout the structure can also be predicted when one or more members are being varied independently. If  $x_j$  is the deflexion at a joint  $j$  due to external loads and  $\psi_j$  is this deflexion after changing member  $i$ , then the third theorem states that

$$\psi_j = x_j - \alpha_i p_i \chi_{ji} / (1 + \alpha_i f_{ii}) \quad \dots 7.5$$

In this hyperbolic relationship  $\chi_{ji}$  is the deflexion at  $j$  due to unit loads acting at the ends of member  $i$ . When member  $i$  is totally removed  $\alpha_i$  ( $= \delta a_i / a_i$ ) takes the value of  $-1$ .

The above exact formulae make it possible to forecast

- (i) The necessary changes of the volume of a resulting structure, to maintain design feasibility, while members are being altered or removed, and hence
- (ii) To decide upon a policy of removing members and/or joints, thus changing the shape of the structure.

#### 7.2.1 Assumptions

The proposed method is limited by the following assumptions:

- (i) That the load-deflexion behaviour of the structure is elastic and linear;
- (ii) That the global optimum of the mathematical non-linear programming problem lies within the boundaries of the feasible domain. Usually the nature of the problem, the derivation of the constraints and the sectional properties of the available members define the boundaries of the feasible domain. However, the global optimum can only be obtained if the initial as



well as the resulting mathematical programming problems have convex constraints and objective function. Using matrix displacement, it is possible to satisfy this condition.

(iii) It is also assumed that there is a continuous set of sections to select the sectional properties of the members. In practice, a continuous set of sections cannot be manufactured and the problem can be resolved by using integer programming techniques. The use of integer programming, however, grossly reduces the capability of any non-linear programming method. For this reason integer programming has been avoided. Previous workers have shown however that the approximation involved by this assumption is not always unreasonable.

### 7.3 The Tactics of Geometrical Synthesis

The fact that it is possible to evaluate the forces  $\pi$  and the displacements  $\psi$  can be utilized to calculate, in advance, the material saving achieved by altering the topology of a structure. This forecast is made by first predicting the weight of the new feasible structure with each member removed in turn. Members are then arranged in a benefit vector  $\underline{b}$  in the order in which their removal contributes to save weight. The member that reduces the weight most is removed first. Provided the structure remains feasible, further members listed in  $\underline{b}$  are also removed. During the construction of the benefit vector both stress and deflexion constraints are considered. Details for each case are now given.

#### 7.3.1 Dominating Stress Constraints

In the case where stress constraints dominate, the stress  $\sigma_j$  in member  $j$  due to the removal of member  $i$  is given by

$$\sigma_j = \pi_{ji}/a_j$$

... 7.6

The allowable stress in this member is  $\sigma_j^*$  and for fully stressed conditions its area may be changed by  $\delta a_j$  so that

$$\sigma_j^* = \pi_{ji} / (a_j + \delta a_j) \quad \dots 7.7$$

Equations (7.6) and (7.7) give

$$\delta a_j = a_j \sigma_j / \sigma_j^* - a_j$$

In which

$$1 - \text{if } \pi_{ji} > 0; \quad \sigma_j^* = \sigma_t^* \quad \dots 7.8$$

and

$$2 - \text{if } \pi_{ji} < 0; \quad \sigma_j^* = \sigma_c^*$$

where  $\sigma_t^*$  and  $\sigma_c^*$  are the allowable stresses in tension and compression respectively.

Equations (7.8) represent two straight lines expressing the fully stressed condition in member  $j$ . When  $\sigma_j = 0$  then  $\delta a_j = a_j$  indicating that this member can be removed altogether. On the other hand, for  $-\sigma_c^* < \sigma_j < \sigma_t^*$ ,  $\delta a_j$  is negative and the area of the member can be reduced. Otherwise, to achieve fully stressed condition, the area has to be increased.

From equation (7.2) the stress in  $j$  is

$$\sigma_j = (p_j + r_{ai} f_{ji}) / a_j \quad \dots 7.9$$

Therefore, equation (7.8) gives the change in area necessary to render  $j$  fully stressed as

$$\delta a_j = a_j (p_j + r_{ai} f_{ji}) / a_j \sigma_j^* - a_j \quad \dots 7.10$$

The corresponding change in the volume of the structure is

$$l_j \delta a_j = l_j a_j \left( \frac{p_j + r_{ai} f_{ji}}{a_j \sigma_j^*} - 1 \right)$$

where  $l_j$  is the length of the member.

When all the  $n$  members are altered, the total increase  $\delta v_i$  in the volume of the structure due to the removal of member  $i$  is

$$\delta v_i = \sum_{j=1}^{j=n} \{ l_j a_j [ -1 + (p_j + r_{ai} f_{ji}) / \sigma_j^* a_j ] \} \quad \dots 7.11$$

provided that  $i \neq j$  as  $i$  is being removed. The removal of  $i$  reduces the volume by  $l_i a_i$  and the net saving in volume is  $l_i a_i - \delta v_i$ . This is the difference between the old volume  $v$  and the new volume  $v_i$ . Thus

$$v_i = v + \delta v_i - l_i a_i \quad \dots 7.12$$

where

$$v = \sum_{k=1}^n l_k a_k$$

and the new volume is obtained from equations (7.11) and (7.12) to be

$$v_i = \sum_{\substack{j=1 \\ i \neq j}}^n l_j (p_j + r_{ai} f_{ji}) / \sigma_j^* a_j, \quad \dots 7.13$$

The quantity  $\pi_j = p_j + r_{ai} f_{ji}$  is an element of a vector  $\underline{\pi}$ . It is convenient to normalise the behaviour of vector  $\underline{\pi}$ , as in Chapter 4, so

that an inspection of the resulting normalised vector  $\underline{G}$  may indicate the constraint that violates the design requirements. An element  $g_{ji}$  of  $\underline{G}$  corresponding to  $\pi_{ji}$  is of the form

$$g_{ji} = d(1 - \pi_{ji}/a_j \sigma_j^*)$$

In which

$$\sigma_j^* = \sigma_t^* \text{ for } \pi_{ji} > 0 ; \quad \dots 7.14$$

and

$$\sigma_j^* = -\sigma_c^* \text{ for } \pi_{ji} < 0$$

where  $d$  is a conveniently selected constant. It is possible for the elements of  $\underline{G}_i$ , corresponding to the removal of member  $i$ , to be all positive. In that case member  $i$  can be removed without the necessity of increasing the weight of the new structure.

In real structures several members are often grouped together to have the same sectional properties. Assuming that there are  $n_g$  groups in a structure, one of which  $k$  is the group that member  $j$  belongs to, and denoting  $g_{ki}$  to the value of the most critical normalised stress constraint associated with area group  $k$ , equations (7.13) and (7.14) can be combined to calculate the new volume of the structure as

$$v_i = \sum_{j=1}^n l_j a_k (1 - g_{ki}/d) \quad \dots 7.15$$

provided that the summation does not cover member  $i$ .

It is significant to point out that when  $r_i = \infty$ ,  $\pi_{ji}$  becomes infinite, and hence drives  $g_{ji}$  to  $-\infty$  and  $v_i$  to  $+\infty$ . This indicates that the

removal of member  $i$  renders the structure (or part of it) into a mechanism. Care should be taken, therefore, to place  $i$  as the last element of the benefit vector so that this member may not be removed. Similarly the removal of  $i$  that causes large forces  $\pi_{ji}$  indicates that it is not advantageous to remove such a member.

In this manner it is possible to forecast the order in which members should be removed. This is accomplished by scanning the members so that they may be placed in the benefit vector in the order of their decreasing benefit.

Equation (7.15) is such that one member in each group is assumed fully stressed. This does not however produce a fully stressed design since  $v_i$  is used only to forecast the order of member removal. The outcome of this forecast is influenced by many other factors as will be shown later.

### 7.3.2 Dominating Deflexion Constraints

In the case where deflexion constraints dominate, equation (7.5) gives the deflexion  $\psi_j$  at node  $j$  after the removal of member  $i$ . In this case  $\alpha_i = -1$  and equation (7.5) reduces to

$$\psi_j = x_j + p_i \chi_{ji} / (1 - f_{ii}) \quad \dots 7.16$$

On the other hand, for an all round proportional increase of the members by a constant factor  $\alpha$ , equation (7.4) gives the deflexion at node  $j$  as

$$x_j^* = x_j / (1 + \alpha) \quad \dots 7.17$$

After such an all round increase  $\chi_{ji}^*$ , which is the deflexion at  $j$  due to a unit load at the ends of member  $i$ , is also related to  $\chi_{ji}$  by equation (7.4)

which may be rewritten as

$$\chi_{ji}^* = \chi_{ji}/(1 + \alpha) \quad \dots 7.18$$

Consider now the case where the all round increase of the structural members is followed by the removal of member i. Equation (7.16) can be used to calculate the final deflexion  $\psi_j^*$  at j. This takes the form

$$\psi_j^* = x_j^* + p_i \chi_{ji}^*/(1 - f_{ii}) \quad \dots 7.19$$

Member i can only be removed provided that the all round increase in the members is sufficient to prevent  $\psi^*$  from exceeding the allowable deflexion  $\Delta_j$  at j. This condition is achieved by substituting  $\Delta_j$  for  $\psi_j^*$  in equation (7.19). This, together with equations (7.17) and (7.18) gives the unknown factor  $\alpha$  as

$$\alpha = x_j/\Delta_j + p_i \chi_{ji}/\Delta_j(1 - f_{ii})^{-1}$$

which, by using equation (7.16) becomes

$$\alpha_{ji} = (\psi_j - \Delta_j)/\Delta_j \quad \dots 7.20$$

The suffixes j and i are allocated to  $\alpha$  to indicate that the all round factor  $\alpha$  is calculated for the condition in which member i is being removed and the deflexion at j is becoming critical.

A similar expression can be obtained for each deflexion constraint and each member. The largest  $\alpha_{jk}$  for any member k amongst these is denoted  $\alpha_k^*$ . This set of  $\alpha_k^*$  gives the value by which all the areas of the resulting structure should be increased so that any member k can be removed without violating any of the deflexion constraints.

At this stage it is possible to predict the new volume of the resulting structure. Consider the case when, for instance, member  $k$  has to be removed. The predicted volume  $v_k$  of the new structure is given by the sum of the original volume  $\sum a_i$  and the increase in this volume  $\sum a_i a_k$ , less the volume saved for removing member  $k$ . Thus

$$v_k = -l_k a_k (1 + a_k^*) + \sum_{i=1}^n l_i a_i (1 + a_k^*) \quad \dots 7.21$$

Using this equation, the new volume of the structure due to the removal of each member can be forecast.

Consideration of members for removal is embarked upon only if the structure is feasible and will remain so. However, in the early stages of the design process some members may act as a burden on the structure. These have negative overall removal factors. Their removal, therefore, saves not only their own weight but also some of the weight of the remaining structure. Members of this type are placed at the top of the benefit vector for early removal.

### 7.3.3 The Preparation of the Benefit Vector

So far two methods have been devised for the preparation of the benefit vector, depending upon whether stress or deflexion constraints are dominant. These two methods are combined to prepare a single overall benefit vector using the "Mini-Max" principle. For the removal of a given member  $m$ , the larger of the two values of  $v_m$  obtained by equations (7.15) and (7.21) decides the position of member  $m$  in vector  $\underline{b}$ . This ensures that weight is not saved at the expense of feasibility.

As an example, a structure with seven members and an original volume of 30 units is considered for the preparation of the benefit vector. It is assumed that table (7.1) gives the new volume of the resulting structure, due to the removal of each member. These figures are obtainable using equations (7.15) and (7.21). If only stresses were considered, then the second column of this table suggests that member 6 with a maximum volumetric benefit of 10 units would appear as the first element of the benefit vector. Similarly the last column of the table suggests that, when considering deflexion only, member 1 gives the maximum benefit. The table also indicates that the removal of members such as 6 or 7 saves material without violating stresses but actually causes the violation of deflexion constraints. Indeed the last column suggests that these members can only be removed if the volume of the resulting structure is increased to 41 or 31 units respectively.

In table (7.1) the larger value in each row is underlined to indicate that it decides the position of that member in the benefit vector. An inspection of these figures enables the arrangement of these members so that the first member in the list may be removed with the largest reduction in the volume of the structure and without loss of any feasibility. For this reason member 5 forms the first element of vector  $\underline{b}$ . Removal of this member represents a possible saving of 4 units in volume. Similarly the other members are graded in vector  $\underline{b}$ , which is shown, in its final form in table (7.2).

The benefit vector only gives the order in which members may be removed from the structure provided that this results in a feasible and lighter structure. However the removal of several members may alter the geometry of the initial structure significantly, and possibly render the forecast erroneous. For this reason, in the actual computer programme, prepared for the proposed method, care was taken to terminate the process of



member removal as soon as this entailed increases in the overall weight of the structure. This prevented the removal of essential members. Care was also taken that members of equal benefit had the same order in vector  $\underline{b}$ , so that they were removed simultaneously. This is particularly necessary in symmetrical structures where the removal of one member at a time may distort symmetry.

#### 7.4 The Mathematical Programming

Matrix displacement method was used to formulate the mathematical programming problem. At a given instant, the problem is of the form

$$\text{Minimize } Z = \sum_{i=1}^n l_i a_i \quad \dots 7.22$$

subject to the deflexion constraints

$$(\underline{A}' \underline{k} \underline{A})^{-1} \underline{L} \leq \underline{\Delta} \quad \dots 7.23$$

and stress constraints

$$\underline{\sigma}_c^* \leq \underline{a}^{-1} \underline{k} \underline{A} (\underline{A}' \underline{k} \underline{A})^{-1} \underline{L} \leq \underline{\sigma}_t^* \quad \dots 7.24$$

and further

$$a_i \geq 0$$

with  $i = 1, 1, n$ ,

where  $Z$  is the objective function, matrix  $\underline{A}$  is the displacement transformation matrix whose transpose is  $\underline{A}'$ . The member stiffnesses are given by  $\underline{k}$  and for a pin-jointed structure matrix  $\underline{a}$  is diagonal having the areas of the

members as its diagonal elements. The load matrix is  $\underline{L}$  and  $(\underline{A}' \underline{k} \underline{A})^{-1} \underline{L}$  are the actual joint displacements that are limited by their permissible values given by vector  $\underline{\Delta}$ . Usually not all the displacements of a structure are constrained and therefore, when deriving a feasible solution, only the active deflexion constraints of inequalities (7.23) are safeguarded. The vectors  $\frac{\sigma}{c}^*$  and  $\frac{\sigma}{t}^*$  contain the permissible compressive and tensile stresses.

The design problem gives rise to a set of non-linear constraints with a linear objective function. However it is now shown that the mathematical problem is in fact of a new type fundamentally different from those covered by available algorithms.

Once a member or joint in a structure is removed, the initial mathematical programming problem itself changes basically. This is because as members or groups of members are removed the number of variables as well as the number of stress constraints are reduced. Furthermore, unless the existence of some unloaded joints is an architectural necessity, these joints may also be removed, hence reducing the number of deflexion constraints. The composition of each remaining constraint also changes during this process. These factors contribute to modifying the dimensions of the mathematical problem, the objective function and the boundary of the feasible region.

The effect of the removal of a member on the non-linear programming problem is shown diagrammatically in figure (7.1). Variables  $x_1$  and  $x_2$  represent two area groups, each one consisting of several members. In figure (7.1a), point a represents a boundary solution before a member is removed. The boundary itself is represented by a dotted curve (1). At this stage, line (2) represents the constant objective function  $Z_1$ . The removal of a member from group  $x_1$  alters the boundary of the feasible area from curve (1) to curve (3). The gradient of the objective function also changes due to a reduction in the effect of  $x_1$ . The value of the objective function

$Z_2$  is now represented by line (4) which also passes through point a. In this figure line (5) represents the new objective function, corresponding in value to the original  $Z_1$ .

It is noticed that point a is now within the new feasible area, indicating that feasibility has improved. As a result a further member may be removed, which may give rise to an infeasible solution as shown in figure (7.1b). Here point a remains fixed at its original position, while the boundary of the feasible area is once again altered and is now represented by curve (6). Lines (7), (8) and (9) represent the new objective functions corresponding to constants  $Z_3, Z_2$  and  $Z_1$  respectively, with  $Z_3$  as the latest value.

A new boundary solution can be obtained at the intersection of the line of steepest ascent ab with the boundary of the feasible region. This is best achieved by first restoring the original value  $Z_2$  to the new objective function. In the case of dominating local factors or as the optimal solution is approached, the possibility may, increasingly, arise where the feasible region is considerably displaced with respect to the original point a. In these circumstances the steepest ascent does not yield a feasible solution and it is necessary to adopt a new direction vector. Such a case is also shown in figure (7.1b), where the original point a is now represented by  $a_1$ . A movement from  $a_1$  to  $b_1$  only yields another infeasible solution. For this reason it is necessary to select a new direction vector that moves towards a feasible point such as  $b_2$ .

#### 7.4.1 Determination of a Feasible Solution

It was shown above that the mathematical programming problem under consideration is continuously changing. Furthermore it was shown that once a solution becomes infeasible a direction vector orthogonal to the constant

objective function may not result in a feasible solution. When using the non-linear programming method, described in Chapter 4 of this thesis, it is clear that the direction vector of search has to be continuously changed, in a dynamic manner, to cater for these circumstances.

Consider a general  $n$  dimensional problem in which the new solution vector  $\underline{x}_b$  is obtained from an older one  $\underline{x}_a$  by

$$\underline{x}_b = \underline{x}_a - \lambda \underline{\delta x} \quad \dots 7.25$$

where  $\underline{\delta x}$  is the direction vector of search while the step length  $\lambda$  defines the magnitude of this vector. To evaluate the elements of this new direction vector it is necessary first to calculate the slopes of the new constraints. These correspond to point  $a_1$  in figure (7.1b). In this manner the slope matrix  $\underline{S}$  is constructed in which each element  $s_{ij}$  is the partial derivative of constraint  $j$  with respect to a variable  $i$ . The elements of  $\underline{S}$  are then once again weighted so that the sensitivity of the inactive constraints is damped down. However, this process is now performed in a manner that maintains the elements of the column for the most critical, negative normalised constraint, as constant. An element of the resulting modified slope matrix  $\underline{S}^*$  is given by

$$s_{ij}^* = s_{ij} / [1 + \beta(g_j - g_{\min})] \quad \dots 7.26$$

where  $g_{\min}$  is the value of the most negative normalised constraint. The factor  $\beta$  is a convenient constant. Increasing the value of  $\beta$  rotates the direction vector towards the normal of the most critical constraint.

Equation (7.26) also demonstrates that when  $g_{\min} = g_j$ , then  $s_{ij}^* = s_{ij}$ .

On the other hand for  $g_j \gg g_{\min}$ ,  $s_{ij}^* \ll s_{ij}$  and the corresponding constraint  $j$  becomes ineffective.

An element  $\delta x_i$  of the direction vector  $\underline{\delta x}$  may be obtained by the sum of the elements of the corresponding row of  $\underline{S}^*$ , i.e.

$$\delta x_i = - \sum_{j=1}^m s_{ij}^* \quad \dots 7.27$$

where  $m$  is the total number of constraints currently in the problem. The larger elements in  $\underline{\delta x}$  in equation (7.27) correspond to the more beneficial variable in the programming problem. To improve these variables most effectively at the expense of the inferior variables, the deviation of the elements of  $\underline{\delta x}$  from the average is magnified. A magnification power  $D$  is therefore applied to each element  $i$  of  $\underline{\delta x}$  to convert it to  $\delta^* x_i$ , thus

$$\delta^* x_i = - (\delta x_i / e)^D \quad \dots 7.28$$

where  $e$  is the average value of the  $n$  elements of  $\delta x_i$ , i.e.

$$e = \sum_{i=1}^n \delta x_i / n \quad \dots 7.29$$

An inspection of equation (7.28) reveals that increasing  $D$  rotates the direction vector towards a line parallel to the axis of the most beneficial variable. In figure (7.1b) for instance, if  $x_1$  is a more beneficial variable than  $x_2$ , then large values of  $D$  tend to rotate  $a_1 b_2$  to become parallel to  $x_1$  axis while  $\beta$  directs it to become normal to the feasible boundary given by curve (6). To illustrate these new aspects of the mathematical programming problem consider the following example, which consists of a simple, but non-linear problem of two variables  $x_1$  and  $x_2$  subject to the constraints

$$60/x_1^2 + 4/x_2^3 \leq 6$$

$$11/x_1 + 13/x_2^2 \leq 7$$

$$1/x_1 + 14/x_2^2 \leq 8$$

required to minimize

$$z = 3x_1 + 5x_2$$

Before removing a constituent element associated with a variable such as  $x_1$ , let a feasible boundary solution be given by  $x_1 = 2.25$ ,  $x_2 = 2.65$  and  $z = 25$ . After the removal of the constituent element of  $x_1$ , suppose that  $z$  changes to 20, with  $x_1$  and  $x_2$  remaining at their original values but now infeasible. This state of affairs, as well as the boundaries of each of the modified constraints are shown graphically in figure (7.2), where the feasible space is shown shaded. It is noticed that the current solution at point a with  $\underline{x}_a = \{2.25 \quad 2.65\}$  is infeasible violating the first constraint.

An ascent step is obtained with  $\lambda = 2.5$  and  $\delta x = \{-1/3 \quad -1/5\}$  so that the original value of 25 is restored to the objective function. Equation (7.25) now gives the new solution vector  $\underline{x}_b = \{3.08 \quad 3.15\}$ . This corresponds to point b on the graph. Line ab is influenced by both the coefficients  $c_1$  and  $c_2$ , in the objective function, and hence is not perpendicular to the line of constant  $z$ . Point b is less infeasible compared to a, nonetheless a feasible direction vector has yet to be calculated. At point a, a partial derivative of the first constraint with respect to  $x_1$  and with values of  $x_1 = 2.25$  and  $x_2 = 2.65$ , is equal to 16.46. The other elements of the slope matrix are calculated in a similar manner. These are

$$\underline{S} = \begin{bmatrix} s_{11} & s_{12} & s_{13} \\ s_{21} & s_{22} & s_{23} \end{bmatrix} = \begin{bmatrix} 16.460 & 2.970 & 0.013 \\ 0.380 & 1.890 & 1.780 \end{bmatrix}$$

with  $\beta = 0$ , equation (7.26) gives  $\underline{S}^* = \underline{S}$  and with  $D = 1$ , equations (7.28) and (7.29) give

$$\underline{\delta x}^* = \{-1.6569 \quad -0.3430\}$$

with  $z = z_2 - z_1 = 5$ , the value of  $\lambda (= \delta z / \delta x_i c_i)$  is 0.748 and a new solution represented by point c in the figure, can be calculated from equation (7.25), with point c replacing b, hence

$$\underline{x}_c = \{3.49 \quad 2.90\}$$

Point c is noticed in figure (7.2) to be feasible.

A better direction of search which improves the optimality of the problem further can be obtained by changing the values of  $\beta$  and  $D$ . With  $\beta = 2$ , for instance

$$\underline{S}^* = \begin{bmatrix} 16.4600 & 0.1084 & 0.0003 \\ 0.3800 & 0.0690 & 0.0494 \end{bmatrix}$$

Comparing  $\underline{S}$  and  $\underline{S}^*$ , it is noticed that, in  $\underline{S}^*$ , the first column, corresponding to the violated constraint (1) is unaltered. The other two columns corresponding to the non-critical constraints have been reduced considerably. In this manner the influence of the non-critical constraints on the new direction vector is reduced. With  $D = 3$ , equations (7.28) and (7.29) now

give

$$\underline{\delta x}^* = \{ -7.3194 \quad -0.0001 \}$$

Recalculating  $\lambda$ , equation (7.25) gives a new solution. This is represented by point d in the figure and for which

$$\underline{x}_d = \{ 3.92 \quad 2.65 \}$$

Points b, c and d are all on the original line of the constant objective function  $z = 25$ . It is noticed that point e which is the intersection of line ad with the boundary of the feasible region yields an improved solution compared to point f obtained with ac.

## 7.5 The Design Procedure

The design procedure starts by developing the ground structure, either from a network of nodes or, more conveniently, from the combination of a number of candidate structures. The members are then grouped together so that those in a group may all have the same cross-section. The design constraints are now formulated. These include aesthetic constraints which are satisfied either by removing certain members or joints, or by permanently including other members or joints. To do this it may be necessary to impose certain artificial deflexion constraints at some nodes so that these are never removed from the final structure. The design constraints may also include upper and lower bounds on sectional properties due to practical considerations which may prevent the selection of certain unacceptable member properties.

Once a ground structure is developed the design problem is formulated automatically by the computer, and the sectional properties of the members are set at their lower bound values. The search process of Chapter 4



is initiated by the computer, by embarking upon the stage 1 ascent mode. This increases the volume of all the groups equally until the first feasible boundary solution is obtained. From this a new and improved boundary solution is derived using stages 2 and 3 of the non-linear programming procedure before the removal of any members takes place.

Before leaving subsequent boundary solutions however the policy for removing members is tested. This consists of first arranging the members in the appropriate order in the benefit vector. The less advantageous members are then removed provided that feasibility is not lost, or that once an infeasible structure is obtained, additional volume is not required to restore feasibility. In this way several boundary solutions are arrived at by repeatedly using stages 2 and 3 of the non-linear programming procedure, until finally the optimum design is located. At each boundary solution it is possible for the topology of the structure to change, which may also involve the removal of superfluous joints. These are joints that contribute neither to the maintenance of equilibrium nor to the rigidity of the structure.

As the optimum design is approached, there arises the possibility that once a member is removed the structure becomes indefinitely infeasible. This is when a direction vector that restores feasibility without increasing the structural volume is unobtainable. In that case the member in question is restored and the constant weight mode, stage 2, is commenced. The final design is attained when such a move is impossible.

The following possibilities may arise during the design procedure:

- (i) The derived structure may turn out to be statically determinate. In that case no further members can be removed.
- (ii) More frequently, in cases where deflexion constraints are

governing, the derived local optimum structure is hyperstatic. Here the search continues, even though the resulting structures have increased weight. This search is terminated when case (i) is arrived at. In this manner all the possible derived structures become available. Amongst these there sometimes exists a structure which is not the lightest but is more economical from an overall construction point of view. It is this latter structure which interests engineers most.

The proposed procedure does not claim that the design obtained is globally optimum. The removal of a vital member erroneously may exclude this and divert the search to one of the remaining local optima. It is to safeguard against this possibility that the computer programme devised for the proposed method includes facilities:

- (a) Not to remove members at the early stages since the areas of the members may bear false relationships to each other. This may lead to the erroneous removal of important members which can never be reintroduced into the structure. Instead attention is directed to reduce weight without altering the shape of the structure, thus improving the relationships between the areas and making the forecast of the benefit vector more realistic.
- (b) At each boundary solution member removal is terminated as soon as feasibility can only be maintained at the expense of additional volume.

In the following chapter the proposed method is used to carry out a series of design studies.

Table 7.1 : The New Volume of a Structure with Seven Members

Member Number	New Volume By:	
	Equation (15)	Equation (21)
1	<u>29</u>	25
2	26	<u>30</u>
3	<u>40</u>	39
4	27	<u>28</u>
5	21	<u>26</u>
6	20	<u>41</u>
7	24	<u>31</u>

Table 7.2 : The Benefit Vector

Member Order	5	4	1	2	7	3	6
Possible New Volume	26	28	29	30	31	40	41

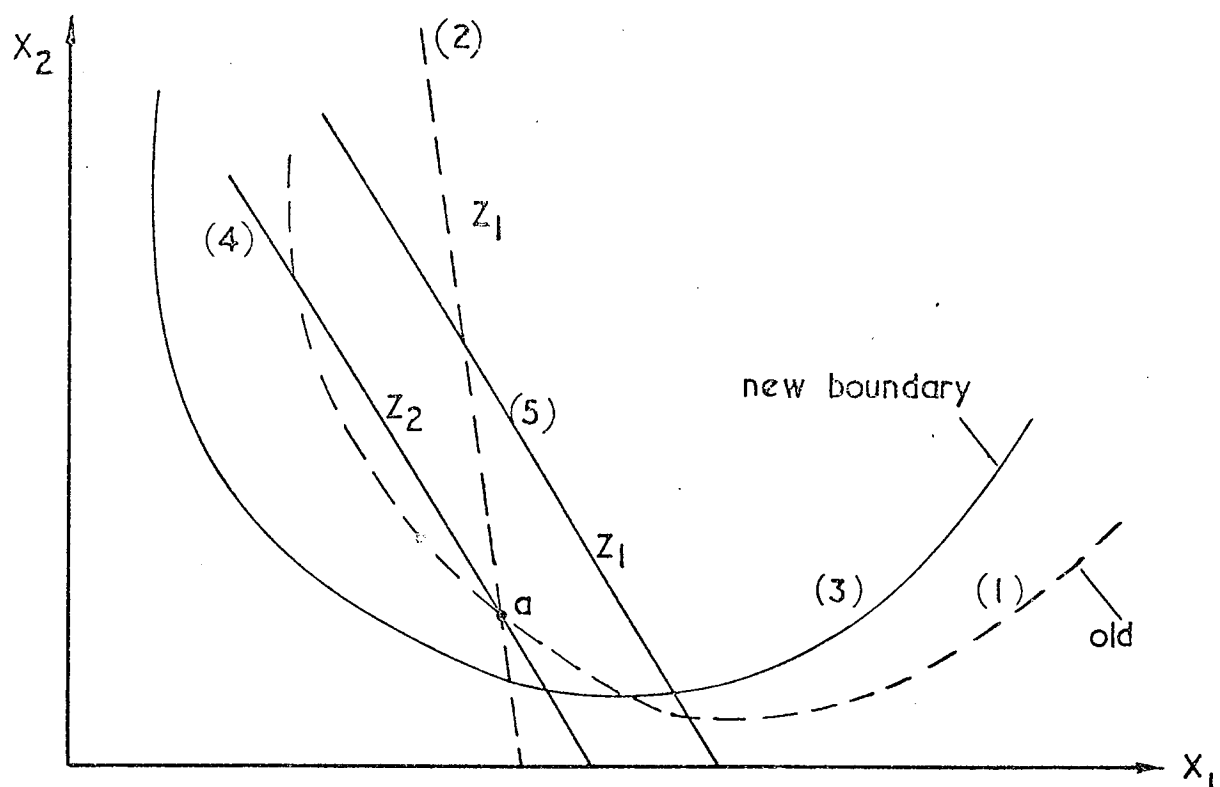


Figure 7.1 a.

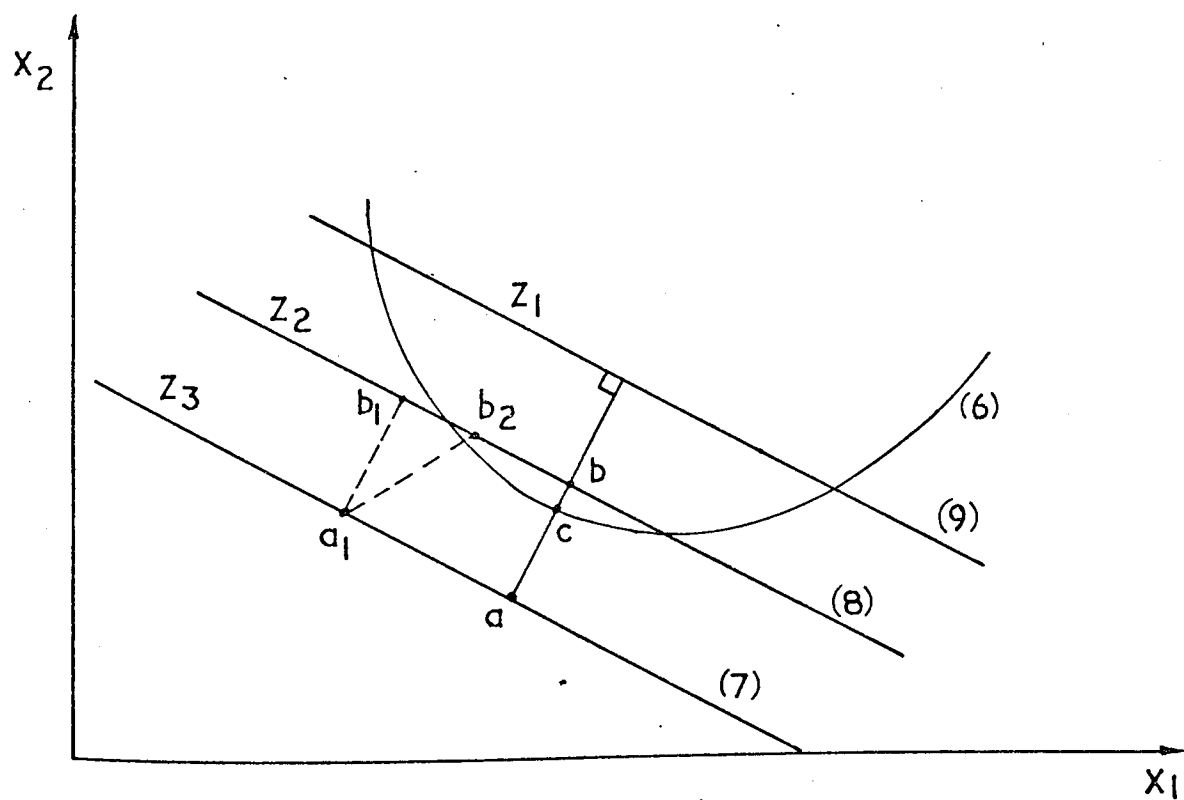


Figure 7.1 b.

Figure 7.1. Variation of the mathematical problem.

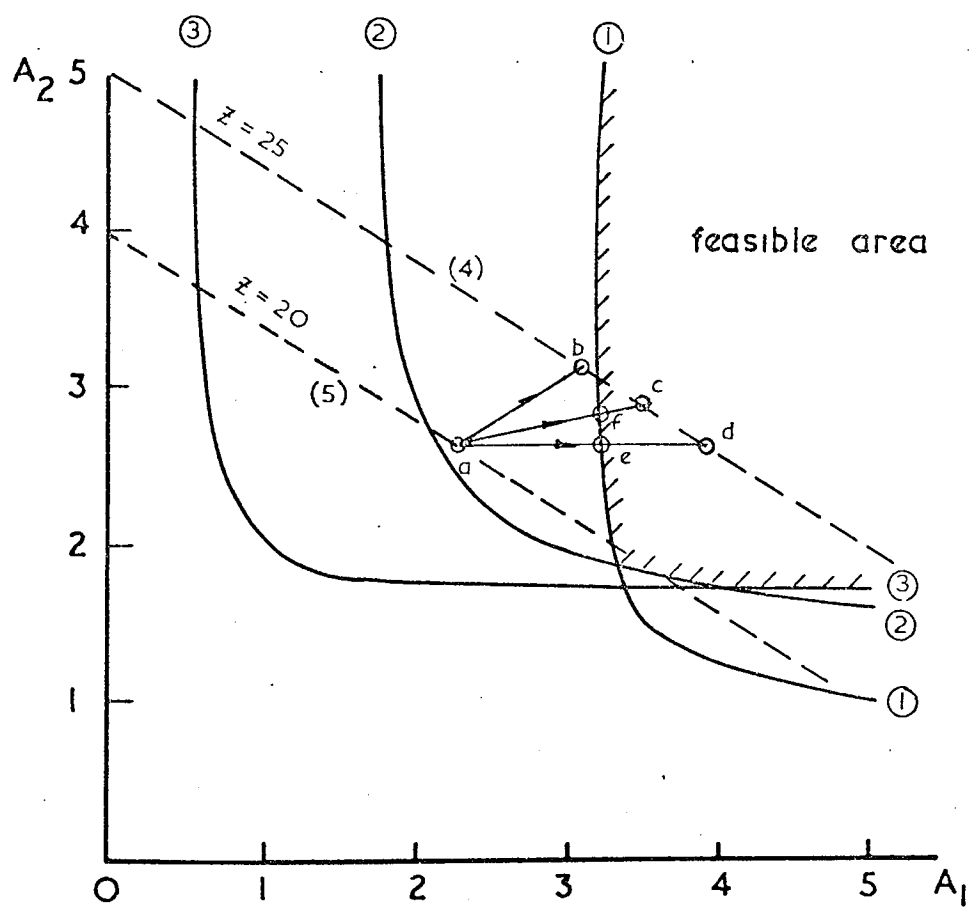


Figure 7.2. Possible directions of search from infeasible point  $a$ .

## CHAPTER 8

### DESIGN STUDIES

#### 8.1 Introduction

In this section a number of design examples are given, not only to demonstrate the efficacy of the proposed method, but also to carry out an investigation into the various factors that influence the shape of the final design. These factors include the nature and number of deflexion or stress constraints, the type of loading and the number of loading cases, including the self weight of the structure as well as the effect of the shape of the initial ground structure upon the final shape.

#### 8.2 Hand Design

In order to demonstrate numerically and graphically some of the steps involved in the proposed method the plane frame of figure (8.1), previously dealt with in Chapter 6, is again considered. This is now taken as a ground structure from which it is required to obtain a structure having minimum volume and optimum topology. In figure (8.1), point A is subject to a horizontal load  $H$  of 10 tons (99.64 kN) and the horizontal deflexion of this node is not to exceed 0.1 inches (2.54 mm). The members of the structure are initially grouped together into two area groups so that the progress of the design may be represented as a two-dimensional graph. In this manner members BC and BE are grouped with common area  $a_1$  and members BA and AD with common area  $a_2$ .

Using the matrix displacement method the problem is formulated as

Minimize:

$$z = 2\sqrt{2} a_1 + (1 + \sqrt{2}) a_2$$

subject to the deflection constraint

$$2\sqrt{2} [ 2a_1 + (1 + 2\sqrt{2})a_2 ] L^3 / \{ (2a_1 + a_2) [ 2a_1 + (1 + 2\sqrt{2})a_2 ] + a_2^2 \}$$

$$\leq 0.01E$$

$$\text{and } 0 \leq a_1, a_2 \leq 30$$

where  $L$  is 100 inches (2540 mm) and  $E$  is the modulus of elasticity, which is 13400 ton/in<sup>2</sup> (207 kN/mm<sup>2</sup>).

A first boundary solution is obtained using stage 1 of the non-linear optimization procedure as  $a_1 = 7.313$  square inches (4718 mm<sup>2</sup>) and  $a_2 = 8.567$  square inches (5527 mm<sup>2</sup>). In figure (8.2) the entire process up to the final optimum design is given graphically. Curve 1 on this figure is the boundary of the feasible region before any member is removed, and the current design is indicated by point A on this boundary.

In table (8.1) the results of analysing this structure under the external load are given in the third column. The last four columns give the horizontal and vertical deflexion at point A and the member forces due to unit equal and opposite forces acting at the end of each member in turn. These are the results of matrix multiplications of the type given by equations (6.10) and (6.11). The removal factor  $r$  of each member, obtained from equation (7.3), is also given in the last row of the table.

Using these factors the deflexions and the forces, due to the removal of each member, were calculated. These are tabulated in table (8.2). As it is the deflexion of node A that dominates the design, the factor which gives the amount by which all the areas have to be increased before any member can be removed was calculated using equation (7.20). The resulting values are given as the last row in the table. From an inspection of these values it is evident that member AD is the least efficient and

should be removed first. From equation (7.21), the new volume of the feasible structure will then be 3509.3 cubic inches. This is to be compared with 4140.0 cubic inches, the current volume of the structure before the removal of any member.

Having removed member AD the non-linear programming problem is altered and may now be restated as

Minimize

$$z = 2\sqrt{2} a_1 + \sqrt{2} a_2$$

subject to the deflexion constraint

$$2\sqrt{2} (2a_1 + a_2)EH / \{4a_1(1 + a_2)\} \leq 0.01E$$

and  $0 \leq a_1, a_2 \leq 30$

The new boundary of the feasible region is shown in figure (8.2) as curve 2 and the current design as point B. The new feasible boundary passes through B.

The design was then continued by obtaining another boundary solution vector. This caused a movement which maintained constant volume to C and then, reducing the volume, to D on the boundary curve 2. At this point  $a_1$  is 3.91 square inches and  $a_2 = 4.00$  square inches.

The structure is now once again inspected for possible member removal and it is found that member AB reaches the top of the benefit vector with  $\alpha = 0.1726$ . It is interesting to note that at this stage member AC has an infinite value for  $\alpha$ . This indicates that the removal of this member leads to the formation of a mechanism.

Due to the removal of member AB the volume of the feasible structure



is reduced from 3086 cubic inches to 2935 cubic inches. At this stage the structure is statically determinate and is therefore in its final shape with two members AC and AE. The new mathematical programming problem is of the form

$$\text{minimize } z = 2\sqrt{2} a_1$$

subject to the deflexion constraint

$$\sqrt{2} lH/a_1 \leq 0.01E$$

Area group  $a_2$  has been eliminated from the design. The current design is indicated by point E in figure (8.2) on the new boundary curve 3. This boundary is now a vertical straight line due to the absence of the second area group. The final step in the design is to formally reduce  $a_2$  to zero, and point F vertically below E gives the final value of  $a_1$  as 10.554 square inches.

This structure was then designed starting with the same ground structure but with the members grouped together in different manners. Progress toward the final shape as recorded above is shown in figure (8.5a). In figure (8.3b) progress toward the final shape is shown when members AB and AC form the first area group while members AD and AE form the second area group. The final design shape, in this case, differs from the first having members AC and AB as shown.

When the members of the ground structure are not grouped so that the area of each member may vary independently yet another final design shape is obtained. Progress of the design in this case is shown in figure (8.3c) and leads to a structure with three members AB, AC and AE. Once this stage is reached it is found that no further members can be removed without

an overall increase in the volume of the structure. It is noticed however that the volume of the final structure is the same as those of the two previous designs. In fact the final shape of figures (8.3a) and (8.3b) can be obtained from the final shape in figure (8.3c) by making either  $a_2$  or  $a_4$  equal to zero.

Before leaving this section it is interesting to return once more to figure (8.2). In this figure it is noticed that although the boundary of the feasible design space is continually changing, all three positions of this boundary pass through the optimum point F. This indicates that the non-linear programming procedure, above, could have been employed to obtain the final result by merely eliminating the members of group 2 when their cross-sectional area became zero. Indeed this is the approach adopted by Dobbs and Felton. It is to be expected however that the proposed method saves computer time and storage by eliminating inefficient members, thereby reducing the size of the problem, before member areas assume a zero value. This is especially so when area grouping is employed as an insignificant member may be grouped with a structurally important member.

### 8.3 Design of Hanging Structures

The second study was concerned with ground structures consisting of a number of hanging members all meeting at a single free joint. These members were grouped together into pairs so that the ground structures were symmetrical. The modulus of elasticity of the material was taken as  $70 \text{ kN/mm}^2$ . The lower bound on the member areas was  $5 \text{ mm}^2$  while the upper bound was  $2000 \text{ mm}^2$ , thus allowing a wide variation in the member areas. The design requirements included deflexion constraints and there were always two stress constraints on each member. These limited the allowable tensile and

compressive stresses to  $0.1379 \text{ kN/mm}^2$  and  $-0.1054 \text{ kN/mm}^2$  respectively.

The first investigation was initiated with ten members and five area groups which is shown as ground structure (I) in figure (8.4). The structure was subject to two loads  $L_1$  and  $L_2$ , each one being 89 kN, acting as two independent loading cases. This structure was initially designed so that the stresses are satisfactory while the vertical deflexion at the common joint J does not exceed 0.1 mm. The final shape obtained was a statically determinate structure consisting of two members shown by design (a) in figure (8.4). The resulting members were of the same area group and had an area of  $1811.09 \text{ mm}^2$ . It was found that the vertical deflexion at J in the derived structure was exactly 0.1 mm while the stresses were satisfactory.

The structure was then redesigned several times with the severity of the vertical deflexion constraint reduced, by increasing the allowable deflexion at J in steps of 0.05 mm up to 0.35 mm. Each time the final design had the same shape but the volume of the structure reduced as the deflexion constraint was relaxed. This is indicated by the full line in the graph of figure (8.5). It was found that once the allowable vertical deflexion became greater than 0.26 mm this line became horizontal and no further saving in the volume of the structure could be obtained. This was because at this point it was the stress constraints that began to dominate the design.

The second investigation was initiated with a ground structure of eleven members. This was achieved by adding a vertical member, as a sixth area group, to the original ground structure. This structure is given as ground structure (II) in figure (8.4). With the vertical deflexion at J once again limited to 0.1 mm, the final design resulted in a statically indeterminate structure with three members. This is given as design (d) in figure (8.4) with the vertical member having an area of  $1479.52 \text{ mm}^2$  and the

two inclined members having an area of  $637 \text{ mm}^2$ . It is to be noticed that the insertion of the vertical member into the ground structure has reduced the volume of the final design by 30%. This indicates that for a deflexion constraint of this type and severity the most effective distribution of the structural volume is toward the centre line of the region covered by the ground structure.

This structure was also redesigned several times, each time reducing the severity of the deflexion constraint at J. The resulting variation of the volume of the structure is shown as a dashed line in the graph of figure (8.5). Once again the structural volume required decreases as the deflexion constraint is eased until the stress constraints become dominant, at which point the curve levels off. It is noticed, however, that as the deflexion constraint became less dominant, the shape of the final design changed to that shown as design (g) in figure (8.4), with five members. Finally with the deflexion at J limited to  $0.3 \text{ mm}$ , the vertical member became useless and was omitted from the final design. At this stage, in common with the ten member ground structure, design (a) was obtained as the best shape for the structure. For larger values of this deflexion both ground structures gave the same shape for the final structure with the two inclined members both having a sectional area of  $709.44 \text{ mm}^2$ .

It should be pointed out that in every case, where the deflexion constraint dominated, the value of this deflexion was exactly equal to its allowable value. This was also the case with stresses when stress constraints dominated.

A further design example was also initiated with a ground structure of ten hanging members and the same dimensions and material properties as the previous example. The design requirement was altered, however, by

removing the vertical deflexion constraint and imposing a horizontal deflexion limitation at J together with stress constraints, as before. Once again the value of the limiting deflexion was altered by increments and, in figure (8.6), the variation of the volume of the final design is shown against the severity of the imposed deflexion. The various shapes obtained are also indicated in this figure and shown in figure (8.4).

It is noticed that, once again, the topologies obtained for this series of designs depend upon the severity of the deflexion constraint. As this is eased the best shape changes from design (c) to (b), then (e) and finally to (a). It is interesting to compare the shapes obtained when severe vertical or horizontal deflexion limitations are imposed. In the former case the volume of the structure was distributed about the centre line of the ground structure. This was emphasised when the eleven member ground structure was used to commence the design. In the latter case, however, the volume is distributed away from the centre line. In this way the horizontal displacement of node J is more effectively restricted. However, a balance is struck between this effectiveness and the length of the structural members involved. Finally, as a vertical member is useless when restricting the horizontal displacement, the same results are obtained when using the eleven member ground structure.

A fourth set of designs were initiated by ground structure (I) but with both horizontal and vertical deflexions constrained simultaneously. In figure (8.7) the variation of the volume of the final design is shown plotted against the severity of the horizontal deflexion constraint. The ratio between the two allowable deflexions is also given numerically for each design, adjacent to the corresponding point on the graph. These ratios were obtained from the two separate deflexions of figures (8.5) and (8.6). It

was decided to investigate how the shape of the structure changes when both these deflexion constraints were imposed simultaneously. For this reason the numerical values of these deflexion constraints were selected from the final design structures having the same weight as when these deflexions were imposed individually.

It is noticed that while the deflexion constraints dominated, the final design always had the design shape (f). This shape has, not unexpectedly, a combination of the properties required of the final design shapes obtained when the horizontal and vertical deflexions were constrained independently. When the severity of the allowable deflexions was reduced and the stress constraints became critical, design shape (a), once more emerged as the final design. In every case where the deflexion constraints dominate both the horizontal and vertical deflexion at node J was equal to its allowable value.

In figure (8.7) the final design shown boxed had a volume of  $4.72 \times 10^5 \text{ mm}^3$  and the deflexion constraints were 0.252 mm vertically and 0.6 mm horizontally. It was noticed that with this final design both the deflexion constraints were critical while the stress constraints were also on the point of criticality. These stress and deflexion constraints were therefore imposed on a new design to investigate further the influence of the shape of the ground structure upon the shape of the final design.

For this purpose the structure was redesigned twice. The first was initiated with the eleven member ground structure (II). This also produced the final design shape (f) with exactly the same volume as that obtained starting from ground structure (I). However, when the design was initiated with a ground structure of 45 members grouped into 23 area groups, as shown in figure (8.8), it was noticed that the final design gave a

statically determinate structure with a volume reduced to  $4.65 \times 10^5 \text{ mm}^3$ . This is shown as design (b) in figure (8.4) which is made up of members that are non-existent in ground structures (I) and (II).

In figure (8.9) the progress toward the final design, starting with the 45 member ground structure, is shown. It is noticed that the shape of the structure was altered 22 times before the optimum geometry was obtained. It is also noticed in the figure that several local optima were located, but the non-linear mathematical programming method used overcame these in its progress to a final statically determinate result. It is interesting to note that to overcome stagnation at a local optimum, it is necessary to increase the volume of the structure before reducing it again.

These investigations show that the final shape of the structure, both its volume and its degree of redundancy, depends upon the type and numbers of the design constraints and their severity. They also show that the final shape depends upon the original shape of the ground structure.

#### 8.4 Design of Trusses

As a further example the ground structure shown in figure (8.10) was selected for the design of various trusses subject to different loads and design criteria. The ground structure is pin-jointed with support A fixed in position while support G is on a roller. In this ground structure each of the 9 joints is connected to every other joint by a member so that there is a total of 36 members. In the figure, the dashed lines connecting joints A to H, A to G and G to J represent straight members coaxial with members AJ, JH and HG.

Throughout the following series of designs the allowable member stresses were  $0.16 \text{ kN/mm}^2$  in tension and  $0.1 \text{ kN/mm}^2$  in compression. In the

first instance however the vertical loads, applied at joints J and H were each considered to be equal to 150 kN and to act simultaneously. The modulus of elasticity of the material was taken as  $207 \text{ kN/mm}^2$ .

In the first design to be considered, in addition to the stress constraints, the design requirements also limited the vertical deflexion at J and H to 6.5 mm. The members were grouped together into thirteen area groups in a manner indicated in the second column of table (8.3). Lower and upper bound values were imposed upon these groups of  $5 \text{ mm}^2$  and  $12000 \text{ mm}^2$  respectively. The volume of the first local optimum obtained was  $8.30 \times 10^7 \text{ mm}^3$  and the shape of the structure is shown in figure (8.10) as design (a). It is noticed that this structure is symmetrical and statically indeterminate with 20 members of which 5 are redundant. At this stage of the design 6 of the area groups have been completely removed and the mathematical problem is now one of 7 variables. The current values of these variables are given in the fourth column of table (8.3) where the superfluous area groups are indicated with a dash.

It is also noticed in this current design that joints A and H and J and G are connected to each other. This means that during the construction of this structure parallel elements should be used to connect these joints which by-pass the intermediate joints. Such an effort may add to the cost of the structure and lead to the selection of an alternative design.

The proposed algorithm, however, does not terminate at such a design and further removal of members from the local optimum design initially led to an increase in the volume of the remaining structure. After removing the five redundant members the volume was once again reducing and the resulting statically determinate structure was lighter than design (a) having a volume of  $7.60 \times 10^7 \text{ mm}^3$ . This structure is shown as design (b) in



figure (8.10) and the sectional properties of the 5 remaining area groups are given in the final column of table (8.3). In this design the deflexions at joints J and H are exactly equal to their limiting value. It is also noticed that joints A, H and J, G are no longer directly linked and therefore this structure does not involve any constructional difficulties.

The ground structure of figure (8.10) was used to initiate a series of redesigns. The resulting structures were to be subject to the same loading conditions and stress constraints but more severe deflexion limitations. The allowable deflexions at J and H were limited to 3 mm first and then to 2 mm. The manner in which the volume of the design proceeded and the number of topological changes that were made are shown in figure (8.11) by graphs (1) and (2) respectively. In both cases the lowest volume recorded was with 29 members, having the shape shown in figure (8.10) as design (c). This structure has 14 redundant members and 10 remaining area groups. The sectional properties of the area groups are given in the second and third columns of table (8.4) and correspond to structural volumes of  $2.13 \times 10^8 \text{ mm}^3$  and  $3.21 \times 10^8 \text{ mm}^3$  respectively.

A further local optimum was obtained which had 19 members. Once again the shape was the same for both the design criteria and is shown as design (d) in figure (8.11). This structure has only 5 of the original 13 member groups and the cross-sectional areas of these are indicated in the fourth and fifth columns of table (8.4) with corresponding structural volumes of  $2.17 \times 10^8 \text{ mm}^3$  and  $3.47 \times 10^8 \text{ mm}^3$ .

It is interesting to note that the area groups remaining in these designs with severe deflexion limitations are different from those remaining in the previous design. It is also noticed that the computer has automatically removed the joint at D. The statically determinate structure as obtained by the computer, therefore, had only 13 members and graphs (1) and

(2) of figure (8.11) show that such a structure is very heavy compared to designs (c) or (d).

It is noticed in figures (8.10) and (8.11) that although design (c) is lighter than design (d) from a construction cost point of view it is cheaper to adopt design (d) as this has far fewer members and has no overlapping of members at joints J and H.

The truss was again redesigned but this time the allowable deflexions at J and H were different. Joint J was allowed to deflect not more than 2 mm while joint H was limited to a maximum of 3 mm. The progress of the design for this unsymmetrical design requirement is also shown in figure (8.11) as graph (3).

The structure with the least volume obtained,  $2.66 \times 10^8 \text{ mm}^3$ , has 18 members and 6 remaining area groups, the properties of which are given in table (8.5). This is shown in figure (8.10) as design (e) where it is noticed that the final shape is unsymmetrical. The area groups differ from those remaining when the design criteria were symmetrical and the volume of the structure is distributed so that the deflexion at J is 2.000 mm and that at H is 2.978 mm. Once again therefore both of the limited deflexions are at their maximum allowable value in the final design. The statically determinate structure in this case proved to be by far the heaviest.

## 8.5 Design Including Self Weight

A major facility of the computer procedure was the capability of dealing with not only the case of several loading conditions, but also the inclusion of the structure's own weight. This latter facility was found to speed up the design operation considerably. This is due to the fact that on the removal of a structural member the loads applied to the structure are reduced.

The ground structure of figure (8.10) was once again used to initiate the design of two further trusses. The members of the ground structure, however, were now collected into 26 independent area groups which could range in value between  $5 \text{ mm}^2$  and  $12000 \text{ mm}^2$ . For both designs the truss was subject to two loading conditions. In the first condition  $L_1$  was 150 kN while  $L_2$  was removed. Under the second load condition  $L_2$  was 150 kN while  $L_1$  was removed. In both cases variation in the self weight of the members was included as a design parameter. To achieve this the density of the material was taken as  $7.69 \times 10^{-8} \text{ kN/mm}^3$ . The weight of any member in the structure was represented by equal vertical forces acting at the two joints to which the particular member was connected. In this way forces were applied to every single joint in the structure.

The inclusion of self weight into the problem necessitated an alteration in the procedure to determine the benefit vector. To achieve this the load vector at any stage was of two types, the actual external loading and the self loading. Each of the structural members had a different self load vector which contained the forces due to the weight of all the members except the corresponding member. To predict the behaviour of the structure on the removal of a member, the behaviours under the external load vector and the corresponding self load vector were considered independently. The results obtained were then summated using the principle of superposition. In this way the unknown factor  $\alpha_{ji}$  of equation (7.20) was now given by

$$\alpha_{ji} = (\psi_{Ej} + \psi_{Dij} - \Delta_j) / \Delta_j \quad \dots 8.1$$

Here  $\alpha_{ji}$  was the all round increase in the area of the members necessary before the removal of member  $i$  results in a limiting value  $\Delta_j$  for the deflexion at node  $j$ .  $\psi_{Ej}$  and  $\psi_{Dij}$  were the deflexions at node  $j$  after the removal of member  $i$  when the structure is subject to the external loading

vector and the self load vector corresponding to member  $i$  respectively.

Returning to the current design, apart from stress constraints, the deflexions at joints J and H were initially restricted to an allowable 3 mm. In figure (8.12) the variation of the volume of the structure is shown as its shape was altered. The structure with lowest weight was obtained at once with 22 members in 12 remaining area groups. The cross-sectional areas of those groups are given in the fourth column of table (8.6) where the area grouping is also indicated together with the initial feasible values.

The shape of this least volume design is shown in figure (8.12). It is noticed that this is symmetrical and once again includes undesirable members connecting joints A to H and G to J. The final statically determinate structure was obtained after four changes in topology. Although this has a volume of  $1.294 \times 10^8 \text{ mm}^3$  as compared with  $1.276 \times 10^8 \text{ mm}^3$  of the least volume design, it is clear that it is easier and cheaper to construct. This structure has 5 remaining area groups the cross-sectional properties of which are given in the final column of table (8.6).

In the second design the ground structure was once again subject to the same two loading cases but with unsymmetrical design requirements. No deflexion requirement was imposed at H. However, under the first loading condition the allowable deflexion at J was limited to 3 mm while with the second loading case acting this deflexion was limited to 2 mm.

The results of the design process are summarised in figure (8.13). It is noticed that the structure with the lowest weight was obtained in two steps. This structure is shown in the figure and is noticed to be unsymmetrical as is to be expected from the imposition of unsymmetrical deflexion criteria. Automatically proceeding to the statically determinate structure indicated the existence of another local optimum. The shape of this structure

is also shown in the figure and has 18 members. Before obtaining the statically determinate structure the computer automatically removed the joint at E so that this structure has only 13 members.

Once again there is little difference in volume between the least volume design and the statically determinate design. It is noticed in both these designs that the volume of the structure is distributed toward the pinned support A thereby restricting the deflexion of node J in an efficient manner.

The foregoing truss designs have indicated that with heavy loads and severe deflexion criteria the least volume design is often statically indeterminate.

#### 8.6 Design of Cantilever Truss

The ground structure shown in figure (8.14) was obtained by superimposing a number of familiar structures. A selection of these candidate structures, commonly selected by practising designers, are the X, N and K type trusses shown in figure (8.15). This ground structure has 21 joints and 72 members collected into 26 area groups as tabulated in figure (8.14). A ground structure with this number of joints, three of which are fixed in position, would require 207 members if every joint were to be connected to every other joint. The use of the reduced ground structure therefore reduces the size of the initial problem and eliminates undesirably long compression members such as that necessary to connect joints A and P.

The designed structure was required to sustain its self weight and two independent loading cases. The first load case consisted of point loads of 50 kN acting vertically at joints J, K, L, M, N and P. The second case consisted of vertical loads of 100 kN at K, 150 kN at M and 50 kN at P.

The elastic modulus and the density of the structural material was  $207 \text{ kN/mm}^2$  and  $7.69 \times 10^{-8} \text{ kN/mm}^3$ . The member stresses were to be limited to  $0.1 \text{ kN/mm}^2$  in compression and  $0.16 \text{ kN/mm}^2$  in tension. The deflexions at joints B and C were limited to  $1/240$  of their distance from A. On the other hand a more severe deflexion limitation was imposed at D and E. These deflexions were limited to  $1/300$  of their distance from A. There were no deflexion limitations imposed at F or G. It is clear that the trial and error approach, usually adopted by practising designers is not very helpful in this design. It is also clear that the outcome of the design exercise cannot be forecast intuitively.

The variation of the volume of the structure with its topological changes is shown in figure (8.16). It was noticed that for the first seven changes in the shape of the structure, the stress considerations dominated the design. After this stage, however, both stress and deflexion considerations became critical. The structure with the lowest volume obtained is shown in the figure. This had 20 joints and 42 members in 20 remaining area groups. The cross-sectional areas of these groups are given in the third column of table (8.7) which also indicates the initial feasible areas allotted to the groups.

Having obtained the structure of least volume the automatic process reduced the structure to one which was statically determinate. This had 20 joints and  $34$  members but a considerably higher volume. This is shown in figure (8.17).

It is interesting to note that in the design of least volume both stress and deflexion criteria are critical. The structural volume is distributed so that the deflexion at E is exactly equal to its maximum allowable value together with the compressive stresses in members AB and CD.

The portion of the structure beyond point E, away from the supports, is allocated just sufficient volume to prevent violation of the tensile stress constraint of members MU and UG. It is also noticed that the redundant members are contained in the part of the structure between A and E over which the deflexion constraints are imposed.

The design of this structure was initiated several times, but from different positions on the graph of figure (8.16), by manually intervening and removing joints and members. The volume of the structure however was never improved below that shown in the figure.

It is noticed in the figure that joint Q with its connecting members may be removed to be replaced by members JD and RS. Such an alteration, however, does not reduce the volume of the structure. Furthermore instability and construction considerations may prevent this.

The ground structure of figure (8.14) was also used to initiate a design with a more normal deflexion requirement. The two load cases of the previous design were once again applied and the structure was required to support its own weight. At each of the nodes B, C, D, E, F and G the vertical deflexion was not to exceed  $1/240$  the distance from A.

The progress of this design and the structure of least volume obtained is given in figure (8.18). It is noticed that once again the stresses dominate the design for the first 7 topological changes whereupon the vertical deflexion at G also becomes critical. The inclusion of this constraint into the design has resulted in the selection of a structure with 48 members and 21 joints. Also, by comparison of this with the structure selected in the previous design it can be seen that the section of the cantilever between nodes E and G now contains more redundant members.

## 8.7 Conclusions

Structures, subject to one loading case, designed to satisfy stress constraints only, may turn out to be statically determinate. However the preceding design studies have shown that structures subject to dominating deflexion requirements and under several loading cases are often hyperstatic. This is also the case with unsymmetrical design conditions. Furthermore it has been shown that structures selected as statically determinate may be very heavy, although in some cases these may be better from a constructional stand point.

It has also been shown that it is advantageous to include the self weight of the structure as a design variable. This is because including the weight of a member makes its position in the benefit vector more realistic. Including the self weight also enables the removal of long members. These are either heavy or buckle easily, and in either case are unsuitable.

The investigation also showed that the final shape of a structure depends upon the shape of the initial ground structure and the severity as well as the nature of the design constraints. The first example considered showed that the manner in which the members are grouped together also affects the shape of the final design.

It was found that the shape of a structure at its final stage could be considerably different from that of an initial ground structure. It was also found that many of these shapes could be unusual and difficult to select intuitively. This was particularly the case when the design requirements were varied and themselves unusual. It was shown that for a given set of design requirements, more than one shape could be obtained. The structure with least volume is not always the cheapest to construct but the proposed method makes several shapes available and from these the cheapest may be adopted.

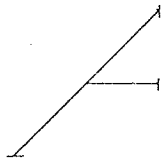

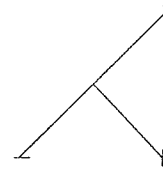



Remarks	Under external loads	Under unit axial loads at the ends of member			
		AC	AE	AD	AB
Horizontal deflexion	97.5116	8.1406	-5.6494	1.7616	5.6494
Vertical deflexion	-17.6160	-4.6176	-2.1264	-4.7688	2.1264
Member forces	AC	0.6250	-0.1726	0.3201	0.1726
	AE	-0.1726	0.5809	0.1473	-0.3809
	AD	0.5300	0.2441	0.5474	-0.2441
	AB	0.2022	-0.4463	-0.1726	0.4463
Removal factor	r	15.0429	-6.3225	4.4679	8.2822

x 10<sup>-4</sup> inches

Tons

Table 8.1 : Deflexions and member forces for structure of figure (8.1)

Remarks	Behaviour under external loading on removal of member			
	AC	AE	AD	AB
Possible New Structure				
Horizontal deflexion	219.9698	133.2299	105.3822	144.3010
Vertical deflexion	-87.0780	-4.1719	-38.9225	-0.0048
Member forces	AC	-	8.0988	7.0706
	AE	-6.5107	-3.2562	7.0689
	AD	9.9949	-	0.0006
	AB	7.6275	3.8148	-
Overall increase $\alpha$	1.1990	0.3320	0.0528	0.1440

$\times 10^{-4}$  inches

Tons

Table 8.2 : Behaviour of possible new structures

Group No.	comprises members	Area in mm <sup>2</sup>		
		Initial Feasible Values	1st Local Optimum	Statically Determinate Optimum
1	AJ, JH, HG	806.77	921.04	1742.77
2	CD, DE	1523.46	1795.54	1809.83
3	AB, BC, EF, FG	1447.31	1978.29	2289.60
4	DJ, DH	933.43	1055.19	562.11
5	JB, JC, HE, HF	621.94	1099.41	1275.52
6	AC, GE	1066.57	-	-
7	CE	1499.76	-	-
8	CH, JE	710.73	-	-
9	AD, DG	615.34	-	-
10	BH, JF, BG, AF, CG, AE	5.00	-	-
11	BF, BE, CF	270.62	-	-
12	BD, DF	855.93	320.64	-
13	AH, JG, AG	491.79	663.92	-

Table 8.3 : Properties of the members at various stages of the truss design of figure (8.10)

Group No.	Area in mm <sup>2</sup>			
	29 Member Structure		19 Member Structure	
	Allowable Deflexion at J and H		Allowable Deflexion at J and H	
	3mm	2 mm	3 mm	2 mm
1	1975.64	2964.89	4009.29	6012.15
2	3668.11	5511.82	-	-
3	2373.05	3539.81	4757.34	7112.47
4	2301.62	3462.47	-	-
5	1790.21	2687.64	3555.18	5352.30
6	2207.81	3306.48	-	-
7	-	-	-	-
8	-	-	-	-
9	-	-	-	-
10	423.14	650.5046	877.98	1331.68
11	943.26	1424.69	2652.82	3986.35
12	2138.26	3211.49	-	-
13	1408.77	2122.05	-	-

Table 8.4 : Properties of the members of the symmetrical truss designs of figure (8.11)



Group No.	Compressive Members	Group No.	Area (mm <sup>2</sup> )
1	AD, GH, HG	1	5640.12
2	CD, DE	2	5302.09
3	AB, BC, EF, FG	3	4906.68
4	DE, EH	4	4504.80
5	DB, AC, CE, BE	5	3731.02
6	AC	6	group removed
7	BC	7	group removed
8	CD	8	group removed
9	DE	9	group removed
10	EF	10	1560.32
11	FG	11	group removed
12	GH	12	group removed
13	AD	13	group removed

Table 8.5 : Properties of the members of the least volume truss obtained in the unsymmetrical design of figure (8.11)

Group No.	Comprises Members	Initial area (mm <sup>2</sup> )	Least Volume Areas (mm <sup>2</sup> )	Final Area (mm <sup>2</sup> )
1	AJ, JH, HG	1013.31	1618.52	2486.83
2	CD, DE	1165.40	1060.39	2216.70
3	AB, BC, EF, FG	1573.85	2889.39	3476.27
4	DJ, DH	1068.63	1256.39	1974.56
5	JB, JC, HE, HF	1818.14	2220.21	2555.95
6	AC	1323.51	-	-
7	CE	1159.35	789.97	-
8	EG	1324.00	-	-
9	CH	1046.32	829.53	-
10	JE	1046.02	826.25	-
11	AD	790.65	-	-
12	DG	790.60	-	-
13	BH	778.56	-	-
14	EJ	770.29	-	-
15	BG	390.19	-	-
16	FA	390.08	-	-
17	BF	532.44	-	-
18	BE	765.39	-	-
19	CF	765.29	-	-
20	BD	1154.29	732.87	-
21	DF	1154.42	734.91	-
22	CG	518.14	-	-
23	EA	510.70	-	-
24	AH	711.97	694.83	-
25	GJ	713.63	703.74	-
26	AG	482.13	-	-

Table 8.6 : Properties of the members at various stages of the truss design of figure (8.12)



Area Group	Initial area in square millimetres	Final value in square millimetres
1	19039.44	14350.45
2	8646.30	5787.53
3	16865.83	11229.49
4	10760.68	8854.68
5	7962.10	4214.39
6	9853.81	5971.34
7	8730.15	4314.47
8	794.66	group removed
9	8479.57	3633.65
10	0.1	group removed
11	0.1	group removed
12	9775.96	5163.60
13	13219.27	8812.91
14	13225.83	9585.63
15	9356.04	group removed
16	8962.80	4732.39
17	9807.82	group removed
18	8577.99	2211.32
19	74.71	1399.73
20	491.41	1849.15
21	8049.73	2309.97
22	5850.93	2802.85
23	4951.13	2324.59
24	8492.67	4612.72
25	7933.31	4470.92
26	9536.29	group removed

Table 8.7 : Properties of initial and final members of the structures shown in figures (8.14) and (8.16)

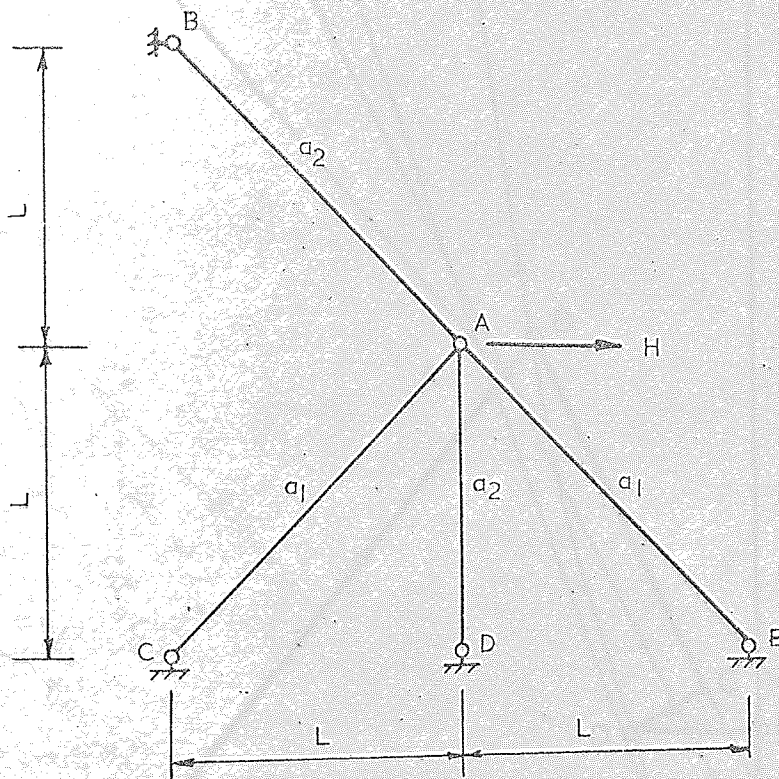


Figure 8.1. Planar frame.





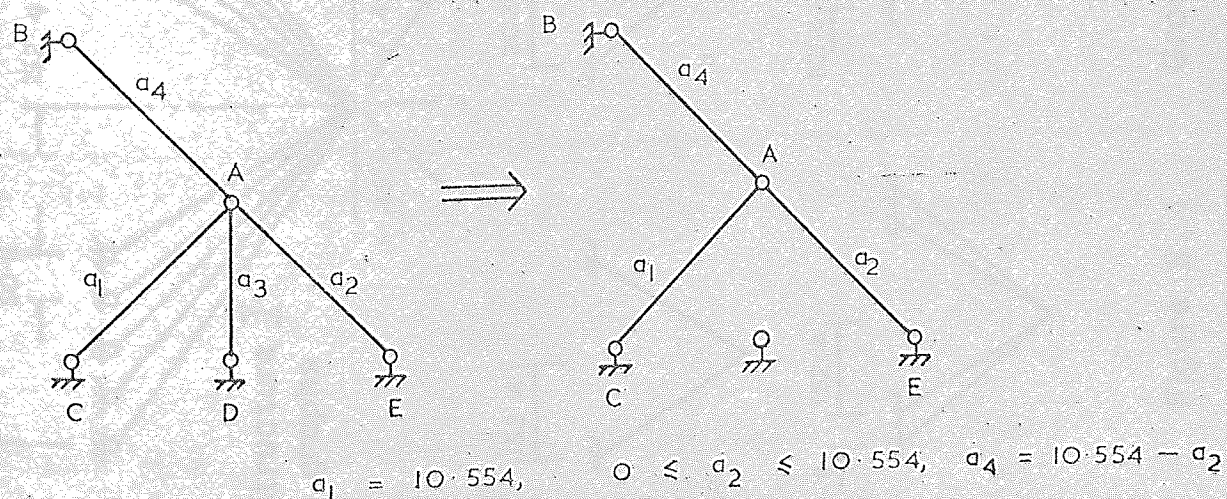
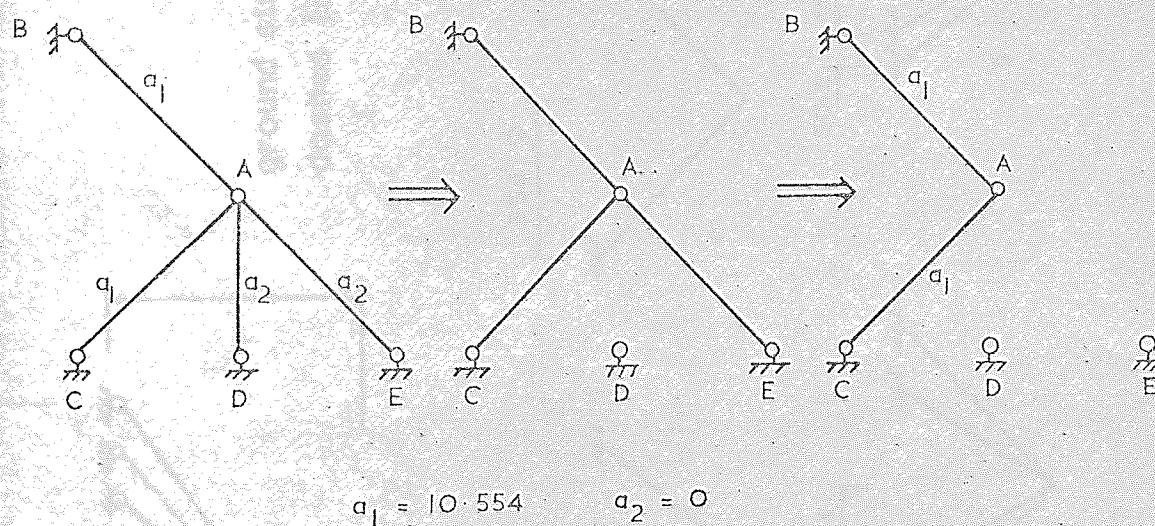
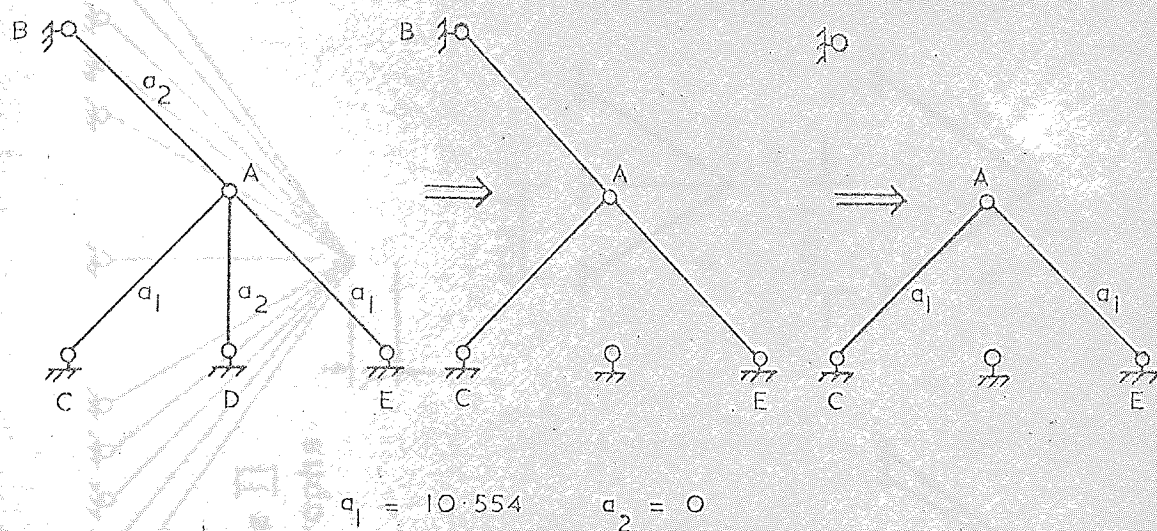


Figure 8.3 Various least volume structural shapes

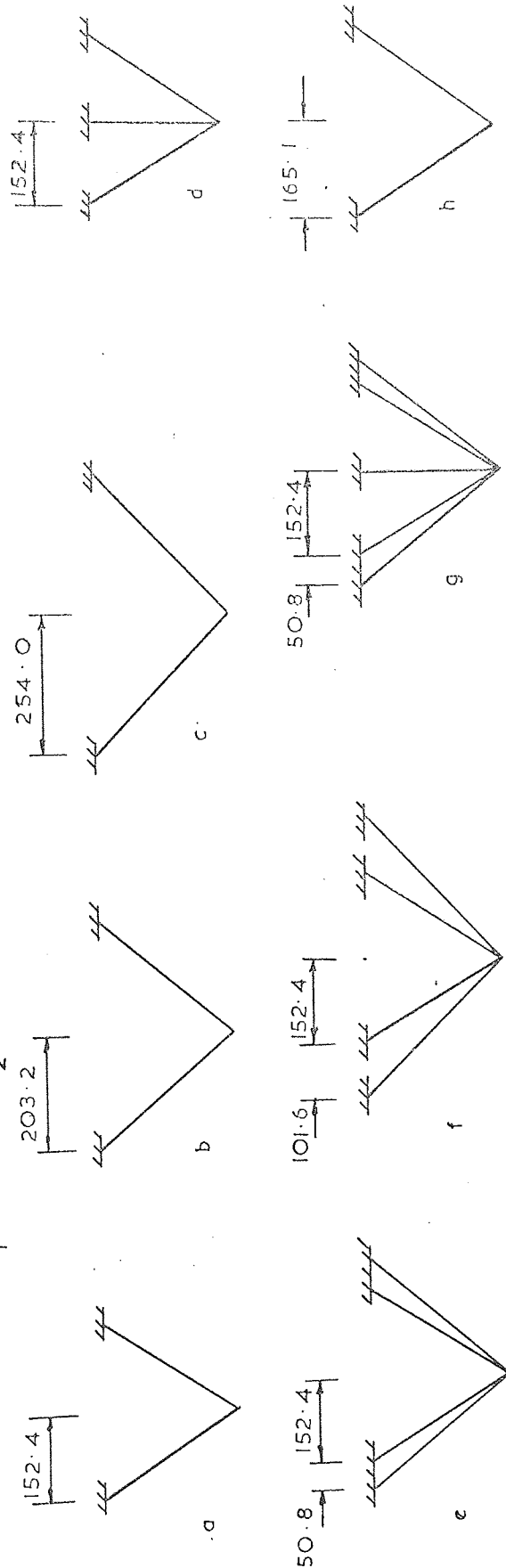
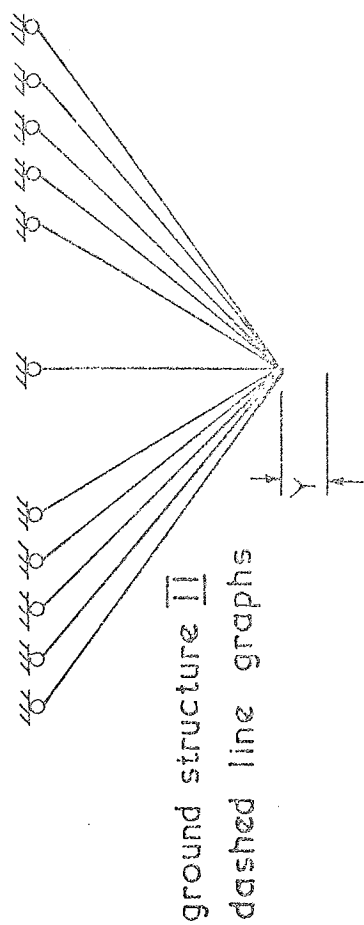
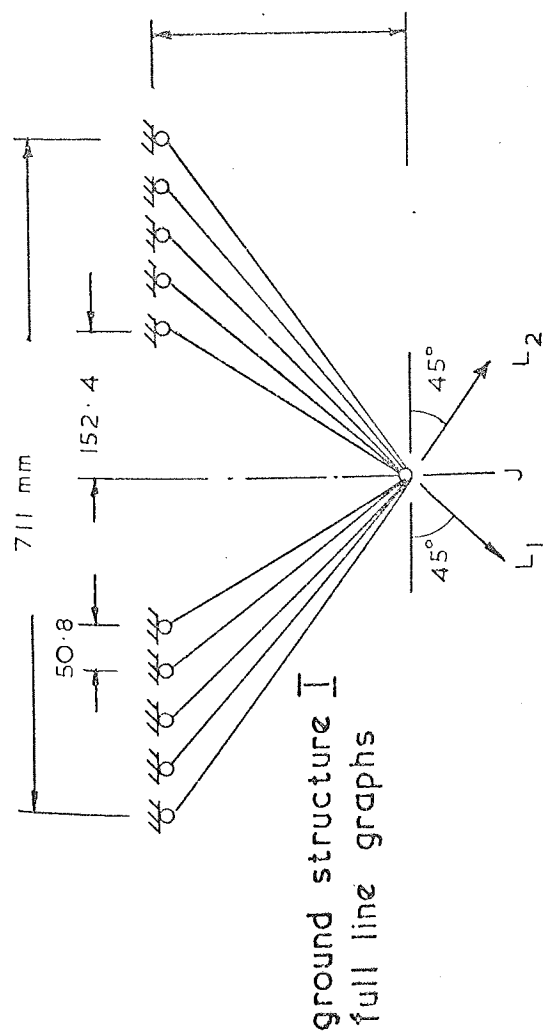


Figure 8.4 Ground structures and various derived final designs



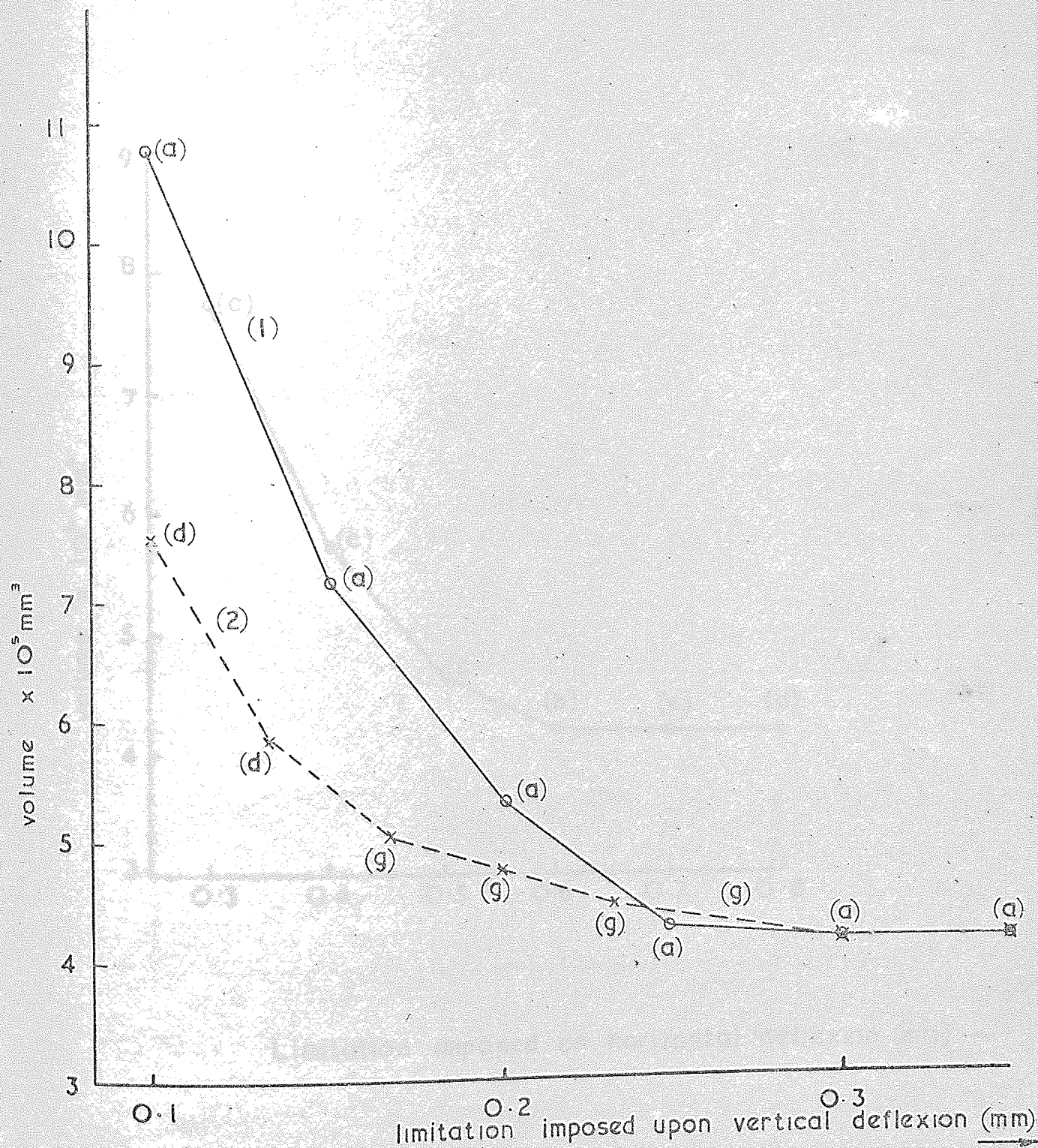
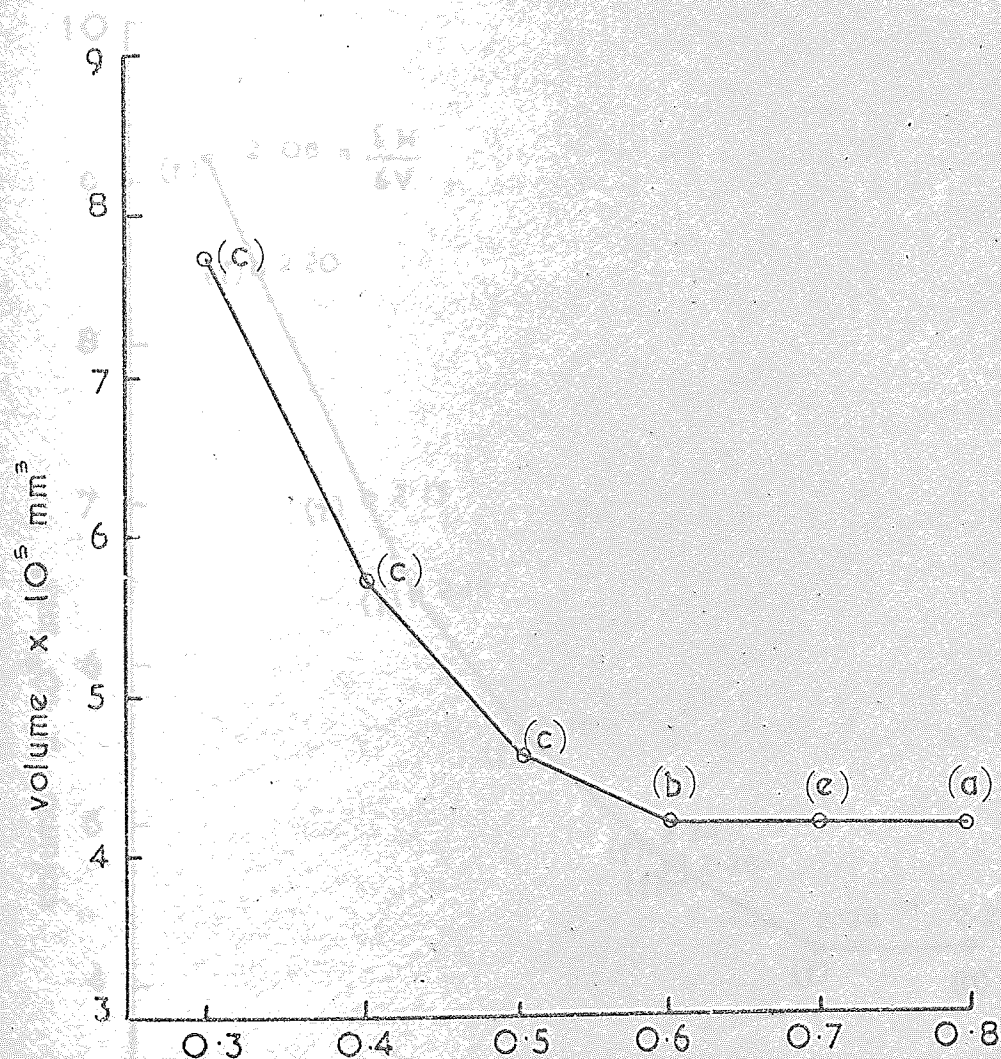


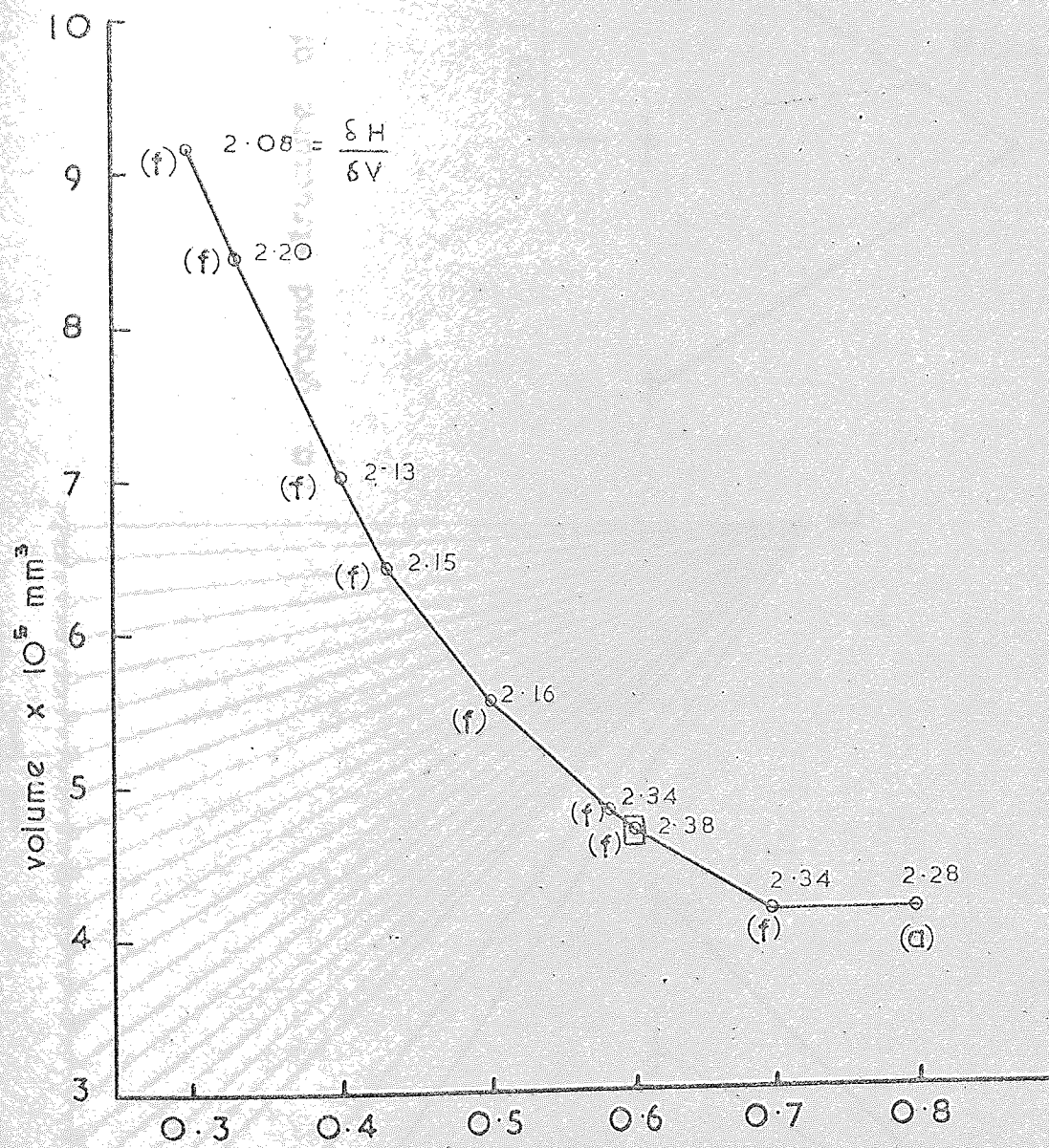
Figure 8.5 Final designs of hanging truss with vertical deflection constrained



Limitation imposed on horizontal deflexion (mm) →

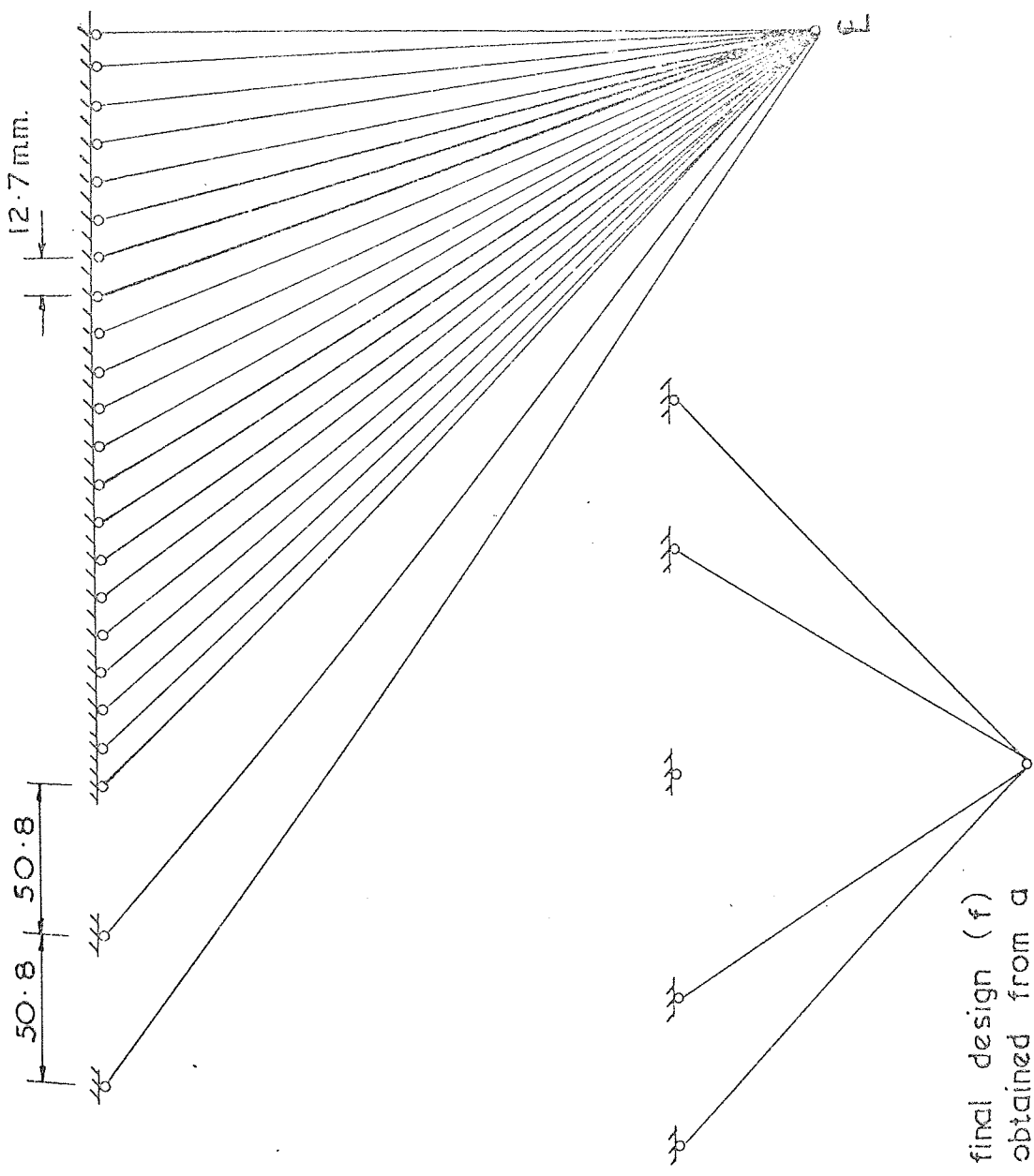
Figure 8.6. Final designs of hanging truss with horizontal deflexions constrained.





Limitation imposed upon horizontal deflexion (mm) →

Figure 8.7 Final designs of hanging truss with both vertical and horizontal deflexions constrained.



b. final design (f)  
obtained from a  
ground structure  
with eleven members

c. final design (h)  
obtained from a  
ground structure  
with forty five  
members

Figure 8.8. Redesign of hanging truss using a ground structure of 45 members

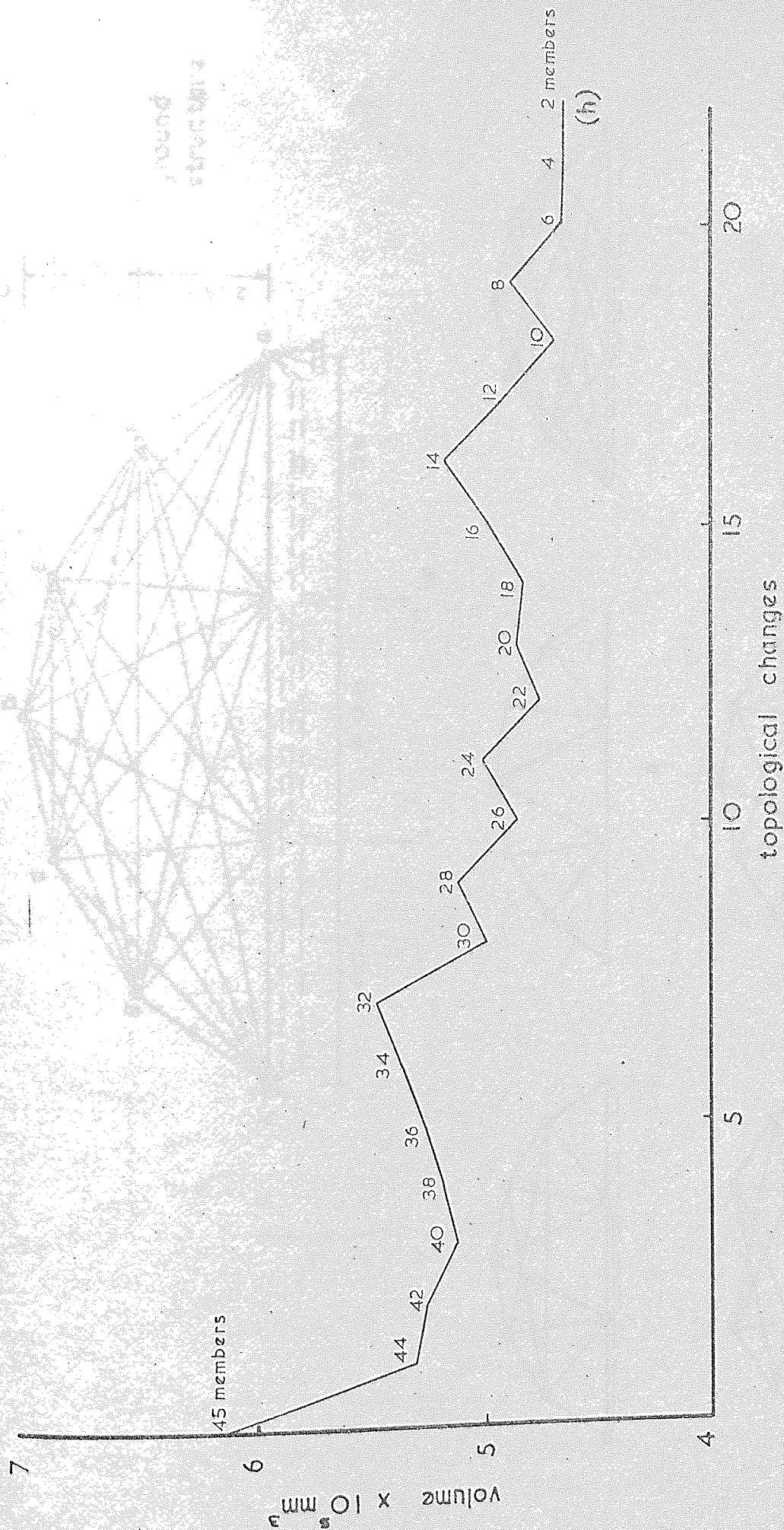


Figure 8.9. Progress of design commencing with ground structure of 45 member



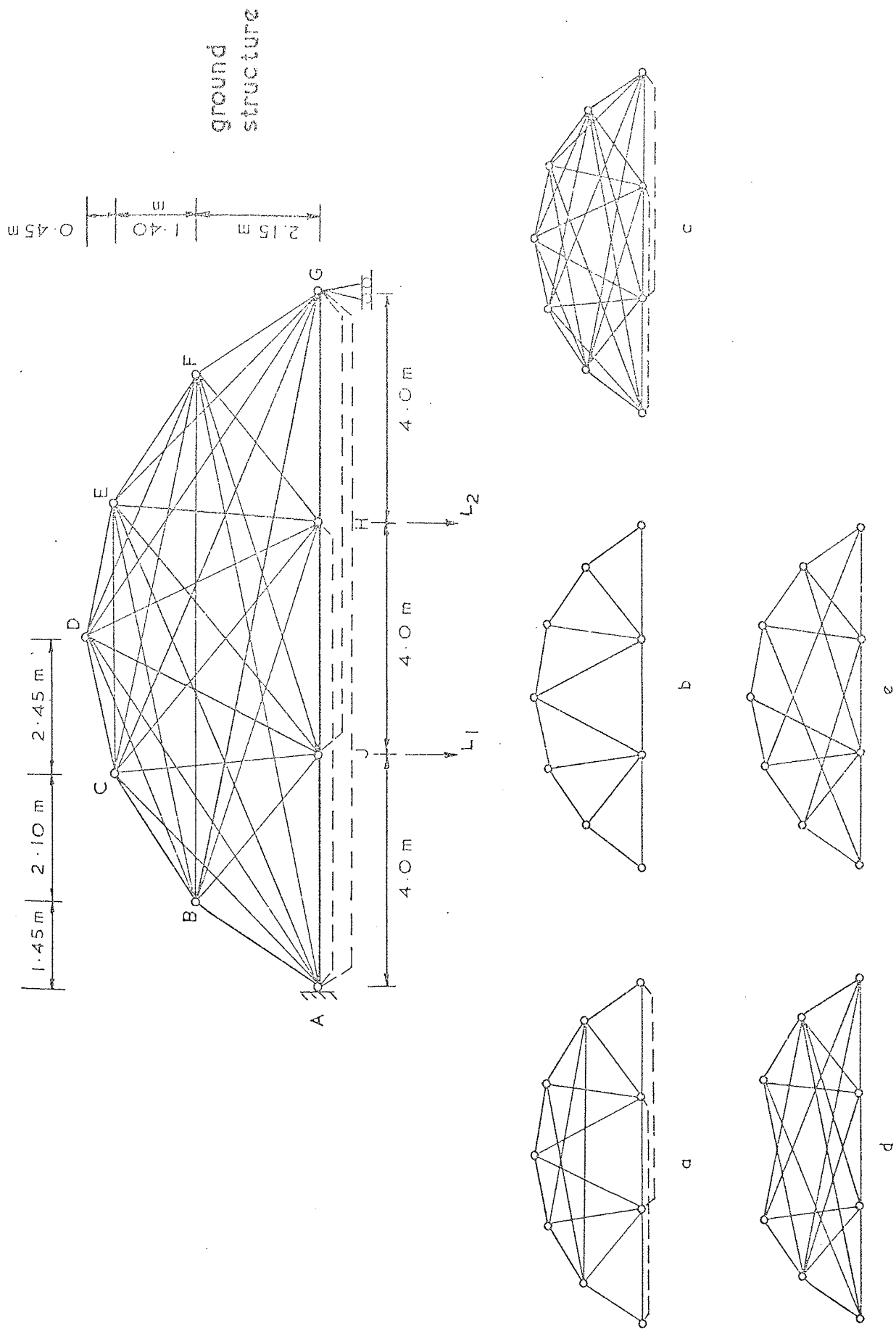


Figure 8.10. Details of truss showing ground structure and various derived structures

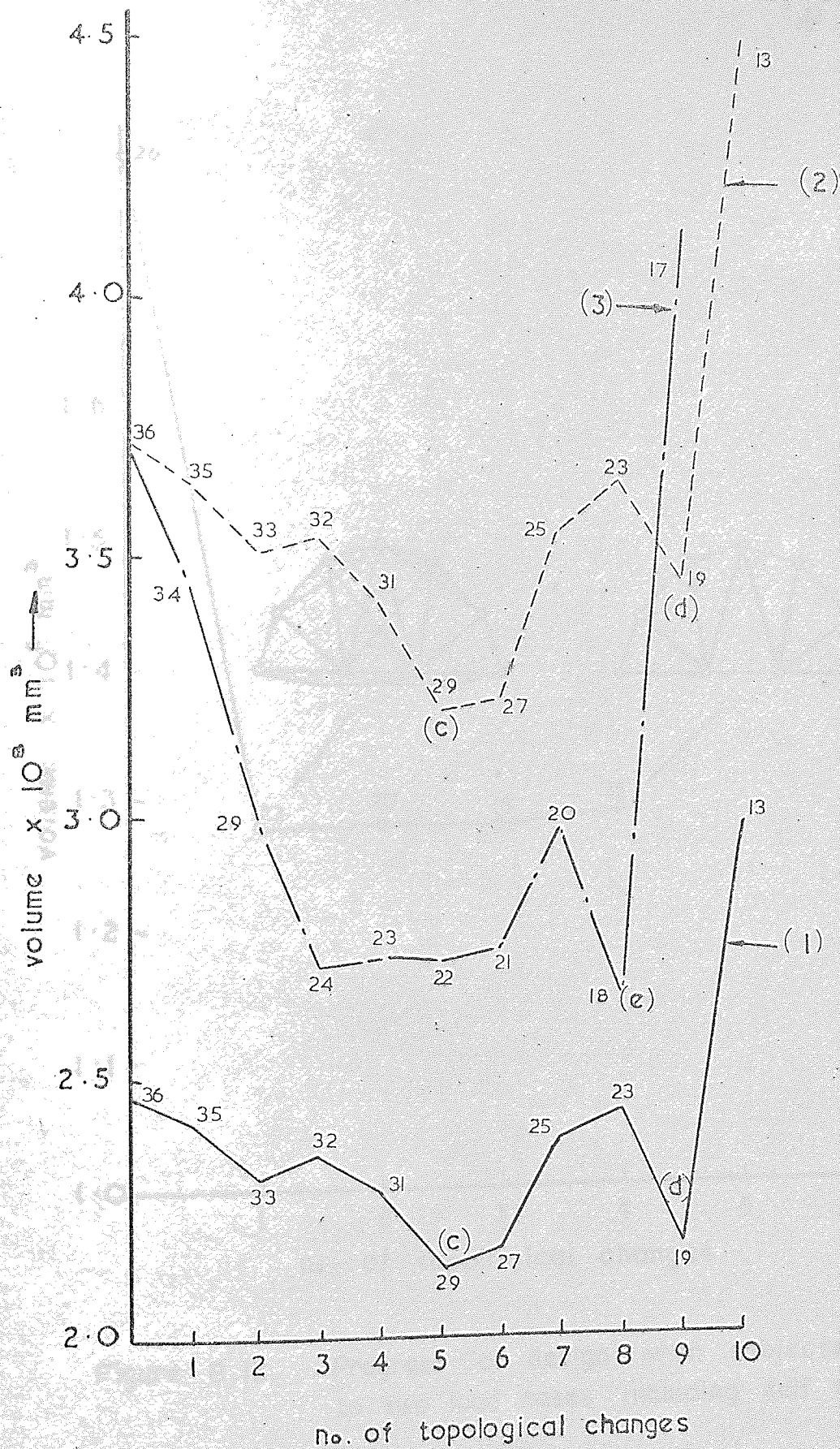


Figure 8.11. Progress of design when subjected to a single load case and three sets of deflexion criteria.

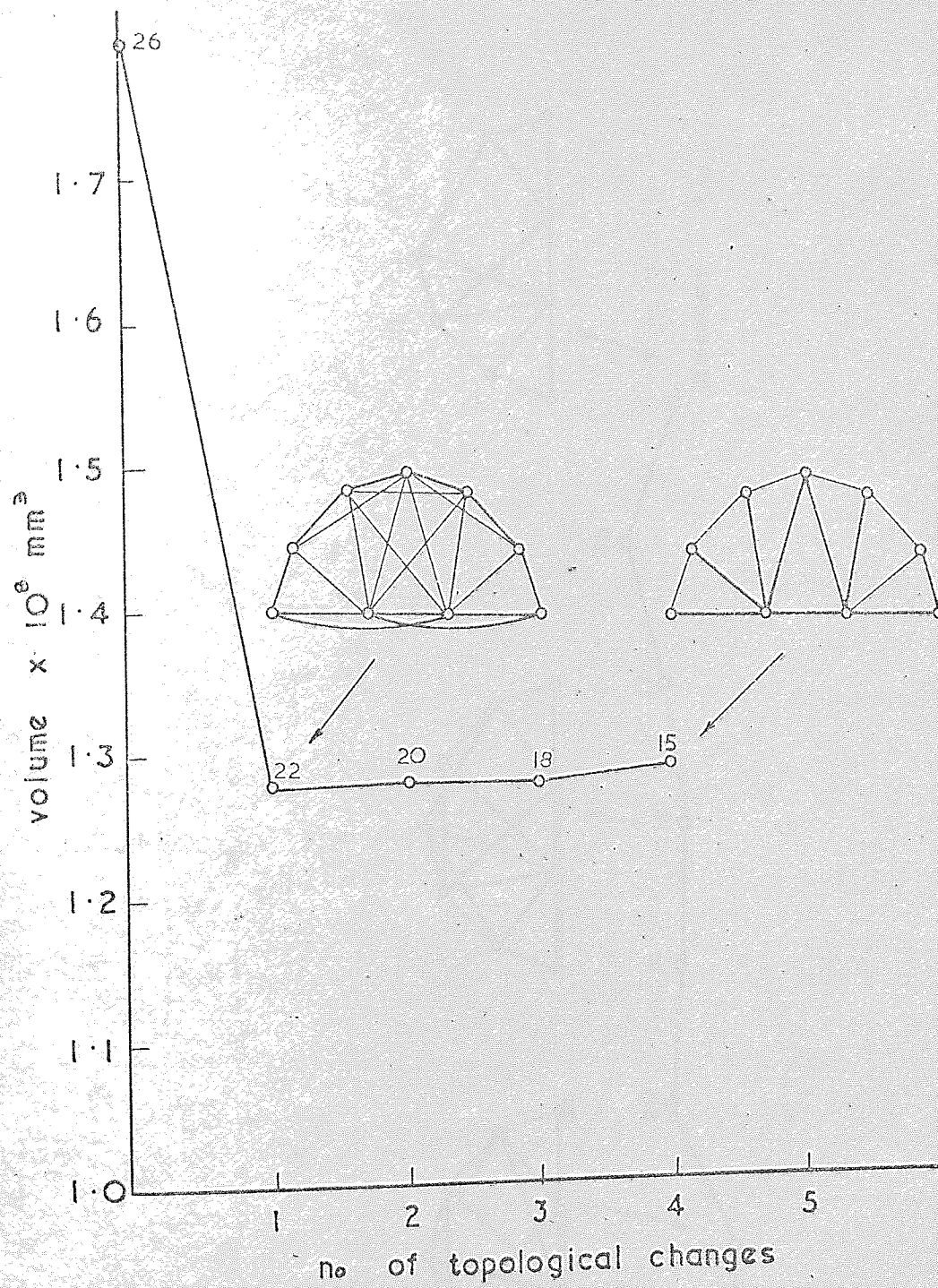


Figure 8.12. Progress of design when subjected to two load cases including self weight.



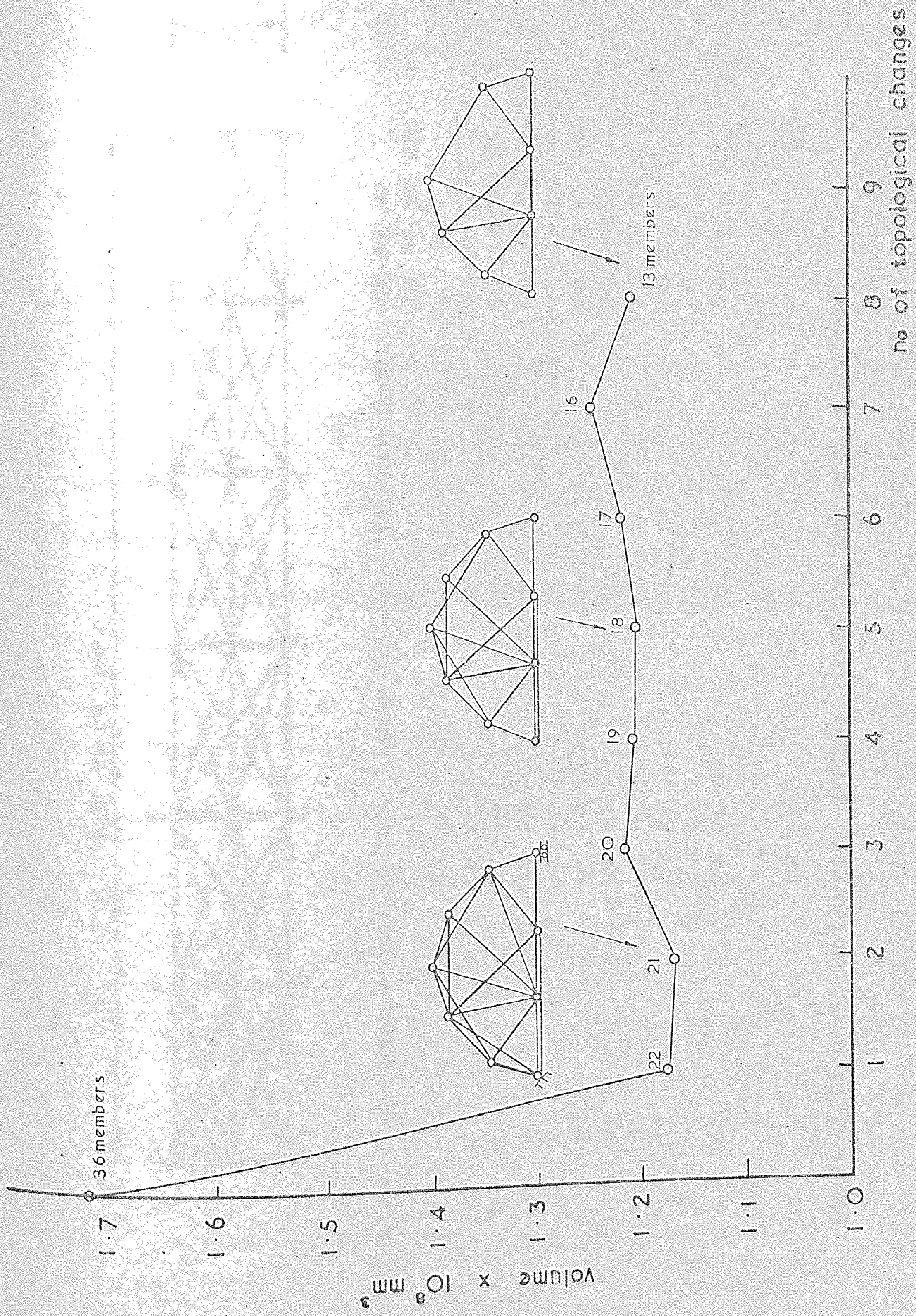


Figure 8.13. Progress of unsymmetrical design

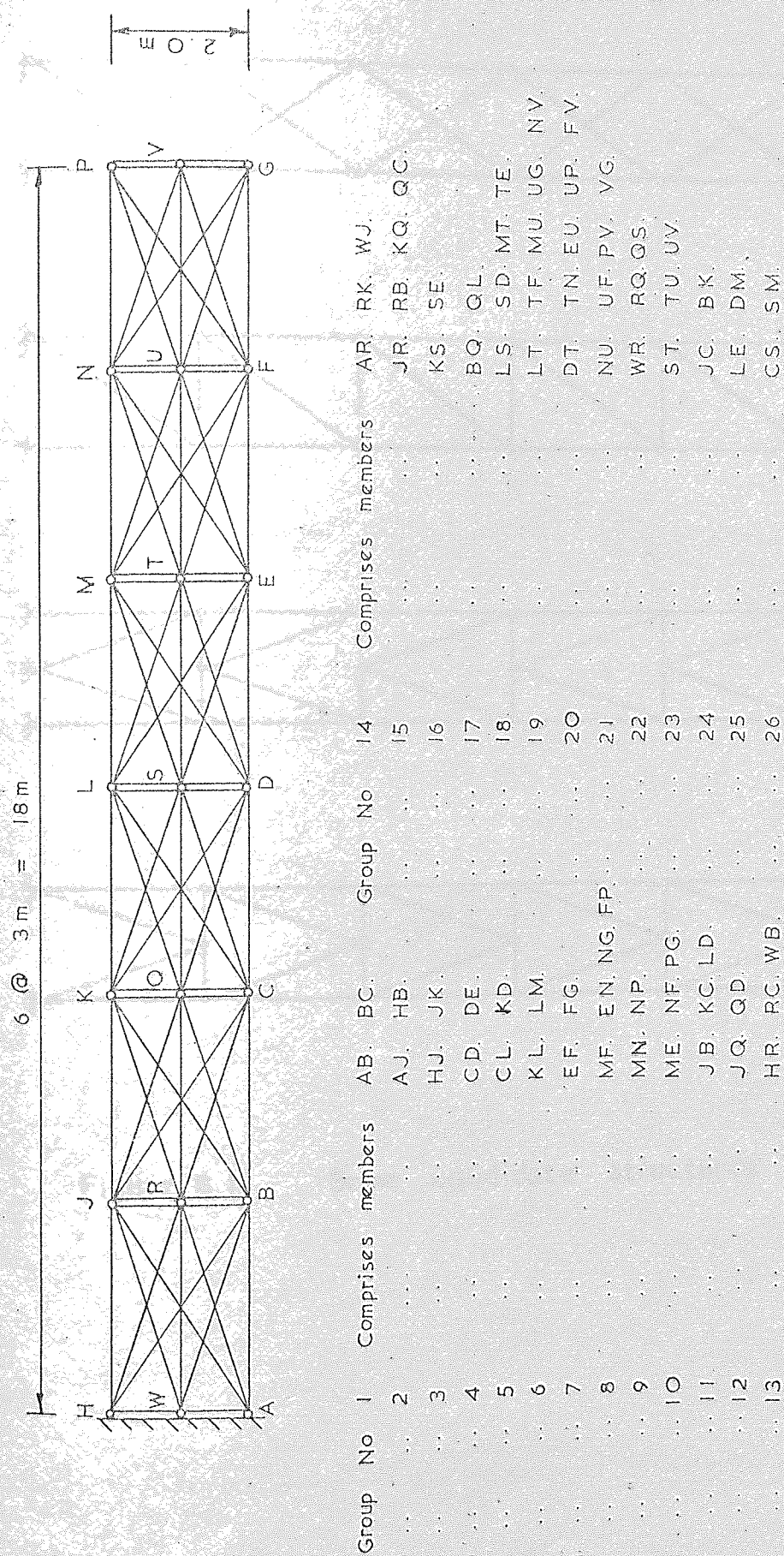


Figure 8.14. Cantilever ground structure and area groupings

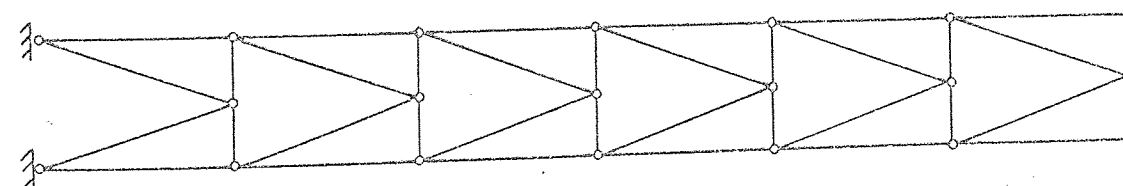
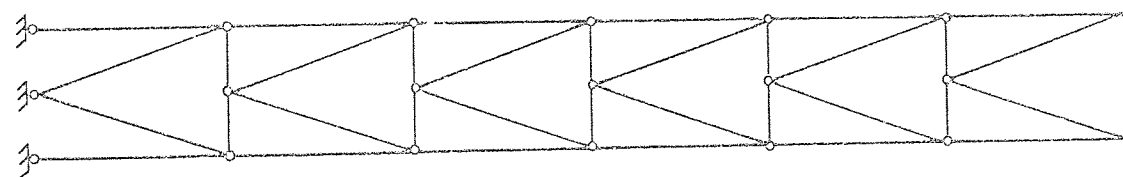
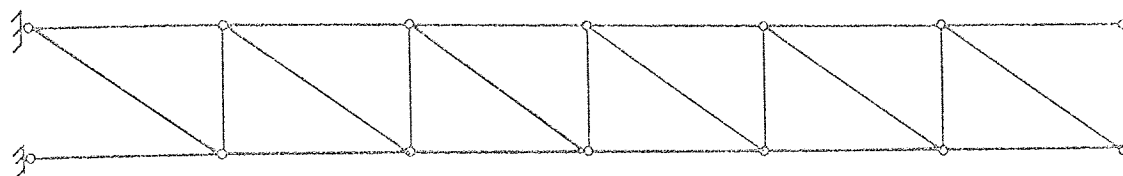
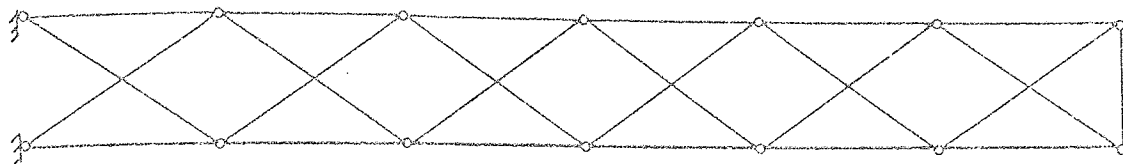


Figure 8.15. Some candidate structures



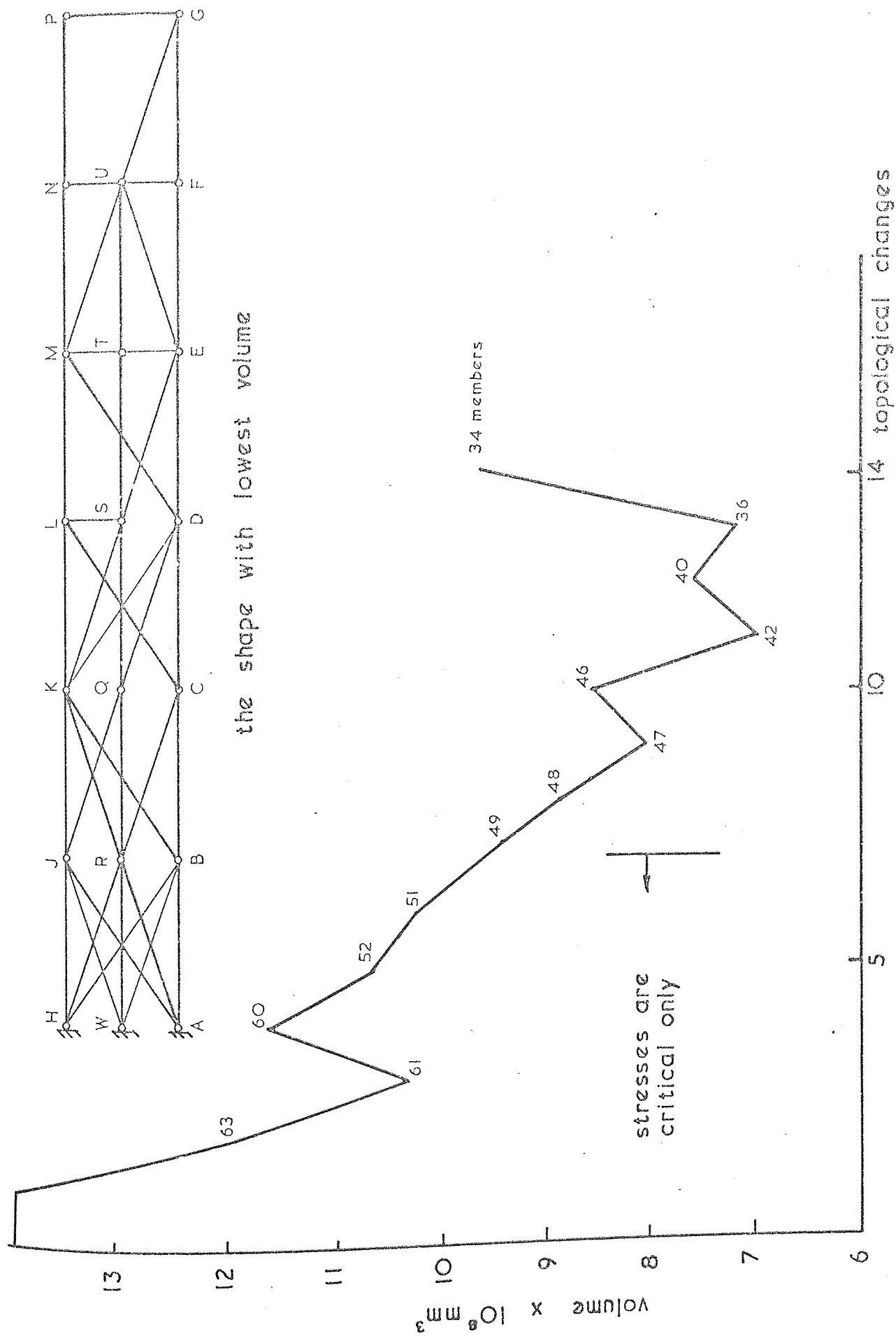


Figure 8.16. Progress of cantilever design

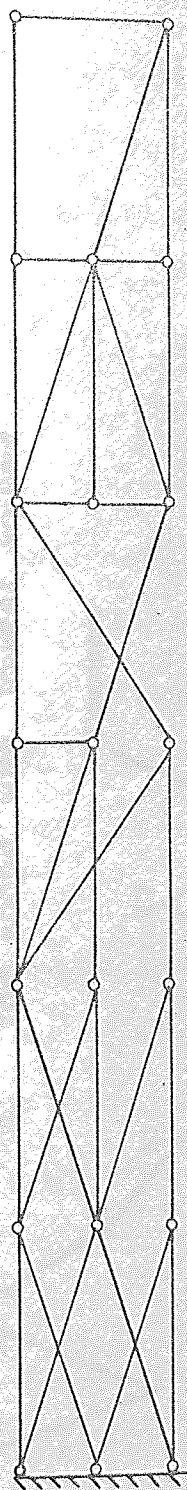


Figure 9.17 Final statically determinate structure



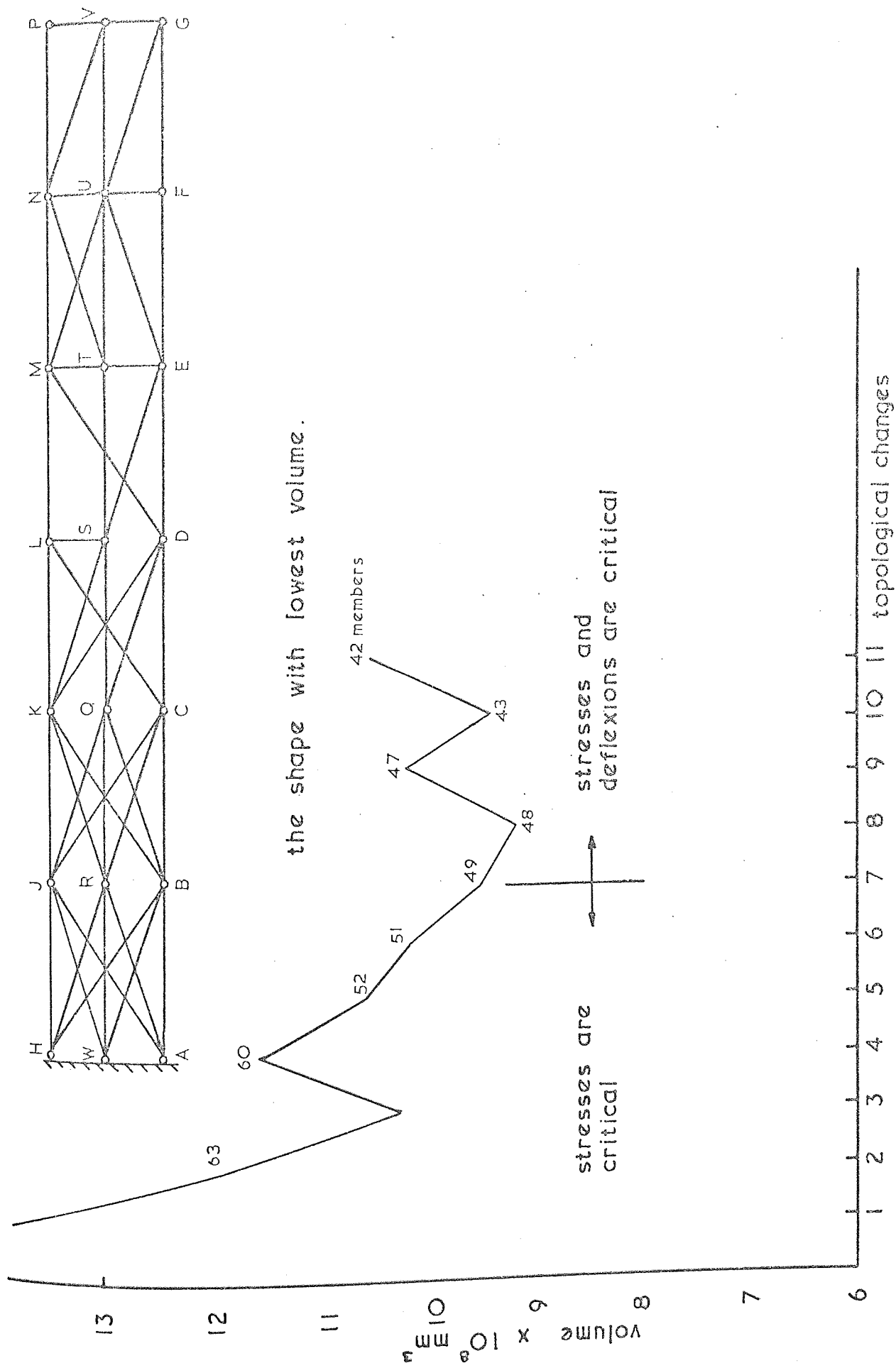


Figure 8.18. Progress of 2nd. cantilever design

CHAPTER 9SUGGESTIONS FOR FURTHER WORK

The dynamic search method of non-linear programming is successful in designing both rigid and pin jointed frames when subject to deflexion criteria. The design problem can be formulated using either the matrix displacement or matrix force methods. However, the size of the design is limited by the concept of sub-optimization and as a result no attempt has been made to produce a computer program capable of designing general structures that utilizes this method.

With a few refinements this could be achieved and the proposed procedure form the basis of a practical design method for redundant frames with small numbers of variables. Stress constraints, including buckling considerations, may also be introduced with little difficulty. However, it may be found that with an increasing number of constraints the method becomes less efficient.

The alternate mode non-linear programming algorithms proposed are encouraging and these may be extended to deal with rigidly jointed frames. In this way a practical automatic design procedure could be produced for such frames as well as pin jointed frames. In such a procedure it would be necessary to formulate the force transformation matrices automatically for all types of frame.

For the pin jointed frames dealt with in this thesis the permissible compressive stresses have been introduced into the problem as functions of the unknown cross-sectional areas. This was achieved by using a single general relationship for the radius of gyration to include several types of section. A more exact approach however would involve the determination of a suitable relationship between the area and the least radius of gyration

for each type of section used. Due to the flexible nature of the proposed method these relationships could be easily introduced into the automatic design procedure.

When designing rigidly jointed frames the effects of axial deformations could be introduced into the design problem by replacing the unknown sectional areas by functions of the unknown second moments of area. Due to the bending of members a further variable would also be introduced into the design problem, namely, the distance to the extreme fibres of a section from the neutral axis. This may be eliminated by determining a relationship with the second moment of area for various types of section. In this way all the constraints and the objective function can be expressed in terms of the second moment of area.

The alternate mode algorithm can readily be adapted to deal with the resulting non-linear objective function. This can be achieved by considering the objective function coefficients to be variable quantities equal to the instantaneous partial derivatives of the objective function with respect to the corresponding design variable. The convex nature of the objective function will probably accelerate the progress of the design as was demonstrated in this thesis in connection with dynamic search.

It should also be possible to develop an automatic optimum non-linear elastic design procedure based on the proposed algorithms.

The theorems of structural variation put forward in this thesis have been proved capable of calculating in advance the effect of variation or removal of members upon the behaviour of pin jointed structures. It is therefore possible to calculate the volume of a derived structure by studying its parent structure. These facts may be used to vary the properties of structural members for the purpose of design economy. Once the ground structure is analysed there is no further necessity for the analysis

of the derived structures.

These theorems may be utilized to produce a computer procedure to obtain the minimum weight design of structures of fixed geometry. When using the alternate mode procedure a large proportion of the computer time is spent deciding upon the direction of constant weight. By using the theorems of structural variation this is available without further analysis and thus it is possible to avoid a considerable amount of computation.

The work presented on minimum weight design with shape as a design variable is encouraging as it avoids arbitrary decisions and selects the shape of a structure as dictated by the design requirements and by a scientific method. The extension of the proposed theorems of structural variation to include rigidly jointed structures does not involve any fundamental difficulty. It is possible, therefore, to produce computer methods, based on these theorems, to design such rigid jointed structures with fixed or variable shape for minimum weight.

# REFERENCES

1. Maxwell, J. C., Scientific Papers, ii, pp. 175-177, 1869.
2. Michell, A.G.M., Phil. Mag. S.6. Vol. 8, No. 47, 1904.
3. Heyman, J., 'Plastic design of beams and plane frames for minimum material consumption', Quat. Appl. Math., Vol. 8, 1951.
4. Heyman, J., 'Plastic design of plane frames for minimum weight', Struct. Eng., Vol. 31, 1953.
5. Foulkes, J., 'Minimum weight design and theory of plastic collapse', Quat. Appl. Math., Vol. 10, 1953.
6. Foulkes, J., 'Minimum weight design of structural frames', Proc. Roy. Soc., Vol. 223, 1954.
7. Livesley, R. K., 'The automatic design of structural frames', Quat. J. Mech. Appl. Math., Vol. 9, Part III, 1956.
8. Kicher, T. P., 'Optimum design - minimum weight versus fully stressed', Proc. A.S.C.E., Vol. 92, No. ST6, 1966.
9. Rubinstein, M.F., & Karagozian, J., 'Building design using linear programming', Proc. A.S.C.E. Vol. 92, No. ST6, 1966.
10. Majid, K.I., & Anderson, D., 'Optimum design of hyperstatic structures', J. Num. Meth. in Eng. to be published.
11. Hadley, G., 'Non-linear and Dynamic programming', Addison-Wesley Publishing Co., 1964.
12. Moses, F., 'Optimum structural design using linear programming', Proc. A.S.C.E., Vol. 90, No. ST6, 1964.
13. Toakley, A. R., 'The optimum elastic-plastic design of rigid jointed sway frames', Research report No. 4, Dept. of Civ. Eng., Univ. of Manch. 1967.
14. Jennings, A., & Majid, K.I., 'An elastic-plastic analysis for framed structures loaded to collapse', Struct. Eng., Vol. 43, 1965.
15. Toakley, A. R., 'Optimum design using available sections', Proc. A.S.C.E., Vol. 94, No. ST5, 1968.
16. Gomory, R. E., 'An algorithm for mixed integer problems ', Rand. Corp., P-1885, 1960.
17. Jennings, A., & Majid, K.I., 'Computer analysis of space frames using sparse matrix techniques', Paper C4., Int. Conf. on Space Structures, University of Surrey, 1966.

18. Toakley, A. R., 'The optimum design of triangulated frameworks', Int. J. of Mech. Sci., Vol. 10., 1968.
19. Schmit, L.A., & Kicher, T.P., 'Synthesis of material and configuration selection', Proc. A.S.C.E., Vol. 88, No. ST3, 1962.
20. Schmit, L.A., & Morrow, W.M., 'Structural synthesis with buckling constraints', Proc. A.S.C.E., Vol. 89, No. ST2, 1963.
21. Schmit, L.A., & Mallet, R.H., 'Structural synthesis and the design parameter hierarchy', Proc. A.S.C.E., Vol. 89, No. ST4, 1963.
22. Brown, D.M., & Ang, H.-S., 'Structural optimization by non-linear programming', Proc. A.S.C.E., Vol. 92, No. ST6, 1966.
23. Rozen, J. B., 'The gradient projection method for non-linear programming', J. Soc. Indust. Appl. Math., Vol. 9, No. 4, 1961.
24. Schmit, L.A., & Fox, R.L., 'An integrated approach to structural synthesis and analysis', A.I.A.A., J., Vol. 3, No. 6, 1965.
25. Palmer, A.C., 'Optimal structural design by dynamic programming', Proc. A.S.C.E., Vol. 94, No. ST8, 1968.
26. Bellman, R. E., 'Dynamic Programming', Princetown University Press, 1957.
27. Pearson, C. E., 'Structural design by high speed computing machines', Conf. on Electronic Computation of the A.S.C.E., Kansas City, 1958.
28. Hemp, W. S., 'Studies in the theory of Michell structures', 11th Int. Cong. Appl. Mech., Munich 1964.
29. Chan, H.S.Y., 'Optimum structural design and linear programming', Coll. of Aeronautics, Rep. No. 175, 1964.
30. Dorn, W.S., Gomory, R.E., & Greenberg, H.J., 'Automatic design of optimal structures', J. de Mécanique, Vol. 3, No. 1, 1964.
31. Palmer, A.C., & Sheppard, D.J., 'Optimizing the shape of pin-jointed structures', Proc. I.C.E., Vol. 47, 1970.
32. Dobbs, M.W., & Felton, L.P., 'Optimization of truss geometry', Proc. A.S.C.E., Vol. 95, No. ST10, 1969.
33. Clarkson, J., 'The elastic analysis of flat grillages', Cambridge University Press, 1965.
34. Wolfe, P., 'Methods of non-linear programming', The Rand Corporation, R-401-PR., 1962.

35. Majid, K. I., 'Non-linear structures', Butterworths, 1972.
36. Toakley, A. R., 'The optimum design of triangulated frameworks', Research Report No. 3, Dept. of Civ. Eng., Univ. of Manch., 1966.
37. Mohr, O., 'Beiträge zur theorie des fachwerks', Z. Architekten-Ingenieur-Ver. Hannover, 509, 1874.
- 38a. Castigliano, A., Trans. Acad. Sci., Turin, 11, 127, 1876.
- 38b. Castigliano, A., 'Théorème de l'équilibre des systèmes élastiques et ses applications', Paris, 1879.
39. Maxwell, J. C., Phil. Mag., Vol. 27, No. 250, 1864.
40. Muller-Breslau, H., 'Die graphische statik der Baukonstruktionen', 4th ed. 2, 59, 1866.
41. Matheson, J.A.L., 'Hyperstatic structures', Butterworths, Vol. 1, 1959.



PUBLISHED WORK

The work presented in Chapter 2 of this thesis has been published in the form of a paper, written jointly by the author and Professor K.I.Majid. The paper, entitled 'Optimum Design of Frames with Deflexion Constraints by Non-Linear Programming' was published in 'The Structural Engineer', Volume 49, Number 4, April 1971.

The work of Chapter 4 has been presented at a symposium of the Planning and Transport Research and Computation Co. Ltd., entitled 'Cost Models and Optimization in Road Location, Design and Construction', held in London from 8th to 11th June 1971. This paper also written jointly with Professor K.I.Majid is entitled 'On the Optimization of Problems with Non-Linear Constraints' and will be published shortly in the proceedings of the above symposium.

A paper on the theorems of structural variation, based on the work presented in Chapter 6 has been submitted to Professor Sir John Baker, OBE., Sc.D., F.R.S., C.Eng., for consideration for publication by the Royal Society. It is hoped to follow this in the near future by a paper that encompasses the work presented in Chapters 7 and 8.